# Durham E-Theses

## *The crystal growth and properties op some chalcogenides of zinc and cadmium*

Cutter, J. R.

**How to cite:**

Cutter, J. R. (1977) *The crystal growth and properties op some chalcogenides of zinc and cadmium,* Durham theses, Durham University. Available at Durham E-Theses Online: http://etheses.dur.ac.uk/8207/

**Use policy**

THE CRYSTAL GROWTH AND PROPERTIES

OF SOME CHALCOGENIDES OF ZINC AND CADMIUM

by

J. R. CUTTER, B.Sc.

Presented in candidature for the

Degree of Doctor of Philosophy

in the University of Durham

May 1977

*Dedicated to my wife Valerie*

## ACKNOWLEDGEMENTS

## ABSTRACT

The main purpose of the work described in this thesis was to develop techniques for producing boules of ZnSe and $ZnS_xSe_{1-x}$ suitable for research purposes. This was accomplished by extending the method that Clark and Woods[1] used for CdS to the higher temperatures needed to grow ZnSe and $ZnS_xSe_{1-x}$ in the range $x = 0 - 0.6$. In this system the capsule is connected to a reservoir of one of the components via a narrow orifice to maintain constant growth conditions. The system has been examined theoretically in an attempt to learn more about the actual conditions of growth within the capsule. It was concluded that growth occurs close to stoichiometry with $A_0$ (the ratio of $P_{Se_2}/P_{Zn}$ at the growth face) approximately 0.194 or 1.12 according to the element in the reservoir.

Particular emphasis was placed upon the incorporation of manganese into the zinc selenide lattice. Concentrations of the order 300 p.p.m. were obtained when the element was added to the charge and $MnCl_2$ was placed in the reservoir. Higher levels of manganese ($\sim 1\%$) were obtained using chemical vapour transport with iodine as the transport agent.

Boules of solid solutions within the range of compositions from ZnSe to $ZnSe_{0.4}S_{0.6}$ were examined using a transmission electron microscope. The dominant crystallographic defects were found to change from thin twins to stacking faults as the amount of ZnS was increased. The origin of the defects was probably post growth stress.

Finally, the anomalous photovoltaic effect was discovered in ZnSe needle crystals, and was explained qualitatively in terms of asymmetrical barriers along the polar axis of the crystal.

(1)  J Woods  and  L Clark  (1968)  J. Crystal Growth  3  4  127-130

# CONTENTS

# CHAPTER 1

## INTRODUCTION

The zinc and cadmium chalcogenides have been studied for many years because of their interesting photoconductive and luminescent properties. They have direct band gaps, of a magnitude that at low temperatures varies between 1.6 eV for CdTe and 3.91 eV for hexagonal ZnS[1]. These values correspond to photons with wavelengths varying from the infra-red to the ultra violet. The work described in this thesis was directed towards producing materials suitable for the fabrication of two types of practical device.

The first, as part of a project sponsored by S.R.C. was a light emitting diode of the Schottky barrier type made from zinc selenide or solid solutions of zinc selenide/sulphide. The second was a scintillator made from single crystal CdS:Te, for the detection of nuclear particles. This was intended for use in conjunction with a silicon photo-diode.

The early work on II-VI compounds was performed on polycrystalline material and powders. Single crystal studies began essentially in 1947 when Frerichs[2] first grew cadmium sulphide crystals from the vapour phase, and produced crystals of a purity not found in nature. Since that time bulk crystals have been produced by a number of techniques, but still have not reached the perfection of those crystals used in semiconductor and laser technology.

The difficulty in growing crystals of II-VI compounds stems from a combination of relatively high melting temperatures and high vapour pressures, with quite high chemical reactivity.

The evaporation of II-VI compounds involves dissociation of the form

$$2MN \rightleftharpoons 2M + N_2$$

$$\text{Solid} \qquad \text{Gas} \quad \text{Gas}$$

M and N are used to denote the metal and non-metal respectively.

The relative vapour pressures of the two elements are governed by the relationship

$$Kp = P_M^2 P_N \qquad (1.1)$$

$Kp$ is the reaction constant, $P_M$ is the partial pressure of metal, $P_N$ the partial pressure of non-metal and $P_T$ is the total pressure. As

$$P_T = P_M + P_N \qquad (1.2)$$

the total pressure must vary rapidly with the relative proportions of the constituents within the limits set by the vapour pressures of the elements at that temperature.

Let

$$P_N = A P_M \qquad , \qquad (1.3)$$

then

$$Kp = A P_M^3 \qquad , \qquad (1.4)$$

$$P_T = P_M (A+1) \qquad , \qquad (1.5)$$

and

$$Kp = \frac{A P_T^3}{(A+1)^3} \qquad . \qquad (1.6)$$

Rearranging the last expression gives

$$\frac{P_T}{Kp^{1/3}} = \frac{1}{A^{1/3}}(A+1) \qquad . \qquad (1.7)$$

Differentiating to find the minimum value of the total pressure gives,

$$\left(\frac{1}{Kp}\right)^{1/3} \cdot \frac{dP_T}{dA} = \frac{2}{3}A^{-1/3} - \frac{1}{3}A^{-4/3} \qquad . \qquad (1.8)$$

Equating the right hand side to zero yields $A = \frac{1}{2}$ for a minimum.

i.e. $P_T = \frac{3}{2}(2Kp)^{1/3}$, $P_M = (2Kp)^{1/3}$ and $P_N = \frac{(2Kp)^{1/3}}{2}$ (1.9)

At the maximum melting point the dissociation pressure $P_{MIN}$ is significant as the following table[3] shows.

| | Maximum Melting Pt. °C | $P_{MIN}$ Atmospheres |
|---|---|---|
| ZnS | 1830 | 3.7 |
| ZnSe | 1520 | 0.53 |
| ZnTe | 1295 | 0.64 |
| CdS | 1475 | 3.8 |
| CdSe | 1239 | 0.41 |
| CdTe | 1092 | 0.23 |

The values of $P_{MIN}$ are extrapolated from data obtained at low temperatures, and would therefore have to be revised upwards if the non-metal were to be monatomic in the vapour at the higher temperatures.

Melt growth thus poses an interesting problem, the materials must be heated some 50°C above their melting points to ensure complete melting before crystal growth is begun. They should also be contained in a sealed capsule to prevent their evaporation. However silica glass, which provides by far the easiest sealing system, softens above 1200°C making it unsuitable in its simple unsupported form as a container. The difficulty is compounded because material sealed in a tube at room temperature almost certainly will not lead to $P_{MIN}$ conditions at the melting point, and may well give a pressure many times $P_{MIN}$ at that temperature. An alternative to sealing the material in a capsule, is to provide an overpressure

of one of the constituents, thus suppressing the evaporation of the compound by reducing the vapour pressure of the other constituent. Another approach is to apply a large overpressure of inert gas, which increases the time for the charge to evaporate completely.

One of the first reports of melt growth of CdTe in a sealed silica capsule was by De Nobel[4]. He used a horizontal boat system and prevented the cadmium telluride from leaving the boat by applying an overpressure of either cadmium or tellurium. Tsujimoto et al.[5] grew ZnSe under a pressure of 120 Atmospheres, while Fischer used a highly complex system of a graphite container sealed in silica. An overpressure of argon was used to support the silica. Both these workers used R.F. heating of a graphite crucible, but Fischer[6] sealed his crucible in a quartz envelope and held one of the elemental components in a reservoir at a fixed temperature to control the stoichiometry while growth was in progress. Wardinski[7] used unsupported silica to grow CdSe by the Bridgeman-Stockbarger technique; this is probably the limit of what can be performed with confidence in unsupported silica. Graphite supporting envelopes are sometimes used as reinforcement for the silica which expands under the internal pressure until it is compressed against the graphite (e.g. Ref. 8).

The pressure on the capsule may be minimised by baking the compound under vacuum at a high temperature before sealing the capsule. During the bake some of the material sublimes and the charge moves towards the composition required to establish $P_{MIN}$ conditions at that temperature. All the melt techniques used to date have been variations of the Stockbarger theme (e.g. Refs. 8-12). There have been no successful attempts at Czolchralski pulling. This is because of the difficulty of preventing evaporation of the melt and growing crystal; a similar problem to that encountered with

III-V compounds. However with the III-V compounds liquid encapsulation with boric oxide has been successfully employed[13,14].

With this technique the loss of volatile components is prevented because the melt is covered with a layer of molten glass, and an overpressure of inert gas greater than the vapour pressure of the melt is applied. Many of the difficulties of the melt growth of II-VI compounds would be removed if a suitable encapsulent could be found. The requirements for such an encapsulent are quite stringent. With zinc telluride for example, it must melt below $900^{\circ}$C, and with ZnS boil above $2,000^{\circ}$C. It must not react with the melt or the apparatus. The compound must not dissolve in it. II-VI compounds unfortunately react with boric oxide, the usual encapsulent, and dissolve in all the molten salts tried in this laboratory, including KI, CaI and $CaCl_2$. However if a suitable encapsulent were found the stoichiometry of the crystal could be readily controlled in a quite low pressure apparatus by adding an excess of one of the components to the charge, and allowing it to boil off through the encapsulation until the desired total pressure (related to the partial pressures by equations 1.1 and 1.2) equalled the pressure outside the encapsulent.

Solution growth has been attempted to avoid the problems encountered with high temperatures and pressures. Parker and Pinnel[15] used a KI-$ZnCl_2$ flux to produce small crystals of ZnS at temperatures around $800^{\circ}$C. The resultant crystals were of moderate quality and highly doped with solvent. Since most crystals are studied for their luminescence and electrical properties, which may be affected by impurity concentration of a few parts per million, this method of crystal growth is not likely to find wide application.

One might also seek to grow crystals from a non-stoichiometric

melt, i.e. a solution of the II-VI compound in one of its con-
stituents. However, the details of the phase diagrams[16] (shown
in Fig. 1.1) make this approach difficult. The vapour pressure
above a dilute solution approaches that of the solvent element.
In most cases the solvent must be taken well above its boiling
point to increase the solubility to a reasonable level. Consequently,
to gain a worthwhile reduction of temperature and pressure, a very
dilute solution must be used. So far only poor quality crystals
have been produced by this method. Moreover, there is the difficulty
of separating the crystals from the solvent. The crystals are
likely to be damaged by the stress involved in cooling in a solid
matrix. However, temperature gradient solution zoning has been used
with success for ZnTe[17]. This technique produces a very worth-
while reduction in temperature for the growth of zinc telluride
which is brought to a comfortable temperature for use with wire
wound furnaces and silica glass. De Nobel[4] when growing cadmium
telluride under a heavy excess pressure of one element found that
his melt was non-stoichiometric, not as one might have expected
by suffering from constitutional supercooling, but from bubble
formation from the boiling solvent. For the same reasons that con-
stitutional supercooling occurs, there is a build-up of rejected
solvent in front of the growth face, considerably increasing the
vapour pressure of the melt locally. To avoid bubble formation it
is consequently necessary to pull slowly to avoid reaching the
critical supersaturation for bubble formation, or to put an over-
pressure of inert gas on the melt, thus employing a liquid encap-
sulation technique. A similar problem is encountered using
overpressures of inert gas with an unsealed capsule[18]. The two
constituents diffuse at different rates, (particularly in the case

# THE LIQUIDUS COMPOSITION AS A FUNCTION OF TEMPERATURE FOR Zn Se, Zn Te, CdS AND Cd Se

## Fig. 1 : 1
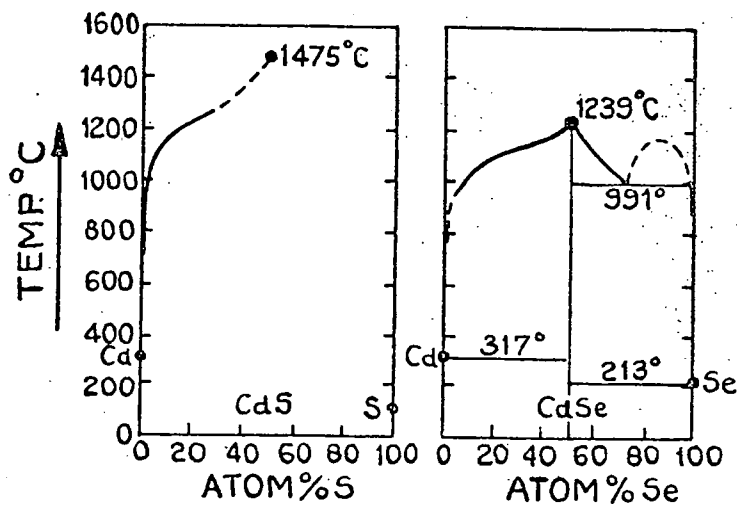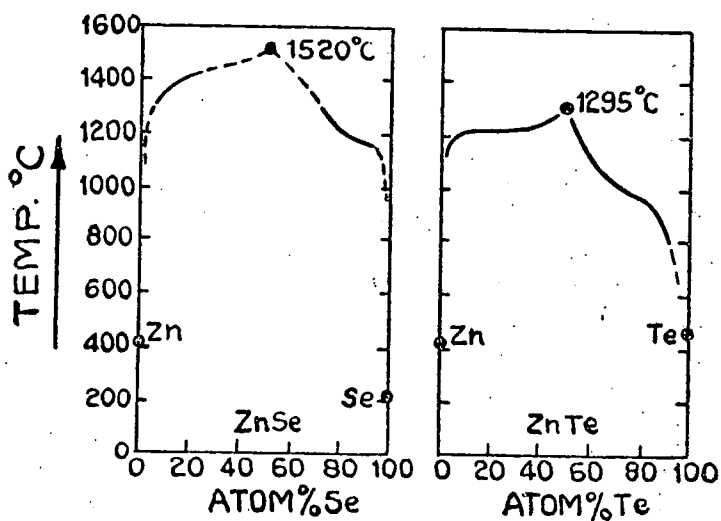
of tellurides) leaving a concentration gradient in the melt. As high overpressures are applied, bubbles do not form, but constitutional supercooling and cellular growth may do so. This phenomenon is likely when any II-VI compound is grown from the melt, because the melt can easily have a composition outside the narrow existence region of the solid. This difficulty could be overcome by using Fischer's method and applying a suitable partial pressure of one element to keep the melt stoichiometric. The temperature of the reservoir would have to be controlled very accurately.

Another promising piece of work was that of Rubenstein[19] who investigated the solubilities of various II-VI compounds in tin and bismuth. Several of the compounds were found to have useful solubilities which is particularly interesting because although these solubilities are only a little higher than those in the parent metal, higher temperatures can be used without exceeding a pressure of one atmosphere because tin does not boil until $2600^{\circ}$C. Rubenstein demonstrated the possibility of growing CdS by this method. A temperature difference of $500^{\circ}$C was maintained between the top and bottom of a tin bath with CdS floating on top. Platelets grew from the bottom of the bath. Epitaxial layers of ZnTe on ZnTe have been grown[20] by this method, and the growth of ZnSe layers on ZnTe will be described in this thesis. As tin is a group IV element it does not have a serious effect on the electronic properties of the material when incorporated as an impurity.

Another possibility is the growth of crystals in a gel. Very high crystalline quality with surprisingly high growth rates has been reported by Z. Blank et al[21].

The other general method that has found favour is growth from the vapour phase. While slower than melt growth the capital expenditure is less, making it particularly suitable for the small quantities of crystals required for research purposes.

Frerichs[2] used a horizontal, two-zone furnace to produce the first high purity crystals of CdS. Two separate streams of hydrogen carrier gas were passed down a silica tube within the furnace, and mixed in the hotter zone. One stream also contained $H_2S$, and the other carried cadmium vapour from a boat positioned in the cooler of the two zones. The following reaction occurred in the hot zone:

$$Cd + H_2S \longrightarrow CdS\downarrow + H_2$$

CdS crystals grew from the walls of the silica glass reaction tube. Many modifications of the technique have been used and CdS, CdSe, CdTe, ZnSe and ZnS have all been grown in a similar manner. Preformed compounds and a single flow of inert gas are often used. Kremheller[22] used a cold finger to encourage the precipitation of ZnS, while Fochs and Lunn[23] have studied extensively the growth of CdS needles and plates on various nucleation sites. ZnTe grown by this technique in our research group quickly coalesced to form polycrystalline lumps rather than discrete single crystals.

Reynolds and Czyzack[24] used a method later modified by Green[25] to grow large single crystal boules from the vapour phase. A charge of the preformed compound was placed in a quartz tube in the centre of a symmetrical temperature gradient. The quartz tube was not sealed but the compound was protected from the atmosphere by a mullite muffle containing argon or non-metal hydride. The charge sublimed to form a crystal at each end of the quartz tube.

Piper and Polich[26] modified this technique to produce very good single crystals. In their arrangement a quartz ampoule with a conical growth tip and a heat sink was employed. At the other end of the capsule a charge of sintered compound was closely backed by a tightly fitting quartz tube, and the whole was pro= tected by a mullite tube containing an argon atmosphere.

The growth tip was positioned at the centre of the furnace and the mullite envelope evacuated and baked at $500^{\circ}C$ to remove volatile impurities. Argon was admitted at atmospheric pressure, and the furnace raised to the growth temperature. The mullite tube was pushed towards the cool zone at between 0.3 and 1.5 mm $hr^{-1}$. Often a single seed predominated and a single crystal boule grew. CdS, ZnS and ZnSe have all been grown by this technique. Numerous modifications have been suggested, most of which have been concerned with sealing the capsule under vacuum after baking, and pulling the capsule vertically instead of horizontally. See for example Ref. 27.

A number of experimenters have endeavoured to control the stoichiometry of the charge at the growing crystal. Lunn[28] accomplished this by utilising a Knudsen hole in the capsule, and Woods and Clark[29], and Fochs et al[30] did so by connecting the capsule to a reservoir of one of the constituent elements held at a known temperature.

A final variation of the vapour transport technique is the chemical vapour transport method. Kaldis[31], Nitsche[32] and Schaeffer[33] have developed this technique extensively using a variety of transport agents. The two-six compound is sealed in a quartz tube with a small quantity of transporting agent which might be iodine. The method depends on the principle of a chemical

reaction occurring at one temperature and being reversed at another, releasing the transport agent again.

e.g.
$$2ZnSe \; + \; 2I_2 \; \overset{HOT}{\underset{COLD}{\rightleftharpoons}} \; 2ZnI_2 \; + \; Se_2$$

SOLID      GAS      COLD
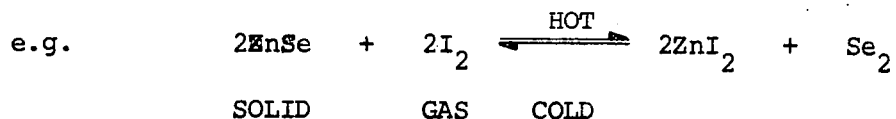
In practice the two ends of the growth tube are held at different temperatures;  at the hot end, the reaction proceeds left to right transporting ZnSe as $ZnI_2$ and $Se_2$ which have much higher vapour pressures than ZnSe.  At the cold end, solid ZnSe is deposited and $I_2$ is freed to diffuse back to the source and recycle.  There is a relationship between total pressure in the capsule and temperature for optimising the transport rate for each reaction.  J.H.E. Jeffes has discussed this in a review paper[34].

# CHAPTER 1

## REFERENCES

1. B Ray (1969) II-VI Compounds (Pergamon-London) p.54

2. R Frerichs (1947) Phys. Rev. 72 594

3. M R Lorenz (1967) Physics and Chemistry of II-VI Compounds
   ed. M Aven and J S Prener (Amsterdam: North Holland) 86

4. D De Nobel (1959) Philips Research Reports 14 361-430

5. Y Tsujimoto, Y Onodern and M Fukai (1966) Jap. J. Appl. Phys.
   5 636

6. A G Fischer (1966) Investigation of Carrier Injection Electro-
   luminescence, Contract No. AF(604) 8018 USAF Cambridge
   Research Laboratories Bedford Massachusetts

7. W Wardinski (1961) Proc. Roy. Soc. A260 370-378

8. W C Holton et al (1970) J. Cryst. Growth 6 97-100

9. A G Fischer, J N Carides and J Dresner (1964) Sol. St. Comm.
   2 157-9

10. M Inove, I Teramoto and S Takamagi (1962) J. Appl. Phys. 33
    2578-82

11. H J McSkinnon and D G Thomas (1962) J. Appl. Phys. 33 56-59

12. S Yamada (1960) J. Phys. Soc. Japan 15 1940-4

13. E P A Metz, R C Millar and R Mazelsky (1962) J. Appl. Phys. 33 2016-17

14. J B Mullin, B W Straughan and W S Brickell (1965) J. Phys.
    and Chem. of Sol. 26 782-4

15. S G Parker and J E Pinnel (1968) J. Cryst. Growth 480-495

16. M R Lorenz (1967) Phys. and Chem. of II-VI Compounds,
    ed. M Aven and J-S Prener (Amsterdam: North Holland) 85

17.  J Steininger and R E England (1968) Trans. Metallurgical Soc. of A.I.M.E. 242 p.444-448

18.  H Kimura and H Komiya (1973) J. Cryst. Growth 20 p.283-291

19.  M Rubenstein (1968) J. Cryst. Growth 3,4 p.309-312

20.  R Widner et al (1970) J. Cryst. Growth 6 p.237-240

21.  Z Blank et al (1972) J. Cryst. Growth 11 p.255-259

22.  A Kremheller (1955) Sylv. Techno. 8 p.11

23.  P D Foch and B Lunn (1963) J. Appl. Phys. 34 p.1762-6

24.  D C Reynolds and S J Czyzak (1950) Phys. Rev. 79 p.543-544

25.  L C Greene, D C Reynolds, S J Czyzak and W M Baker (1958) J. Chem. Phys. 29 p.1375

26.  W W Piper and S J Polich (1961) J. Appl. Phys. 32 p.1278-1279

27.  B M Bulakh (1971) J. Cryst. Growth 7 p.196-198

28.  B Lunn, W Freer and P Wright (1968) Report Min. of Technology Contract No. PD/119/04/AT

29.  J Woods and L Clark (1968) J. Cryst. Growth 3,4 p.127-130

30.  P D Fochs, W George and P D Augustus (1968) J. Cryst. Growth 3,4 p.112-125

31.  E Kaldis (1969) J. Cryst. Growth 5 p.376-390

32.  R Nitsche et al (1961) J. Phys. Chem. Sol. 21 p.119-205

33.  H Schafer (1964) Chem. Transport Reactions (Academic Press New York)

34.  J H E Jeffes (1968) J. Cryst. Growth 3,4 p.13-32

## CHAPTER 2

## MATERIAL PREPARATION

The original intention was to buy the materials used in this research as high purity compounds from chemical suppliers, but in practice only B.D.H. "Optran" cadmium sulphide proved satisfactory for crystal growth, and it became necessary to synthesize ZnSe, ZnTe and ZnS from the elements. A primary object was, therefore, to develop a method of producing these compounds in a form suitable for growing crystals from the vapour phase.

### 2.1 CdS

"Optran" CdS polycrystalline lump was purchased from B.D.H., and as a first step towards growing large crystals was sublimed in a flow of argon using the equipment shown in Fig. 2.1. The argon (B.O.C. 99.9995% argon) was passed over hot copper filings to remove any oxygen present, and then through a molecular sieve to extract water vapour, before being passed down the silica furnace tube at 200 ml/min.

After the furnace had been flushed with argon for one hour it was heated to 600°C to drive off volatile impurities from the charge. Six hours later the furnace temperature was increased to 1165°C for the sublimation. The process was controlled by a motor driven programmer, but was switched off manually, typically after 15 hours.

Most of the 50 gm charge was transported from the boat in the hot part of the tube and formed needles and platelets of CdS on the wall of the first liner. If good needles or plates were required for an experiment their growth was observed through the window and the furnace switched off at an appropriate time. The furnace was wound with Kanthal Al wire and was controlled by an Ether "Transitrol 990" switching a mercury relay. A temperature fluctuation of a few

# FLOW RUN TUBE. Fig. 2:1



1:5    1:

COMPRESSED AIR COOLING OF JOINT.

PYREX END CAP + WINDOW

ARGON OUT TO DUST TRAP. SILICONE OIL BUBBLE AND FUME CUPBOARD EXHAUST.

B40 CONE AND SOCKET

SPRINGS

WASTE COLLECTING LINER.

KANTHAL A1 WINDINGS.

CRYSTALS

SILICA LINER

SILICA BOAT CONTAINING SOURCE MATERIAL

CONTROL THERMO COUPLE 1165°C

O-RING SEAL SPEEDIVAC

SYNDANIO PLUG

ARGON

42

12

TEMP. °C

1200

900

600

300

0
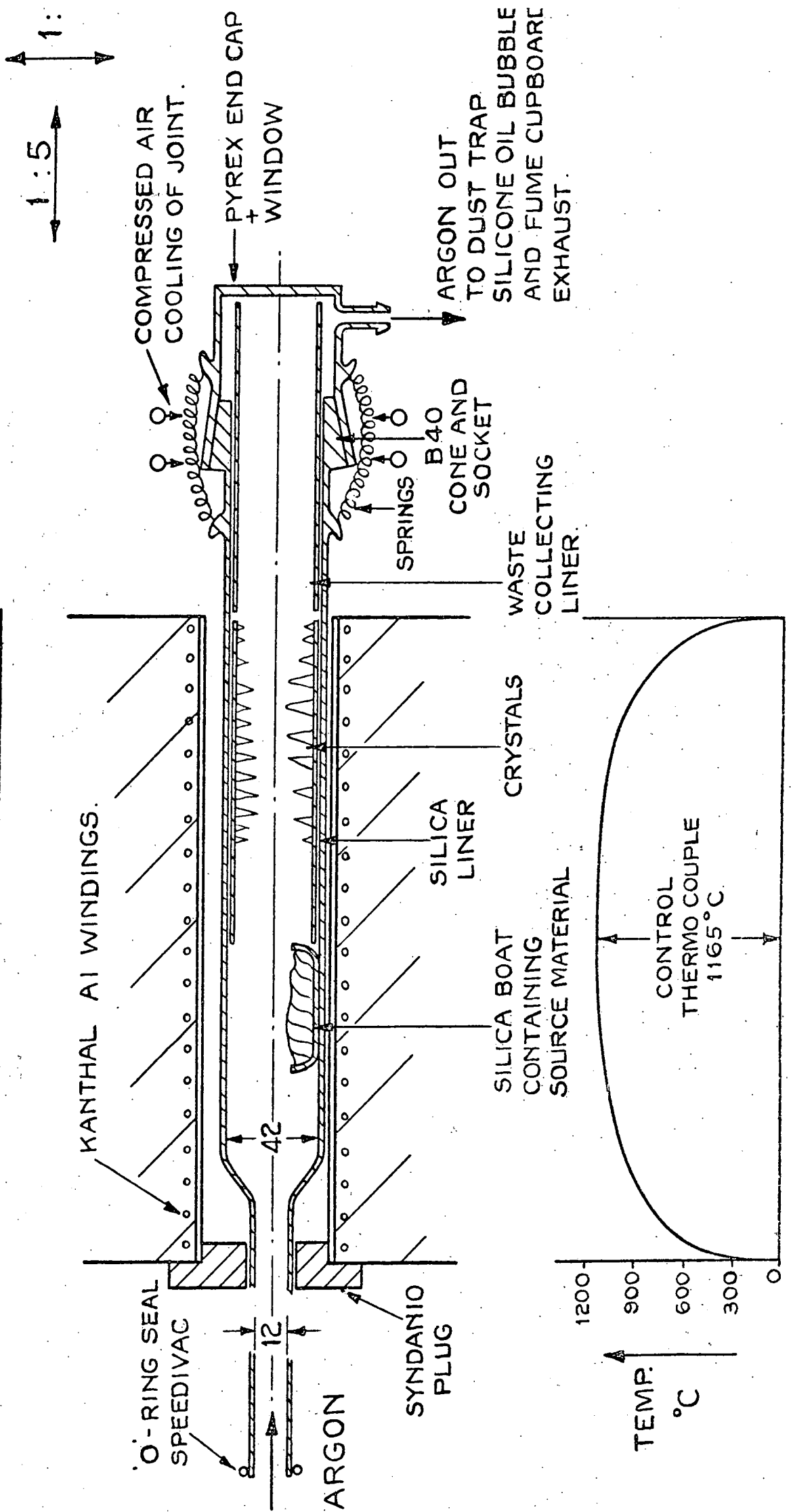
degrees was present, but did not affect the process noticeably.

To ensure the correct and reproducible assembly of the apparatus, all the components were made to a standard size, and were loaded with the liners, boat and pyrex cap touching. The second or 'dirt' liner was cleaned each time the apparatus was used. The 'dirt' consisted of volatile impurities and CdS dust that had failed to condense on the walls of the first liner. No attempt was made to clean the first liner, the loose CdS crystals were shaken off and the remaining layer left attached to the liner to absorb any impurities diffusing out of the silica. Impurities less volatile than CdS accumulated in the charge; consequently the small amount left in the boat was rejected.

## 2.2  Zinc Selenide

Zinc selenide was initially purchased from Derby Luminescents Ltd., and was found to contain quite a large percentage of zinc oxide. In an attempt to remove this, the material was sublimed under vacuum, but the product still required heating in excess zinc before it was suitable for the growth of large crystals. The technique used for purifying CdS was therefore adapted for zinc selenide, and 90 gms could be sublimed in one week using an argon flow of 350 ml/min and a temperature of $1160^{\circ}C$. This produced yellow-green plates and needles of very pleasing appearance, the plates had triangular growth features on one face and waves on the other, while the needles were of hexagonal cross section. Typically 1-5 gms of zinc oxide were left in the source boat, and the brown colour towards the ends of the boules grown from material purified in this way suggested the presence of oxygen.

A change to B.D.H. material improved this situation initially, but the quality of the material supplied declined, and later batches were found to contain several percent of carbon in the form of

hydrocarbons which decomposed on heating. This forced a further

change in the procedure, and led to the synthesis of ZnSe from the

elements which were purchased from Metals Research or from Koch-Light.

Consideration was first given to the direct combination of

zinc and selenium in a sealed quartz tube, but the results were

variable and several explosions occurred. As a result the synthesis

tube of Fig. 2.2 was developed. A similar technique was used by

W.C. Holton et al.[2]. Zinc selenide decomposes almost entirely into

zinc and selenium molecules in the vapour phase, so if a well mixed

vapour can be produced from separate sources of zinc and selenium, it

should be possible to produce solid zinc selenide by supersaturating

the vapour. The vapour phase reactor contained a separate source for

each element, from which the vapour was carried in two separate streams

of argon to the reaction zone where they merged. To obtain a satisfactory

yield, it proved necessary to close the end of the zinc tube except for

four small nozzles which produced jets of zinc vapour and broke up the

laminar flow in the reaction chamber. Before this was done a sheet of

solid zinc selenide formed between the two gas flows until they had

cooled sufficiently to precipitate zinc in elemental form again, this

resulted in a low yield.

Large amounts of zinc selenide dust were formed in the tube,

and sometimes needle crystals were found. These were often of mixed

hexagonal and cubic structure, as indicated by their birefringence,

Fig. 2.3.

The design of the reactor tube proved difficult to simplify.

A buttress end with teflon sealing ring was used to avoid greased end

caps and consequent risk of contamination. This also had the advantage

that the joint could not separate and leak zinc selenide or selenium

SILICA REACTION TUBE FOR SYNTHESIS OF ZnSe.

WATER COOLED DURALUMIN

GLASS WOOL

O-RING SE

O-RING SE

ARGON OUT

TO SILICON OIL TRAP AND NaOH BUBBLER.

TEFLON O'RING

BUTTRESS END

SILICA LINER IN SECTIONS

NOZZLES OR BELL END TO DESTROY LAMINA FLOW.

2-INDEPENDENT ARGON INLETS

O-RING SEALS

1:5

1:2

150

50

180

150

200

800

630

Se

Zn

ZnSe DEPOSITION ZONE

TEMP. °C

1000
800
600
400
200
0

FURNACE PROFILE.
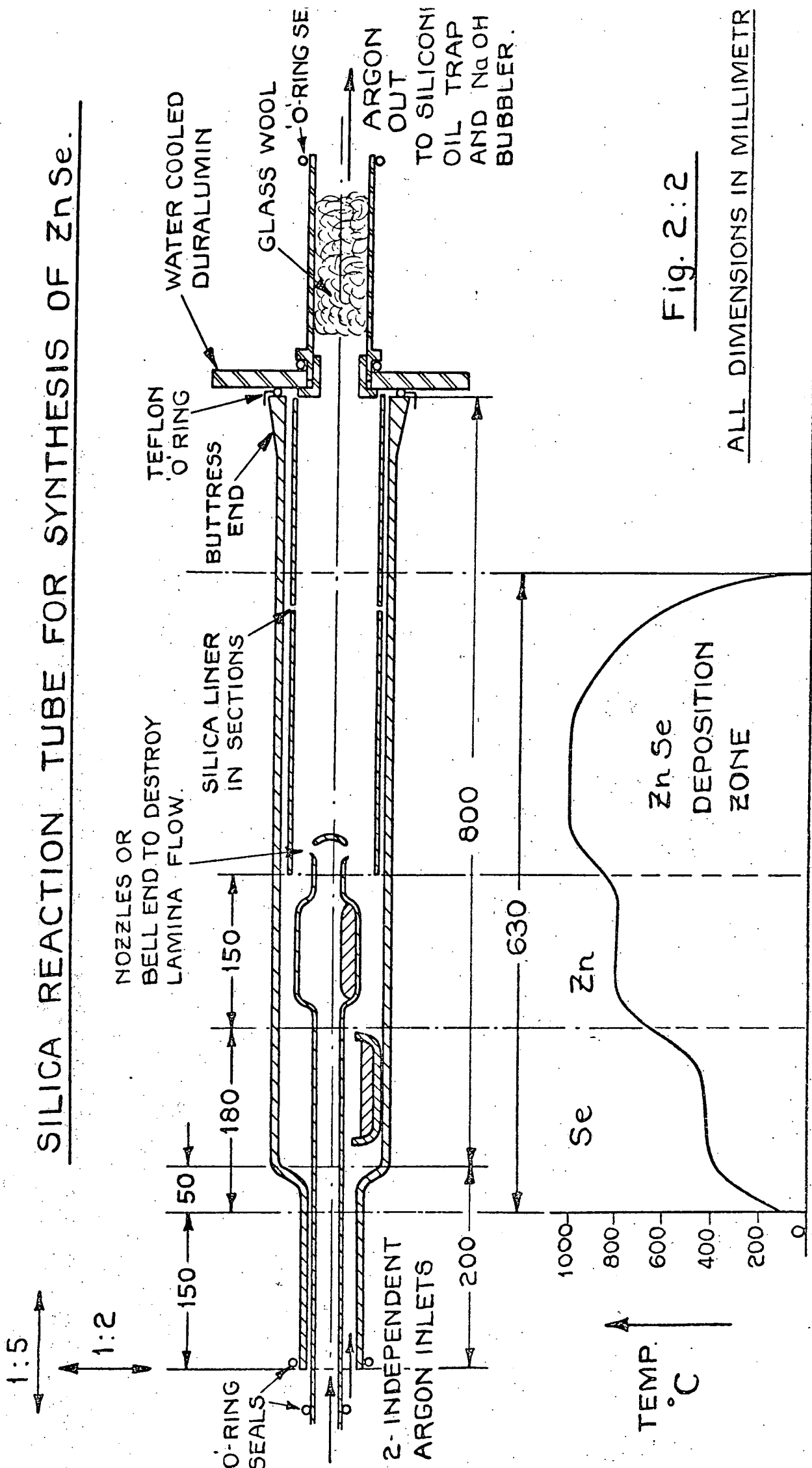
Fig. 2:2
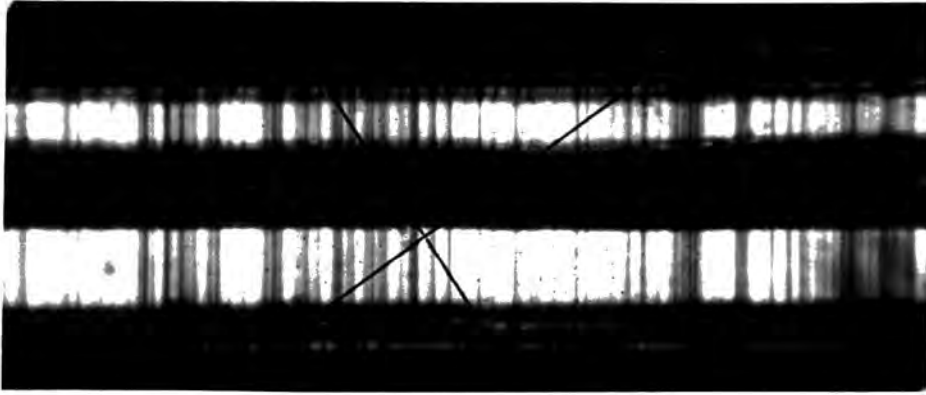
ALL DIMENSIONS IN MILLIMETR

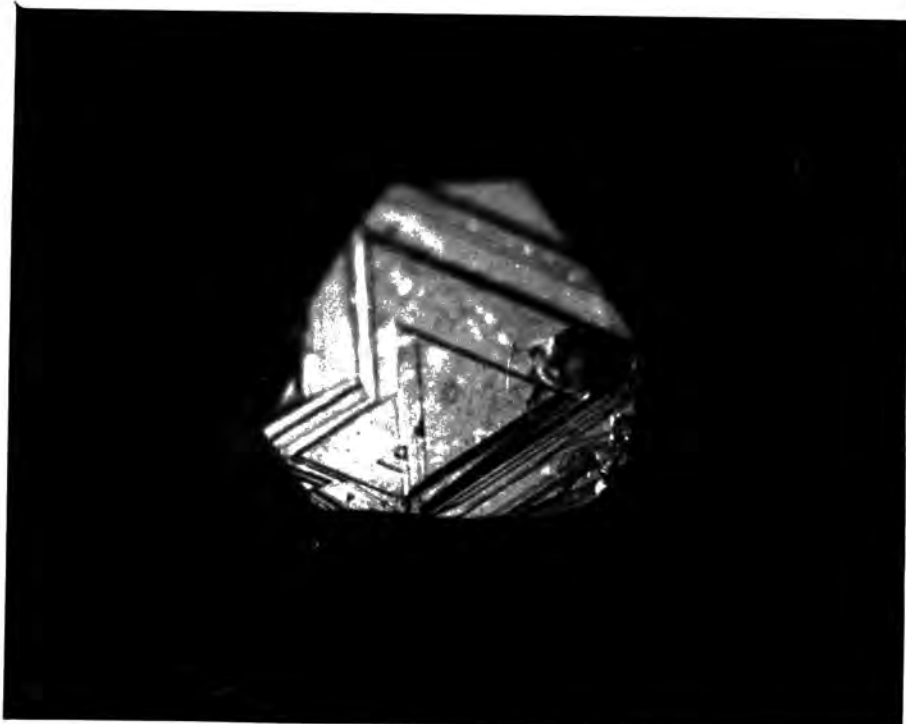Figure 2.3A:  Birefringent needle crystal.  (Magnification x 400)



Figure 2.3B:  Triangular growth features on typical flow

crystal.  (Magnification x 30)

dust into the atmosphere in the event of pressure building up because of a blockage in the outlet pipe. Zinc selenide dust was trapped at the outlet by a silica wool plug, which was replaced after each run.

The end plate was fabricated from two 3/16" duralumin plates screwed together with two 'O'-rings clamped between them to form a channel to permit water cooling, thus eliminating the possibility of the end plate being over-heated by the furnace. A 25 mm bore tube containing the silica wool plug conducted the waste gases away through a silicone oil bubbler and a sodium hydroxide trap, and finally to a fume cupboard extract duct. The viewing window of the cadmium sulphide tube design was discarded because it quickly became obscured by dust in this case, and the straight through design was free from blockages and allowed the filter to be changed quickly. Safety from selenides in the laboratory was provided by extracting acidic material in the caustic soda bubbler, while the silicone oil prevented back diffusion of water vapour into the system.

The material produced was often mixed with unreacted zinc and selenium and was, therefore, sublimed in an argon flow in a similar manner to the B.D.H. and Derby Luminescents Ltd. material. Because of the low density of the powder formed in the process a mass of 30 gms only could be loaded and this was sublimed in 48 hours. The optimum temperatures for the three zones were found by trial to be $400^{\circ}$C for the selenium, $710^{\circ}$C for the zinc and $1050^{\circ}$C for the combination zone, the relatively low temperature of the combination zone ensured a reasonable life for the expensive reaction tube. Each zone was controlled by a thyristor controller with a platinum/platinum 13% rhodium thermocouple placed between the silica reaction tube and the furnace tube. It is clear that the material in the boats must have been at a lower temperature than that registered by the thermocouples, but

nevertheless conditions were reproducible from run to run, and so

from the production point of view this was immaterial. As the partial

pressures of zinc and selenium were much higher than $P_{min}$ for zinc

selenide at $1050^\circ$C, powder and crystalline material formed along the

whole length of the reaction chamber.

The chief danger with the apparatus was that uncombined zinc

would form a pool at the cold end of the reaction chamber. Since molten

zinc wets silica this would cause the silica to crack on cooling.

To avoid any risk of this occurring, excess selenium was provided to

maintain a selenium rich vapour at all times. At first rather

variable results were obtained. The rate of sublimation of ZnSe in

vertical growth tubes is critically dependent on the quantity of

impurities present. Some batches of selenium charge were shown by atomic

absorption analysis to have significant (p.p.m. level) amounts of copper

present. Results were improved by obtaining 6N grade selenium, and

constructing a zone refiner for zinc bars.


## 2.3    Zinc Sulphide

A similar reactor to that used for zinc selenide was employed

to produce zinc sulphide from the elements. However, the super-

saturation in the growth chamber was several times greater than that

for ZnSe, so that all the zinc sulphide produced was in the form of

a fine white powder. During unloading, the powder was unavoidably

mixed with unreacted zinc and sulphur, which were subsequently removed

by heating to $1165^\circ$C in a flow of argon. No significant transport of

zinc sulphide occurred because of the low vapour pressure of the

material at that temperature. The optimum temperatures were found

experimentally to be: sulphur $300^\circ$C, zinc $750^\circ$C, and the reaction

zone $1050^\circ$C.

Further purification was provided for later batches by sublimation at diffusion pump pressure ($5 \times 10^{-6}$ torr) in a simple silica tube closed at one end. The product lined the tube in the entrance to the furnace and showed a gradient of colour on cooling to room temperature. White material was removed for use, while the darker coloured material was recycled.

## 2.4    Zinc Telluride

Because zinc and tellurium have similar vapour pressures it was possible to react the two quite safely in a sealed quartz tube. However, heating a mixture of the two melts was found to produce a small boundary layer of zinc telluride only and the remainder of the charge was left unreacted.

The technique adopted to overcome this difficulty was to use the three zone furnace employed for ZnSe and ZnS with a bent silica reaction tube, Fig. 2.4. The tube was evacuated to $10^{-6}$ torr and sealed. When heated each element was trapped at its own end of the tube and the two vapours met in the middle. Each end was controlled at $800^{\circ}C$ while the middle was $100^{\circ}C$ hotter to prevent condensation of the elements. After between 6 and 24 hours all the unreacted material accumulated at one end, and was cycled from end to end of the reaction tube by altering the end zone temperatures as appropriate.

When several cycles had been performed most of the material had reacted.

The method varies from the techniques of other workers. Fischer[2] reacted extruded bars of tellurium and zinc in close contact by igniting one end, while other workers have used autoclaves and Schaffer[3] has suggested an iodine transport technique.

ZnTe REACTION TUBE. Fig. 2:4



FIREBRICK EXPLOSION SHIELD.

FURNACE

Te

FIREBRICK SUPPORT.

Zn

TEMP. °C

900
800
600
400
200
0

1:5

1:2
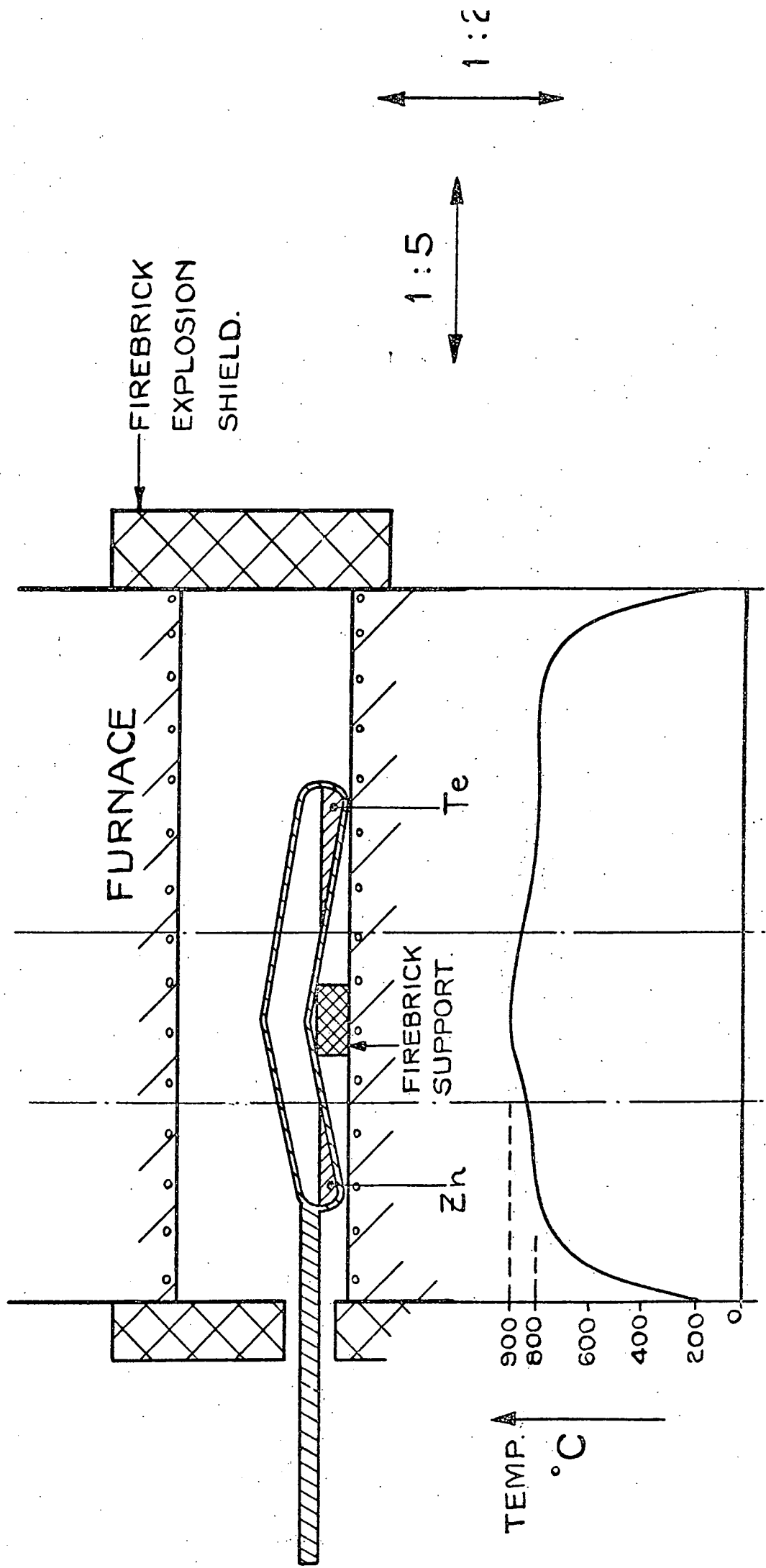
## CHAPTER  2

## REFERENCES

1.  W C Holton,  R K Watts  and  R D Stineford  (1969)  J. Cryst. Growth
    6  p.97-100

2.  A G Fischer  (1963)  Investigation of Carrier Injection Electro-
    luminescence,  Contract No. AF19(604)8018  U.S. Air Force Cambridge
    Research Laboratories  Bedford  Massachussetts

3.  M Schaefer  (1964)  Chemical Transport Reactions  Academic Press
    New York

CHAPTER 3

VERTICAL GROWTH SYSTEM

3.1   ZnSe

The vertical growth system described by Woods and Clark[1] was developed for use with zinc selenide.  Diagram 3.1.1 shows the arrangement of the furnace and crystal growth tube.  In this technique, a charge of preformed II-VI compound is sublimed under vacuum between the ends of a silica growth capsule.  The capsule is connected via a narrow orifice to a reservoir containing one of the components of the compound, which is held at a constant temperature to maintain a constant partial pressure of that component in the growth capsule.  Clark and Woods[1] found that the colour, conductivity and optical quality of CdS boules could be controlled by varying the temperature of the reservoir.

The first objective of the research into the growth of ZnSe was to develop the technique used for CdS into a reliable production method for ZnSe boules with centimetre dimensions for research purposes within the group.  A grain size of at least several millimetres was required, but single crystal boules were not a necessity.  Burr and Woods[2] reported growth of this technique in 1969, but in practice poor transport and frequent equipment failure resulted in an unreliable supply of material for research.  As noted in Chapter 2, the initial starting material used by Burr and Woods, namely vacuum sublimed Derby Luminescents Ltd. Electronic Grade ZnSe, was unsatisfactory.  It sometimes contained several percent of oxide as supplied, and consequently was vacuum sublimed to purify it.  A brown material resulted.  The material adhered strongly to the silica and later experience showed that sticking was associated with a high impurity content.  Before a

# VERTICAL GROWTH FURNACE.

## GROWTH TUBE IS IN STARTING POSITION.

CONTROL
THERMO COUPLE

1:2

1:5

1165°C

600

ZnSe

KANTHAL A1
WINDING

VERMICULITE
INSULATION

SYNDANIO

450

Zn OR Se

TAIL GUIDE

CONTROL
THERMO COUPLE.
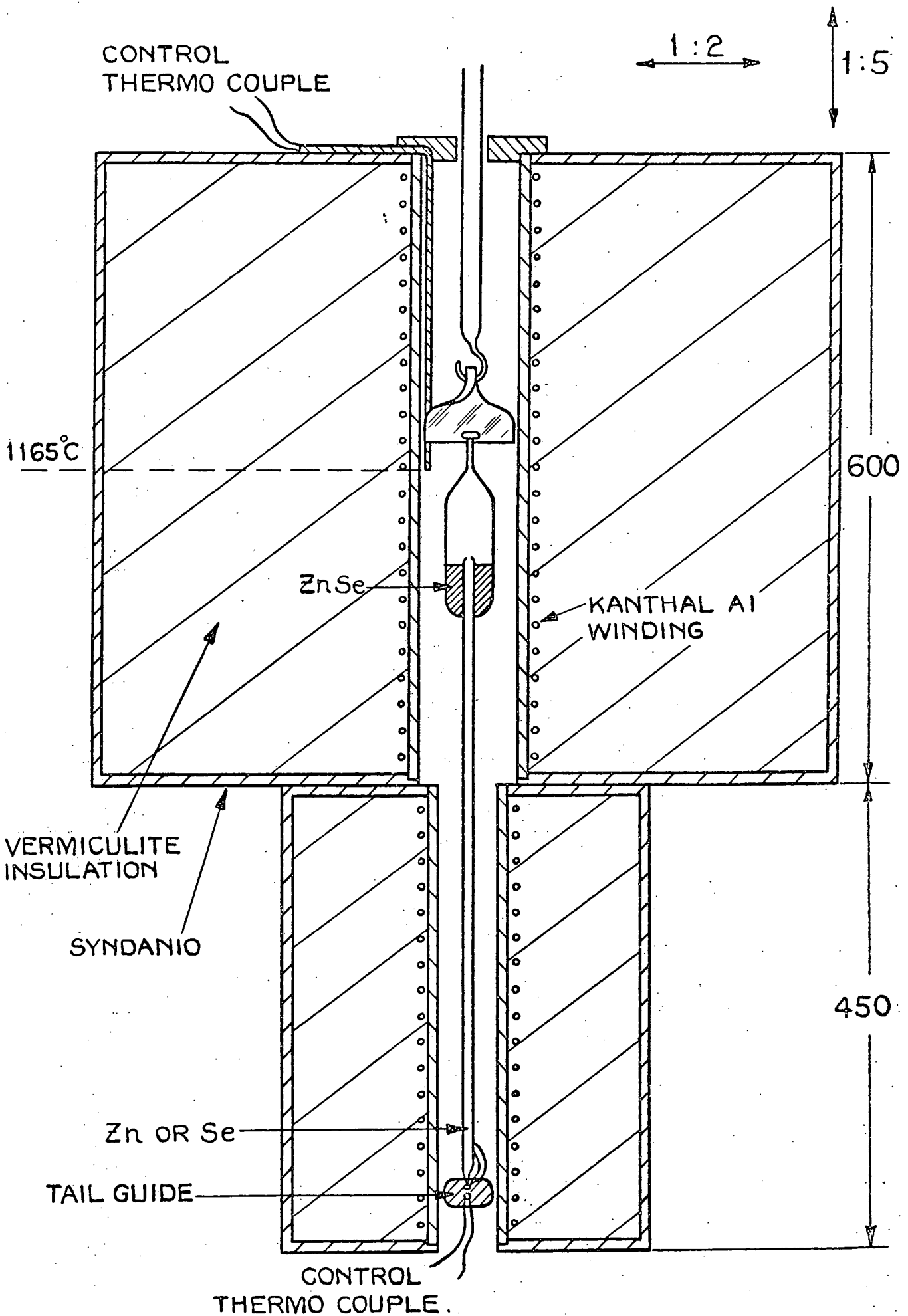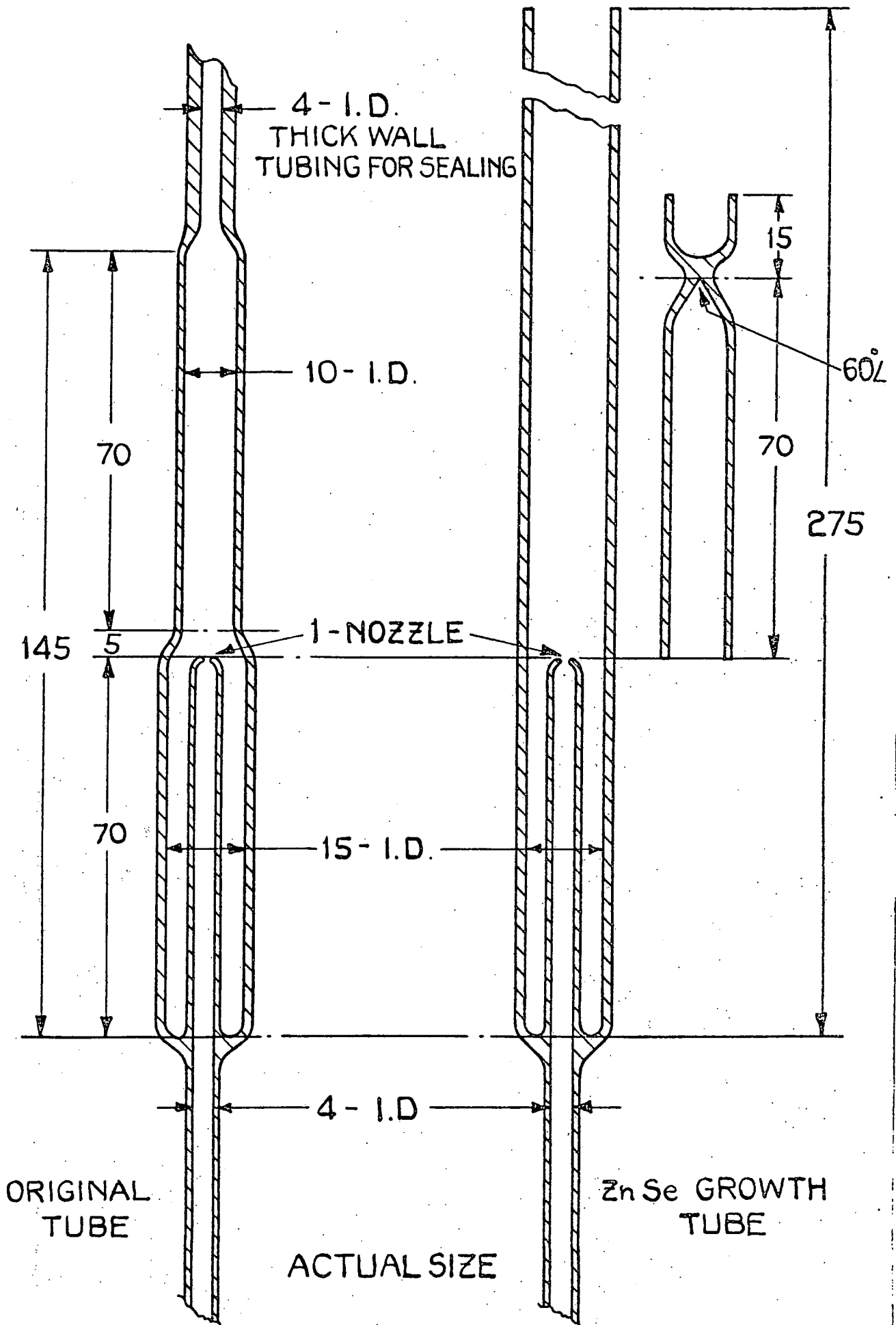
ALL DIMENSIONS IN MILLIMETRES.

crystal could be grown, it was necessary to heat the ZnSe with excess zinc in a crystal growth tube (Figure 3.1.2) for a period of several days at $1150^{\circ}$C. The material obtained was crushed and reloaded into a new crystal growth tube before any attempt was made to grow a crystal. As the growth tube was cooled after a run, it was frequently cracked by the ZnSe which stuck to it. Both the remaining charge and the ZnSe boule were oxidised as a result. Furthermore, selenium dioxide vapour escaped from the capsule to the laboratory and needle crystals of $SeO_2$ were found round the top of the mullite furnace tube and the pull rod. The fact that selenium compounds are poisonous provided an added incentive to cure the cracking problem. Other failures were the result of broken pull rods and furnace guides, the loss of tail thermocouples and furnaces burning out mid-way through a growth run.

A final cause of failure was the collapse of the silica glass capsule. The pressure over stoichiometric ZnSe at $1150^{\circ}$C is only 20 torr, and the unsupported capsule sometimes collapsed under the external atmospheric pressure. The weakest parts of the silica were those where the glass had been worked by a glassblower. Water vapour and other impurities are absorbed from the gas flame, rendering the glass softer, and more susceptible to devitrification. For example, the original guides failed very quickly at $1150^{\circ}$C because of the devitrification of the silica at the joint between the 3 mm rod and the 36 mm O.D. tubing. Such failures caused several growth tubes to drop out of the furnace and smash on the floor. A modified guide without any joints is shown in Figure 3.1.3B; it is produced by twisting a single plate of silica through $90^{\circ}$. The holes were made with an ultrasonic drill.

Pull rod failures were eliminated by replacing the devitrified end of each rod after 2 or 3 runs, but furnace failure was more

# ORIGINAL AND NEW GROWTH CAPSULES

Fig. 3:1:2

4 - I.D.
THICK WALL
TUBING FOR SEALING

15

70°

10 - I.D.

70

70

275

145

5

1 - NOZZLE

70

15 - I.D.

4 - I.D

ORIGINAL
TUBE

Zn Se GROWTH
TUBE

ACTUAL SIZE
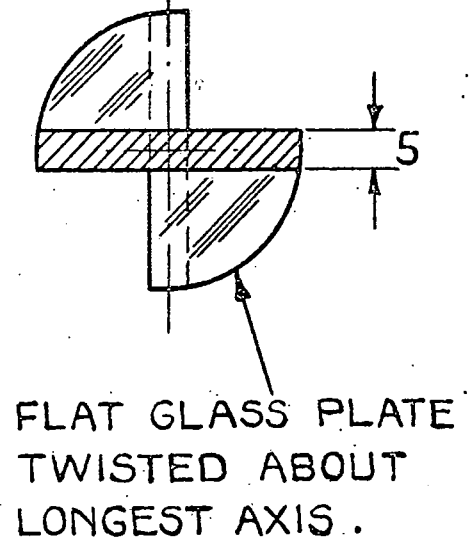
ALL DIMENSIONS IN MILLIMETRES

# MODIFIED FURNACE GUIDE

A   ORIGINAL

B   MODIFIED.



## A ORIGINAL

- 25
- 3-ROD
- 3-ROD
- 2-WALL
- 40
- 36-O.D. TUBE
- 25
- WEAK JOINT.

3-ROD

2-WALL

THERMO COUPLE CUT OUT.

ROD - TUBE JOINT DEVITRIFIED.

## B MODIFIED.

- 5
- 8
- 6-HOLE
- 25
- 70
- 20
- 6-HOLE
- 25
- 8
- 36

5

FLAT GLASS PLATE TWISTED ABOUT LONGEST AXIS.

ALL DIMENSIONS IN MILLIMETRES
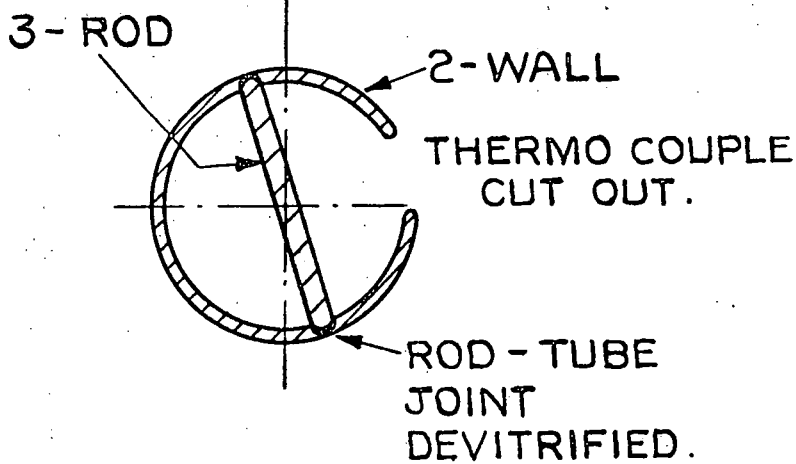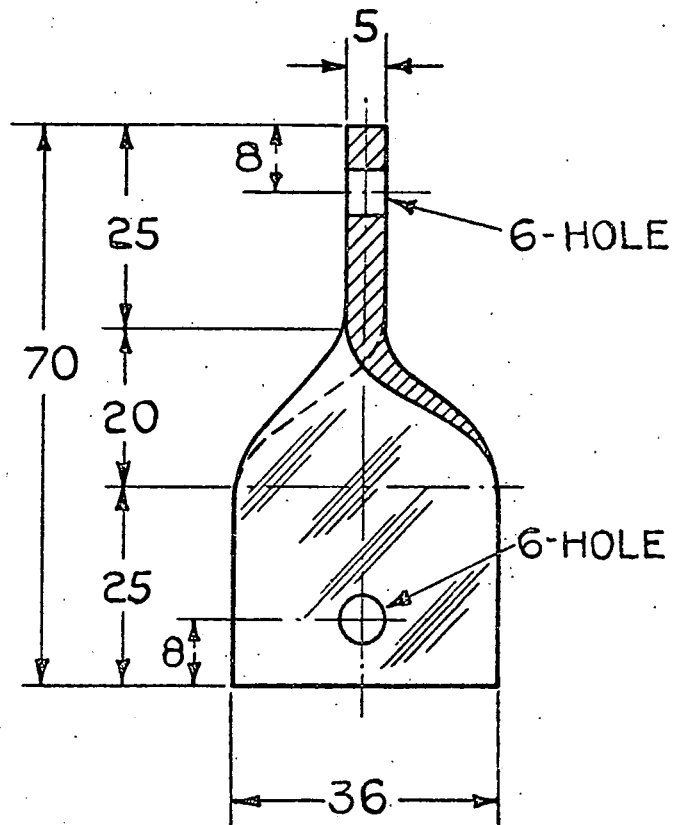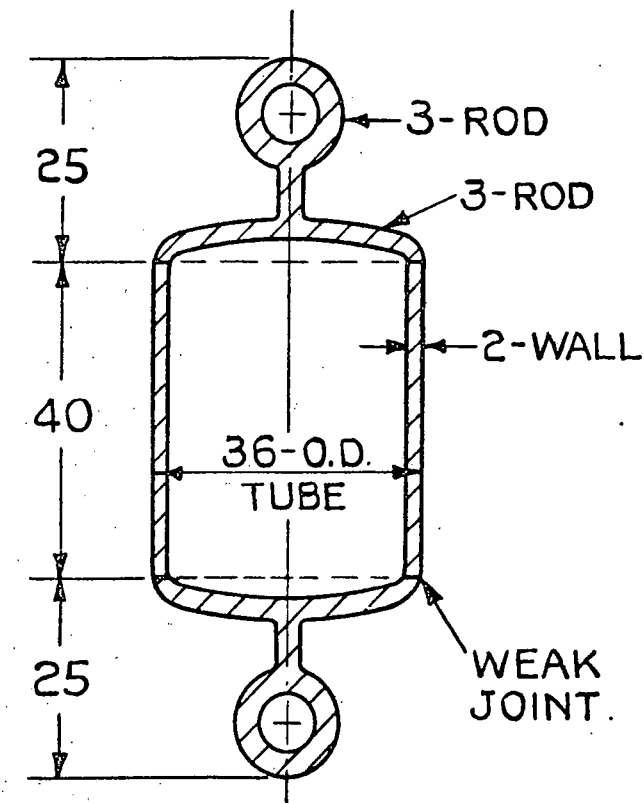
difficult to overcome. The top furnace was initially 38 mm internal diameter, and 680 mm long; later this was reduced to 32 mm internal diameter by 600 mm long to reduce the convection currents round the growth tube, and to increase the temperature gradient. The 32 mm tubes have a longer average life due to better insulation and smaller heat losses from convection inside the furnace tube. This would lower the element temperature slightly. However, the main factor was the compromise between the temperature required to grow a crystal, and furnace life. 1165$^{\circ}$C was the optimum temperature, it gave a reasonable furnace life (about four months at temperature) and was a little hotter than the minimum for the satisfactory growth of undoped boules (1150$^{\circ}$C). This gave a slight margin for error in the reservoir temperature and the effect of dopants and impurities.

Difficulties with the lower furnace stemmed from losing the thermocouple from the growth tube, which caused the furnace to heat up to its maximum temperature, and the sticking of the mechanical relays in Ether Mini temperature controllers. Appendix 1 shows a method of converting these controllers to 'Triac' switching. The thermocouples are now secured by threading them through the tail guide.

A modified growth tube was devised (Figure 3.1.2b) which had many advantages including:

1.      A large cross-section for evacuation.

2.      A large hole for loading the charge. This meant that the crushing of the charge could be reduced to a minimum.

3.      A double thickness of silica over the boule. This provided added resistance to collapse, and protected the boule from oxidation if the inner layer of silica cracked during cooling.

4.      The growth tip was reproducibly shaped, and could be altered

        as desired.

5.      A minimum of working was done on the silica.

6.      The length of the capsule could be altered at will.

The weakest point of the new growth tube was the joint between

the base of the capsule and the tail.

Before use the silica growth tube and growth tip were soaked in

aqua regia, washed in deionised water and methanol, and stored in a

drying cabinet.

Figure 3.1.4 shows the stages of loading a standard crystal

growth tube before putting it in the furnace. Usually, tubes were

prepared in batches of three. First the growth tube was attached to

an expanded section of silica, which terminated in a ground glass joint.

The tube was then evacuated, flushed with argon and baked out using a

gas torch to heat the tube. 0.5 gms of zinc or selenium were added to

the tail reservoir, which was then sealed and bent, Figure 3.1.4B. The

element was sublimed into the tail of the tube under vacuum. When the

tail had been resealed, the bent section of glass was discarded. To load

the 20 gm charge of slightly crushed ZnSe, the tube was removed from the

vacuum system, and the charge dropped in. A growth tip was placed in

the expanded section of tube, followed by a piece of soft iron encapsulated

in silica. The tubes were evacuated and flushed with argon several times,

before the tubes were finally pumped out overnight using a mercury

diffusion pump (Figure 3.1.4D). A growth tip was moved into position

using a magnet, and the tubes were sealed off at a pressure between

2 and 3 x $10^{-6}$ torr which was measured using an ionisation gauge,

Figure 3.1.4E.

# LOADING A CRYSTAL GROWTH TUBE.

## Fig. 3:1:4

1:2

1:4

### A

B.24

VACUUM

21-I.D

16-I.D

JOIN

15-I.D

200

125

275

70

HEAT

SEAL

HEAT
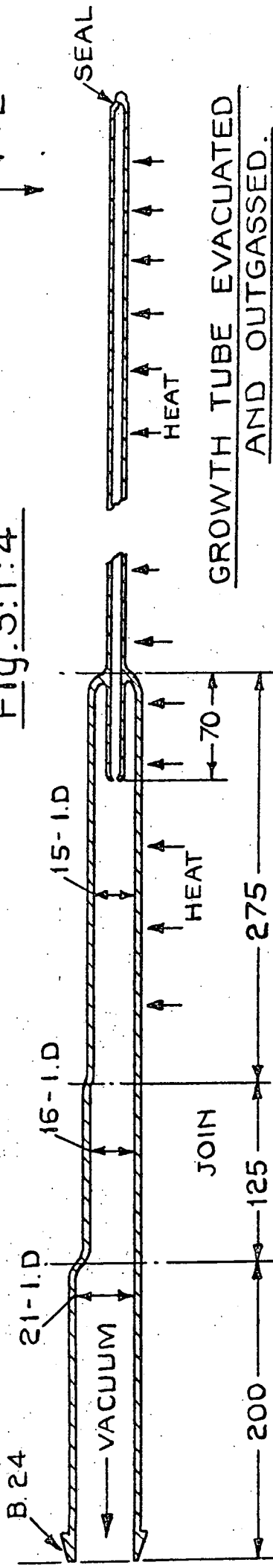
GROWTH TUBE EVACUATED
AND OUTGASSED.

### B

PELLETS OF
RESERVOIR
ELEMENT.

HEATED GENTLY

VACUUM
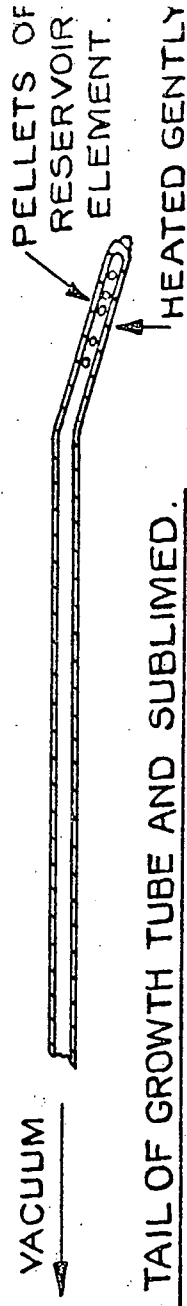
RESERVOIR ELEMENT LOADED INTO TAIL OF GROWTH TUBE AND SUBLIMED.

### C

TUBE RESEALED
END DISCARDED

ELEMENT

VACUUM

TUBE RESEALED.

### D

SOFT IRON
SEALED IN
SILICA

GROWTH TIP.

ZnSe
CHARGE
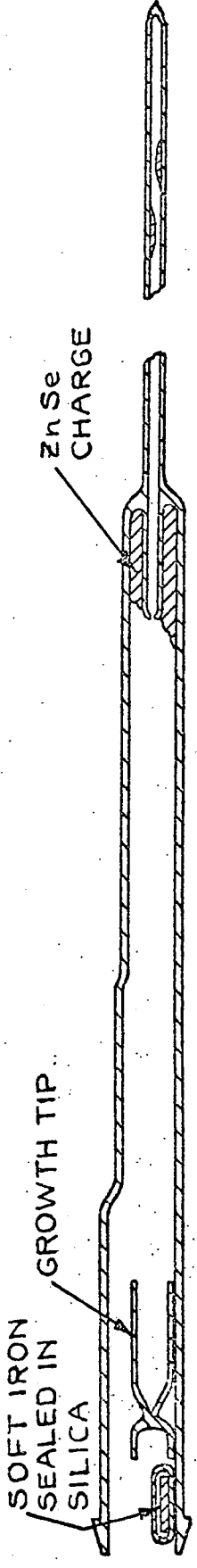
CHARGE AND GROWTH TIP LOADED. TUBE ARGON FLUSHED THREE
TIMES. AND EVACUATED.

ALL DIMENSIONS IN MILLIMETRES.

# Fig. 3:1:4 CONT.

FIRST SEAL HERE

VACUUM

MAGNET
USED TO MOVE
SOFT IRON
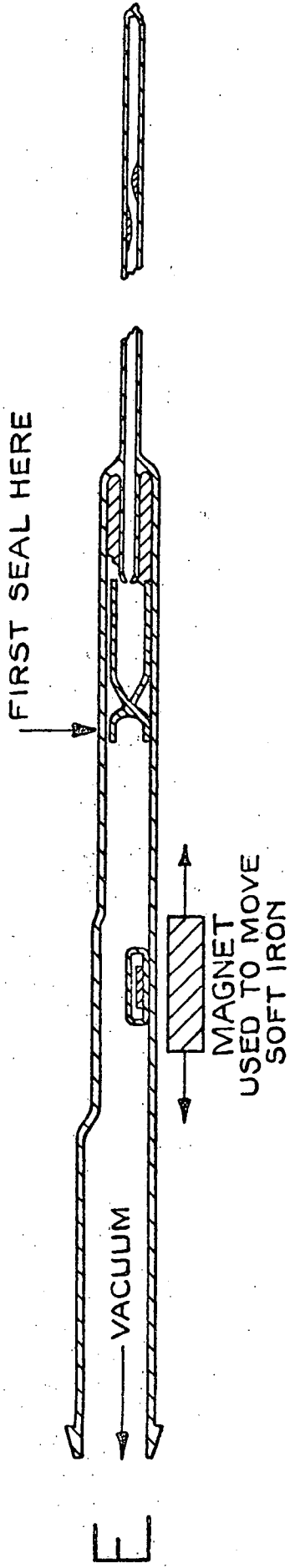
THE GROWTH TIP IS PUSHED INTO PLACE AND THE TUBE
SEALED OFF AT $10^{-6}$ TORR.

E

2 ND SEAL
OUTER TUBE COLLAPSED AND
SEALED ONTO INNER

TUBE COLLAPSED
AND HOOK ADDED.
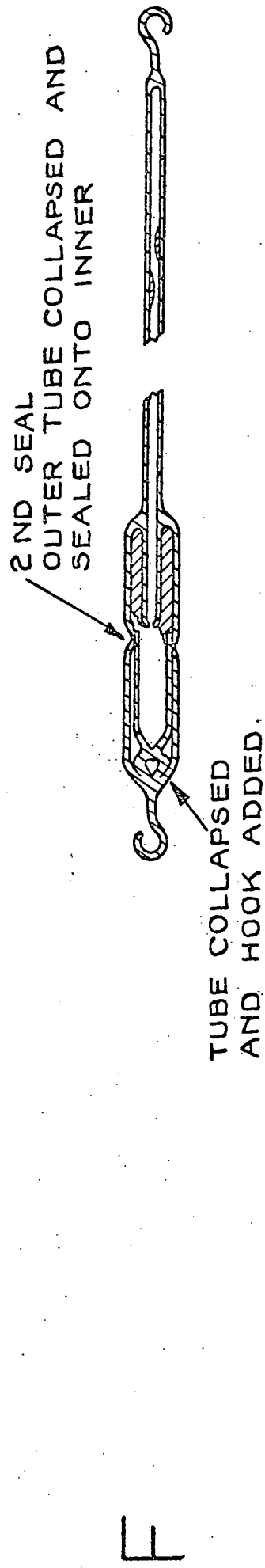
THE FINISHED GROWTH TUBE IS SEALED AT THE BOTTOM OF THE GROWTH
TIP AND HAS A HOOK AT EACH END.

F

Finally, the tubes were removed from the vacuum system, the growth tube collapsed on to the bottom end of the silica growth tip and a hook was added at either end of the tube.

The tubes were then ready for loading into the furnaces. Each tube was positioned so that its growth tip was at the centre of the furnace. The power and the pull were then turned on. Two rates of pull were available, 0.1 and 0.2 mms/hr. Initially the growth tip was in the hottest part of the furnace, and material transported towards the base of the capsule. In this way the charge was compacted and any ZnSe dust was removed from the growth tip. This reduced the number of nucleating centres in the capsule. As the tube was pulled through the furnace (see Figure 3.1.1) the charge became hotter than the growth tip and a boule grew from the tip of the capsule. Using flow crystals and a reservoir temperature calculated to give $P_{MIN}$ conditions inside the capsule, ZnSe boules 3 cms long by 1.1 cms diameter were grown reproducibly. The boules had convex bases, and a good greenish colour. Twin bands could be seen running across a boule. Boules grown from Derby Luminescents Ltd. material frequently had a brown appearance in the last few millimetres grown. The material as purchased from the manufacturer had a high oxide content, and the brown colour may well be attributable to oxygen.

At first an attempt was made to transport only two-thirds of the charge, and to obtain purification of the boule by leaving most of the impurities in the residue of the charge. In practice it was found that some of the tubes cracked round the base of the growth chamber when the boules were cooled, a weak point noted above. This cracking was caused by the remnants of the charge sticking to the silica. To avoid this difficulty the charge was transported completely and the bottom

section of the boules were discarded. Occasionally a boule stuck to the silica growth tip and cracked it on cooling. This did not matter as the outer layer of silica protected the boule from the atmosphere. These problems were reduced when higher purity material from B.D.H. Ltd. became available.

The boules were usually cooled over a period of 80 hours using a ramp function e.m.f. generator in series with the thermocouple.

Low resistivity zinc selenide was required for research into Schottky barrier light emitting diodes. Naturally it was desired to reduce the resistivity of the bulk material to as low a value as possible in order to avoid heating the crystal and losing efficiency. When the tail temperatures were altered away from those required to give $P_{MIN}$ conditions in the capsule, the resistivity of the undoped ZnSe boules remained high, $\sim 10^{12}$ $\Omega$cm. This contrasts strongly with the behaviour of CdS[1]. It was necessary to heat slices of 'as grown' material in liquid zinc to reduce their resistivity. This process has two effects; it produces a saturation concentration of selenium vacancies, and it removes compensating impurities such as copper and silver by solvent extraction.[3] In view of this, the use of a tail reservoir to control stoichiometry would appear superfluous, and the simple sealed capsule often used for CdS ought to have been adequate (see, for example, reference 4). This was tried without success; usually no transport was obtained, but following a vacuum bake at $800^{\circ}$C for six hours prior to sealing the tube a small amount of transport did occur. However, instead of growing a crystal in the tip of the capsule, the material was deposited in the form of tiny crystallites and dendritic spikes lower down on the wall. Figure 3.1.5 shows a typical result. A long tube extending to the cooler part of the furnace was added to the simple capsule (Figure 3.1.6),

Distillate consists of tiny crystallites at the top of the tube, and dendritic spikes in the middle.

The charge has annealed to a solid mass.

Figure 3.1.5:    An attempt to grow ZnSe in a Simple Sealed Capsule.

# EXPERIMENTAL GROWTH TUBE.

## Fig. 3:1:6

4 - I.D.

150

1 - I.D.
NOZZLE

FACETTED
CRYSTAL.

11 - I.D.

100

CHARGE
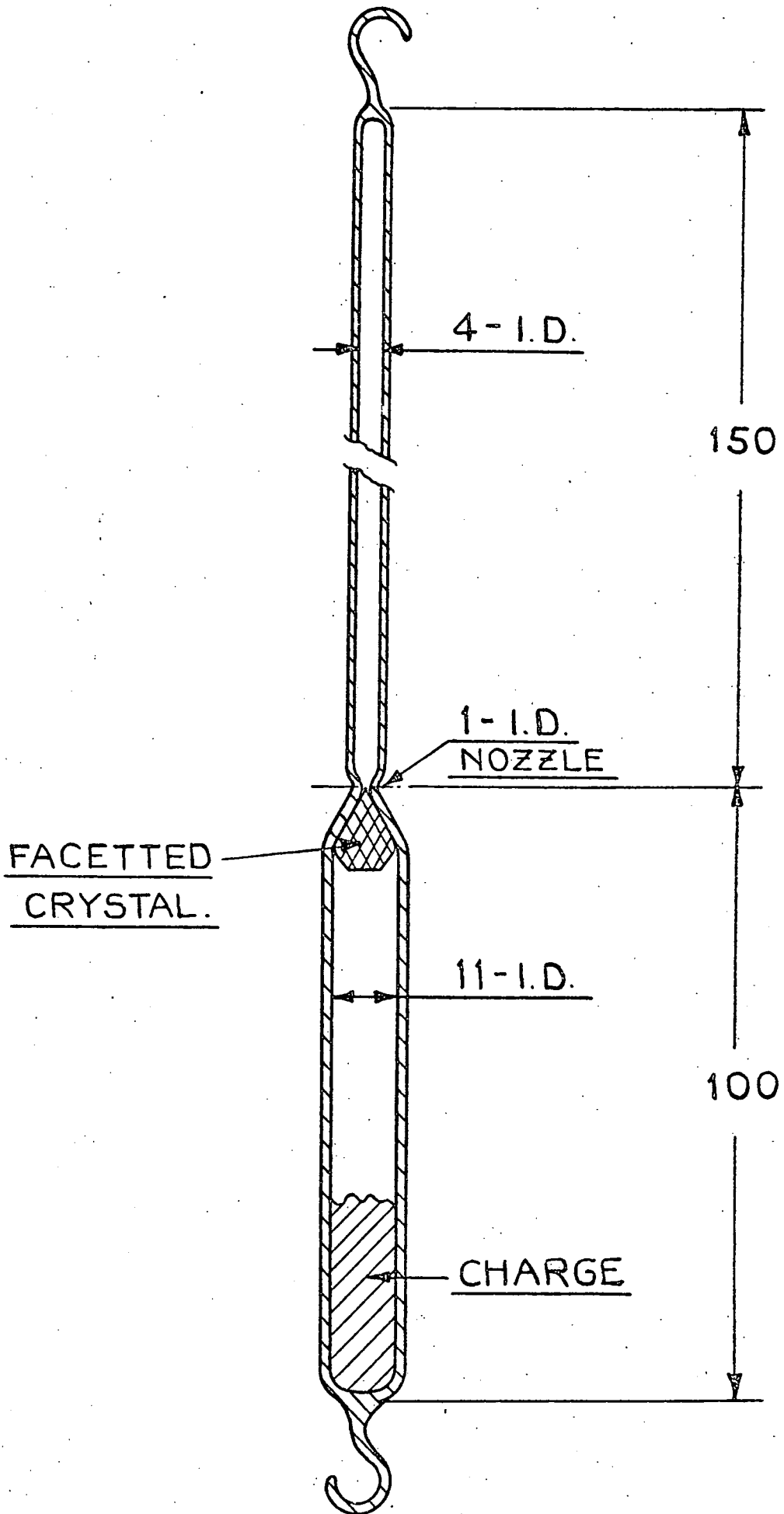
ACTUAL SIZE.     ALL DIMENSIONS IN MILLIMETRES.

and two crystals were grown. They grew rather slowly and were heavily facetted. As a production technique this method was unreliable in comparison with the reservoir system. However, it did prove useful in demonstrating a technique of producing thin films of ZnSe and the luminescent samples of Section 3.6.

## 3.2 Doped ZnSe

ZnSe boules doped with manganese chloride, chlorine, indium, gallium, copper, antimony, tellurium and erbium chloride have all been grown in the vertical system. Elemental indium, gallium, copper and tellurium were added to the charge and found to transport satisfactorily. Indium and gallium led to orange coloured boules, while copper reduced the transport significantly. Concentrations of the order 0.1 p.p.m. affect the luminescent properties[5] and heavy precipitates of copper were found in boules nominally containing 100 p.p.m. copper. An antimony doped crystal was grown to test the effect of this element on the growth and luminescence of zinc selenide. This was related to work involving the evaporation of zinc selenide on to glass coated with tin oxide, when a pressure of antimony was found to be helpful in maintaining the conductivity of the tin oxide. Tellurium doped crystals were dark in colour, with no unusual luminescent properties in the visible region.

Erbium chloride, zinc chloride and manganese chloride were added to the tail reservoir in the manner described for manganese chloride below. This arrangement allowed a constant partial pressure of the dopant compound to be maintained during the growth of the crystal. Tables 3.2.1, 2, 3, 4 summarize the experimental results for the growth of crystals doped with gallium, copper, antimony, indium and tellurium.

## INDIUM AND GALLIUM DOPED CRYSTALS

| Crystal No. | Dopant | | | Temperature °C | | Silica | Description of Boule |
|---|---|---|---|---|---|---|---|
| | Charge | Tail | Amount | Charge | Reservoir | | |
| 139 | In | Zn | D.F.C. | 1150 | 555 | Good | 3 cms, orange tapered |
| 140 | Ga | Zn | 1000p.p.m. | 1150 | 555 | Good | 3 cms, deep orange-brown |
| 142 | In | Zn | D.F.C. | 1150 | 555 | Good | 3 cms, orange |
| 150 | In | Zn | 100p.p.m. | 1150 | 555 | Good | 3 cms, orange |
| 154 | In | Zn | 1000p.p.m. | 1150 | 555 | Cracked | ½ cms, oxidised |
| 174 | In | Zn | 1000p.p.m. | 1175 | 555 | Cracked by boule | 3 cms, T.T. |
| 176 | Ga | Zn | 1000p.p.m. | 1175 | 555 | Good | 4 cms, Red |
| 180 | In | Se | 100p.p.m. | 1175 | 360 | Collapsed | ½ cm |
| 188 | Ga | Zn | 100p.p.m. | 1165 | 555 | Good | 3 cm, T.T. medium sherry |

D.F.C. = Doped flow crystal

T.T. = Total transport

Table 3.2.1

## Copper Doped Crystals

| No. | Dopant | Proportion WT. | Temperature °C | | Silica | Description of Boule |
| --- | --- | --- | --- | --- | --- | --- |
| | | | Charge | Reservoir (Zn) | | |
| 157 | CuSe | 1000p.p.m. | 1150 | 555 | Cracked | Green under heavy Oxide layer |
| 158 | CuSe | 1000p.p.m. | 1150 | 555 | Normal | Almost Black 1 cm. |
| 168 | Cu | 1000p.p.m. | 1150 | 555 | Cracked | Dark Green under Oxide |
| 169 | Cu | 1% | 1150 | 555 | Cracked | Bottom half dendritic Dark Green under Oxide. 3 cms. |

Crystal growth was somewhat inhibited by the copper, the growth tubes were cracked on cooling by the residue sticking to the silica. They failed where the tail joined the growth ampoule. The dopant was added to the ZnSe charge.

Table 3.2.2

## In/Manganese Doped Crystals

| Crystal No. | Dopant | | | Temperature °C | | Silica | Description of Boule |
|---|---|---|---|---|---|---|---|
| | Charge | Tail | Amount | Charge | Reservoir | | |
| 184 | In Mn | Zn Zn | 100p.p.m. 1% | 1175 | 555 | Good | T.T. Dark Yellow-Orange |
| 186 | In Mn | Se | 100p.p.m. 1% | 1175 | 360 | Cracked | 1.5 cms Oxidised |

Table   3.2.3

## Antimony and Tellurium Doped Crystals

| Crystal No. | Dopant | | | Temperature °C | | Silica | Description of Boule |
|---|---|---|---|---|---|---|---|
| | Charge | Tail | Amount | Charge | Tail | | |
| 192 | Te | | 1000p.p.m. | 1165 | | Cracked | 1 cm Surface oxidised. Green inside |
| | | Se | | | 365 | | |
| 206 | Te | | ½% | 1165 | | Good | 3 cms Brown-Green |
| | | Zn | | | 560 | | |
| 211 | Sb | | 1000p.p.m. | 1165 | | Good | Lime Green |
| | | Zn | | | 560 | | |

Table   3.2.4

For application in d.c. electroluminescent devices, samples with high conductivities are necessary to reduce the series resistance of a device. Some dopants increase the photoluminescent efficiency of ZnSe, and it was hoped to find a dopant that would simultaneously enhance the luminescence and the conductivity of samples. Gallium and indium were found to decrease the resistivity of the ZnSe boules from the usual undoped value of $10^{14} \, \Omega$ cm to about $3 \times 10^3 \, \Omega$ cm. One boule (139) lightly doped with indium had a conductivity of 2.0 $\text{ohm}^{-1} \, \text{cm}^{-1}$, and it is thought that this sample had a particularly low concentration of acceptor impurities. Atomic absorption analysis indicated that there was less than 50 p.p.m. indium in the boule. A more typical sample (152) had 100 p.p.m. in the boule, as determined by atomic absorption analysis, and a resistivity of $3 \times 10^3$ ohm cms. In practice, however, it was found that these dopants had little effect on the electroluminescence, and manganese was more efficient. To investigate the luminescence effects of manganese in a crystal, it was necessary to identify the characteristic luminescence associated with manganese and distinguish it from that associated with co-dopants. G. Jones[6] found that all the boules grown were slightly contaminated with copper and chlorine (less than 1 p.p.m.) and that photoluminescence bands due to these two impurities overlap in the red region of the spectrum and mask the manganese emission when samples are excited with U.V. (3656 angstroms) radiation . To obtain samples for comparison purposes, chlorine, water and copper doped samples were grown, together with highly doped boules of ZnSe:Mn (Section 3.3) and polycrystalline samples of ZnSe:Mn, $MnCl_2$ and Al (Section 3.6). G. Jones[6] investigated these samples rigorously, measuring excitation spectra to distinguish between different impurities,

and he eventually isolated the luminescence associated with each, see

Table 3.2.5. He showed that copper, but not the chlorine, could be

removed by leaching in liquid zinc. A substantial amount of indium and

gallium was precipitated when the samples were heated in liquid zinc,

but was redissolved when the crystals were heated in selenium or vacuum.

It is believed that this is due to the removal and replacement of compen-

sating acceptors in the form of impurities or zinc vacancies. Most of the

manganese remains in the lattice during the treatment in molten zinc,

but afterwards it is found that the characteristic photoluminescence of

manganese is quenched. Evidence that the manganese is still in the lattice

after the zinc treatment comes from the electroluminescence spectrum

(Figure 3.2.1) [9] in which the manganese peak was clearly present, and

from atomic absorption analysis of samples before and after treatment in

zinc. J. Allen [7] has explained the absence of photoluminescence after

leaching in zinc by suggesting that in semiconducting zinc selenide the

manganese ions are rapidly de-excited by giving up their energy to con-

duction electrons in an Auger type interaction. This cannot happen in

insulating material. In an electroluminescent device the useful manganese

ions are in the depletion region of the device close to the metal Schottky

contact, and so once again there are no conduction electrons available

to participate in Auger de-excitation processes.

| Emission Band | Dopant | Position of Emission Band Å | | Position of Excitation Band Å | |
|---|---|---|---|---|---|
| | | 293 K | 85 K | 293 K | 85 K |
| Copper – Red | Cu | 6480 | 6400 | 5350 | 5150 |
| Copper – Green | Cu | | 5300 | | 4440 |
| Copper – Green | Cu | | 5450 | | ≃ 4600 |
| | | | | | ≃ 4750 |
| S.A. | – | 6050 | 6150 | 4650 | 4480 |
| S.A. | Cl | 6050 | 6150 | 4700 | ≃ 4550 |
| | | | | 4950 | 4800 |
| S.A. | I | 6050 | 6150 | ≃ 4700 | ≃ 4600 |
| | | | | 5100 | 4890 |
| S.A. | Al | ≃ 6240 | 6360 | 4700 | ≃ 4550 |
| | | | | 4900 | 4800 |
| S.A. | In | ≃ 6200 | ≃ 6300 | | |
| Group III – Green | Al | | 5570 | | 4450 |
| Group III – Green | In | | 5600 | | 4530 |
| Group III – Green | Ga | | 5630 | | 4550 |
| Undoped – Green | – | | 5650 | | |
| Undoped – Green | – | | ≃ 5600 | | |
| Undoped – Green | – | | 5420 | | ≃ 4550 |
| | | | | | ≃ 4750 |
| Undoped – Green | | | 5350 | | |
| Undoped – Green | – | | 5300 | | 4480 |

Table 3.2.5:   Emission bands observed in Zinc Selenide

S.A. = Self Activated.

# THE SPECTRAL DISTRIBUTION OF THE E.L. EMISSION OF A Zn Se: Mn DIODE.
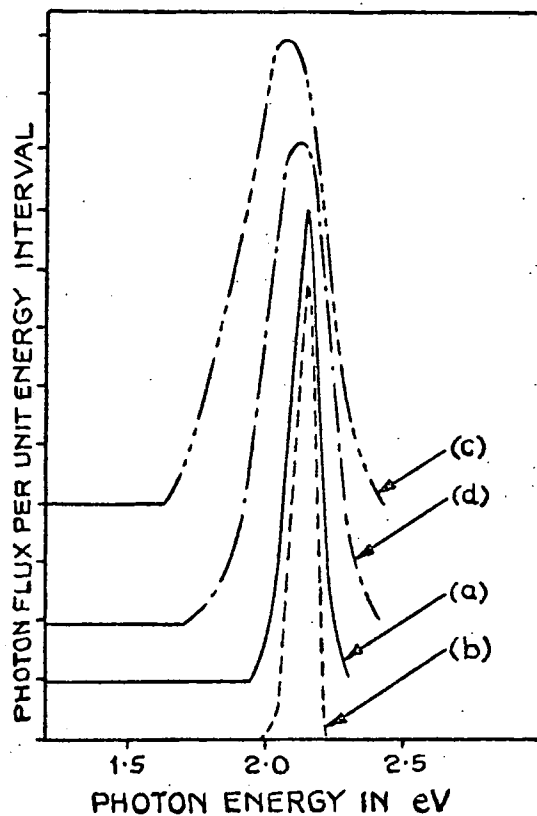
SPECTRAL DISTRIBUTION OF A Zn Se: Mn DIODE,
(a) ELECTROLUMINESCENCE IN REVERSE BIAS AT 290°K,
(b) ELECTROLUMINESCENCE IN REVERSE BIAS AT 18°K,
(c) PHOTOLUMINESCENCE AT 290°K EXCITED BY U.V. RADIATION,
(d) FORWARD EL AT 90°K.
    THE UNITS OF THE ORDINATES ARE ARBITRARY AND
    THE MAXIMA OF THE CURVES ARE DISPLACED TO
    REVEAL MORE EASILY THE SHAPES OF THE CURVES.

## 3.3    Manganese and Aluminium Doped ZnSe

Manganese doped samples were required for photo and electro-luminescence studies.    J Allen et al.[8] attributed efficient electro-luminescence in ZnSe to manganese doping.  The best L.E.D's. were reported to be fabricated from ZnSe:Mn:Al, in which the function of the aluminium was to increase the conductivity.

Manganese, however, proved more difficult to incorporate than the dopants mentioned above.  It has a low vapour pressure in the form of the element or the selenide, and it rapidly attacked any silica that it came into contact with.  To avoid excessive attack in any one section of the capsule, which would have led to a leak, the manganese and ZnSe were ground together to form an intimate mixture, from which a boule was grown in the usual way.  Manganese could not be detected in the resulting crystal using luminescence techniques, and very little was revealed by spark source mass spectroscopy.  Similar results were obtained with MnSe doping.  To grow manganese into the boules it was necessary to introduce manganese chloride, which has an appreciable vapour pressure, into the system.  In this way many doped boules were grown.  The most satisfactory technique was to sublime the chloride into the tail which contained the usual zinc.  Unfortunately, $MnCl_2$ is deliquescent, and undoubtedly some water was introduced at the same time.  To minimise the amount of water, the $MnCl_2$ was placed in a capsule which was con-tinuously pumped with a rotary vacuum pump, and gently warmed for several hours before being loaded as quickly as possible into the tail of a growth tube.  The chloride was heated gently under vacuum until it melted, and was then sublimed.  Nevertheless, growth tubes containing $MnCl_2$ had to be pumped individually instead of in batches of three, and a much longer time was required to reach the final vacuum, usually

$\sim 8 \times 10^{-6}$ torr. Recent tubes have been equipped with an extended tail and the manganese chloride has been sublimed twice. A wet cloth was used to cool the glass and induce the $MnCl_2$ to condense at the correct place. With this technique boules containing $\sim 200$ p.p.m. were readily obtained. Adding manganese powder to the charge increased the resultant concentration to $\sim 1000$ p.p.m. Samples from such boules (e.g. No.213) were fabricated into L.E.D's. with the highest brightness of any observed to date. Figure 3.3.1 shows a typical characteristic (Woods and Ozsan[9]). S. Gezci[10] observed the manganese absorption spectra in such a sample and was able to detect the zero phonon line at 5137.4 Å. Boules grown with manganese chloride in the tail only, appeared reasonably homogeneous when removed from the capsule, while those with additional manganese in the charge were less so. This is to be expected because the reservoir maintains a constant vapour pressure of the dopant.

Aluminium doped boules were also difficult to produce. The element reacts with silica to produce a white fluffy residue. As a result only small amounts were incorporated into the boule. Even when 1000 p.p.m. aluminium was loaded with the charge very little was transported, and that mainly into the last part of the boule to grow. Sometimes small pieces of ZnSe grew round the base of the growth tip.

When aluminium was added to the charge, the resultant boules were usually the standard green/yellow in colour, but contained very little aluminium, while small pieces round the base of the capsule were orange. These pieces contained aluminium at a concentration of around 20 p.p.m., and had a resistivity reduced from $\sim 10^{14}$ $\Omega$cms to $10^{10}$ $\Omega$cms. It is thought that the aluminium diffused into the wall of the capsule from the top of the charge, and then out again into the ZnSe as it grew on that part of the capsule.

# CHARACTERISTIC OF A TYPICAL
## Zn Se:Mn DIODE.

### Fig. 3:3:1
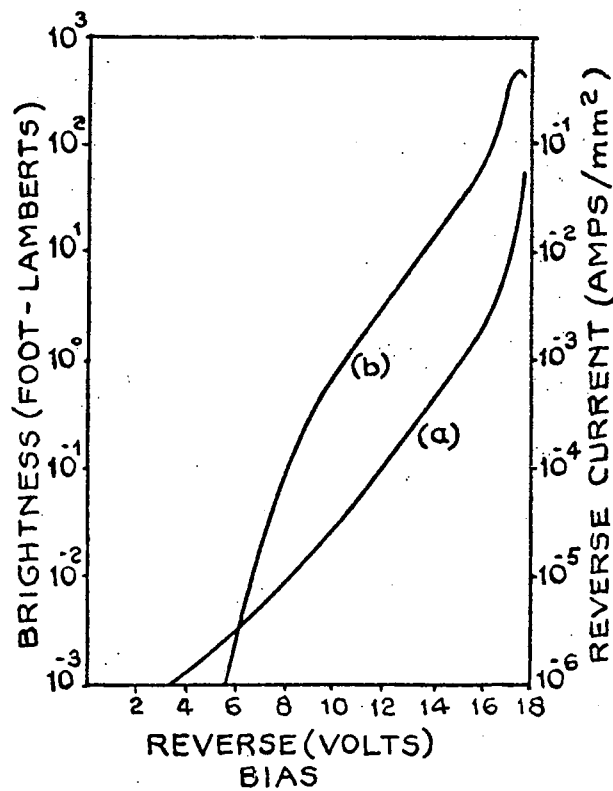


(a) CURRENT-VOLTAGE CHARACTERISTICS IN REVERSE
   BIAS FOR A Zn Se:Mn DIODE.
(b) LUMINANCE OF THE ELECTROLUMINESCENCE AS
   A FUNCTION OF BIAS VOLTAGE.

## 3.4    Crystallinity of Doped Boules

As the quantity of manganese in the boules was increased, the growth rate and quality declined; often a three or four centimetre boule would grow dendritically for the last 2 cms.  This should not necessarily be attributed to the manganese since chlorine ($ZnCl_2$) doped boules behaved similarly, although erbium chloride doped boules behaved much better.  Both $MnCl_2$ and $ZnCl_2$ are highly deliquescent and the trouble is probably due to water vapour in the system.  Figure 3.4.1 shows voids nucleating in a $ZnSe:MnCl_2$ crystal.  The boule was pulled at the slowest rate available (0.5 mm/hr) and was then held stationary in a temperature gradient for one week.  Facets formed indicating that a very slow pull rate should allow non-dendritic boules to be grown.  The photograph of the voids was taken through the facetted face of the crystal, which displayed triangular growth features indicating a $\{111\}$ Zn face, and many growth ridges.  The common facets found on ZnSe were $\{110\}$ and $\{111\}$ planes as identified by Laue back-reflection photographs.

The mechanism for the growth of chlorine doped boules is certainly different from that of the undoped boules.  Boules numbered 226 and 230 were grown with manganese chloride only in the tail  and no zinc so that the stoichiometry of the vapour was not controlled in the usual way.  Normally no growth would occur in these circumstances, because the pressure in the capsule would move well away from $P_{MIN}$.  The growth process must be at least in part a chlorine transport reaction, e.g.

$$2ZnSe \; + \; 2Cl_2 \; \underset{COLD}{\overset{HOT}{\rightleftharpoons}} \; 2ZnCl_2 \; + \; Se_2$$
$$\text{SOLID} \qquad \text{GAS} \qquad\qquad \text{GAS} \qquad \text{GAS}$$

The free chlorine may be released by a variety of reactions, but the most likely seems to be the simple dissociation of $MnCl_2$ to $MnCl + \frac{1}{2}Cl_2$

A. Triangular growth features on a facet. The dark
   spots are globules of selenium which sublimed from
   the tail reservoir as the crystal cooled (Mag. x 25)
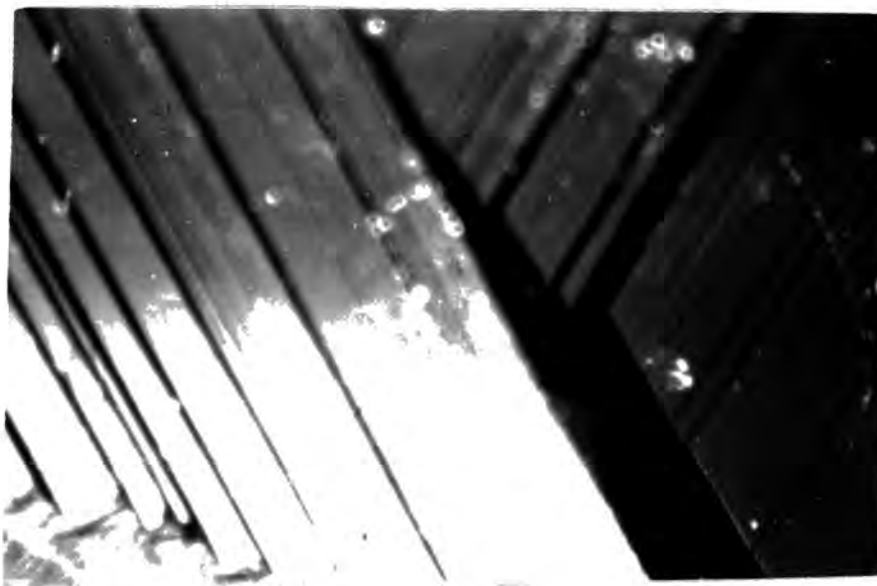


B. Detail of growth ridges    (Mag. x 50)

Figure 3.4.1:    Some Growth Features of a Manganese
                 Doped Boule
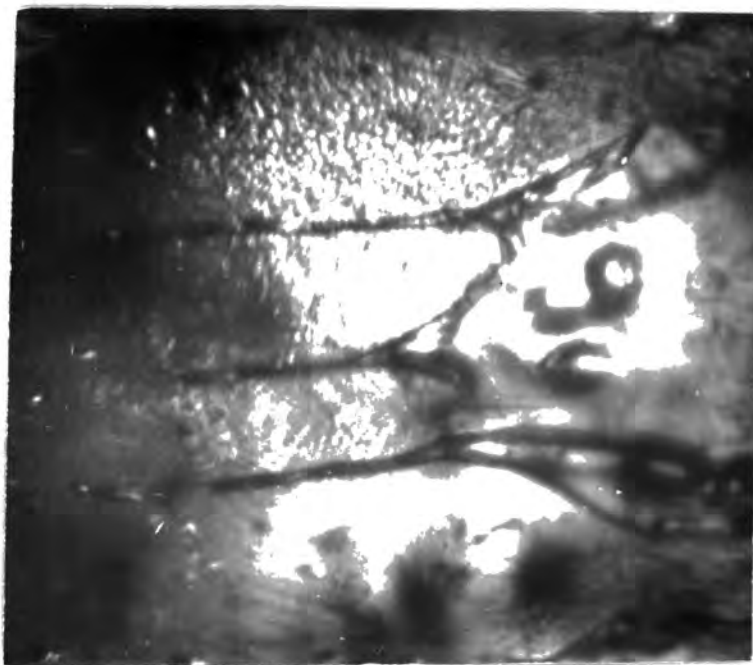
C. Nucleation of voids. Photograph taken through
   facet shown in 3.4.1A, growth direction left to
   right  (Mag. x 50)



D.  Detail of voids    (Mag. x 50)

Figure 3.4.1 (Continued)

Possibly some HCl is formed, this has been used as a transport

agent for ZnSe[11]. Further evidence for the chemical vapour transport

process is the large increase in the quantity of dopant incorporated

in the boule when Mn is added to the charge in addition to $MnCl_2$ in the

tail reservoir. Adding the chlorides of most recalcitrant dopants might

be expected to assist in doping ZnSe crystals, although chlorine will

be incorporated also, and cannot be removed by any known method. For

example, crystals doped with terbium chloride and erbium chloride grew

particularly well. In fact they grew better even than many manganese

chloride doped boules, because of the lower water content of the chloride

used, Figure 3.4.2. A summary of the crystals grown is given in

Tables 3.4.1 and 3.4.2.

3.5    Seeded Single Crystal Growth

The standard crystal growth tip was modified to accommodate a

flow crystal as a seed (Figure 3.5.1), and a differential thermocouple

was attached to the capsule with one junction close to the seed, and

the other against the charge. Flow platelets of appropriate size were

selected and inserted so that growth would take place either on the

{111} zinc face or the {$\overline{1}\overline{1}\overline{1}$} selenium face.

The growth tube was loaded into the furnace in the usual manner,

except that the midpoint of the capsule was located so as to be at the

hottest part of the furnace when full temperature was reached. When

the furnace attained the growth temperature the tube was lowered until

Figure 3.4.2:    An Erbium Chloride Doped

Boule of ZnSe

# ALUMINIUM, MANGANESE AND MANGANESE CHLORIDE DOPED BOULES

| Boule No. | Dopant | | | Temperature $^{\circ}$C | | Silica | Description of Boule |
|---|---|---|---|---|---|---|---|
| | Charge | Tail | Quantity | Charge | Reservoir | | |
| 141 | MnSe | Zn | 1000 p.p.m. | 1150 | 550 | White | 1 cm. Green Dendritic |
| 145 | MnSe Al | Zn | 1000 p.p.m. 1000 p.p.m. | 1150 | 555 | S.D. | 3 cm. Orange |
| 147 | Al | Zn | 1000 p.p.m. | 1150 | 555 | Normal | Good 2½ cms. White fluffy residue |
| 149 | Mn Al | Zn | 100 p.p.m. 1000 p.p.m. | 1150 | 555 | S.D. | 5 cms. |
| 153 | MnSe Al | Zn | 100 p.p.m. 1000 p.p.m. | 1150 | 555 | S.D. | 3 cms. Green White fluffy residue |
| 156 | MnSe | | 1% | 1200 | | Highly Devitrified | 1 cm. Very Dendritic |
| 160 | Mn | Zn | 1% | 1150 | 555 | Good | 4 cm. Yellow Residue Black Sponge |
| 161 | Al | | 1000 p.p.m. | 1200 | 570 | S.D. | 3 cms. Top Yellow-Green Bottom Orange |
| 162 | | $MnCl_2$ Zn | 1% | 1200 | 570 | Poor Collapsed | Small. Orange |
| 163 | $MnCl_2$ | Zn Zn | 1% | 1200 | 570 | Fair. Partly Collapsed | Small. Orange-Red |
| 165 | | $MnCl_2$ Zn | 1% | 1160 | | S.D. Growth Tip | 1.5 cms. Orange |
| 170 | | $MnCl_2$ Zn | ½% | 1150 | 555 | S.D. | 4 cms. Dendritic |
| 183 | | $MnCl_2$ Zn | | 1165 | 555 | S.D. Growth Tip | 1.5 cms. |
| 187 | Al | Zn | 1000 p.p.m. | 1165 | 555 | Normal | 2.5 cms. T.T. |

Table 3.4.1

Table 3.4.1 (Continued)

| Boule No. | Dopant | | | Temperature °C | | Silica | Description of Boule |
|---|---|---|---|---|---|---|---|
| | Charge | Tail | Quantity | Charge | Reservoir | | |
| 189 | MnSe Al | Se | 1% 1000 p.p.m. | 1165 | 365 | Normal | 3 cm. Green |
| 190 | Zn | MnCl$_2$ Zn | | 1165 | 560 | S.D. | 4 cms. |
| 195 | | MnCl$_2$ Zn | 2½% | 1165 | 560 | S.D. | 2 cms. |
| 200 | | MnCl$_2$ Zn | | 1165 | 460 | S.D. | 3 cms. Orange |
| 202 | | MnCl$_2$ Zn | | 1165 | 680 | Cracked on cooling | 0.3 mm.Orange |
| 204 | | MnCl$_2$ Zn | | 1180 | 360 | Normal | 3 cms. Orange |
| 209 | | MnCl$_2$ Se | | 1165 | 360 | Normal | Small Red. Poor |
| 226 | Mn | MnCl$_2$ | | 1160 | 560 | Normal | 1 cms. Dendritic |
| 230 | Mn | MnCl$_2$ | | 1160 | | Attacked by contact with Mn. | Orange. Dendritic |
| 246 | Mn | MnCl$_2$ Zn | 1000 p.p.m. | 1160 | 560 | Cracked Devitrified | 1 cm. Orange |
| 247 | Al | Zn | 1% | | | S.D. | Red T.T. |
| 252 | Mn | MnCl$_2$ Zn | 1000 p.p.m. | 1165 | 600 | S.D. at Base | 3 cms. Red. |
| 304 | Mn | MnCl$_2$ (D.S.) | 1500 p.p.m. | 1165 | 600 | | 2.75 cms. Orange |

S.D. = Slightly devitrified

T.T. = Total transport

D.S. = Double sublimed

CHLORINE and $H_2O$ DOPED BOULES

| Boule No. | Dopant | | | Temperature °C | | Silica | Description of Boule. |
|---|---|---|---|---|---|---|---|
| | Charge | Tail | Quantity | Charge | Reservoir | | |
| 122 | $ZnCl_2$ | Zn | | 1150 | 555 | | Small Red Crystallites |
| 123 | $ZnCl_2$ | | | 1150 | 555 | S.D. | 2 cms. Red Tapered |
| 134 | $ZnCl_2$ | Zn | 1% | 1150 | 550 | S.D. | 0.5 cms. Orange |
| 135 | $ZnCl_2$ CuSe | Zn | 0.25% 10 p.p.m | 1150 | 555 | S.D. | 3 cms. Orange |
| 136 | $ZnCl_2$ CuSe | Zn | 1% | 1150 | 555 | S.D. | 3cms. Orange Tapered |
| 146 | $ZnCl_2$ | Zn | D.F.C. | 1150 | 550 | Cracked | 15 cms. Oxidised |
| 148 | $H_2O$ | Zn | D.F.C. | 1150 | 555 | Normal | 4 cms. |
| 242 | | $ZnCl_2$ | 1% | 1160 | 450 | S.D. | 3 cms. Quite Good |
| 244 | | $ZnCl_2$ | 1% | 1160 | 600 | S.D. | ½ cm. Orange |

D.F.C. = Doped flow crystals

S.D. = Slightly devitrified

Table 3.4.2

# SEEDED GROWTH TIP.

## Fig.3 : 5 :1
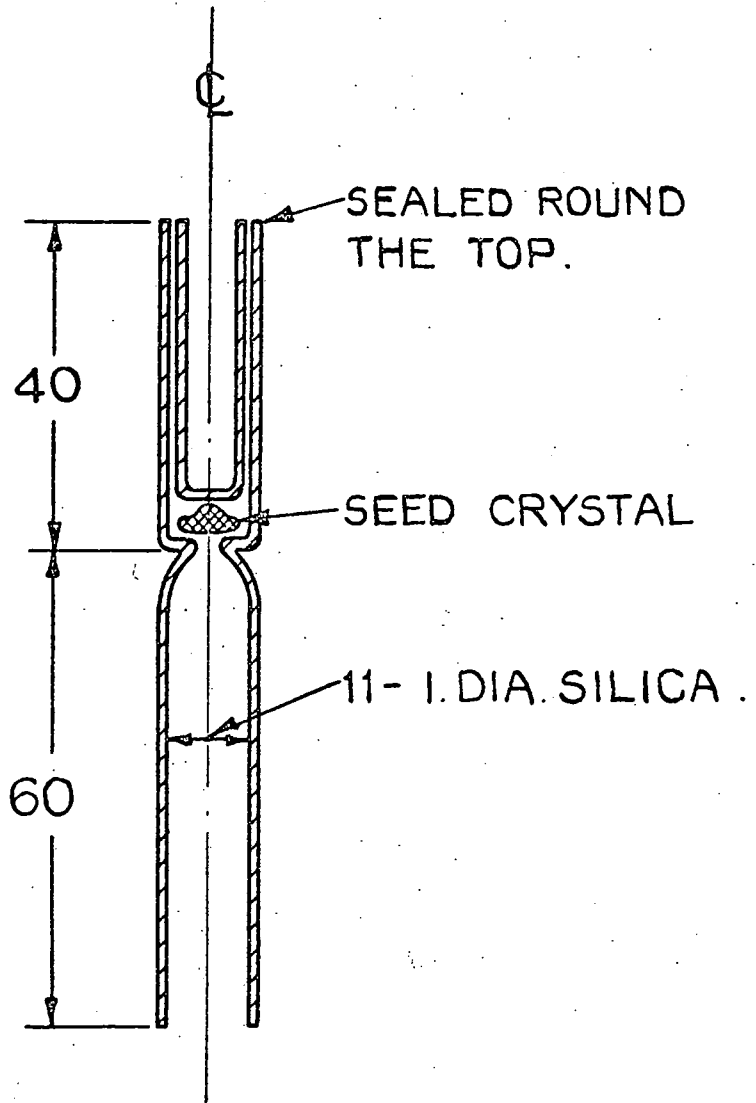


SEEDED GROWTH TIP READY TO BE LOADED
INTO VERTICAL GROWTH TUBE.

a reverse temperature difference of $10^\circ$C was obtained, as measured

using a potentiometer and the differential thermocouple. This situa-

tion was maintained for 30 minutes to clean the seed, after which time

growth was begun by raising the tube until a forward temperature

gradient of approximately $5^\circ$C was established. After 24 hours the

temperature gradient was increased to $10^\circ$C for 48 hours, when the

mechanical pull was started at the slowest rate. The technique of

quickly removing the growth tube from the furnace and examining the

crystal as used by Shiozawa[12] proved impractical because of the

geometry of the furnace. Firstly the tail guide came clear of the tail

furnace and could not be replaced while hot. Secondly, even if the

furnace had been altered to avoid this, the reservoir entered a hotter

part of the furnace and the zinc distilled into the crystal growth

chamber disturbing the growth conditions for a considerable period of

time. Lastly, being a vertical furnace, the temperature profile was

grossly distorted by convection currents as soon as the bungs were

removed.

Out of 10 attempts to grow crystals only the first two on zinc

faces were successful. In these a 0.5 cms, and a 1.5 cm boule, Figure

3.5.2, were grown using a charge temperature of $1165^\circ$C and a zinc

reservoir at $555^\circ$C. In the other attempts, one of the seeds evaporated,

and one very dendritic polycrystalline growth resulted. It has become

clear, however, that the reason for the failures was connected with the

deteriorating quality of the ZnSe supplied by the manufacturers. In

fact it later proved very difficult to grow unseeded crystals with the

material then being used.

The two boules actually produced grew free from the walls of

the capsule, and had six facets round the sides. They were dark green

Figure 3.5.2:   A Boule of Zinc Selenide grown from a Seed

The crystal was grown on the {111} zinc face
of a flow platelet.  Note the six facets on
the top part of the boule, which grew free
of the silica capsule.

in colour and showed no signs of twinning. The method therefore shows great promise for growing high quality, twin free boules. No other reports of this technique being applied to ZnSe have been found, although it has been used for iodine transported cystals[13]. Selenium faces usually grow faster than zinc when the chemical vapour transport technique is used and thus the failure to grow crystals on the selenium faces of flow crystals is almost certainly due to the poor quality of the starting material employed.

## 3.6     Photoluminescence Samples

A series of very heavily doped samples of ZnSe was required for the work of G. Jones on the photoluminescence of ZnSe. In attempts to obtain very high concentrations of impurities, very fast evaporation rates were employed and these were produced by using a very large temperature gradient. As noted in Section 3.1, ZnSe will not sublime at a useful rate unless some method is adopted to maintain the stoichiometry of the vapour phase. Consequently the arrangement of Figure 3.6.1 was devised, the growth tube is similar in principle to the capsule of Figure 3.1.6, and provides a cold region to condense non-stoichiometric material. The 7 mm I.D. tube was evacuated and sealed at $\sim 10^{-6}$ torr. Polycrystalline samples were produced by subliming the zinc selenide down the temperature gradient, the charge was held at $1000^{\circ}C$ and the other end below $200^{\circ}C$. Crystalline material condensed at temperatures between $800^{\circ}C$ and $450^{\circ}C$. Excess dopants and zinc or selenium collected at the cold tip. With aluminium doped samples a certain amount of $Al_2Se_3$ was formed at the cold end of the tube. When such a tube is opened $Al_2Se_3$ hydrolises on meeting water in the air and releases toxic $H_2Se$. The simplest way to avoid this danger is to open the tube in a fume cupboard and to wash the samples and glass before removing them from the cupboard. This ensures that the reaction proceeds to completion safely.

# PRODUCTION OF LUMINESCENCE SAMPLES.

## Fig. 3:6:1

1:2

1:1

1000°C  800°C  450°C  <200°C

EXCESS Se
DOPANTS.

MATERIAL
DEPOSITED

CHARGE AND
DOPANTS
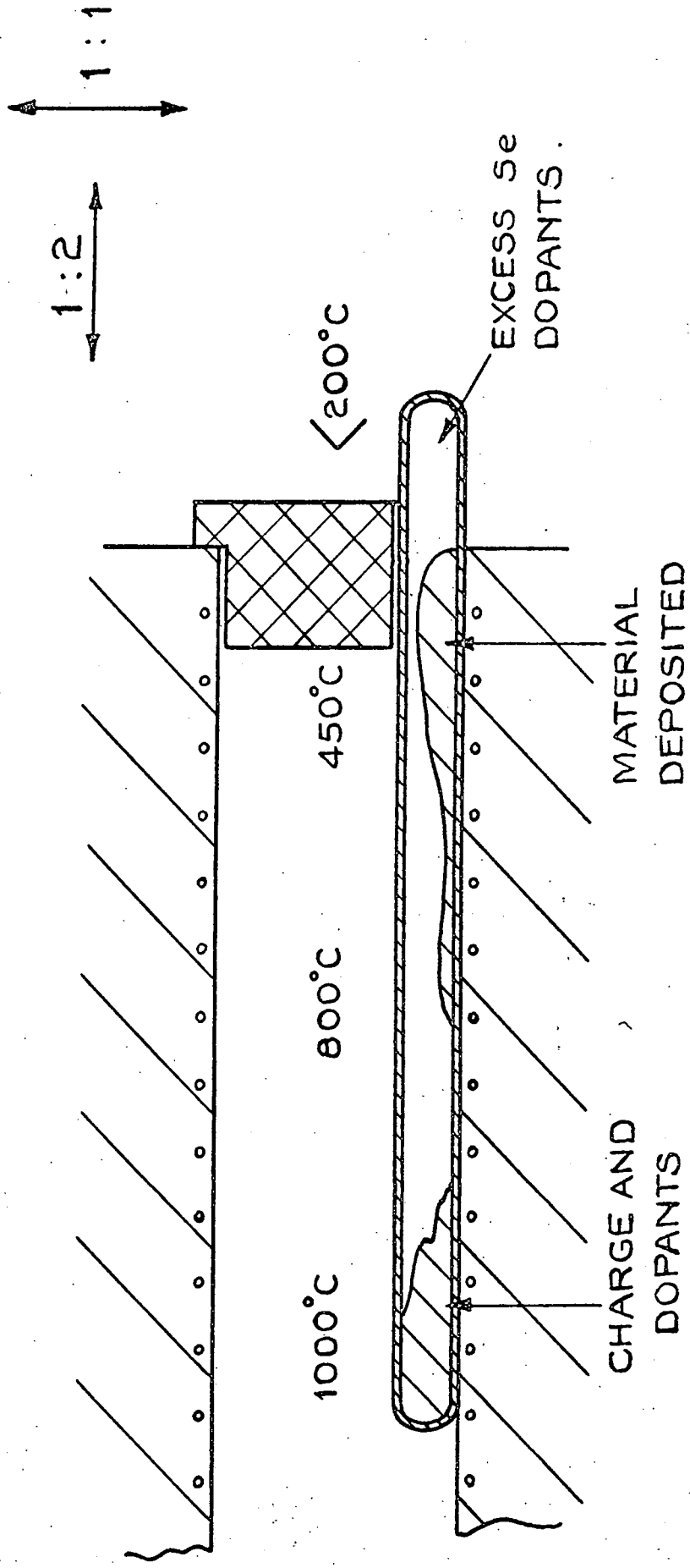
# CHAPTER 3

## REFERENCES

1.  L Clark  and  J Woods  (1968)  J. Cryst. Growth  3,4  p.127-130

2.  K F Burr  and  J Woods  (1971)  J. Cryst. Growth  9  p.183-189

3.  M Aven  and  H H Woodbury  (1962)  Appl. Phys. Lett.  1  p.53

4.  E Kaldis  (1969)  J. Cryst. Growth  5  p.376-390

5.  L Ya Markovskii,  I A Mironov  and  Yu S Ryzhkin  (1969)  Optics and
    Spectroscopy  27  p.84-85

6.  G Jones  (1973)  Ph.D. Thesis  University of Durham  Chap. 5  p.83-85

7.  J W Allen,  M D Ryall  and  E M Wray  (1973)  Phys. Stat. Solidi
    A17  p.101-105

8.  A W Livingstone,  K Turvey  and  J W Allen  (1973)  Sol. St. Electronics
    16  p.351-356

9.  M E Ozsan  and  J Woods  (1975)  Sol. St. Electronics  18  p.519-527

10.  G Jones  and  J Woods  (1973)  J. Phys. D.  6  p.1640-1651

11.  H J Hovel  and  A G Milnes  (1969)  J. Electrochem. Soc.  116  No.6  p.843

12.  L R Shiozawa,  J M Jost,  S S Devlin  and  R M Broady  (1963-1964)
    Research on II-VI Compound Semiconductors, 8th, 9th, 10th Quarterly
    Repts.  Contract AF33  (616)  6865  U S Air Force Aeronautical
    Research Labs.  Wright-Patterson Air Force Base  Ohio

13.  S G Parker  (1971)  J. Cryst. Growth  9  p.177-182

## CHAPTER 4

THEORETICAL CONSIDERATION OF VERTICAL GROWTH

TUBE WITH RESERVOIR

### 4.1    Introduction

The theory of crystal growth from the vapour phase has been

investigated by many authors, including Reed and Lafleur[1], Reed,

Lafleur and Strauss[2] and Faktor and Garrett[3]. Ballentyne et al[4],

Rouse and White[5], Tempest and Ballentyne[6] have given particular

attention to the crystal growth of II-VI compounds from the vapour phase.

The object of this chapter is not to add to the general theory of the

subject, but to attempt to apply some relevant parts of crystal growth

theory to the experimental system described in Chapter 3, parts 1-4.

This has been done in order to understand what is happening inside the

sealed system, and to arrive at the approximate composition of the vapour

over the growing crystal. Because the system was designed to grow crystals

reliably, rather than to investigate the limits of the possible growth

conditions, the data available is restricted, and many assumptions have

to be made to obtain the information required. However, Clark and Woods[7],

Burr and Woods[8] and Cutter, Russell and Woods[9] have reported the

growth of CdS, ZnSe and $ZnSe_xS_{1-x}$ respectively. The apparatus has also

been used successfully to grow CdSe, ZnTe and $ZnTe_{1-x}Se_x$. With each com-

pound a furnace temperature of $1150^\circ C$ was used and the tail reservoir

contained one of the elements. The tail temperature was set, as usual,

to give a pressure of the reservoir element equal to its partial pressure

in the capsule at $P_{MIN}$. CdSe, ZnTe and $ZnTe_{1-x}Se_x$ all transported well

to provide substantial boules. This was expected because CdSe and ZnTe

have much higher values of Kp than ZnSe at $1150^\circ C$. All the boules

produced had hollow growth faces indicating that heat extraction from the growth face was governing its shape. During one ZnTe run the tail furnace failed, then in contrast with ZnSe and CdS, the ZnTe transported to the tail and completely blocked it in a period of approximately 72 hours. Another report of crystal growth in a system with a separate reservoir has come from Fochs et al[10], who grew CdS in a similar system. It would seem worthwhile, therefore, to investigate why the system works so well, and to enquire how much deviation from the ideal charge with exact stoichiometry can be tolerated before the growth is disturbed significantly.

First, however, it is necessary to review some of the background theory. The basis of the crystal growth technique is transport in a sealed tube, either in vacuum or in the presence of an inert gas. The growth process may be conveniently divided into three stages:

(i)      Evaporation of the charge.

(ii)      Transport in the vapour phase.

(iii)      Condensation on to the growing crystal.

The three processes may be regarded as analogous to three resistors in series with a current (growth rate) and a driving voltage ($\Delta T$ between source and seed). If the resistance of one step is much greater than the others it will control the growth rate almost entirely, e.g. the growth rate may be said to be 'diffusion limited' if the process is controlled by the rate of diffusion of one component in the vapour phase, or 'condensation limited' if the kinetics at the growth face is the controlling factor.

In a sealed tube, evaporation is much less likely to be limiting than condensation. Intuitively this appears reasonable because condensation takes place at a lower temperature and thus constitutes a greater

disturbance of the equilibrium rates of evaporation and condensation. With II-VI compounds the stoichiometry of the material affects the evaporation rate. Somorjai and Jepson[11] investigated the evaporation rate of CdS and found that an induction period of several hours was necessary before a non-stoichiometric charge reached its full evaporation rate. In another experiment[12], they found that bombarding the surface with cadmium had little effect on the evaporation rate, and concluded that the retardation was a bulk rather than a surface phenomenon. In a sealed growth tube non-stoichiometry of the charge could affect the evaporation rate sufficiently to make it the rate limiting step, rather than the diffusion of the minority component. However, using a growth tube with a tail reservoir the stoichiometry of the gas in the capsule is stabilised. The charge is always slowly evaporating and condensing in the tail, so that any non-stoichiometry of the charge ought to be corrected in the 48 hours period before crystal growth begins. It would appear therefore that the controlling factors during the growth of the crystals described here are processes (ii) and (iii).

Consider the transport process (ii) first. Material may be moved by three basic mechanisms:

(a)     Viscous flow due to a pressure difference between the ends of the capsule.

(b)     Diffusion.

(c)     Convection.

In the simplest possible system, namely with an elemental charge in a perfectly evacuated capsule, transport occurs when a temperature difference is established along the capsule, because of the resultant pressure difference between the ends. However, only a very small pressure difference would be required to obtain a high transport rate, and the

growth rate would be limited by the heat flows into the source and out from the crystal, which supply and remove the latent heat of sublimation. The system is, in fact, a simple heat pipe, in which the flow of gas from one end of the capsule to the other constitutes what may be termed a 'wind' inside the capsule. Gas is introduced at the source and removed at the crystal. Faktor et al[3] refer to this effect as 'Stefan' flow.

If an inert gas is introduced into the system it will be swept along by the wind. A steady state will be set up in which there is a smaller 'wind' from source to crystal, while superimposed on this will be the forward diffusion of the element, and the backward diffusion of the inert gas. To formulate this mathematically (see Figure 4.1.1), let the 'Stefan' flow be U, the pressure of gas be P, the material flux be J, and the number of moles/unit volume be N. Further, let the subscripts E, I and T added to these symbols represent the elemental gas, the inert gas, and total, respectively. The pressure difference between the ends of the capsule is assumed to be zero.

$$J_T = J_E + J_I .$$

However, in the steady state the flow of inert gas must be zero, so $J_I = 0$ and $J_T = J_E$.

Consider the flow of the element being transported

$$J_E = N_E U - D \frac{d N_E}{dx} = J_T \tag{4.1.1}$$

i.e.     Flux of Element = Stefan Flow + Diffusive Flow = Total Flux

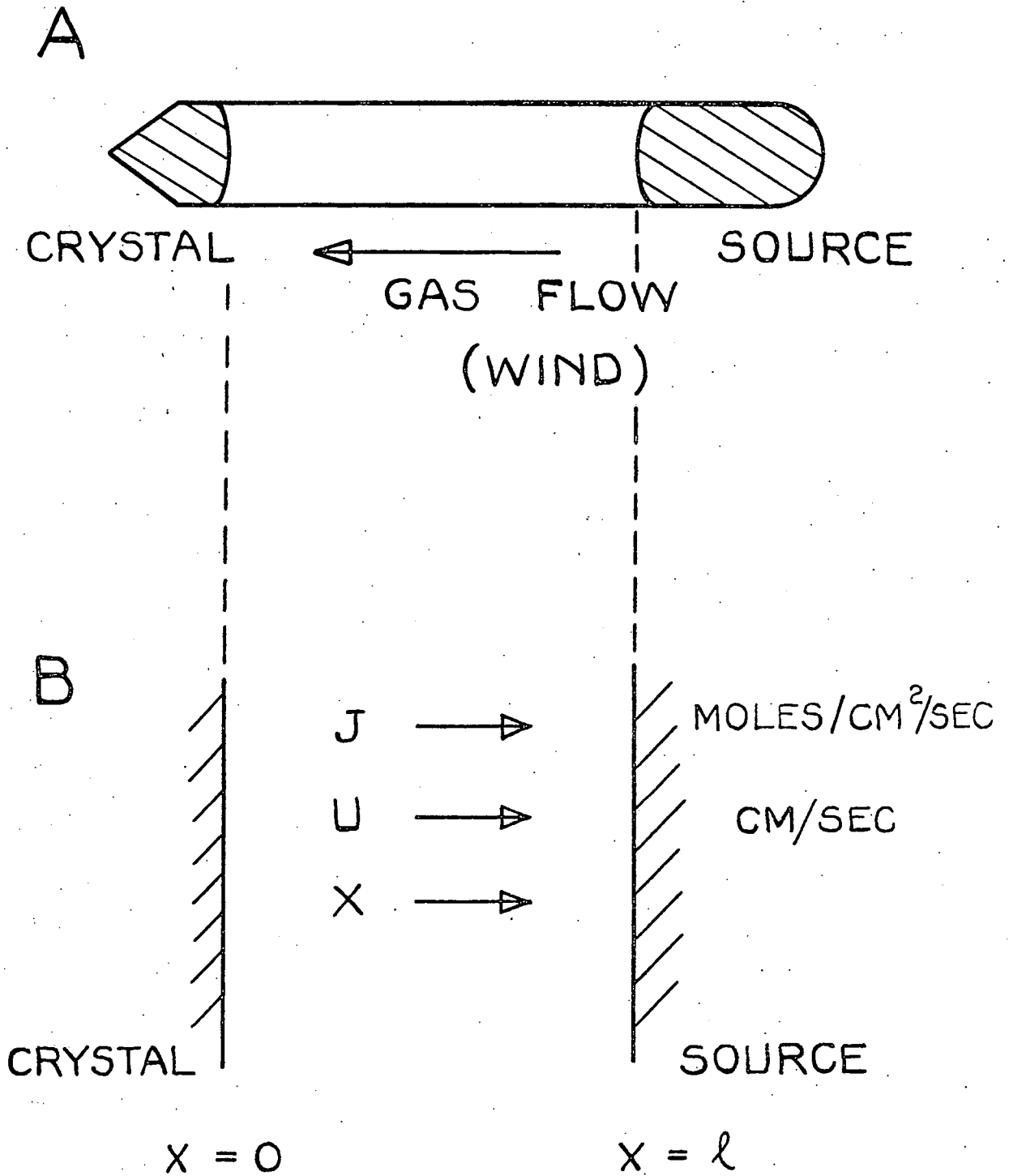But

$$J_T = U N_T \tag{4.1.2}$$

so,

$$J_T = \frac{N_E}{N_T} \cdot J_T - D \frac{d N_E}{dx} \tag{4.1.3}$$

# SIMPLE SEALED CAPSULE.

A

CRYSTAL ← GAS FLOW SOURCE
(WIND)

B

J → MOLES/CM$^2$/SEC

U → CM/SEC

X → 

CRYSTAL SOURCE

X = O X = $\ell$

and

$$J_T \, dx = D \, N_T \cdot \frac{d \, N_E}{(N_E - N_T)} \qquad (4.1.4)$$

If the crystal grows at $x = 0$, where $N_E = N_E(0)$, and the source is at $x = \ell$ where $N_E = N_E(\ell)$, then by integration between $x = 0$ and $x = \ell$,

$$J_T = \frac{D \, N_T}{\ell} \cdot \ell n \left\{ \frac{(N_E(\ell) - N_T)}{(N_E(0) - N_T)} \right\} \qquad (4.1.5)$$

Or in terms of pressure,

$$J_T = \frac{D \cdot P_T}{\ell \, R \, T} \cdot \ell n \left\{ \frac{P_E(\ell) - P_T}{P_E(0) - P_T} \right\} \qquad (4.1.6)$$
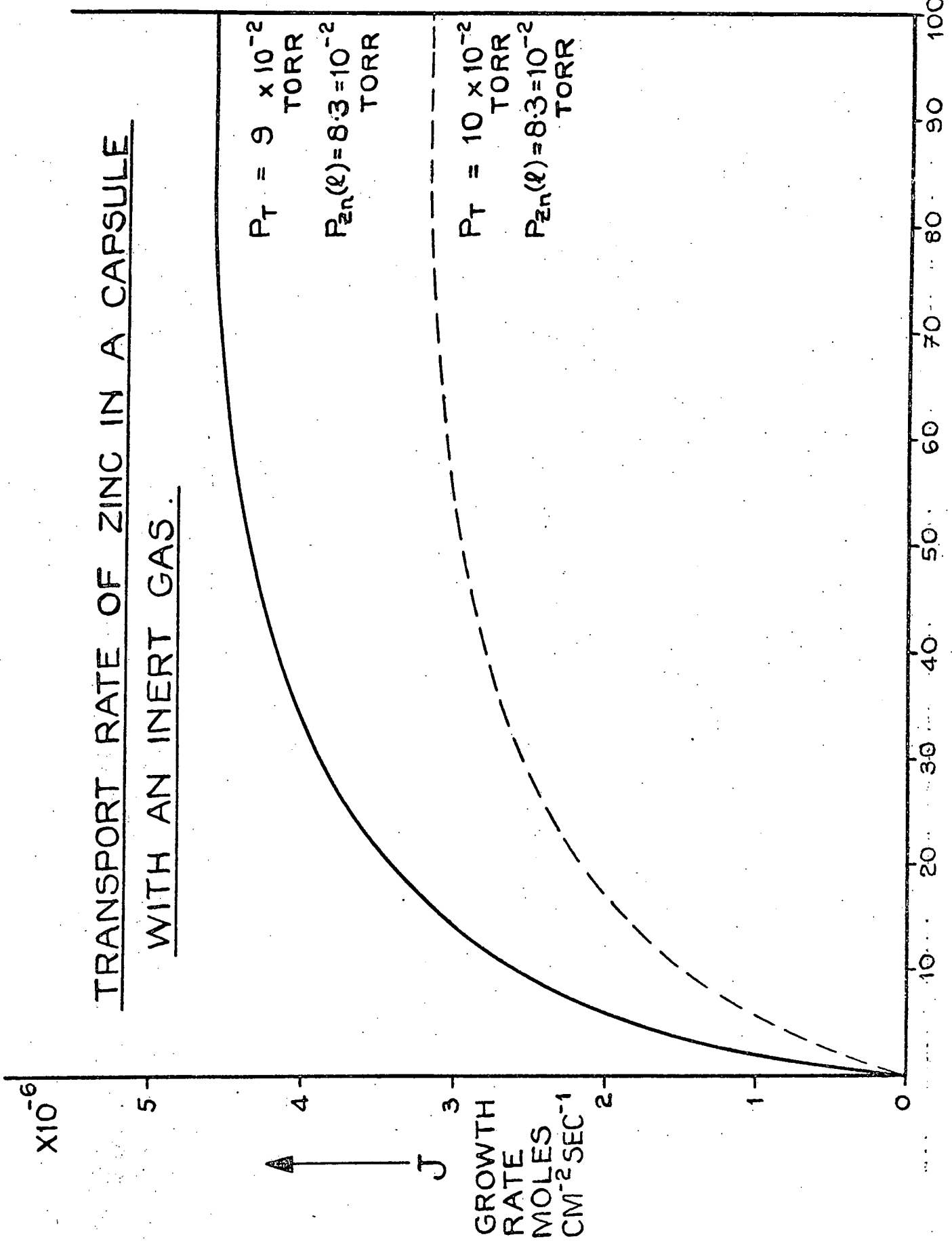
where R and T have their usual significance.

As an example consider the growth of a zinc crystal from the vapour at a temperature just below its melting point. A temperature of $400^\circ C$ is used for the charge. Figure 4.1.2 shows the variation of the growth rate $(J_T)$ with $\Delta T$ for two values of total pressure $(P_T)$. In Figure 4.1.3 the variation of the partial pressures of the zinc and the inert gas along the capsule is shown. The curvature of the partial pressure lines is a consequence of the Stefan flow. As the value of $P_T$ is increased the flow velocity falls rapidly and the curves approach straight lines when $P_T \gg P_{Zn}(\ell)$. Similar effects may be seen in multi-component systems, and a similar curvature of the partial pressure lines occurs when the Stefan flow has a significant velocity.

If the capsule geometry permits, the situation may be further complicated (particularly in a vertical system) by convection currents, which are difficult to treat theoretically. A reasonable approximation may often be made by assuming perfect mixing of the source gas up to a boundary layer close to the growing crystal, and then assuming diffusion controlled growth takes over again, with a source to seed distance equal to the boundary layer thickness. Reed, Lafleur and Strauss[2] point out

TRANSPORT RATE OF ZINC IN A CAPSULE WITH AN INERT GAS.

Fig. 4:1:2

$P_T = 9 \times 10^{-2}$ TORR

$P_{Zn}(\ell) = 8.3 = 10^{-2}$ TORR

$P_T = 10 \times 10^{-2}$ TORR

$P_{Zn}(\ell) = 8.3 = 10^{-2}$ TORR

$\Delta T \, ^\circ C$

$J$ GROWTH RATE MOLES $CM^{-2} SEC^{-1}$

$X10^{-6}$

# PARTIAL PRESSURES OF ZINC AND AN INERT GAS IN A SEALED CAPSULE.

## Fig. 4:1:3
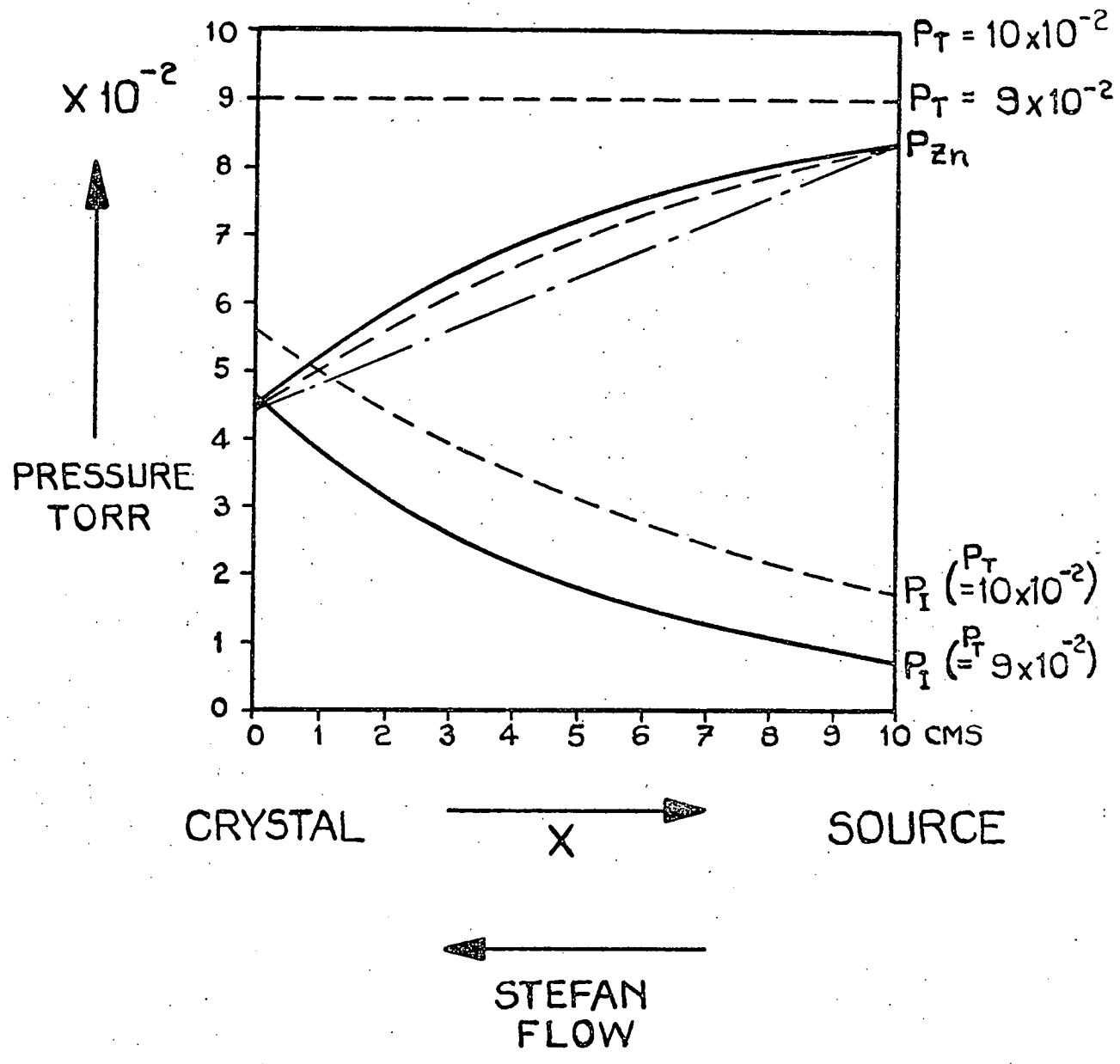


$P_T \gg P_{Zn}(\ell)$

$P_T = 10 \times 10^{-2}$

$P_T = 9 \times 10^{-2}$

NOTE THE CURVATURE OF THE PARTIAL PRESSURE LINES DUE TO THE INCLUSION OF STEFAN FLOW IN THE TRANSPORT EQUATION. AS $P_T$ INCREASES THE CURVES APPROACH STRAIGHT LINES, WHICH AGREES WITH A "DIFFUSION ONLY" TREATMENT.

that this approximation may also be used to describe growth in an open tube with forced convection, (i.e. the conventional vapour phase epitaxy apparatus) by the insertion of an appropriate boundary layer thickness.

4.2    Interface Effects

The surface effects on the growing interface have also been sub-divided into three main classes by Ballentyne et al[4] following the work of Brice[13] on melt growth.

(i)    Growth on a perfect singular interface, where it is necessary to nucleate each successive growth layer requiring a supersaturation ratio $(P/P_{EQUILIBRIUM})$ of at least $2$[14]. A perfect singular interface implies a defect-free surface (no dislocation impurity or other nucleating centre), that corresponds to a sharp dip in the surface energy. This is illustrated in Figure 4.2.1 which shows Wolff's theorem in two dimensions. A singular plane contains no steps. A plane nearly parallel to such a face can minimise its free energy by becoming stepped so that it is made up of steps and singular faces. This type of face is sometimes referred to as a vicinal plane.

(ii)    Growth on a nearly perfect face, e.g. one containing screw dis-locations or some other self regenerative step mechanism. This requires a supersaturation $\sim 1.01$[15].

(iii)    Growth on an atomically rough surface, which always has corner sites available. This requires a very low supersaturation, possibly as low as $1.0001$[16].

4.3    Processes in Sealed Capsules

Before passing on to a consideration of the special peculiarities

# WULFF'S THEOREM TO DETERMINE THE
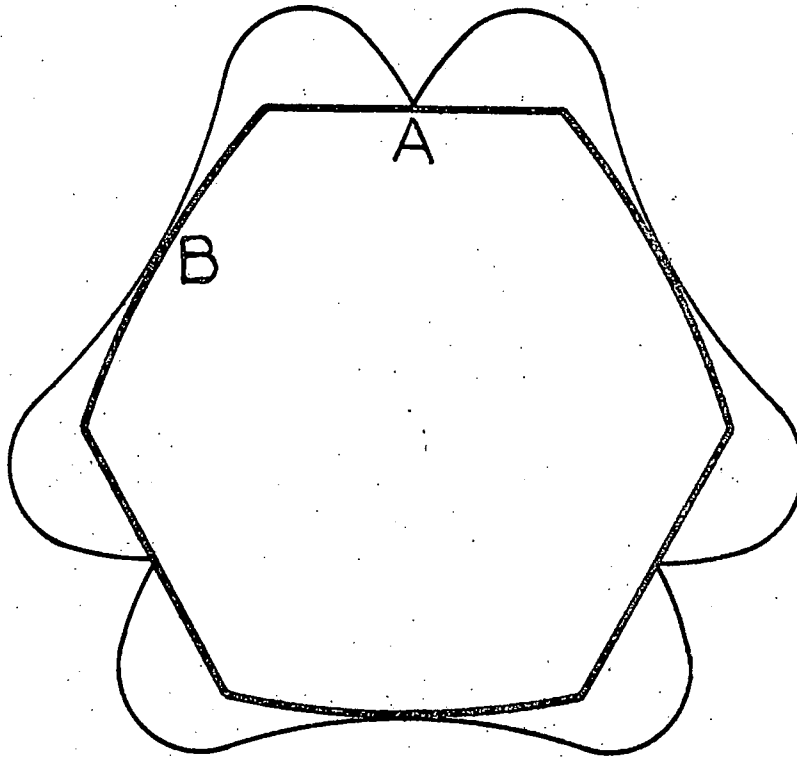# EQUILIBRIUM SHAPE OF A CRYSTAL.



Figure 4.2.1:  Wulff's theorem in two dimensions. The heavy line
is the equilibrium shape and the light line is the
free energy polar diagram. A is a singular inter-
face and B is a rough interface.

If a plot of $\gamma_s(\underline{n})$, (the value of $\gamma_s$ in a direction
defined by a vector $\underline{n}$, where $\gamma_s$ is the surface free
energy of the crystal) is produced, this will be a
closed surface. If at this surface a plane is drawn
normal to each radius vector, then by Wulff's theorem,
the equilibrium shape of a crystal will be geometrically
similar to the volume which can be reached from the
origin without crossing any plane. If a direction $\underline{n}$
corresponds to a sharp minimum of $\gamma_s$, the resulting face
will be flat. In other orientations it will be curved.

of the growth of II-VI compounds, it is perhaps more opportune to consider the processes in an actual growth run. See Figure 3.1.1. If the tail of the capsule is ignored the system reduces to a simple sealed capsule being pulled through a temperature gradient. A run starts with the growth tip in the hottest part of the furnace. The charge tends to sublime and concentrates in the lowest part of the capsule where it coalesces. As the capsule is pulled through the temperature gradient the growth tip becomes cooler than the charge, and at some critical supersaturation, nucleation begins on the walls of the growth tip. Initially the crystallites (invisible to the unaided eye) grow very rapidly reducing the local supersaturation of the gas until their volumes of influence overlap. The crystallites with the largest volumes dominate when this occurs, and the smaller ones are annihilated by re-evaporation as the value of the supersaturation decreases. A reasonably evenly spaced array results. A period of growth follows in which the most favourably oriented crystallites outgrow the others and fill the whole width of the tube. Usually one or two grains are left. Growth will in general proceed at a rate different from the pull rate until $\Delta T$ has been altered by the movement of the growth face so that the two rates become comparable to one another. Of course the pull rate may exceed the maximum possible growth rate in the system, in which case $\Delta T$ will become large. Then the adsorption process may be limited by activation energy. The activation energy is associated with a potential barrier to an energetically favourable reaction (see Figure 4.3.1). In crystal growth, common examples of activated adsoprtion processes are the dissociation of $S_2$ molecules at the surface of ZnS and CdS[6], and the break up of the carrier species at the growth face in chemical vapour transport. The barrier will be most significant at lower growth temperatures, and one of the characteristics of this mode of limitation is that

# SCHEMATIC DIAGRAM OF AN ACTIVATED PROCESS.
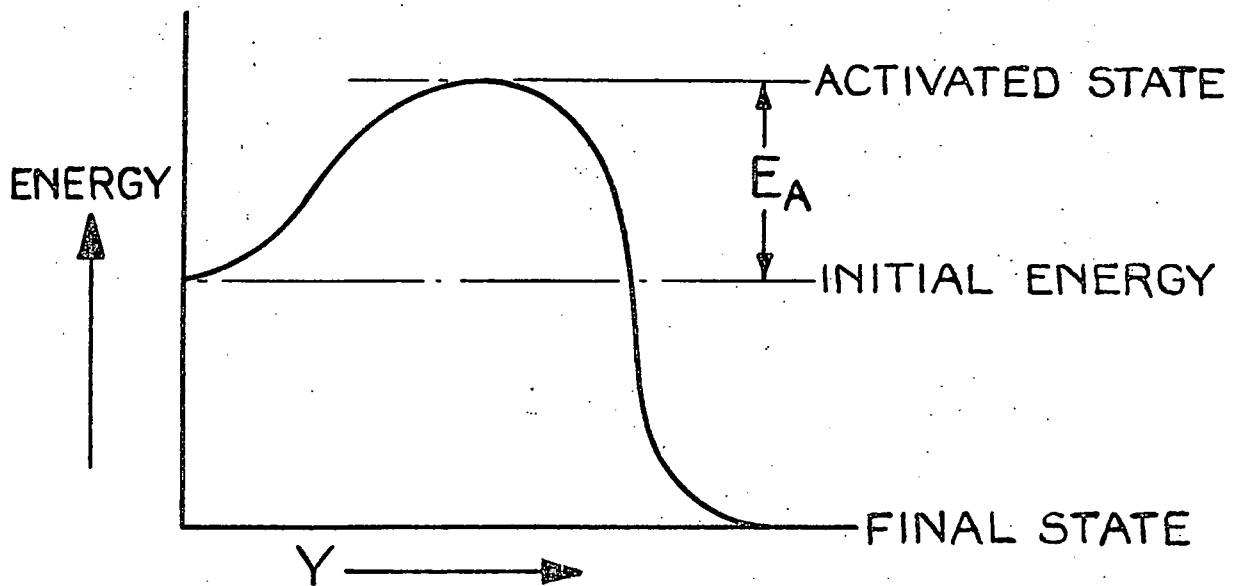
$E_A$ = ACTIVATION ENERGY

Y = SOME FUNCTION OF PROCESS

eg. DISTANCE APART OF MOLECULES.

the growth rate increases exponentially as the temperature of the interface is increased.

## 4.4    Application to II-VI Compounds

Some of the ideas described in Sections 4.1, 2 and 3 can now be applied to the simple sealed capsule containing a II-VI compound.  The essential difference between the sublimation of a II-VI compound and an element is that the II-VI compound dissociates into monatomic metal, and diatomic non-metal molecules.  The pressures of each component are given by the relationship

$$Kp = P_M^2 \, P_{N_2}$$

so clearly there is an extra degree of freedom in the system.

Consider the capsule shown in Figure 4.1.1A.  Material evaporates at the hot end of the capsule, travels to the cold end and condenses. The sealed capsule and reservoir system was developed from a simple capsule to provide more control over the conditions during growth.

Faktor et al.[3] have observed that at normal growth rates the transfer of material from charge to growing crystal constitutes quite a considerable wind inside the capsule.  For example 20 gms of ZnSe transported at a temperature of $1150^{\circ}$C and a pressure of $P_{MIN}$ in five days within an 11 mm I.D. tube constitutes a wind of average velocity 5 cms/sec.

Furthermore, Faktor et al point out that the pressure difference between the ends of the capsule necessary to produce this wind is very small relative to the total pressure inside the capsule.  This presents an interesting picture, the source and seed are at substantially the same pressure, yet at different temperatures.  This may be achieved only

if the composition of the vapour varies along the length of the capsule.
Figure 4.4.1 shows a typical set of curves of composition versus tem-
perature for ZnSe at constant total pressures $(P_T)$ which have been
calculated assuming equilibrium conditions at the two interfaces. The
pressures of the isobars were selected by the computer to be at $50^{\circ}C$
intervals at $P_{MIN}$ ($A = \frac{1}{2}$). The basic assumption of equilibrium must be
justified if the curves are used with reference to a practical system.
Next consider transport of ZnSe in the capsule of Figure 4.1.1A. To
model it mathematically, let the crystal grow at $x = 0$, and the source
be at $x = \ell$. Let the total gas flow be J moles/unit area in unit time.
Each of the moles corresponds to 2/3 mole of solid ZnSe transported
because 1 mole of ZnSe dissociates into 1 mole of Zn and 0.5 moles of $Se_2$
when it evaporates. Let U be the average flow velocity of the wind in
the tube, and N be the number of moles/unit volume, consequently

$$N = \frac{J}{U} \qquad (4.4.1)$$

Let A be the ratio of $Se_2$ to Zn so

$$AP_{Zn} = P_{Se_2}$$

and

$$P_T = P_{Se_2} + P_{Zn} = (A+1)P_{Zn} \qquad (4.4.2)$$

X = Flux due to the wind in the capsule.

Y = Flux due to diffusion.
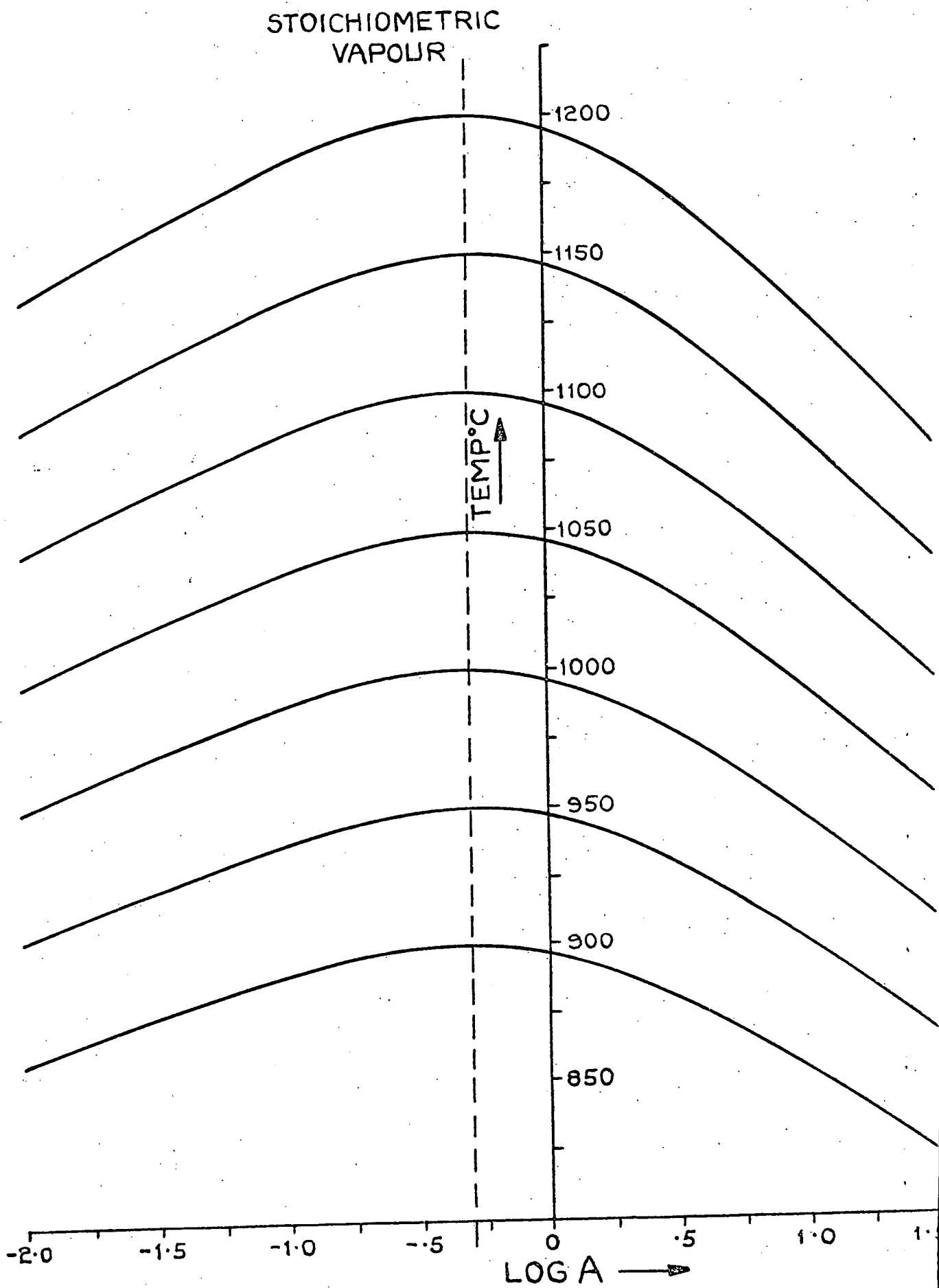
Let the subscripts Zn, Se and T stand for zinc, selenium and total
respectively, e.g. $X_{Zn}$ = Flux of zinc carried by wind, $J_T$ = Total Flux =
$J_{Zn} + J_{Se}$.

CONSTANT PRESSURE CURVES
FOR ZnSe.                    Fig.4:4:1

STOICHIOMETRIC
VAPOUR

TEMP°C

1200
1150
1100
1050
1000
950
900
850

-2·0   -1·5   -1·0   -·5   0   ·5   1·0   1·

LOG A ⟶

$$A = \frac{P_{se_2}}{P_{zn}}$$

So,

$$X_{Zn} = \frac{J_T}{1 + A} \qquad (4.4.3)$$

(i.e. The flux of zinc carried by the wind at any point is the product of the total flux and the proportion of zinc vapour at that point, and,

$$Y_{Zn} = -D \frac{d N_{Zn}}{dx} \qquad (4.4.4)$$

But

$$N_{Zn} = N_T \frac{1}{1 + A} \qquad (4.4.5)$$

so

$$\frac{d N_{Zn}}{d A} = -N_T \frac{1}{(1 + A)^2} \qquad (4.4.6)$$

and substitution in 4.4.4 gives

$$Y_{Zn} = D \frac{N_T}{(1 + A)^2} \cdot \frac{dA}{dx} \qquad (4.4.7)$$

Similarly,

$$X_{Se} = J_T \frac{A}{A + 1} \qquad (4.4.8)$$

$$Y_{Se} = -D \cdot \frac{d N_{Se}}{d x} \qquad (4.4.9)$$

and

$$N_{Se} = N_T \cdot \frac{A}{1 + A} \ .$$

Therefore

$$\frac{d N_{Se}}{d A} = +N_T \frac{1}{(1 + A)^2} \qquad (4.4.10)$$

and

$$Y_{Zn} + Y_{Se} = 0 \ .$$

This is to be expected because the total diffusion flux must be zero under equilibrium conditions, as a result of the assumption of zero change in total pressure $(P_T)$ along the length of the capsule.

The total zinc flux must be constant along the length of the tube at $2/3 \ J_T$, because the zinc is only introduced at the source and $J_T$ must be composed of $2/3$ zinc and $1/3$ selenium. Therefore,

$$X_{Zn} + Y_{Zn} = 2/3 \ J_T = \frac{J_T}{1 + A} + D \cdot \frac{N_T}{(1 + A)^2} \ \frac{dA}{dx} . \qquad (4.4.11)$$

It follows that

$$J_T \left( \frac{2}{3} - \frac{1}{1 + A} \right) = \frac{D \cdot N_T}{(1 + A)^2} \cdot \frac{dA}{dx} \qquad (4.4.12)$$

and substitution from 4.4.1 gives

$$\frac{2A - 1}{3(1 + A)} = \frac{D}{U} \cdot \frac{1}{(1 + A)^2} \cdot \frac{dA}{dx} \qquad (4.4.13)$$

Therefore

$$\frac{U}{D} \cdot dx = \frac{3}{(2A - 1)} \cdot \frac{1}{(1 + A)} \cdot \frac{dA}{dx} \qquad (4.4.14)$$

and

$$\frac{U}{D} \cdot dx = \left\{ \frac{2}{(2A - 1)} - \frac{1}{(1 + A)} \right\} dA \qquad (4.4.15)$$

To find the variation of the composition of the vapour along the capsule it is necessary to integrate between $x = 0$ and $x = \ell$, giving

$$\int_{o}^{\ell} \frac{U}{D} \cdot dx = \int_{A_o}^{A_\ell} \left\{ \frac{2}{(2A - 1)} - \frac{1}{(1 + A)} \right\} dA \qquad (4.4.16)$$

So,

$$\frac{U\ell}{D} = \ell n \ \frac{(2A_\ell - 1)}{(2A_o - 1)} \cdot \frac{(A_o + 1)}{(A_\ell + 1)} \qquad (4.4.17)$$

giving,

$$\text{Exp}\left(\frac{U.\ell}{D}\right) = \frac{(2A_\ell - 1) \cdot (A_o + 1)}{(2A_o - 1) \cdot (A_\ell + 1)}$$

(4.4.18)

The same result may be obtained by putting $X_{Se} + Y_{Se} = \frac{1}{3}$ J.

If the value of $A_o$ is taken as 2 and that of $A_\ell$ as 1, for example, which will be shown later to be rather large for ZnSe in the experiments reported here, the concentration gradient along the capsule may be calculated as shown in Figure 4.4.2A. Knowing the vapour composition, the equilibrium temperature for the vapour over the solid may also be calculated, giving a superlinear curve, Figure 4.4.2b. To avoid constitutional supercooling in the vapour phase, a criterion for stability suggested by Reed and Lafleur[1,2], it is necessary to ensure that the furnace profile is more steeply curved than this. A furnace profile with a sharp knee is usually aimed for (for example, as indicated by the dashed line), which allows for as large a curvature as possible. The criterion for stability is that

$$\frac{dT}{dx}_{\text{FURNACE}} > \frac{dT}{dx}_{\text{SOLID-VAPOUR EQUILIBRIUM}}$$

at the growth face $(x = 0)$.

The choice of the parameter A as the dependent variable was made solely for convenience to obtain an expression in terms of the growth parameters required later, and these results are essentially the same as those of Faktor and Garrett[3]. They went further in their calculations and suggested that crystals should be grown either with an inert gas in the capsule, or slightly off stoichiometry to ensure stability at the growth face.

In practice little evidence was found of instability. Only one

# VARIATION OF A ALONG LENGTH OF CAPSULE.
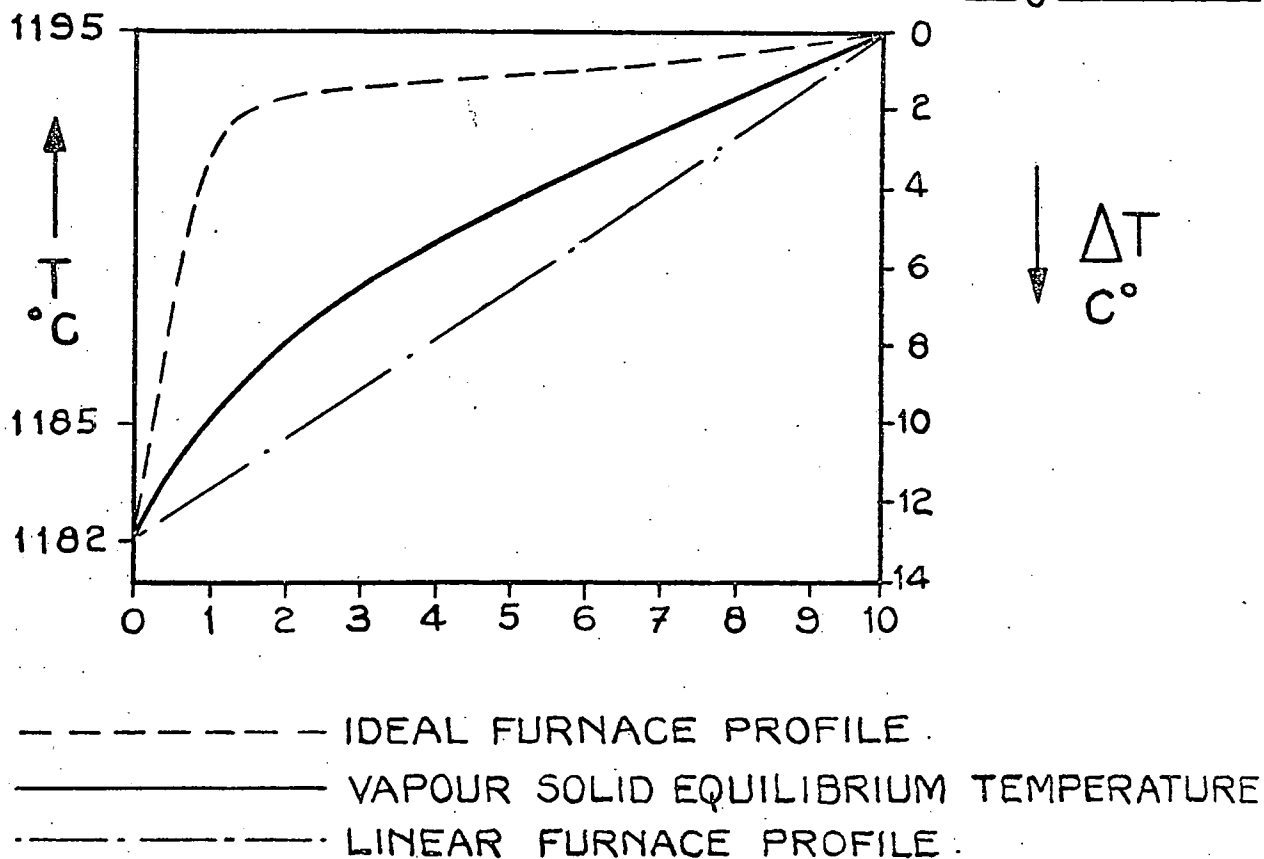
CRYSTAL
1182 °C

SOURCE
1195 °C
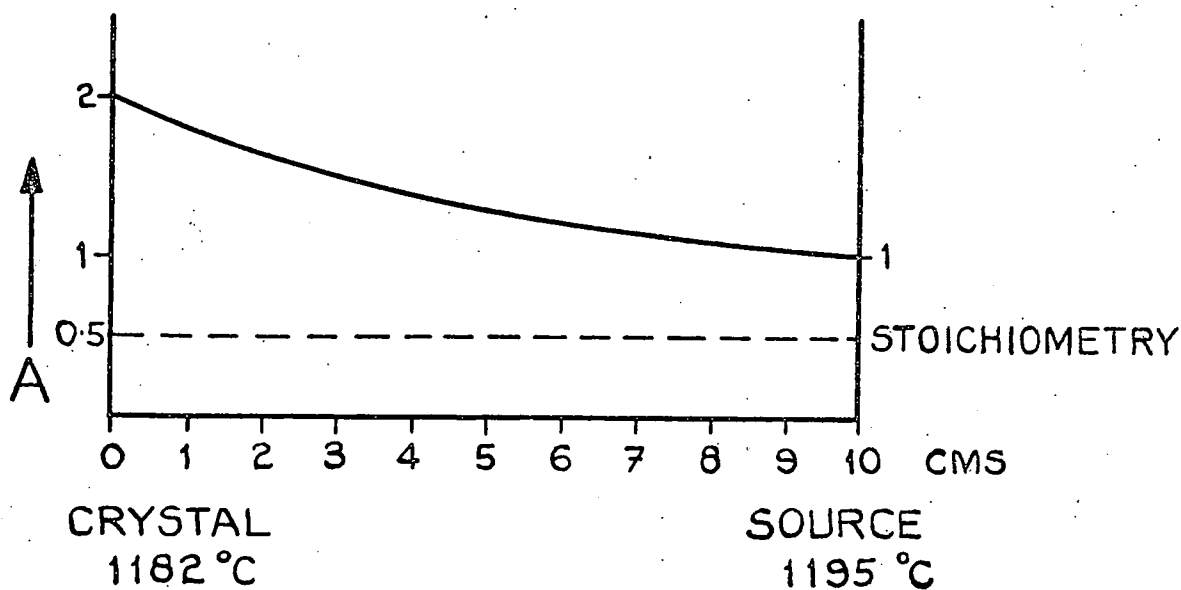
# VARIATION OF VAPOUR – SOLID EQUILIBRIUM TEMPERATURE ALONG CAPSULE LENGTH.

– – – – – – – – IDEAL FURNACE PROFILE.

———————— VAPOUR SOLID EQUILIBRIUM TEMPERATURE

– · – · – · – · – LINEAR FURNACE PROFILE.

undoped boule showed dendritic growth, and this occurred when the capsule was held stationary in a large temperature gradient in an attempt to enlarge a boule after a partially successful run. It is shown below that growth must occur a little off stoichiometry and that there is almost certainly inert gas present. The criteria for stability are therefore satisfied on almost every run.

## 4.5     Experimental Observations

It is possible to compare the predictions of the theory with the results found in practice when growing boules of ZnSe, the best of which were prepared from B.D.H. material. The boules of the highest quality were light green in colour and consisted typically of several large grains. Total transport was regularly obtained. The following observations were made of these boules.

1.     The fastest transport (15 gms in 40 hrs) produced boules with good body colour and rounded ends. The reservoir temperature was chosen to give a partial pressure of the reservoir element corresponding to $P_{MIN}$ in the capsule. Deviation from this temperature by as little as $20^{\circ}C$ led to boules with facets and partial transport only. An experiment was performed to check as closely as possible that these were the optimum conditions for transport within the capsule. Three growth tubes were prepared using starting material from the same batch. They were pumped down on the vacuum system simultaneously, and sealed off at the same time. Growth was performed in a growth rig with three identical furnaces which shared the same pulling mechanism. The charge temperatures were $1175^{\circ}C$ for each of them, but the tail reservoirs were set at $335^{\circ}C$, $360^{\circ}C$ and $385^{\circ}C$. The results are

tabulated in Table 4.5.1.  They showed that the boule with the tail actually set for $P_{MIN}$ grew fastest.  The crystals referred to lower in the table (179, 175, 176, 129) were grown in different runs and are thus more difficult to compare.  Crystals grown with tail temperatures away from the calculated 'best' value were allowed to remain in the temperature gradient for longer times.  Crystal 129 was grown with a heavy overpressure of zinc and the growth rate was slowed, leading to a facetted boule.

Poorer quality starting material gave similar results because the effective value of Kp was altered by the impurities present.  A good example is boule 196, which had an orange colouration instead of the usual lime green colour, and which was produced from a batch of starting material which gave poor transport.

A domed growth face corresponds to what Ballentyne et al have called a face type (iii) i.e. growth on an atomically rough surface, while the facetted face corresponds to their type (ii) i.e. growth on a nearly perfect interface.

A nearly perfect interface requires a supersaturation of the order 1.01, while the rough interface needs very much less.  However, to prevent the rough interface becoming facetted during growth it may be necessary to have the supersaturation required for type (ii) growth.

Using the expression ,

$$\text{supersaturation} \quad = \quad \left[ \frac{P_{Zn}^2 \; P_{Se_2}}{Kp} \right]^{1/3}$$

it is possible to calculate the value of  $\Delta T$  required to give a particular supersaturation.  Using the values quoted in Aven and Prener[17]

| Boule Number | Charge Temperature °C | Tail Temperature °C | (Type) | Result |
|---|---|---|---|---|
| 171 | 1175 | 385 $P_{MIN} + 25$ | (Se) | 2.5 cm boule |
| 172 | 1175 | 360 $P_{MIN}$ | (Se) | total transport |
| 173 | 1175 | 335 $P_{MIN} - 25$ | (Se) | 3 cm boule |

Boules 171, 172, 173 were grown simultaneously giving a good comparison of the growth rates.

| Boule Number | Charge Temperature °C | Tail Temperature °C | (Type) | Result |
|---|---|---|---|---|
| 179 | 1175 | 410 | (Se) | total transport |
| 175 | 1150 | 360 | (Se) | total transport |
| 176 | 1175 | 555 | (Zn) | total transport |
| 129 | 1150 | 655 | (Zn) | 15 mm facetted |
| 196 | 1165 | 560 | (Zn) | 15 mm facetted |

The lower table shows data from four crystals grown from similar starting material. 129 grew slowly because of the high tail temperature. 179, 175 and 129 transported completely, and had domed ends. The fifth crystal, 196, was grown from a bad batch of starting material, and shows a similarity to 129 because of the depression of Kp, which produces an effect similar to raising the reservoir temperature.

Table: 4.5.1

$$\frac{d\left(\log_{10} Kp\right)^{1/3}}{dT} = \frac{37500^*}{T^2}$$

which at $1177^{\circ}C$ yields a value of

$$\frac{d\left(\log_{10} Kp^{1/3}\right)}{dT} \quad \text{of} \sim 0.0059 .$$

while $\log_{10} 1.01$ is 0.0043. So a temperature difference of the order of $1^{\circ}C$ is required to give the necessary supersaturation for growth on a nearly perfect face. This corresponds well with the seeded growth experiments reported in Section 3.5, which showed that initial growth on the seed could be obtained with a temperature difference of $1^{\circ}C$. The growth on the seeds was slow and facetted as would be expected. This demonstrates that the nucleation rate at the crystal cannot be a limitation to the growth rate because the values of $\Delta T$ used were much larger than $1^{\circ}C$.

2.    While it was not possible to monitor the growth rate continually, observation of various capsules which have been stopped in mid run (because of furnace failure, or similar difficulties) indicated that the fastest growth rate obtained did match the capsule velocity used giving a growth time of 36 hours for a 3 cm boule. Most boules grew rather more slowly, completing their growth in 3-5 days.

3.    The temperature of the charge is usually assumed to be the same as the maximum temperature of the furnace, but in fact varies through the growth run as the capsule is pulled, and probably alters by as much as $20^{\circ}C$. $\Delta T$ may be measured by a thermocouple with the cold junction at the crystal and the hot junction near the charge. However, there must be a temperature gradient through the silica, and

*  A more up to date value from Kirk and Raven[18] would replace 37500 by 38260.

such an arrangement only provides a maximum estimate of the magnitude of $\Delta T$. Further, as growth proceeds the junctions are left behind, making it a little difficult to determine exactly what is being measured. Nevertheless, with good quality starting material, growth occurred with $\Delta T$ much less than $30^{\circ}C$, but probably exceeding $10^{\circ}C$ in most runs. This means that nucleation on the growth face was not a limiting parameter.

4.    Because the tail reservoir was used it is unlikely that $P_T$ greatly exceeded $P_{MIN}$, say $P_T < 1.5\, P_{MIN}$ giving $A_\ell < 3$ from Figure 4.5.1. The reason for this is that for $P_T$ to exceed $P_{MIN}$ the vapour must be non-stoichiometric. If this is so, then more of the excess component will be lost to the reservoir, thus tending to restore the system to $P_{MIN}$. This will be discussed further below.

Equation 4.4.18 links the growth rate with the values of $A_o$ and $A_\ell$. If one is known then the other can be calculated, and using Figure 4.4.1. a value of $\Delta T$ can be derived. If it is assumed that the source is in equilibrium with the vapour over it, then a value of $\Delta T$ corresponding to the observed growth rate can be calculated. By comparing this with the experimental value for $\Delta T$ it is possible to decide whether the growth of the crystal was limited by diffusion or by the kinetics of the interface, and this will also be discussed below. The assumption of equilibrium at the source may be justified by the following observations:

(i)    In similar diameter tubes pumped by a diffusion pump, transport of material down a temperature gradient was more than 100 times faster than in a sealed capsule.

# VARIATION OF $P_T/P_{MIN}$ WITH A.

$$\frac{P_T}{P_{MIN}} = \frac{2}{3}(A+1)\left(\frac{1}{2A}\right)^{\frac{1}{3}}$$
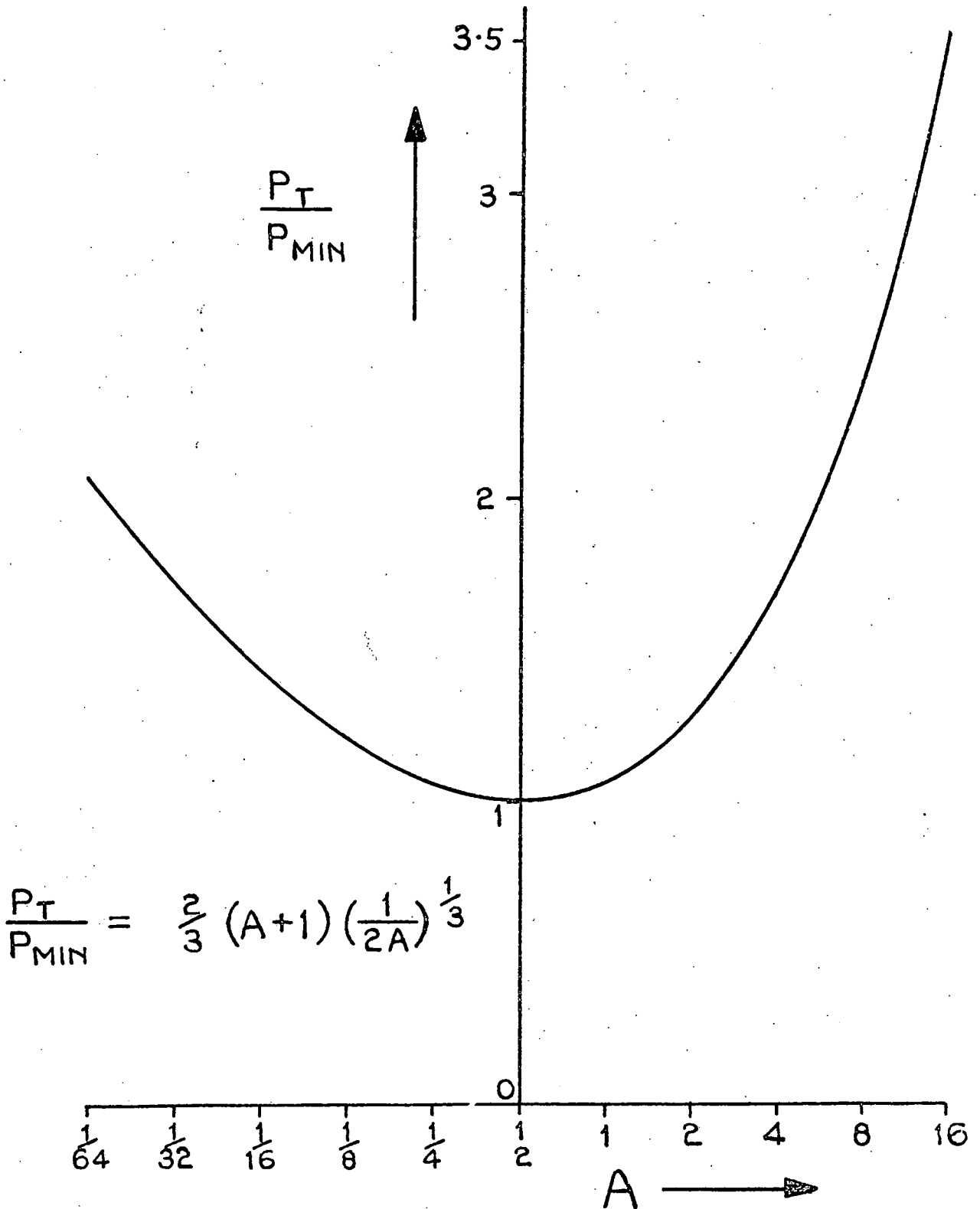
(ii)    Transport in the 11 mm I.D. sealed capsule was slower than in the 7 mm tubes of Section 3.6.

They indicate that the experimental evaporation rate is only a small perturbation of the naturally occurring evaporation and condensation of molecules at the source.

## 4.6    The effects of stoichiometry in a simple sealed capsule

In practice the maximum growth rates theoretically obtainable in a sealed tube are rarely approached.  To obtain a high growth rate one needs a source with the composition to give $P_{MIN}$, which is close to the stoichiometry ratio of 2:1 monatomic zinc molecules to diatomic selenium molecules.  Even if the necessary accuracy could be obtained when weighing the material, only 0.3 mg of oxygen adsorbed over a 20 gm charge in a typical capsule would be sufficient to give an oxygen vapour pressure greater than $P_{MIN}$ for ZnSe.  Clearly this would greatly affect the stoichiometry of the contents of the capsule.  Further contamination may be produced by outgassing and by diffusion through the capsule walls.  To overcome such difficulties, some workers[19,20,4] have baked CdS within the growth capsule at a temperature of the order of $500°C$[4] to outgas the charge and capsule and to bring the charge nearer to the composition required to produce $P_{MIN}$ conditions at that temperature before sealing under vacuum or back filling with argon.  ZnSe has a lower vapour pressure than CdS at the temperature used for growth, and is consequently more difficult to grow in this manner.  When transporting ZnSe it is necessary to maintain the vapour near $P_{MIN}$ conditions continuously by placing some constraint on the composition of the vapour in the capsule or tube.  In Chapter 3 two methods were described;  the vertical tube with tail reservoir in Section 3.1, and the horizontal tube in 3.6.

In the vertical tube the stoichiometry of the charge is controlled by connecting the capsule to a reservoir containing one of the constituents. The two degrees of freedom within the capsule are removed by controlling the charge and reservoir temperatures, and transport occurs while the vapour remains close to $P_{MIN}$ with a temperature difference of $10 - 50^{\circ}C$ between the source and crystal.

In the horizontal tube conditions are very different. Little or no transport takes place when a temperature difference of $\sim 50^{\circ}C$ is employed between the ends of the capsule, see Figure 4.6.1a. If the capsule is displaced in the furnace so that a larger value of $\Delta T$ is obtained as in Figure 4.6.1b, transport is still very slow, but when position 4.6.1c is reached the transport rate increases rapidly. Material is deposited along the walls of the tube when the temperature is between $800$ and $400^{\circ}C$. (The temperature is that deduced from the temperature profile of the furnace. The latent heat of sublimation of the material deposited may well raise the internal temperature of the tube considerably). It is extremely difficult to arrange for material to be deposited right in the tip of a sealed tube even when the tip is held at $400 - 800^{\circ}C$, although material is deposited in this temperature region when the tip is cooler.

The reasons for the processes summarised diagrammatically in Figures 4.6.1a, b and c are quite straightforward. When the source is heated, a total pressure $P_T$ several times $P_{MIN}$ develops because the charge is never perfectly stoichiometric, and also because any impurities present will affect the stoichiometry of the gas. The rate of transport under these conditions is necessarily very low because of the low vapour pressure of the minority component which has to diffuse to the cooler region of the tube. Because the tube must contain a constant pressure

# THE LONG SEALED CAPSULE.

## Fig. 4:6:1

A

NO TRANSPORT

B

LITTLE OR
NO TRANSPORT

C

RAPID TRANSPORT

ZnSe

NON STOICHIOMETRIC
EXCESS.
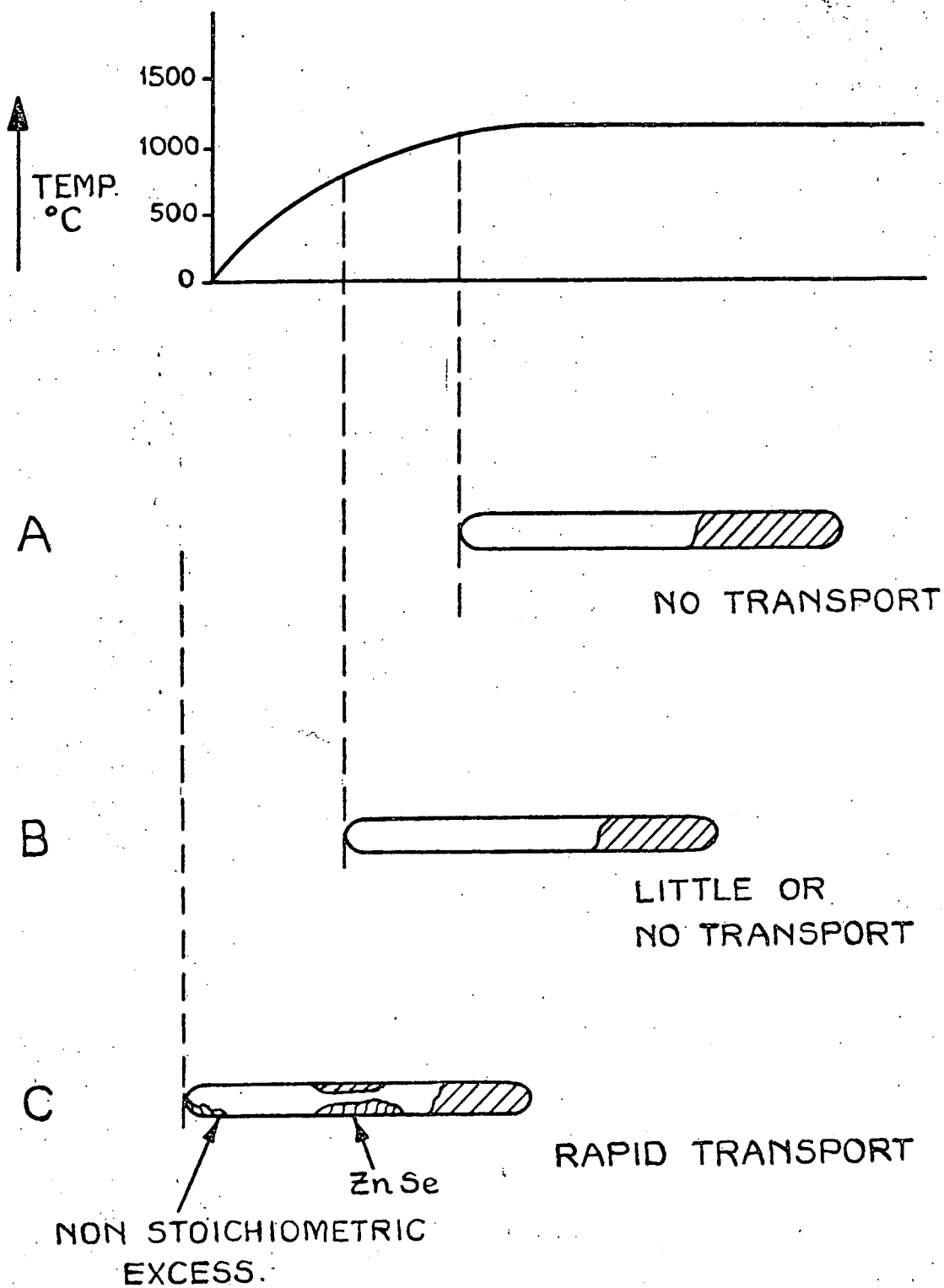
of gas throughout, the value of A rapidly becomes extreme in the cooler regions of the tube. The pressure of the minority component is then so small that $P_{MAJ} \simeq P_T$. This is the situation in Figures 4.6.1a and b. However, when the tube is withdrawn far enough from the furnace, $P_{MAJ}$ will exceed the saturated vapour pressure of the excess element at the coldest part of the tube. The vapour of the element then begins to condense until $P_{MAJ}(\simeq P_T)$ = Saturated Vapour Pressure of the element. In this condition $P_T$ is fixed by the maximum value $P_{MAJ}$ can take, and lowering the temperature of the cold end of the tube brings about a rapid increase in the transport rate as $P_{MIN}$ is approached and the vapour pressure of the minority component increases. When the temperature of the cold end of the tube is such that both constituent elements have a vapour pressure at the cold end which is small relative to $P_{MIN}$, then the transport rate reaches its maximum. The value of $P_T$ cannot be the same throughout the tube and the approximation breaks down. Theoretically such a system should give transport rates which are similar to those in a continuously pumped system. In fact, this is not realised in practice because residual gas and adsorbed impurities raise the background pressure in the sealed tube. However, in the ZnSe system a rapid increase in transport rate definitely occurs when the saturated vapour of selenium at the cold end of the tube approaches 1/3 $P_{MIN}$.

4.7    Application of Theory to Vertical Crystal Growth Tube with

Reservoir

The capsule plus reservoir used in the vertical system combines some of the features of the simple sealed capsule with some of those of the long tube emerging from the furnace. To obtain the maximum mass transport in the crystal growth tube (such conditions will not necessarily produce the best crystals) the vapour over the charge should be

maintained at $P_{MIN}$ throughout the growth run. The partial pressure of zinc in the system would be $^2/3\ P_{MIN}$ and that of selenium would be $^1/3\ P_{MIN}$. The temperature of the reservoir was usually adjusted to maintain the corresponding pressure of whichever element was placed in the reservoir. In practice something approaching $P_{MIN}$ must have been obtained in the capsule because the crystals grew at a reasonable rate.

However, because the system has given good results with CdSe, CdS, ZnSe, ZnS and ZnTe, and often works effectively when considerable quantities of dopants are added, it is of interest to examine why the system works so well, and to discuss the order of magnitude of the deviation from the ideal case which should affect the transport of material.

Clearly the pressure of the element in the reservoir cannot be directly imposed on the charge evaporating in the capsule because under normal conditions there is a significant pressure difference between the capsule at $P_{MIN}$ and the reservoir at $^1/3$ or $^2/3\ P_{MIN}$ (for $Se_2$ or Zn) as appropriate. Gas must flow continuously down from the capsule to the tail because of this pressure difference. Fortunately the gas cools on its passage down the tail tube, and ZnSe is precipitated on the wall of the silica over a length of 200 - 300 mm, stopping a little before the reservoir. The value of $P_{Zn}^2\ P_{Se_2}$ at $700^{\circ}C$ is $\sim 10^{-17}$ (atmospheres)$^3$, so with a zinc reservoir held at $550^{\circ}C$ the equilibrium pressure of selenium at $700^{\circ}C$ is $10^{-13}$ atmospheres. For this reason the reservoir remains uncontaminated. 2 - 4 gms of material are transported to the tail during a typical growth run, which lasts approximately 10 days.

However, assuming laminar flow of the gas to the tail, a pressure difference of $\sim 10^{-3}$ torr will account for the observed rate of loss of material. Compared with the value of $P_{MIN}$ ( $\sim 10$ torr) this is negligible, and the system must therefore be virtually isobaric. This conclusion was

somewhat surprising, and it was necessary to devise an experiment to check it. In principle the idea was to pump continuously from the tail of a growth tube and discover whether or not the rate of loss of material to the tail increased very rapidly as any residual gas was removed. This experiment was performed by lengthening the usual tail tube, so that it extended below the tail furnace, and attaching a rotary pump to it via a flexible hose. No reservoir element was used. The result was most interesting. In 60 hours sufficient material had sublimed to the tail to block it completely, and a crystal had grown at the growth tip. Essentially a system closer to that originally used by Piper and Polich[26] had been obtained. This seems reasonable confirmation that there was a significant amount of unwanted gas present in a sealed-off capsule. This gas has not been identified so far, although spectroscopic studies prove that carbon monoxide is present. J.J. Murray et al.[21] have used a mass spectrometer to investigate the species evolved when sealed silica capsules are heated. When fabricated into capsules the silica supplied by some manufacturers released $4 \times 10^{-6}$ litres $cm^{-2}$ of hydrogen (measured at S.T.P.) when the silica was raised to a temperature of 1300 K, even though it had previously been baked at $600^{\circ}C$. This would correspond to a pressure of greater than 60 torr in a growth capsule at the normal growth temperatures we used. Our growth capsules with tails were made from electrically fused quartz tubing which would not have been subjected to heating by hydrogen during manufacture. However, the tubing was worked with propane gas flames to form the capsules, and then reheated quite severely during the sealing process and may well have absorbed hydrogen or OH radicals quite heavily during these processes.

Some of the gas may well be $SeO_2$. Evidence for this comes from comparison with CdS and ZnTe. Occasionally during a growth run the tail

furnace would fail. When this happened CdS and ZnSe charges were lost to the tail at the usual slow rate when the temperature of the tail reservoir fell to 100 - 200°C, but when this happened to a ZnTe tube the whole charge sublimed to the tail. This could be ascribed to the lower vapour pressure of $TeO_2$[22], which is of the order $10^{-15}$ torr at 200°C compared with 10 torr for $SeO_2$ and a boiling point of -10°C for $SO_2$[23].

The manner in which the tail reservoir acts in controlling the vapour pressure is difficult to analyse quantitatively. Experimentally, it is found that when $P_{RES} \simeq {}^2/3\ P_{MIN}$ in the case of a zinc reservoir, or $^1/3\ P_{MIN}$ for a selenium reservoir, the fastest transport takes place. If no impurities and no residual gas in the tube are assumed, then the mechanism of the controlling action of the reservoir may be examined for the two extreme cases $P_{RES} > P_{MIN}$ and $P_{RES} = 0$.

In the first case the pressure throughout the tube will be approximately that of the tail reservoir. The transport rate will be low, and controlled by the rate of diffusion of the minority component. It would be expected that only a small amount of the compound would form on the walls of the tail, and this is confirmed in practice. The pressure of the minority component can be calculated approximately by inserting the value of $P_{RES}$ into $K_p = P_{Zn}^2\ P_{Se_2}$. The velocity of the gas flow to the tail is very low, and the tail might be regarded as a separate long narrow capsule with a source at the nozzle and a crystal face close to the reservoir liquid.

When $P_{RES} \simeq 0$ the tail reservoir is cold; if it were cold enough, then the vapour pressure of any molecules landing would be negligible, and the system would be indistinguishable from a pump. Under these conditions the charge would start evaporating and rapidly approach $P_{MIN}$. The only obstacle to maximum transport would be the very light reduction in $P_T$ due to the flow out of the capsule through the nozzle, which

reduces the supersaturation at the growth face. This situation is illustrated in Figure 4.7.1.

The effect of the nozzle diameter is important in the case of the cold reservoir. If flow is by diffusion only, then the flow will be proportional to the radius of the tube squared. Assuming a nozzle 1 mm in diameter and 1 mm long, and an effective length for the tail of 250 mm (where the heaviest deposit of the compound occurs) with a diameter of 4 mm, it may be seen that the resistance of the nozzle is only ∼ 6%. However, if the flow is laminar as seems likely in the case of the cold reservoir, then the flow is proportional to $(radius)^4$ giving it a resistance of more than 50% of the total. In this case the nozzle size plays a significant part in deciding how much of the charge is lost to the tail.

As the temperature of the reservoir is increased, the vapour pressure of the element in the reservoir increases, resulting in the compound being precipitated further up the tail tube. In the steady state, atoms of each element must be lost at an equal rate down the capsule, and so the partial pressure in the capsule of the reservoir element must increase slightly to balance the greater rate of diffusion towards the capsule of the majority component in the tail. At low tail pressures the pumping effect of the flow of gas away from the capsule will make the effect very small. However, the value of $P_T$ in the capsule must start to deviate significantly from $P_{MIN}$ when the partial pressure of the reservoir element in the tail exceeds that corresponding to $P_{MIN}$ in the capsule. As the temperature of the reservoir is increased, the point of precipitation of zinc selenide moves closer to the capsule. The net result of the argument is that a selenium reservoir must give a selenium rich atmosphere and a zinc tail a zinc rich atmopshere, even when the selenium

CONCENTRATION OF ZINC AND SELENIUM IN THE VAPOUR PHASE.

Fig.4:7:1.
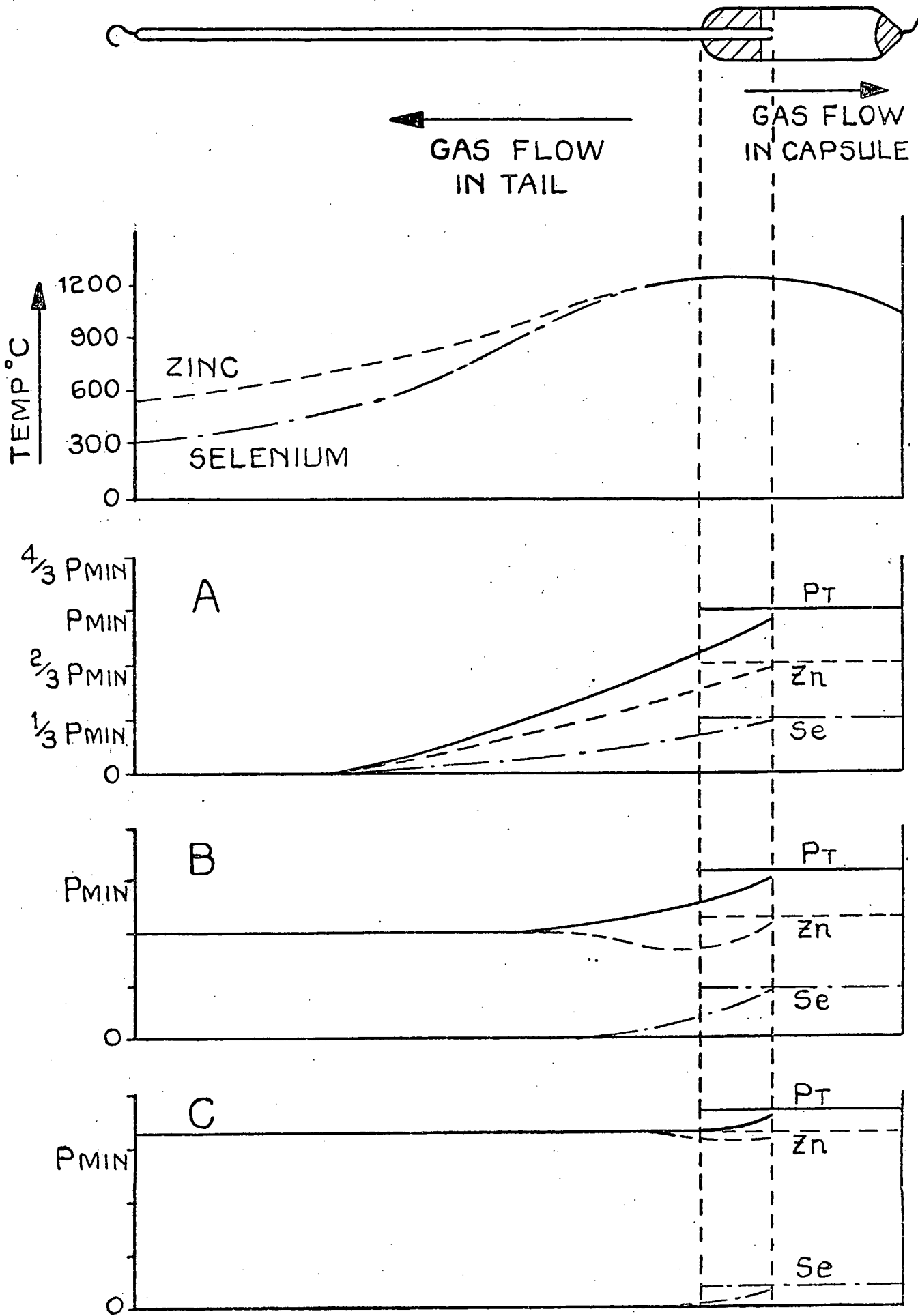
reservoir is at a pressure of $^1/3$ $P_{MIN}$ or the zinc reservoir at $^2/3$ $P_{MIN}$, although the deviation is likely to be small.

This argument also indicates that transport should be fastest when the tail reservoir is cold; this was not found in practice. This is because of the background gas in the system which has so far been ignored, and which affects the growth with a cold tail, (when a large gas flow would otherwise be expected), much more than the growth with a hot tail (when the flow is always small). The flow down the tail of a crystal growth tube is partly attributable to Stefan flow and partly to diffusion. An experimental confirmation of the importance of the Stefan flow contribution was provided by an experiment attempting to grow ZnS in a tube from which the nozzle to the tail reservoir had been removed. Instead of losing the usual 2 - 4 gms of material to the tail, most of the 15 gm charge was lost, blocking the tail completely. If flow had been by diffusion only, the loss would have increased by less than 10%. (It was shown above that the nozzle contributes $\sim 6\%$ resistance in the diffusion only case). As the tail is heated the element in it melts. At this point it is possible that a number of the impurities are removed by dissolution in the reservoir liquid leaving mainly inert gas, which should improve transport considerably. Further, because there is always a plentiful supply of majority molecules available the minority component molecules flowing from the capsule should be rapidly precipitated as the compound, giving good control of the capsule stoichiometry which will be a little rich in the majority element. ZnSe is precipitated in the tail closer to the capsule. However, when the tail is cold the flow will partly break up into the diffusion of the two separate elements through the inert gas or impurities. Under these conditions Zn molecules would diffuse faster than $Se_2$ molecules. (A ratio of 1.5 is obtained from

the square root of the densities). Again, if some of the gas does not reform into ZnSe, but diffuses further down the tail to crystallise in elemental form, the $Se_2$ has further to travel. These considerations would lead to a selenium rich atmosphere in the capsule with a cold tail. Thus the action of the tail is described qualitatively; to obtain more information a mathematical model is required.

## 4.8 A Mathematical Model of the Transport Processes

Having established in Section 4.7 that there is a significant pressure of uncontrolled gas in the system, it is necessary to investigate transport in the presence of an inert gas. Constant pressure is assumed throughout the system. Using the same notation as in Section 4.1, it is possible to write down the transport equations for zinc and selenium For zinc:

$$\frac{2}{3} J_T = \frac{N_T}{N_T} \cdot U N_{Zn} - D \cdot \frac{d N_{Zn}}{dx} \qquad (4.8.1)$$

But $\qquad J_T = U N_T$ ,

so

$$J_T \left( \frac{2}{3} - \frac{N_{Zn}}{N_T} \right) = - D \frac{d N_{Zn}}{dx} \qquad (4.8.2)$$

and

$$\int_0^{\ell} \frac{J_T}{D \cdot N_T} \cdot dx = \int_{N_{Zn}(0)}^{N_{Zn}(\ell)} \frac{3}{3 N_{Zn} - 2 N_T} \cdot d N_{Zn} \qquad (4.8.3)$$

where $N_{Zn}(\ell)$ is the value of $N_{Zn}$ at $x = \ell$, and

$N_{Zn}(0)$ is the value of $N_{Zn}$ at $x = 0$ .

This gives

$$\frac{J_T \ell}{D \cdot N_T} = \ln \left\{ \frac{(3N_{Zn}(\ell) - 2N_T)}{(3N_{Zn}(0) - 2N_T)} \right\} = \frac{U\ell}{D} \qquad (4.8.4)$$

For selenium a similar treatment can be used, and

$$\frac{1}{3} J_T = U N_{Se_2} - D \cdot \frac{d N_{Se_2}}{dx} \qquad (4.8.5)$$

gives

$$\frac{J_T \ell}{D \cdot N_T} = \ln \left\{ \frac{(3N_{Se_2}(\ell) - N_T)}{(3N_{Se_2}(\ell) - N_T)} \right\} = \frac{U\ell}{D} \qquad (4.8.6)$$

In passing it is interesting to enquire what happens if

$$N_T = N_{Se_2} + N_{Zn} \qquad , \qquad (4.8.7)$$

then

$$\exp \frac{U\ell}{D} = \left\{ \frac{2N_{Se_2}(\ell) - N_{Zn}(\ell)}{2N_{Se_2}(0) - N_{Zn}(0)} \right\} \qquad (4.8.8)$$

$$= \frac{N_{Zn}(0)}{N_{Zn}(\ell)} \cdot \left\{ \frac{2\frac{N_{Se_2}(\ell)}{N_{Zn}(\ell)} - 1}{2\frac{N_{Se_2}(0)}{N_{Zn}(0)} - 1} \right\}$$

But

$$N \cdot R T = P V$$

so N is proportional to P

and

$$\frac{N_{Se_2}(\ell)}{N_{Zn}(\ell)} = A_\ell \quad , \quad \frac{N_{Se_2}(0)}{N_{Zn}(0)} = A_o \quad .$$

Further

$$\frac{P_T}{A + 1} = P_{Zn} = k N_{Zn}$$

where k is a constant.

Substitution in 4.8.8 gives

$$\exp \frac{U \cdot \ell}{D} = \left\{ \frac{A_o + 1}{A_\ell + 1} \right\} \cdot \left\{ \frac{2A_\ell - 1}{2A_o - 1} \right\}$$

which is equation 4.1.18 again.

Reverting to the more general problem with a finite value of $P_T$, equations 4.8.4 and 4.8.6 lead to

$$\exp \frac{U\ell}{D} = \frac{3P_{Zn}(\ell) - 2P_T}{3P_{Zn}(0) - 2P_T} = \frac{3P_{Se_2}(\ell) - P_T}{3P_{Se_2}(0) - P_T} \qquad (4.8.9)$$

The values of $U$, $\ell$ and $D$ are known, so to determine conditions at the growth face it is necessary to obtain values for $P_{Se_2}(\ell)$, $P_{Zn}(\ell)$ and $P_T$.
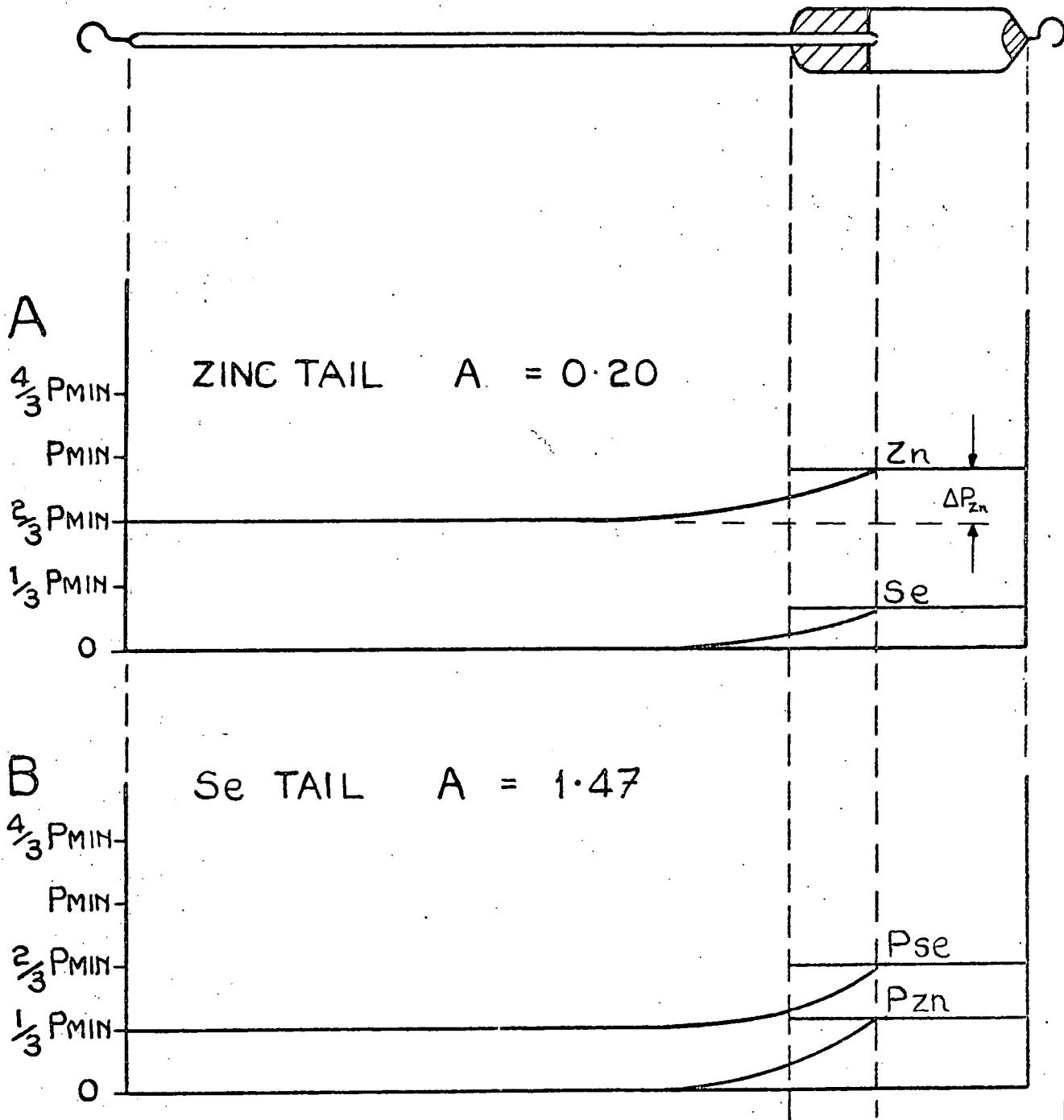
A simple method by which to obtain $P_{Se_2}(\ell)$ and $P_{Zn}(\ell)$ is to assume that the pressure of inert gas is so high that material is lost to the tail by diffusion only. This may be achieved in practice by deliberately admitting inert gas, e.g. argon to a pressure $> 10\ P_{MIN}$. The two elements will then diffuse to the tail and the partial pressures in the capsule would adjust themselves so that equal numbers of zinc and selenium atoms left the capsule (i.e. twice as many molecules of zinc as selenium). To formulate this mathematically, let the subscripts CAP and TAIL stand for capsule and tail respectively, and

$$V = \frac{P_{Se\ TAIL}}{P_{MIN}} \quad \text{and} \quad W = \frac{P_{Zn\ TAIL}}{P_{MIN}} \qquad (4.8.10)$$

The diffusion coefficient of zinc is assumed to be 1.5 times that of selenium because of the difference in mass of the molecules. The diffusion rate of zinc is proportional to $\Delta P_{Zn}$ (Fig.4.8.1), and must be

# TUBE FILLED WITH INERT GAS ~10 $P_{MIN}$

## Fig. 4:8:1

**A**

$\frac{4}{3}$ $P_{MIN}$

ZINC TAIL      A = 0·20

$P_{MIN}$

$\frac{2}{3}$ $P_{MIN}$

Zn

$\Delta P_{Zn}$

$\frac{1}{3}$ $P_{MIN}$

Se

0

**B**

Se TAIL      A = 1·47

$\frac{4}{3}$ $P_{MIN}$

$P_{MIN}$

$\frac{2}{3}$ $P_{MIN}$

Pse

Pzn

$\frac{1}{3}$ $P_{MIN}$

0

twice the diffusion rate of selenium which is proportional to $P_{Se\ CAP}$.

Thus equating the rate of loss of atoms of each species, and allowing for the faster diffusion of zinc, gives

$$\Delta P_{Zn} = P_{Zn\ CAP} - P_{Zn\ TAIL} = \frac{2.0}{1.5} P_{Se\ CAP} \qquad (4.8.11)$$

which gives

$$P_{Zn\ CAP} = P_{Zn\ TAIL} + \frac{2.0}{1.5} P_{Se\ CAP} \qquad (4.8.12)$$

and

$$P_{Se\ CAP} = P_{Se\ TAIL} + \frac{1.5}{2.0} P_{Zn\ CAP} \qquad (4.8.13)$$

for a selenium tailed tube.

Therefore from (4.8.12) and (4.8.10)

$$P_{Zn\ CAP} - \frac{4}{3} P_{Se\ CAP} = W\ P_{MIN} \qquad (4.8.14)$$

But

$$\frac{4}{27} P^3_{MIN} = K_p = P^2_{Zn\ CAP}\ P_{Se\ CAP} \qquad (4.8.15)$$

so

$$\left( P_{Zn\ CAP} - \frac{4}{3} P_{Se\ CAP} \right)^3 = W^3 \frac{27}{4} P^2_{Zn\ CAP}\ P_{Se\ CAP} \qquad (4.8.16)$$

However,

$$A\ P_{Zn\ CAP} = P_{Se\ CAP}$$

so ,

$$\left( 1 - \frac{4}{3} A \right)^3 = W^3 . \frac{27}{4} A \qquad (4.8.17)$$

Similarly, for a selenium tail

$$\left( A - \frac{3}{4} \right)^3 = V^3 . \frac{27}{4} A \qquad (4.8.18)$$

By putting $W = \frac{2}{3}$ , A may be obtained when the reservoir is at the stoichiometric partial pressure for zinc. This yields a value of 0.20 for A. A similar calculation gives $A = 1.47$ for a selenium reservoir. A further interesting result is obtained by putting $A = \frac{1}{2}$ in (4.8.17) and (4.8.18) This gives $W = \frac{1}{6}$ and a negative value for V. Thus it is possible to obtain $P_{MIN}$ in the capsule using a zinc tail limited by diffusion. However, this can never happen with a selenium tail.

In Section 4.7 it was shown that the system, including the tail, is isobaric. This means that the transport equations (4.8.9) may be applied to the tail if suitable values of U, $\ell$ and D are inserted. The growth face in this case is a section of the tail tube about 100 mms long, but most of the deposition occurs in the first 40 mms, and the nozzle is regarded as the source. $P_{Se\ TAIL}$ and $P_{Zn\ TAIL}$ are known. If the tube has a zinc tail $P_{Zn\ TAIL} = \frac{2}{3} P_{MIN}$ and $P_{Se\ TAIL} = 0$, while if the reservoir contains selenium $P_{Se\ TAIL} = \frac{1}{3} P_{MIN}$ and $P_{Zn\ TAIL} = 0$. (See Figure 4.8.1) When these values are inserted into equations 4.8.9 for zinc and selenium, $P_{Zn\ TAIL} = P_{Zn}(0)$ and $P_{Se\ TAIL} = P_{Se_2}(0)$. This gives two equations with three unknowns, $P_{Zn}(\ell)$, $P_{Se_2}(0)$ and $P_T$. However $P_{Zn}(\ell)$ and $P_{Se_2}(\ell)$ are in close equilibrium with the solid source and so

$$Kp = P_{Zn}^2(\ell)\ P_{Se_2}(\ell) .$$

This relationship provides a third equation and the problem may be solved numerically. The following values have been used in the calculation.

(i)     Mass of Material lost to tail:- 4 gms.

This is a typical loss for a charge which was completely transported. Unfortunately no attempt was made to check whether capsules with zinc and selenium tails showed different weight losses. (N.B. when used in equations 4.8.9

and 4.1.18 the transport rate has a negative sign. See Figure 4.1.1).

(ii) Time 7 days:- the time the tube was in the furnace at $1160^{\circ}$C.

(iii) Diffusion Coefficient at N.T.P.:- 0.2 cms sec$^{-1}$, an estimate obtained from Faktor and Garret[3]. The difference between zinc and selenium has been ignored.

(iv) The diffusion coefficient in the growth tube was calculated from the expression

$$D = D_{STAN} \cdot \frac{P_{STAN}}{P_T} \cdot \left(\frac{T_A}{T_{STAN}}\right)^{1.8} \qquad (4.8.19)$$

An average value was used for $T_A$. This expression was also suggested by Faktor and Garrett.

(v) Charge temperature $1158^{\circ}$C. The usual furnace temperature was $1160^{\circ}$C and the charge was unlikely to have been at the hottest spot.

(vi) $T_A = 1000^{\circ}$C, average temperature of tail assuming condensation at $850^{\circ}$C.

(vii) $\ell = 30$ cms, the distance travelled by the material. See Figure 4.8.2. A representative value is taken, clearly it cannot be precise.

(viii) Cross-sectional area of tail tube 0.126 cm$^{-2}$.

(ix) $P_{MIN}$ in capsule 12.3 torr.

Using

$$P_{Se_2}(\ell) + P_{Zn}(\ell) = \frac{2}{3} \cdot P_{MIN} \cdot \left(A_\ell + 1\right) \cdot \left(\frac{1}{2A_\ell}\right)^{1/3} \qquad (4.8.20)$$

and

$$\exp\left(\frac{U\ell}{D}\right) = 0.585$$

# A TYPICAL CRYSTAL GROWTH TUBE AFTER USE.

## Fig: 4:8:2

ACTUAL SIZE 2:5



140-150

70

140

180

760

580

50

100

~50

CRYSTAL ~16GMS

NO DEPOSITION

140-180 DEPOSITION BEGINS

~50MMS LONG REGION OF THICKEST DEPOSITION

SMALL AMOUNT OF DEPOSITION

NO DEPOSITION

WHITE DEPOSIT

ELEMENT
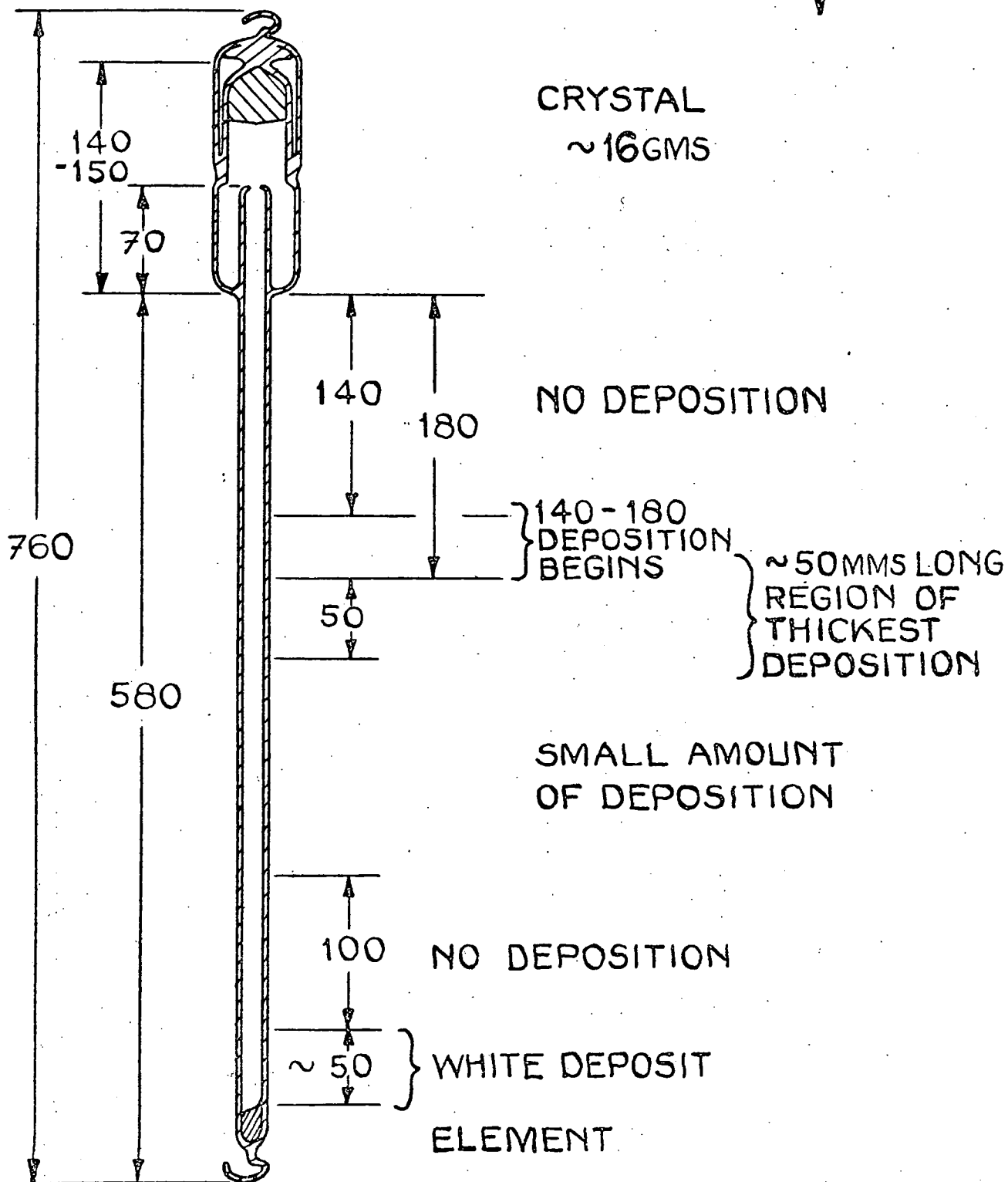
DIMENSIONS IN MILLIMETRES.

It is possible to write, for a selenium tailed tube,

$$P_T = 7.23 . P_{Se_2}(\ell) - 4.23 . P_{Se_2}(0) \tag{4.8.21}$$

and

$$P_T = 3.61 P_{Zn}(\ell) \tag{4.8.22}$$

By selecting a value of $A_\ell$ two values of $P_T$ may be calculated, one from (4.8.21) and one from (4.8.22). The average value of $P_T$ is substituted in these equations to obtain revised values of $P_{Zn}(\ell)$ and $P_{Se_2}(\ell)$, and hence obtain a better value for $A_\ell$. When the cycle is repeated rapid convergence results.

$$A_\ell = 0.85 \qquad P_{Zn}(\ell) = 4.40$$

$$P_{Se_2}(\ell) = 3.76$$

$$P_T = 15.90$$

Using the same value for $\exp \dfrac{u\ell}{D}$, analogous expressions may be derived for a zinc tailed tube .

$$P_T = 3.61 P_{Zn}(\ell) - 2.11 P_{Zn}(0) \tag{4.8.23}$$

$$P_T = 7.23 P_{Se_2}(\ell) . \tag{4.8.24}$$

They give

$$A_\ell = 0.264 \qquad P_{Zn}(\ell) = 6.50$$

$$P_{Se_2}(\ell) = 1.71$$

$$P_T = 12.39$$

The different values of $P_T$ are the result of using the same value of $|J|$ for both zinc and selenium tails. In fact it would be expected that $|J|$ would be larger for a selenium tailed tube because of the lower

pressure of the tail element.

Having obtained a value for $P_T$, it is now possible to obtain values for $P_{Se_2}(0)$ and $P_{Zn}(0)$ in the capsule and hence to calculate $A_o$. The value of $\exp\left(\frac{u\ell}{D}\right)$ in the capsule will be different of course. The following additional values were used to calculate $\left(\frac{u\ell}{D}\right)$ in the capsule.

(i)     Mass of material transported:- 16 gms.

N.B. J requires a negative sign because of the convention used.

(ii)    $\ell$:- 10 cms.

(iii)   Cross sectional area of capsule:- 0.95 $cm^2$.

Then $\exp \dfrac{u\ell}{D} = 0.82$ .

Assuming

$$P_T = 15.90$$
$$P_{Zn}(\ell) = 4.40$$
$$P_{Se_2}(\ell) = 3.76$$

selenium tail $A_\ell = 0.85$

then,

$$P_{Zn}(0) = 3.04$$
$$P_{Se_2}(0) = 3.39$$

$A_o = 0.89$

Assuming

$$P_T = 12.39$$
$$P_{Zn}(\ell) = 6.50$$
$$P_{Se_2}(\ell) = 1.71$$

zinc tail $A_\ell = 0.264$

$$P_{Zn}(0) = 6.12$$
$$P_{Se_2}(0) = 1.19$$

$A_o = 0.194$

However, if no inert gas were present, in the selenium tailed tube;

$$P_T = 8.16$$
$$P_{Zn}(0) = 4.19$$
$$P_{Se_2}(0) = 3.97$$

$A_o = 0.95$

If no inert gas were present $\Delta T$ could be read directly from Figure 4.4.1 using the curve for $1150°$. The other values may be ready by interpolating between the isobars to find the correct position for $P_{Zn} + P_{Se_2}$.

However, a more accurate value can be calculated using the equation

$$\frac{d \log_{10} K_p}{dT} = -\frac{37500}{T^2} \qquad (4.8.25)$$

i.e.

$$\Delta T = 54 \log_{10} \left\{ \frac{P_{Zn}^2(\ell) \, P_{Se_2}(\ell)}{P_{Zn}^2(0) \, P_{Se_2}(0)} \right\} \qquad (4.8.26)$$

The following values were then obtained; with the zinc tailed tube $\Delta T = 11.6°C$, and for the selenium tailed tube $\Delta T = 19.7°C$.

However, if no inert gas were present in the selenium tailed tube, the calculated value of $\Delta T$ is reduced to $1.15°C$, which is clearly too low and confirms the conclusion that inert gas must have been present.

The most uncertain quantity in the calculation is the value of the diffusion coefficient $D_{STAN}$. If the selenium and the zinc are diffusing through lighter molecules then the value of 0.2 would not appear unreasonable. However, if the data of Toyama and Sekiwa[24] is used assuming the gases present to be zinc and diatomic selenium, then the coefficient is approximately 0.1. To check the effect of this variation the analysis was repeated using a value of 0.1 for the diffusion coefficient. The results are tabulated in Table 4.8.1. Their chief features are the value of $P_T$, which indicates a pressure of approximately 5 torr inert gas in the capsule and the difference in the values of $\Delta T$, none of which vary very much from the original estimate from experiments of $\sim 20°C$.

| Source of C and B | D cm²s⁻¹ | a | b | $P_{MIN}$ Torr | $P_{Zn}(\ell)$ Torr | $P_{Se}(\ell)$ Torr | $P_T$ Torr | $P_{Zn}(0)$ Torr | $P_{Se}(0)$ Torr | $A_\ell$ | $A_O$ | $\Delta T$ °C | Reservoir Element |
|---|---|---|---|---|---|---|---|---|---|---|---|---|---|
| A + P | 0.2 | 37153 | 19.8 | 7.875 | 6.50 | 1.71 | 12.39 | 6.12 | 1.19 | 0.264 | .194 | 11.6 | Zn |
|  |  |  |  |  | 4.40 | 3.74 | 15.91 | 3.04 | 3.39 | 0.849 | 1.12 | 19.6 | Se |
| K + R Theory | 0.2 | 39100 | 19.4 | 3.281 | 2.71 | 0.71 | 5.16 | 2.55 | 0.49 | 0.264 | .194 | 11.6 | Zn |
|  |  |  |  |  | 1.83 | 1.56 | 6.63 | 1.27 | 1.41 | 0.849 | 1.12 | 19.6 | Se |
| K + R Expt. | 0.1 | 38260 | 20.24 | 9.811 | 8.10 | 2.13 | 15.43 | 7.62 | 1.47 | 0.264 | .194 | 11.6 | Zn |
|  |  |  |  |  | 5.48 | 4.65 | 19.81 | 3.79 | 4.23 | 0.849 | 1.12 | 19.6 | Se |
| A + P | 0.1 | 37153 | 19.8 | 7.875 | 5.92 | 2.06 | 9.41 | 5.75 | 1.54 | .348 | 0.268 | 8.2 | Zn |
|  |  |  |  |  | 4.71 | 3.26 | 10.75 | 3.52 | 3.10 | .691 | 0.88 | 14.9 | Se |
| K + R Theory | 0.1 | 39100 | 19.4 | 3.281 | 2.47 | 0.86 | 3.92 | 2.40 | 0.64 | .348 | 0.268 | 8.2 | Zn |
|  |  |  |  |  | 1.96 | 1.36 | 4.48 | 1.47 | 1.29 | .691 | 0.88 | 14.9 | Se |
| K + R Expt. | 0.1 | 38260 | 20.64 | 9.811 | 7.38 | 2.57 | 11.72 | 7.16 | 1.92 | .348 | 0.268 | 8.2 | Zn |
|  |  |  |  |  | 5.87 | 4.06 | 13.39 | 4.38 | 3.86 | .691 | 0.88 | 14.9 | Se |

Table 4.8.1:    Calculated Values of Partial Pressures and $\Delta T$ Inside a Crystal Growth Tube.

Table 4.8.1: Continued

Note $\quad P_{MIN} = \frac{3}{2} (2 \text{ Kp})^{\frac{1}{3}}$

where $\log_{10} \text{Kp} = -\frac{a}{T} + b$.

Values of a and b were derived from Aven and Prener[17] (A + P) and Kirk and Raven[18] (K + R). There are two pairs of values from Kirk and Raven, their experimental values, and their experimental values modified by theoretical considerations (Expt. and Theory in table). Because the line has been extrapolated quite considerably the factor of 3 divergence is not surprising. The values of $A_\ell$ and $A_o$ are independent of the value of $P_{MIN}$ because of the initial assumption that the tail reservoir pressure was $\frac{2}{3} P_{MIN}$ (Zn) or $\frac{1}{3} P_{MIN}$ (Se) as appropriate. (See Appendix 4).

Two main conclusions can be drawn from this mathematical analysis.
Firstly, some inert gas is necessary in the system. If it were not
present much of the charge would be lost to the tail reservoir. The
gas also helps to ensure that the growth is mainly transport limited.
Secondly, although the calculated values of $\Delta T$ have quite a spread, they
nevertheless indicate that most, if not all, of the experimentally
observed temperature difference is necessary to sustain the observed
transport rate. This implies that the growth rate is limited mainly
by the transport in the capsule rather than surface kinetics. However
the calculation does not give sufficient precision to dismiss completely
the effect of the processes at the growth face.

### 4.9 The Effect on the Growth Rate of Doped and Non-Stoichiometric Charges

If the charge were non-stoichiometric and the excess were released
at a steady rate throughout the growth run, while the crystal grew with
perfect stoichiometry, then the gas lost to the tail would no longer
contain equal numbers of metal and non-metal atoms. Suppose there were
a non-stoichiometry of 1000 p.p.m., then $\frac{1}{2}$ - 1% of the material lost
through the orifice would be non-stoichiometric excess. This corresponds
to a change in the value of A of 0.005 - 0.01, which would not have a
noticeable effect on the growth rate. (A was found in 4.8 to be of the
order 0.26 for a tube with a zinc tail and 0.85 for one with a selenium
tail).

In practice the charge is extremely unlikely to contain so much
non-stoichiometric material, because this is far outside the existence
range of the material, and could only be present in the form of pre-
cipitates. However, a similar effect would arise from the diffusion of
impurities through the capsule wall or out of the silica during a growth

run. Larger quantities of unwanted material may be removed from the capsule before growth commences without affecting the efficiency of the transport. For example, when 1 gm of excess zinc was added to the charge it sublimed to the tail reservoir as soon as the temperature began to rise, because zinc boils at $985^{\circ}$C. A similar effect occurs when a dopant (e.g. manganese) is added to the charge in the form of a powder, so that it reacts immediately upon heating to displace either zinc or selenium (e.g. manganese displaces zinc). The displaced element is rapidly transferred to the tail, and no longer affects the stoichiometry. It should be noted though, that any impurity in the charge which depressed $K_p$ would slow transport not only because of the lower $P_{MIN}$ over the source, but also because the reservoir temperature would be too high and would create a non-stoichiometric vapour, which would suppress transport.

## 4.10    The Variation of Growth Conditions During a Growth Run

A final point on the action of the tail comes from a consideration of the effect of evaporation on the solid. Normally selenium comes off the charge of zinc selenide when it is first heated up; a similar effect occurs with sulphur and CdS. Buckley[25] observed that when thin films of CdS were grown by evaporation in a vacuum system, the conductivity of the deposited films increased with their thickness, or the time for which the material had been evaporating. It would appear that as CdS or ZnSe is heated, the solid in equilibrium with $P_{MIN}$ deviates from a lattice with equal numbers of metal and non-metal atoms, to one with an excess of non-metal vacancies. In a growth tube with a tail, the initial burst of sulphur or selenium is lost to the tail quite quickly and the solid charge comes to equilibrium with the vapour in the capsule, which will be slightly rich in the reservoir element.

The surface of the charge will clearly do this quite rapidly, but the inside will take a time which depends on the rate of diffusion of selenium vacancies from the surface. To obtain an order of magnitude estimate of the equilibriation time it may be noted that $1\frac{1}{2}$ - 2 mm thick Hall samples can be made conducting by solvent extraction in liquid zinc at $850^{\circ}$C in a few days. At $1150^{\circ}$C the time necessary should be reduced to a few hours. If it is assumed that non-metal vacancies must diffuse in to make ZnSe conducting, at the same time as impurity atoms diffuse out, then the same time constants as for solvent extraction can be taken as the maximum for equilibriation. Because the charge is in a reverse temperature gradient for 1 - 2 days before the tube is pulled far enough for growth to start (Figure 3.1.1) it can be assumed the charge has mainly equilibriated with the vapour by the time growth begins. In consequence the growth should occur from a charge with a uniform composition. In contrast in a simple sealed capsule, growth occurs from a vapour which has an excess of one component. Because the excess element becomes more concentrated in the vapour over the growing crystal than in the vapour over the charge, the crystal must start growing further from stoichiometry than the charge and must finish growing closer to stoichiometry to conserve the number of atoms in the capsule.

## 4.11 Discussion of the Rate Limiting Mechanism within a Vertical Capsule

In the first ten sections of this chapter, an attempt has been made to build up a picture of what is happening inside a typical growth capsule used for producing a boule of a II-VI compound from the vapour phase. Many of the factors influencing the growth rate and quality of the crystals have been investigated. When these are considered in relation to the boules of ZnSe grown in the manner reported here, it is clear that

the evaporation of the charge, and the nucleation of growth steps are not

significant in limiting the process. The main rate limiting step appears

to be the transport process, with possibly an additional effect associated

with the condensation process. It has been suggested by Toyama and

Sekiwa[24] that at $1127^{\circ}C$ the growth of ZnSe is limited by the condensation

process. Using the capsule and reservoir system, the observed growth rate

roughly corresponds to calculated pressures of inert gas in the range

1 - 5 torr, and experimental values of $\Delta T$ near $20^{\circ}C$. The possible errors

in this calculation may be quite large, associated in particular with the

estimation of the magnitude of the diffusion coefficient, and thus the

condensation process may have some significance in limiting the growth rate.

However, the transport process is the dominant mechanism. The boules

which grew fastest all showed convex growth faces, which are usually inter-

preted as indicating diffusion controlled growth[4]. Slower growing

boules were often facetted, and did not reach the full possible size. Many

had one or two grains, while larger boules often contained more. Compari-

sons of these results with those obtained growing crystals of CdS and ZnS,

which are discussed further in Chapter 5, is interesting. At $1150^{\circ}C$, CdS

crystals often grew singly, while pure ZnS transported reasonably well,

but only produced an agglomeration of dendritic needles. Boules of ZnS,

ZnSe and CdS are compared in Figures 4.11.1 A to E. Ballentyne and

Tempest[6] investigated the growth of ZnS and CdS at similar temperatures,

and concluded that CdS grew under diffusion limited conditions, while the

growth of ZnS was condensation limited. The results from our capsule and

reservoir system agree well with their findings, and put ZnSe somewhere

between the two. The higher probability of CdS boules growing as single

crystals may be due either to the hexagonal structure of CdS, or to the

ZnSe growing under partly condensation controlled conditions. It is

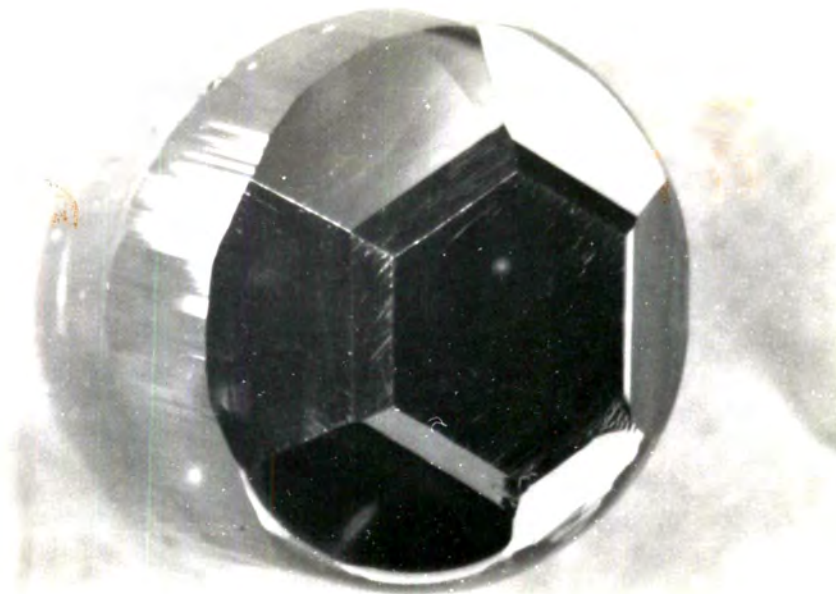interesting to note that the rate of loss of material from the capsule

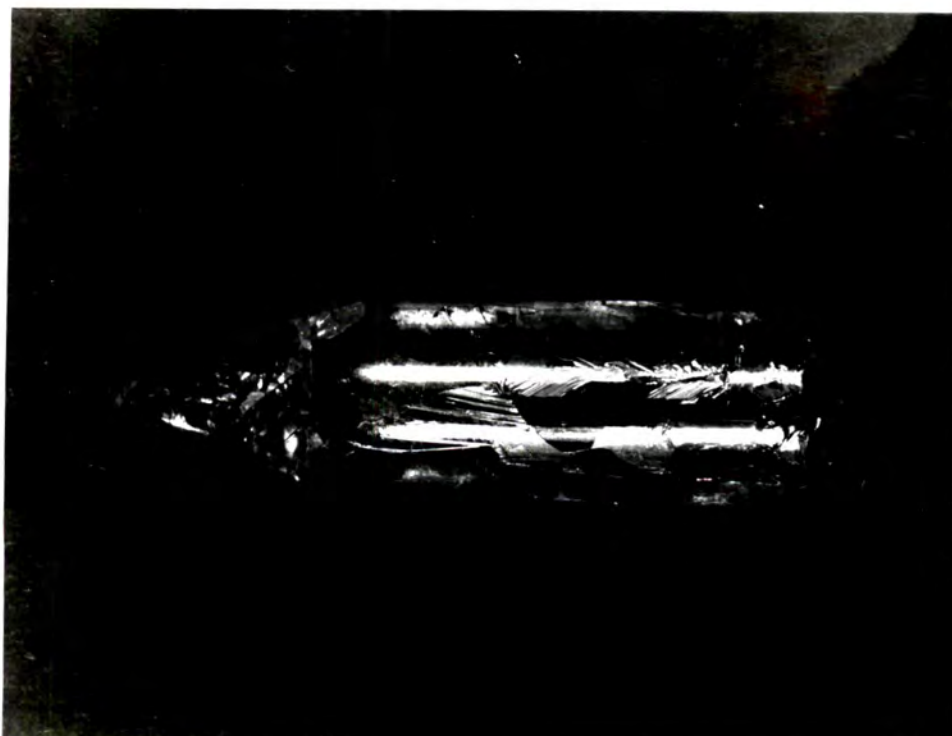Figure 4.11.1    Some boules grown in the vertical growth system.
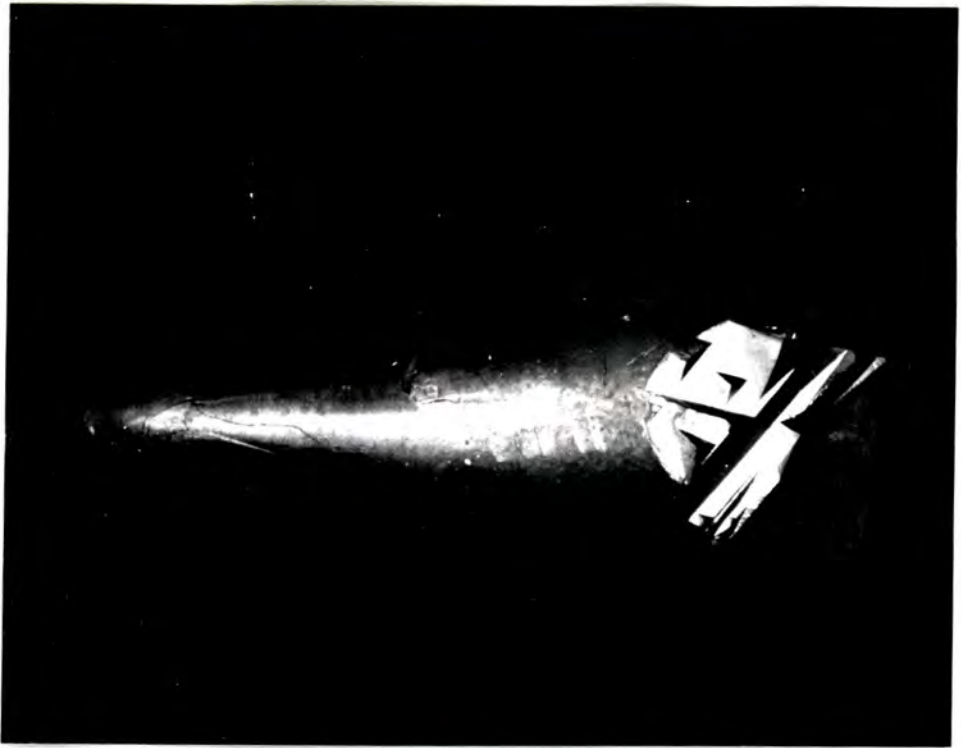


A.   CdS boule



B.   Domed end of CdS boule

C. CdS boule with facetted growth face showing six-fold symmetry.



D.   ZnSe boule

Figure 4.11.1:   Continued

E.   Facetted ZnSe boule showing characteristic triangular
     growth features.
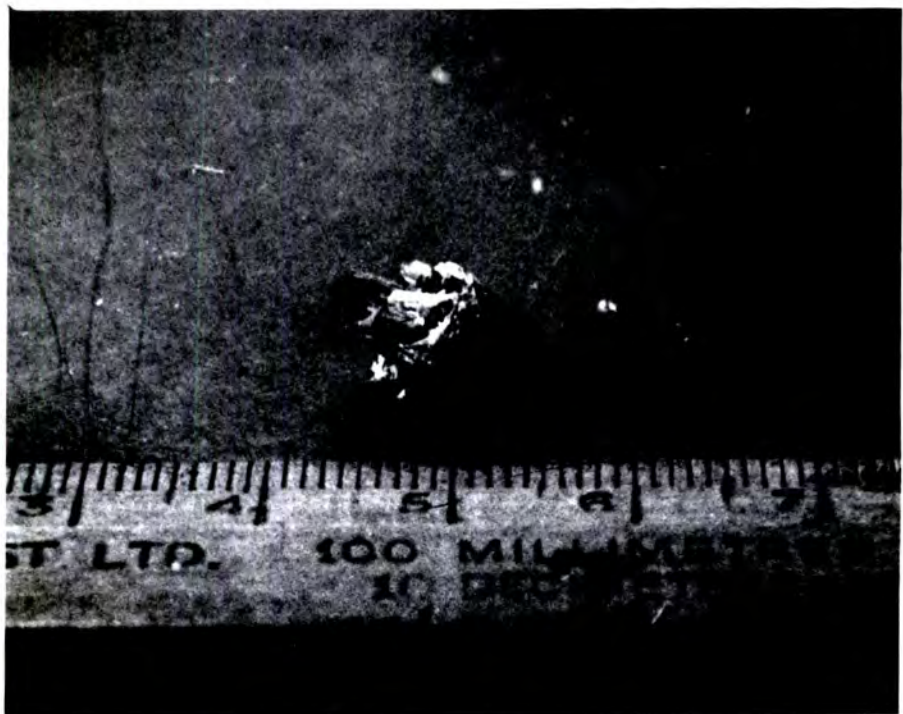


F.   ZnS boule.  The formation of spikes is attributed to
     condensation limited growth.

Figure 4.11.1:   continued

to the tail was similar for CdS, ZnSe and ZnS, suggesting that an unknown
inert gas was present when all the compounds were grown. (Preliminary
experiments indicated that the gas was carbon monoxide). The ZnSe crystals
which did not attain the maximum growth rate (the case examined in
Section 4.8) were probably grown in a regime closer to diffusion limita-
tion initially, but as $\Delta T$ increased during the run so that the temperature
of the growth face was lowered, the growth may well have stopped when
condensation limitation became important. It is not suggested that the
presence of growth facets proves that growth is limited by condensation
processes. The equilibrium form of the crystals is, in general, facetted,
and a slow growth rate will lead to this morphology. However, it is
believed that the break-up of growth into a mass of dendritic needles as
occurred with ZnS does indicate that condensation limitation is important.
If growth is completely condensation limited then the growth rate of the
crystal will increase with increasing temperature. This leads to an effect
analogous to constitutional supercooling. Any random protuberance from
the surface of a growing crystal will enter a warmer area and grow faster.
However, there is a difference between this effect and constitutional
supercooling; in the latter case the latent heat of fusion increases the
temperature of the projection and slows the growth rate, whereas if the
growth rate is condensation limited, the heating effect increases the
growth rate and makes the system more unstable. Ballentyne et al.[4]
showed that growth under condensation limited conditions was undesirable
because it necessarily implies high levels of supersaturation which can
lead to the nucleation of more crystallites. This argument clearly shows
that condensation limitation must lead to unstable growth (unless there
are other very strong stabilising factors), and should be avoided unless
needle crystals are wanted. The ZnS needles had the cubic structure and
grew in a [111] direction (polarity not determined). In Chapter 5 the

growth of solid solutions of $ZnSe_{1-x}S_x$ is reported. As the concentration of sulphur was increased, growth continued quite well until $x > 0.6$ when needle crystals only were formed, and the morphology of the boule closely corresponded to ZnS. No intermediate facetted stage was observed, suggesting that the facets observed on ZnSe boules were attributable rather to growth rate than condensation limitation. It is interesting to speculate on the reason for the abrupt change in morphology of $ZnSe_{1-x}S_x$ boules when x exceeds 0.6. It would appear that the activation energy to decompose the $Se_2$ molecule, $E_{Se_2} < E_{SSe} < E_{S_2}$. The incorporation of sulphur into the boule would then occur most easily from the SSe molecules, and compositions with x a little greater than 0.5 could be obtained by the re-evaporation of $Se_2$ molecules. Smooth growth would stop when the amount of SeS declined too far to support the necessary growth rate. The growth rate would then be condensation limited and the instability would become large as the supersaturation increased because the pull rate exceeded the growth rate.

## 4.12    Conclusions

The growth of a crystal in a vertical tube with a tail reservoir has been analysed in rather crude terms. Nevertheless it has been demonstrated that the reservoir will correct for non-stoichiometry of the charge exceeding 1000 p.p.m. without a significant effect on the transport rate, and that a much greater quantity of volatile material may be removed if it is released as the system warms up, e.g. zinc released by the reaction between the charge and manganese. Further, it has been shown that the tail reservoir will not hold an exact vapour pressure over the material in the capsule, but one which depends on the physical dimensions of the system (which in turn control the velocity of the gas flow to the tail),

the amount of residual gas and the partial pressure of the element in the reservoir. It has been demonstrated that there is a considerable pressure of gas in the system ( $\sim$ 5 torr at temperature) which is neither zinc nor selenium, and that without this gas all the charge would sublime to the tail. An attempt has been made to estimate the total pressure $(P_T)$ of the gases in the system when the optimum transport was obtained. The equations

$$\text{Exp} \frac{u\ell}{D} = \frac{3P_{Zn}(\ell) - 2P_T}{3P_{Zn}(0) - 2P_T} = \frac{3P_{Se_2}(\ell) - P_T}{3P_{Se_2}(0) - P_T}$$

were used to describe the flow of gas to the tail from the capsule. For a tube with zinc in the reservoir it is possible to substitute $P_{Zn}(0) = \frac{2}{3} P_{MIN}$ and $P_{Se_2}(0) = 0$, similarly $P_{Se_2}(0) = \frac{1}{3} P_{MIN}$ and $P_{Zn}(0) = 0$ for a selenium reservoir. $K_p = P_{Zn}^2(\ell) P_{Se_2}(\ell)$ in each case. The equations have been solved numerically, and the most significant error was derived from the assumed value of $D_{STAN}$, the diffusion coefficient, which lies between 0.1 and 0.2 $cm^2 s^{-1}$. Values of $A_o$ and $\Delta T$ were therefore calculated for the two extreme values of $D_{STAN}$.

| D $cm^2 s^{-1}$ | Reservoir Element | $A_o$ | $\Delta T$ $^o$C |
|---|---|---|---|
| 0.2 | Zn | 0.194 | 11.6 |
| 0.2 | Se | 1.12 | 19.6 |
| 0.1 | Zn | 0.268 | 8.2 |
| 0.1 | Se | 0.88 | 14.9 |

The assumption of no residual gas leads to a value of $\Delta T \sim 1^o$C which is unacceptibly low, because this would imply that the boules which grew fastest did so under condensation limited conditions. This is clearly not true because the boules have smooth domed ends typical of diffusion

limited growth. Thus it is concluded that the fastest growing boules grew under transport limited conditions, and that this was due to the presence of an unknown inert gas. Runs in which total transport was not achieved produced boules which grew initially under diffusion limited conditions, but may have stopped growing under condensation limited conditions when $\Delta T$ grew large. The value of $A_\ell$ is maintained close to 0.5 when the tail temperature is set to give a partial pressure of the reservoir element corresponding to $P_{MIN}$ in the capsule, but the exact value is not precisely determined. Known partial pressures can be established away from $P_{MIN}$ using a reservoir of the major constituent element required in the vapour phase.

The reservoir essentially deals with large swings of the partial pressures in the capsule away from those to give $P_{MIN}$. It corrects large deviations quickly because of the increase in $P_T$ associated with such swings. The crystal itself can be grown with a different stoichiometry from the charge, and this remains constant throughout the growth period, unlike that of a crystal grown in a simple sealed capsule. Also a much wider range of dopants may be incorporated by adding them to the charge before growth is inhibited.

In general it would be expected that crystals grown using a selenium reservoir would grow faster than those with zinc reservoirs, because the vapour over the charge is kept closer to stoichiometry. Conditions should also be more stable, because $P_T$ increases faster with deviation from stoichiometry on the selenium rich side of $P_{MIN}$.

## CHAPTER 4

### REFERENCES

1. T B Reed and W J Lafleur (1964) Appl. Phys. Letts. 5 p.191-193

2. T B Reed, W J Lafleur and A J Strauss (1968) J. Cryst. Growth
3,4 p.115-121

3. M M Faktor and I Garrett 'Growth of Crystals from the Vapour
(Chapman and Hall London) Chapter 4

4. D W G Ballentyne, S Wetwatana and E A D White (1970) J. Cryst.
Growth 7 p.79-92

5. L Rouse and E A D White (1972) J. Cryst. Growth 17 .117-122

6. P A Tempest and D W G Ballentyne (1974) J. Cryst. Growth 21
p.219-226

7. L Clark and J Woods (1968) J. Cryst. Growth 3,4 p.127-130

8. K F Burr and J Woods (1971) J. Cryst. Growth 9 p.183-188

9. J R Cutter, G J Russell and J Woods (1976) J. Cryst. Growth
32 p.179-188

10. P D Fochs, W George and P D Augustus (1968) J. Cryst. Growth
3,4 p.122-125

11. G A Somorgai and D W Jepson (1964) J. Chem. Phys. 41 p.1394-1399

12. G A Somorgai and D W Jepson (1964) J. Chem. Phys. 41 p.1389-1393

13. J C Brice (1965) 'The Growth of Crystals from the Melt' (North
Holland Amsterdam) Chapter 2

14. N Cabrera and R V Coleman (1963) in 'The Art and Science of
Growing Crystals', Ed. J J Gilman (Wiley, New York)

15. F C Frank (1949) Discussions Faraday Soc. 5 p.48

16. P Bennema, R Kern and B Simon (1967) Phys. Status Solidi 19 p.211

17. M R Lorenz (1967) in 'Physics and Chemistry of II-VI Compounds'
Ed. M Aven and J S Prener (North Holland Amsterdam) p.103

18. D L Kirk and M S Raven (1976) J. Phys. D. 9 p.2015-2026

19. E Kaldis (1969) J. Cryst. Growth 5 p.376-390

20. L Hildisch (1968) J. Cryst. Growth 3,4 p.131-134

21. J J Murray, R F Pottie and R L Sander (1973) J. Mat. Sci. 8
    p.37-40

22. O Kubaschewski, E El Evans, C B Alcock 'Metallurgical
    Thermochemistry' 4th Edition (1967) (Pergamon Oxford)

23. G W C Kaye and T H Laby 'Table of Physical and Chemical Constants'
    13th Ed. (1966) (Longmans London)

24. M Toyama and T Sekiwa (1969) Japan J. Appl. Phys. 8 p.855-859

25. R W Buckley (1973) Ph.D. Thesis University of Durham

26. W W Piper and S J Polich (1961) J. Appl. Phys. 32 p.1278-1279

## CHAPTER 5

## ZINC SULPHO-SELENIDE AND THE GROWTH OF SOLID SOLUTIONS

### 5.1 Introduction

Work within the research group on zinc selenide L.E.D's. had yielded devices with electroluminescence emission ranging from yellow to red in colour depending on the dopant used. Similar results were found by several other workers, (see references 1-3). In an attempt to extend the range of colours towards the blue, Ozsan and Woods[4] studied Schottky diodes on single crystals of solid solutions of Zn(S,Se). They were able to obtain a reasonably intense green electroluminescence from devices on $ZnS_{0.6}Se_{0.4}$. To sustain work in this field it was necessary to produce boules of zinc sulpho-selenide from the vapour phase similar to the zinc selenide boules described in Chapters 3 and 4. The work is particularly interesting because although ZnSe can just be grown by the technique, it is very difficult to grow ZnS because of the higher temperatures needed. While there is no doubt that the furnace could be modified to provide a higher temperature, the quartz ampoules used are found to collapse at $1200^{\circ}C$, and so to extend the technique to this temperature some means of reducing the pressure difference between the inside and outside of the capsule would be required. Although $P_{MIN}$ for ZnS is only reduced by a factor of two compared with ZnSe, and a satisfactory rate of transport has been obtained experimentally, the resultant boules were only an agglomeration of dendritic needles. Powder photographs showed these needles to have the cubic structure. It would appear that the boule growth is limited by the kinetics of the growth inter-face to an impractical rate in the system used. The value of $\Delta T$ was rather larger than that for ZnSe, although it was probably less than $50^{\circ}C$. Thus the indications are that the growth rate was limited by the activation. energy of adsorption on the growth face.

The additional problems in the growth of solid solutions arise from the extra component. This could lead to separation of the components during crystal growth, giving a varying composition through the boule, or a composition different from that intended. Crystals of $ZnSe_xS_{1-x}$ were of particular interest to the group, but a few boules of $ZnSe_xTe_{1-x}$ and $CdS_xS_{1-x}$ were grown to gain experience with mixed crystals; this was done because ZnSe, ZnTe, CdS and CdSe can all be transported much more easily than ZnS. In fact $CdSe_xS_{1-x}$, $ZnSe_xTe_{1-x}$ and $ZnSe_xS_{1-x}$ were all found to transport easily at $1150-1165^{\circ}C$, and there was no change of colour along the length of the boule, which indicated a reasonably consistent composition. With $ZnSe_xS_{1-x}$ the composition $ZnSe_{0.4}S_{0.6}$ was found to be as far as it was possible to go towards ZnS before the quality of the boule deteriorated and the distillate became a mass of dendritic needles. The composition is a very convenient 50% mixture by weight of ZnSe and ZnS.

## 5.2 Some Theoretical Aspects of the Growth of Solid Solutions

As remarked in 5.1, the main problem in the growth of solid solutions is likely to be the separation of the two compounds involved during crystal growth. This could occur for two reasons; firstly the thermodynamics of the source and crystal interfaces, and secondly the physical nature of the transport system, may aid the separation of the components. In particular, molecules of different masses have different densities and diffusion rates. The difference in density can cause a vertical separation of components according to Archimedes' principle. Naturally this can lead to one element being transported more efficiently than another in a vertical system.

The thermodynamics of the simple binary system are straightforward,

and are described by the equations

$$Kp = P_M^2 P_N \; ,$$

and

$$-RT \ln Kp = G$$

where R, T and Kp have their usual meanings and G is the Gibbs' Free Energy of dissociation. At the temperature of crystal growth ($\sim 1100^{\circ}$C) the compounds appear to interdiffuse freely, which means that the solid solution has a lower energy state than a mixture of the two separate compounds. Expressing this mathematically ,

$$G_{M(N1)_x(N2)_{1-x}} < X \, G_{M(N1)} + (1-x) \, G_{M(N2)} \qquad (5.2.1)$$

Let Kpn represent some average value of Kp that may be ised for the solid solution. It has been observed that transport of the solid solution is easier than the transport of ZnS, which suggests that in the $ZnSe_xS_{1-x}$ system Kpa $>$ Kp(ZnS) for all x. This situation is illustrated graphically in Figure 5.2.1 for the systems $ZnSe_xTe_{1-x}$ and $ZnSe_xS_{1-x}$. $Log_{10}$ Kp is plotted against composition for the systems at $1150^{\circ}$C. ($Log_{10}$ Kp is proportional to $\Delta G$ at a fixed temperature). Line A represents

$$\ln Kpa = X \, \ln Kp \, (Zn \, N1) + (1-X) \, \ln Kp \, (ZnN2) \qquad (5.2.2)$$

while line B is an estimate based on the knowledge that the curve must be sublinear for a stable solid solution, but $\Delta G$ ($ZnSe_xS_{1-x}$) $>$ $\Delta G$(ZnS) to give the observed rate of transport.

The greatest difficulty in analysing the system is to estimate the composition of the gas in equilibrium with a solid solution of a particular composition. In this respect a system with two metals is simpler than one with two non-metals. This is because the vapour over

$(M1)_x(M2)_{1-x}N$ will contain three main constituents (M1),(M2) and N, while the vapour over $M(N1)_x(N2)_{1-x}$ will contain four main constituents, M, $(N1)_2$, $(N2)_2$ and $(N1)(N2)$. The pressure of $(N1)_2$ and $(N2)_2$ is related to the pressure of $(N1)(N2)$ by the equation

$$Ky = \frac{P_{(N1)_2}\ P_{(N2)_2}}{P^2_{(N1)(N2)}} \tag{5.2.3}$$

Consider a mixture of X parts ZnS to (1-X) parts of CdS (parts atomic metal) used as a charge in a capsule. When the capsule is first heated up, the vapour pressure over the mixture would be governed initially by the dissociation of the two binary sulphides

$$Kp(CdS) = P^2_{Cd}\ P_{S_2}$$

and

$$Kp(ZnS) = P^2_{Zn}\ P_{S_2}.$$

Because $P_S$ is the same in each equation

$$\frac{P_{Cd}}{P_{Zn}} = \left(\frac{Kp\ (CdS)}{Kp\ (ZnS)}\right)^{\frac{1}{2}} \tag{5.2.4}$$

which is of the order 100 at $1150^\circ$C. As the zinc and cadmium inter-diffuse, the partial pressures will move closer to those associated with the solid solution and $\frac{P_{Cd}}{P_{Zn}}$ will approach $\frac{x}{1-x}$, although this will not in general be the equilibrium value. Further, it is not clear whether $\frac{P_{Cd}}{P_{Zn}}$ will depend on $P_S$. It is interesting to compare this situation with the variation in partial pressures of the metal and non-metal over a binary II-VI compound. In such a case the pressure of the metal and non-metal can vary within the limits set by the precipitation of another

THE VARIATION OF Kpa WITH X FOR
$ZnSe_xTe_{1-x}$ AND $ZnSe_xS_{1-x}$ AT 1150°C

Fig. 5:2:1
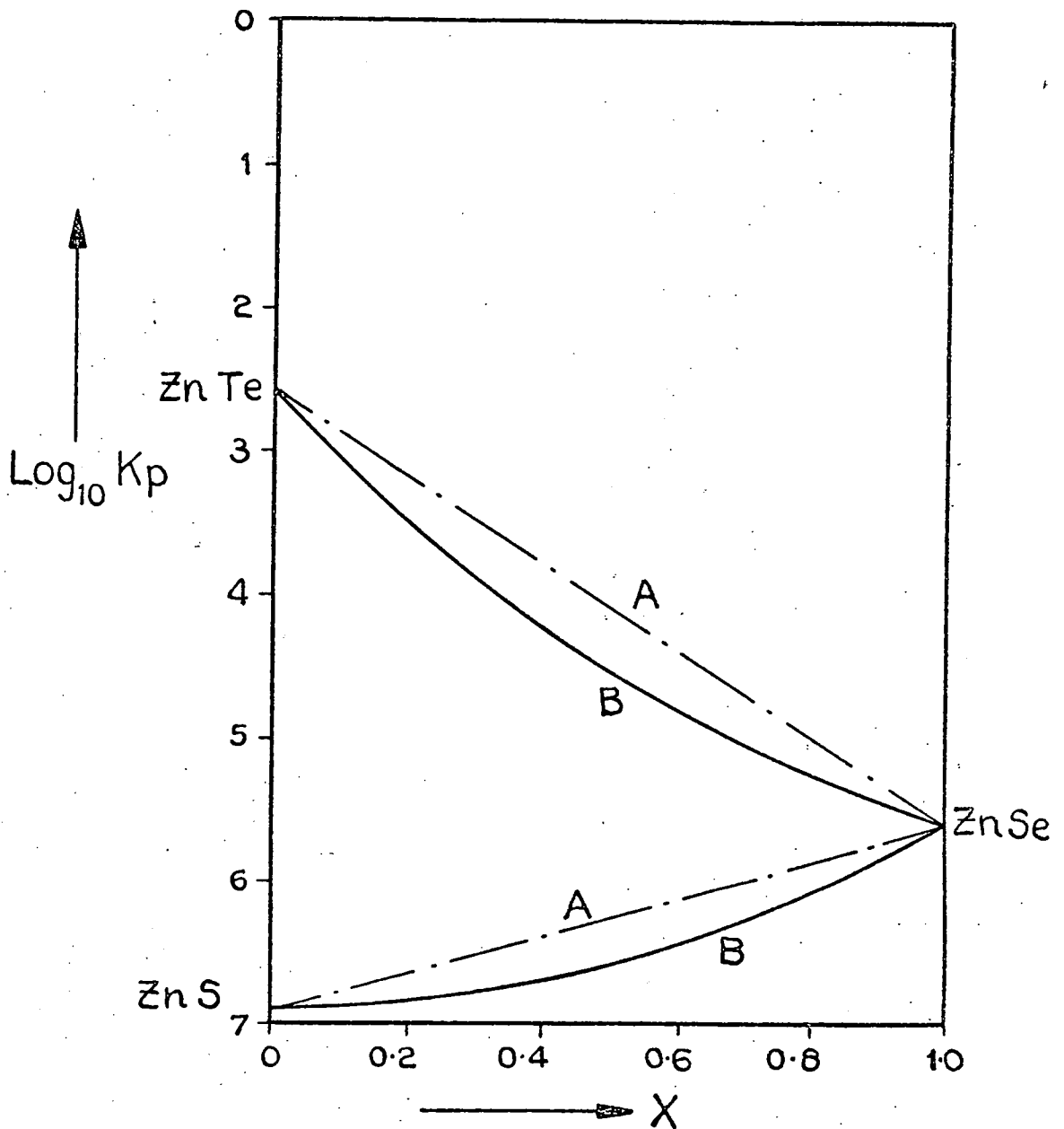
A ——·——·—— $Kpa = X\,Kp(ZnN1) + (1-X)\,Kp(ZnN2)$

B ———————— BETTER APPROXIMATION TO Kpa

phase, and the composition of the solid compound remains virtually unchanged. This contrasts with the case of $Zn_xCd_{1-x}S$ where changing the value of $P_{Cd}/P_{Zn}$ alters the value of $x$ and thus affects the value of Kpa.

Such a discussion of the problems of growing crystals may make the process seem closer to alchemy than to science. Fortunately steps can be taken to minimise the effects of the various uncertainties. Ideally, the system for growing a ternary solution would have three controls to remove all the degrees of freedom, in the same way as the binary system required two. A crystal growth tube with two reservoirs seemed a natural development from previous work, and the capsule illustrated in Figure 5.2.2A was tried. Both a zinc and tellurium reservoir were used in an attempt to grow $ZnSe_{0.5}Te_{0.5}$. Although material was transported in the system, the tellurium reservoir either emptied or became full of ZnTe. Far better results were obtained from a tube with a single zinc reservoir, and a charge of mixed ZnSe and ZnTe. A little reflection shows that this approach (with two reservoirs) has a basic flaw. With a two non-metal system, $(M(N1)_x(N2)_{1-x})$, the metal reservoir remains uncontaminated because all the non-metal gases are precipitated as the compound on the walls of the silica before they reach the reservoir (see Section 4.3). No such reaction prevents two non-metals from contaminating each other. An equivalent effect would occur for two metals and one non-metal, with the metals becoming contaminated. Satisfactory results were obtained with single reservoir tubes, and work on double reservoir systems was abandoned. If it became necessary to use such a technique in an experiment, a tube such as Figure 5.2.2b would probably give better results. The capsules would contain $ZnSe_xTe_{1-x}$, ZnTe and Zn so that the selenium would tend to be precipitated before contaminating the ZnTe reservoir.

In Chapter 4 it was pointed out that crystal growth occurred with near equilibrium conditions at both interfaces, and that $P_T$ remained constant along the length of a growth capsule to a very good approximation. The approximation will also be valid in a three component system and may be used in an analysis of the system. There would be a basic thermodynamic reason for the separation of the components if the composition of the vapour in equilibrium with the solid changed significantly with the temperature difference between the ends of the capsule. It is possible to evaluate the magnitude of this effect for the worst case which would be (for a two non-metal system) when the charge acted as a mixture of two powders M(N1) and M(N2). Then ,

$$\frac{P_{N1}}{P_{N2}} = \frac{Kp \ (M(N1))}{Kp \ (M(N2))} \tag{5.2.5}$$

But

$$-RT \ \ell nKp = \Delta H - T \Delta S \tag{5.2.6}$$

So, representing the compound M(N1) by the subscript 1 and M(N2) by the 2,

$$-R \ \ell n \left(\frac{Kp_1}{Kp_2}\right) = \frac{\Delta H_1 - \Delta H_2}{T} - (\Delta S_1 - \Delta S_2) \tag{5.2.7}$$
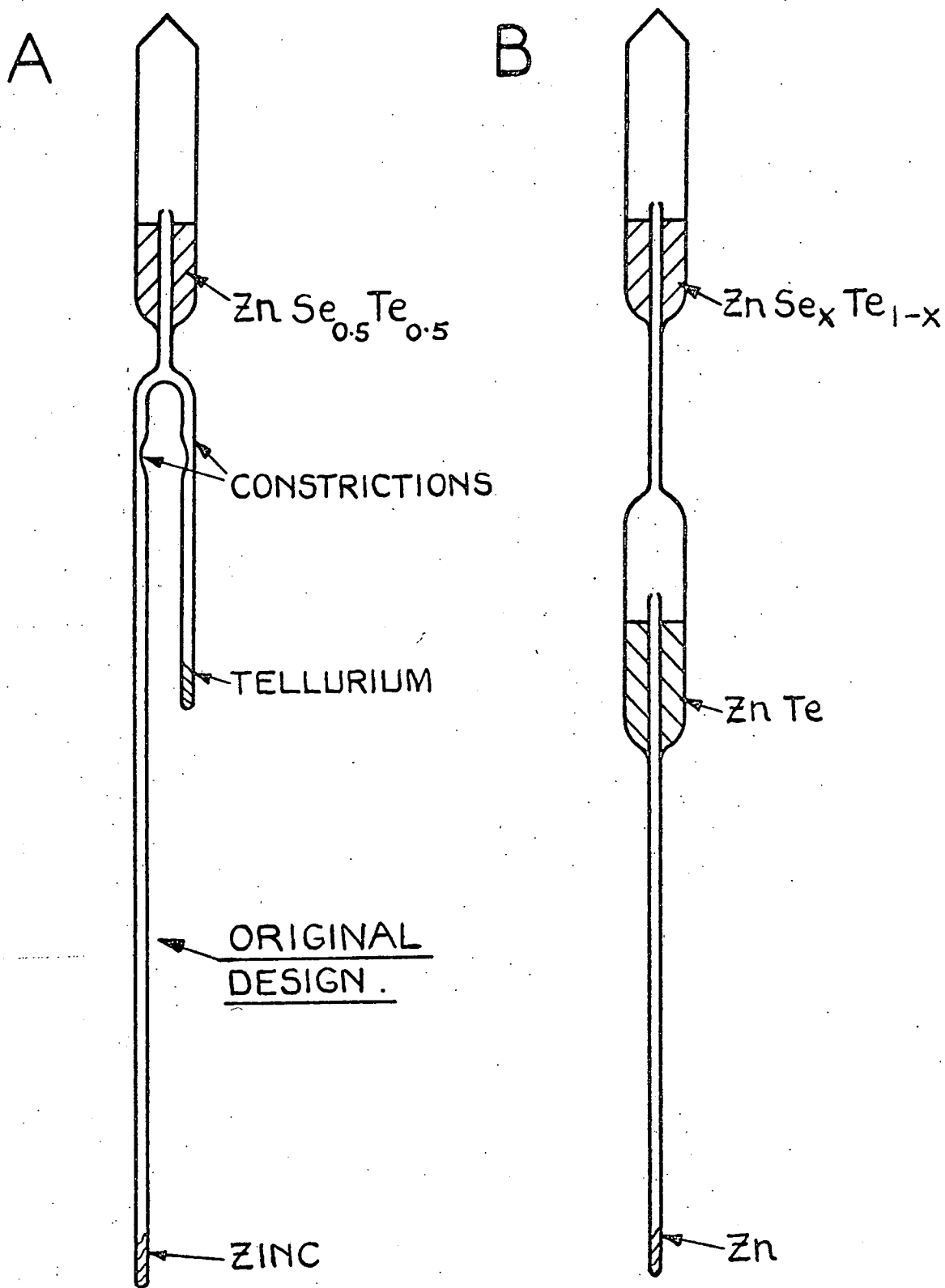
Therefore

$$\frac{d\left(\frac{Kp_1}{Kp_2}\right)}{dT} \bigg/ \frac{Kp_1}{Kp_2} = + \frac{\Delta H_1 - \Delta H_2}{RT^2} \tag{5.2.8}$$

The left-hand side of the expression represents the fractional change in composition with temperature. Fortunately $\log_{10}Kp$ is usually plotted against $1/T$ for II-VI compounds (see for example Aven and Prener[5])

# TWIN RESERVOIR CAPSULES.

A

B

$ZnSe_{0.5}Te_{0.5}$

$ZnSe_xTe_{1-x}$

CONSTRICTIONS

ZnTe

TELLURIUM

ORIGINAL
DESIGN.

ZINC

Zn

giving a line of gradient $-\dfrac{1}{2.3} \dfrac{\Delta H}{R}$ .

Inserting the numbers for $ZnSe_x S_{1-x}$ at $1150^\circ C$ gives a fractional change of $5.5 \times 10^{-4} K^{-1}$; for $ZnSe_x Te_{1-x}$ the value is $2.4 \times 10^{-3} K^{-1}$. These values are not significant, particularly when it is borne in mind that this is an evaluation of an extreme case which cannot actually happen (see equation 5.2.1).

Although there is no basic thermodynamic reason why separation should occur when the solid solution is transported in a temperature gradient, the kinetics of the transport system may cause this to happen. In Chapter 4 the vapour composition along a simple sealed capsule was evaluated for a binary compound. A crystal growth tube with a separate reservoir was found to behave in a similar manner, while the reservoir ensured that the value of $P_T$ was kept close to $P_{MIN}$. The ratio $\dfrac{P_{Se_2}}{P_{Zn}} = A$ was found to vary along the capsule thus maintaining $P_T$ constant. In a simple sealed capsule containing $M(N1)_x (N2)_{1-x}$, $P_T$ must still remain constant, but there are now two ways of achieving this. Either the ratio of metal to non-metal in the vapour can change, or the composition of the charge can differ from that of the growing crystal, leading to a different value of Kpa at the charge and crystal interfaces. For comparison it is worth remembering that Kp(ZnS), Kp(ZnSe) and Kp(ZnTe) are equal when the compounds are at 1229, 1175 and $975^\circ C$ respectively. In order to determine what will actually happen it is necessary to examine the transport process. If transport occurred entirely by diffusion in a system with a large $\Delta T$, the transport rate of each of the two or three minority components (2 metal or 2 non-metal system respectively) would be the product of the diffusion coefficient of that component (proportional to density$^{\frac{1}{2}}$) and its partial pressure

over the source. This approximation assumes that the minority components have very small vapour pressures over the crystal and that the metal is the majority component in a two non-metal system, and the non-metal in a two-metal system, see Figure 5.2.3. (Note the extra component in the two non-metal system is N1N2). The crystal grown would necessarily have the composition dictated by the arrival rate of the gases which will be $\sum_{\ell=1}^{n} P_\ell D_\ell$ where n is the number of components diffusing and P the partial pressure over the source. This will not in general lead to a crystal with the same composition as the charge. As noted in Chapter 4, however, transport occurs by a mixture of the 'wind' and diffusion processes unless the vapour is highly non-stoichiometric or an inert gas filling is present. This means that the diffusion model is once again a 'worst-case' situation. Fortunately $Kp(ZnTe) > Kp(ZnSe) > Kp(ZnS)$ at the same temperature which means that the vapour over the charge is likely to be rich in the heavier, more slowly diffusing component, so the two effects tend to cancel. A further cause of separation, particularly in a vertical system is associated with the different densities of the gases in the system, e.g. the molecular weight of $S_2$ is under half the molecular weight of $Se_2$. An example of this effect was found during attempts to grow boules of $ZnSe_{0.4}S_{0.6}$. The first millimetre to grow, right in the tip of the capsule, often emitted a blue photoluminescence when excited by ultra-violet radiation, which indicates that it was very close to pure ZnS in composition. It might be noted that one way of obtaining an ingot of the desired composition would be to use a charge of sufficient length so that it was much longer than the diffusion length of the separating elements in the solid. The situation would then resemble that which occurs during the first pass in a zone refiner, Figure 5.2.4.

Although this description of the system is qualitative only, certain conclusions can be drawn. $P_T$ in a simple sealed capsule should be as close to $P_{MIN}$ as possible, and $\Delta T$ should be kept small to avoid the 'diffusion only' approximation being valid in the vicinity of the crystal. An inert gas atmosphere should be avoided.

The crystal growth tube described in Chapter 4 was used again with a zinc reservoir to grow crystals of $ZnSe_xS_{1-x}$ and a trial crystal of $ZnSe_{.5}Te_{.5}$. The results were encouraging and are described in the following sections of this chapter. In the tube with a zinc reservoir, the conditions recommended for growth of solid solutions were met admirably. The vapour over the charge was very close to $P_{MIN}$. If the growing crystal were to vary in composition from the charge, the value of $P_{MIN}$ at the crystal would be increased. Clearly it cannot exceed $P_T$ and this provides a negative feedback effect on the growth rate which allows more time for the slowest component to diffuse. Mass transport is as little dependent upon diffusion as possible for stability in the growth system. Against these advantages there must be balanced the possibility of losing unequal amounts of the two components to the tail. Assuming 3 gms of material is lost from a 20 gm charge of $ZnSe_{0.5}S_{0.5}$, and that $A = 1$ in the region of the nozzle, 1 gm of non-metal might be lost. Assuming that this was all selenium, the average composition of the material grown would be $ZnSe_{0.44}S_{0.56}$. This would not be very important for experimental purposes where the quantity of ZnSe could be increased experimentally until the required composition was produced. In practice the material lost did not appear to affect the value of X along the boule, probably because it was lost at a constant rate during growth.

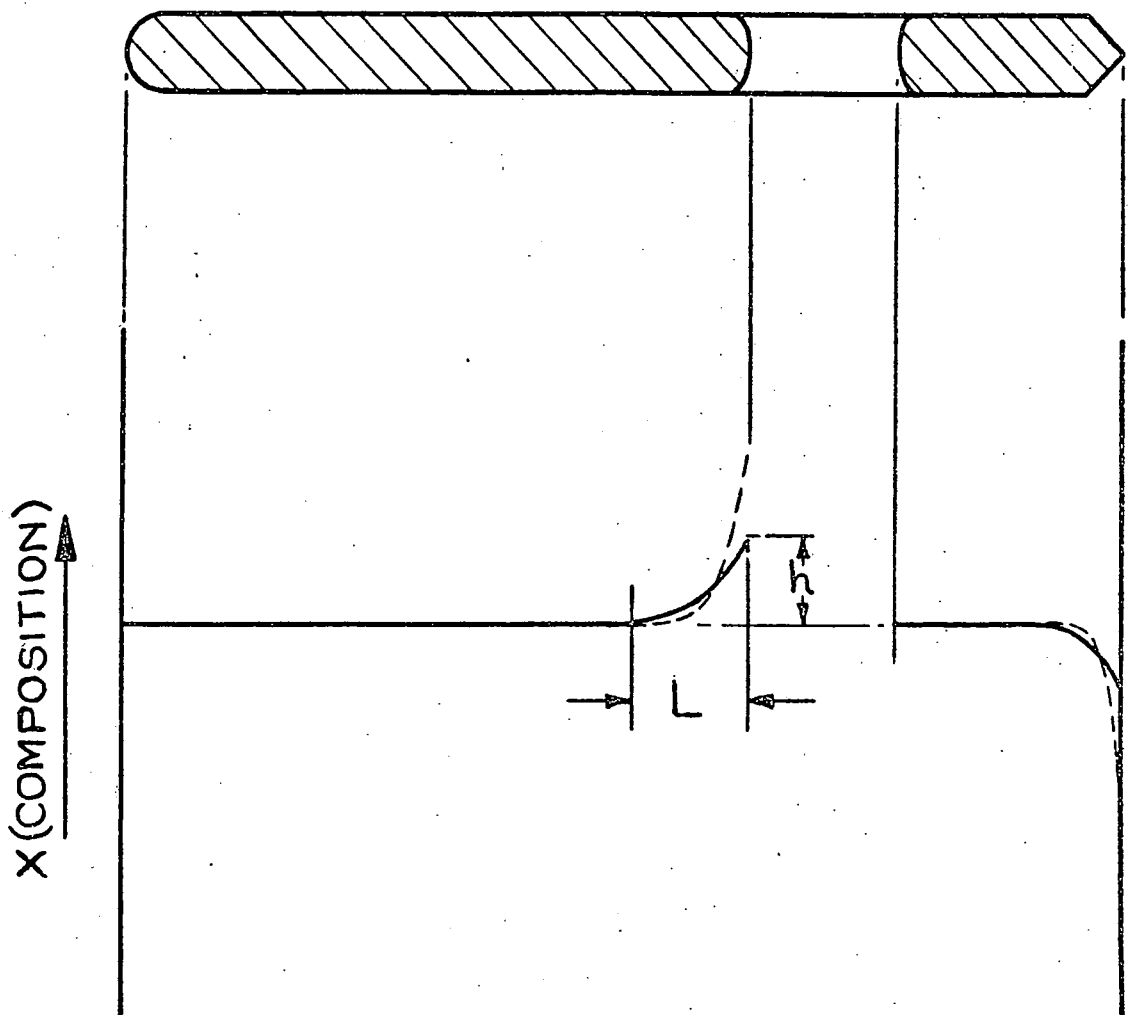# THE DIFFUSION ONLY APPROXIMATION IN A THREE COMPONENT SYSTEM.

Fig. 5 : 2 : 3
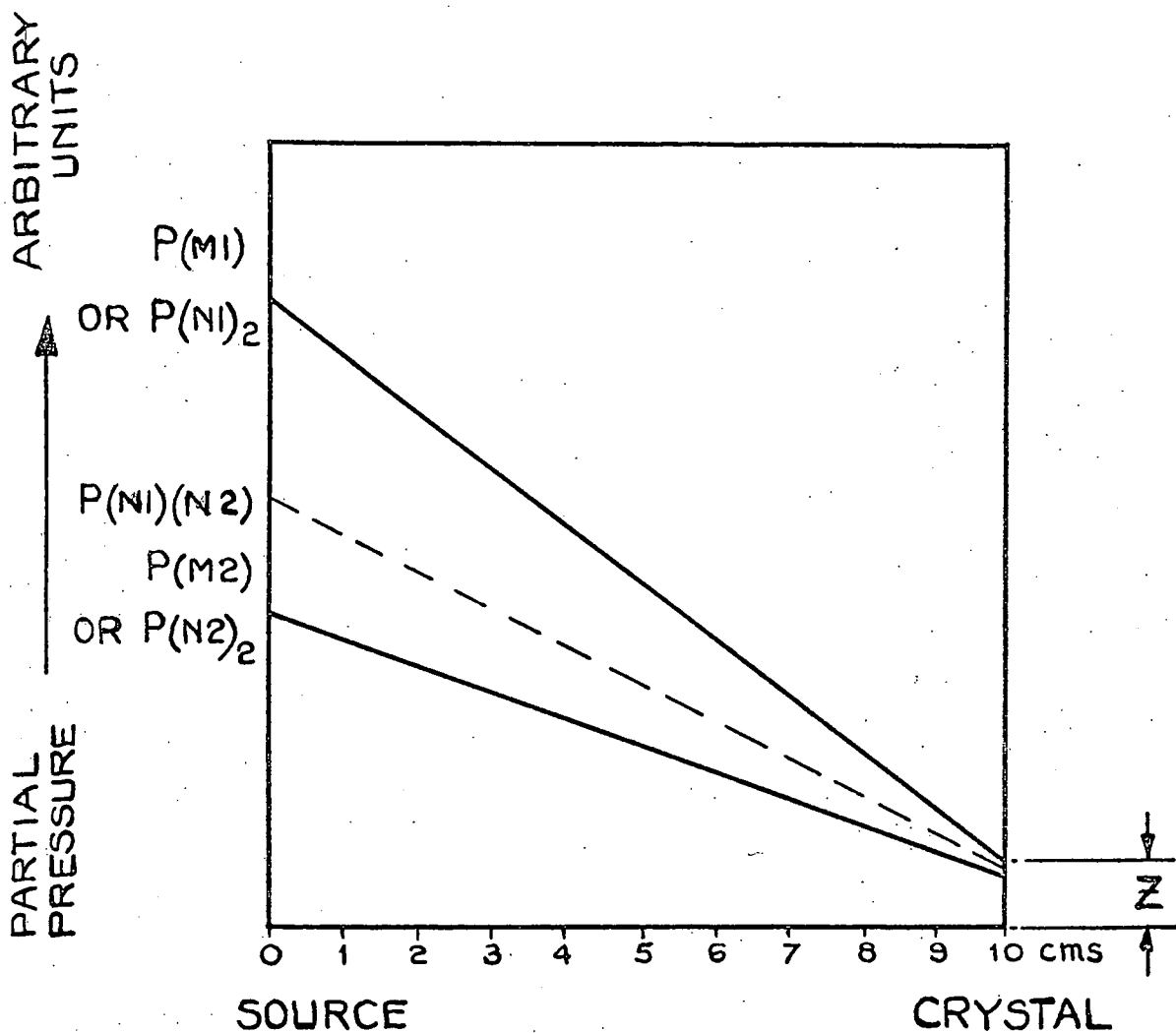


THE MAJORITY COMPONENT AND ANY INERT GAS PRESSURE IS NOT SHOWN. THE ARRIVAL RATE OF THE MINORITY COMPONENTS IS $\sum_{\ell=1}^{n} P_{\ell} D_{\ell}$ IF $z$ IS NEGLIGABLE. $n = 2$ FOR $(M1)_x (M2)_{1-x} N$ AND $n = 3$ FOR $M(N1)_x (N2)_{1-x}$

# THE GROWTH OF AN INGOT OF UNIFORM COMPOSITION IN A LONG SIMPLE SEALED CAPSULE.

## Fig. 5:2:4



IF THE DIFFUSION LENGTH L IS SHORT RELATIVE TO
THE INGOT LENGTH, THE MIDDLE SECTION OF THE
BAR WILL HAVE UNIFORM COMPOSITION. A FAST
GROWTH RATE REDUCES L BUT WOULD INCREASE
h (DASHED LINE). THE AMOUNT OF MATERIAL IN
THE VAPOUR PHASE IS NEGLIGIBLE.

## 5.3    Crystal Growth of $ZnSe_xS_{1-x}$

$ZnSe_xS_{1-x}$ crystals were grown in the crystal growth tube with a separate reservoir as described in Sections 4.3 and 5.2. Initial experiments only required a small amount of sulphur in a boule, and crystals with compositions between ZnSe and $ZnSe_{0.9}S_{0.1}$ were produced by using a charge of ZnSe with 1-2 gms of sulphur in the reservoir. The reservoir was held at the temperature usually used for selenium during the growth of ZnSe. Boules were then grown in the normal manner, and when the reservoir was examined afterwards, it was found that the selenium and sulphur had largely changed places. (Sulphur has a higher vapour pressure than selenium).

To grow the complete range of solid solutions with compositions from ZnSe to ZnS it was necessary to use a charge of mixed ZnSe and ZnS powders which had been ground together to ensure an intimate mixture. (The production of the high purity ZnS and ZnSe starting material was described earlier in Chapter 2). The growth tube was then treated in the usual manner, i.e. it was evacuated and flushed with argon several times before being sealed at a pressure of some $2 \times 10^{-6}$ torr.

During growth the capsule was held at a temperature of $1165^{\circ}C$, while the reservoir, which was filled with zinc, was maintained at the temperature necessary to give the partial pressure of zinc calculated to exist in the capsule under $P_{MIN}$ conditions. This was calculated using the approximation

$$P_{Zn} = (2Kpa)^{\frac{1}{3}}$$

where $\ln Kpa = X \ln Kp(ZnSe) + (1-X) \ln Kp(ZnS)$ which is probably a slight overestimate, (see equation 5.2.1).

Initially, the capsule was arranged in the temperature gradient so that the charge end was at a lower temperature than the end at which the

boule was ultimately to grow. This situation was maintained for three days during which coalescence and sintering of the charge occurred, and a homogeneous, solid solution was produced. The capsule was then pulled through the furnace at a rate of between 0.5 and 1.5 mm/hr for ten days. For most of this time the charge was at $1165^{\circ}$C and the growing crystal interface was at a temperature of between $1145^{\circ}$C and $1065^{\circ}$C, depending on the composition of the crystal being grown. The lower temperatures were used for the more sulphur rich boules. Satisfactory homogeneous crystals, with the cubic, sphalerite structure, were grown for all compositions in the range ZnSe to $ZnSe_{0.4}S_{0.6}$, which suggests that the compound is evaporating so that the vapour has the same composition as the solid. Attempts to grow crystals with more than 60 molar percent of sulphur were unsuccessful, in that no boule was obtained. Some transport did occur but the end product simply consisted of an agglomerate of large numbers of dendritic needles.

The crystals of zinc selenide were wholly cubic in structure and most of the mixed crystals were substantially cubic. This was demonstrated both by electron diffraction and X-ray back-reflection studies. Electron microprobe analysis of a boule with the composition $ZnSe_{0.4}S_{0.6}$ showed that it was substantially homogeneous both radially and from one end to the other. Some samples were thinned for examination in transmission in the electron microscope and were originally obtained by cutting slices 1 cm in diameter and some 0.5 mm thick at right angles to the long axis of a boule, i.e. no attempt was made to ensure that the large area faces of the discs corresponded to any particular low index face.

However, as the work proceeded, it became necessary to produce oriented slices, and it was then discovered that the axes of all the boules examined lay within a few degrees of a <111> direction. Slices

were then cut perpendicularly to this direction and studied to determine
the polarity of the two {111} faces. For this purpose they were polished
mechanically down to 0.25 μm diamond grit and then polished chemically
in HPC[6]. (HPC consists of one part of a saturated solution of chromium
trioxide in orthophosphoric acid with two parts of hydrochloric acid).
Finally they were etched in a 1% solution of bromine in methanol, which
Gezci and Woods[7] have shown to produce triangular pits on the (111)
zinc faces, and conical pits on the ($\bar{1}\bar{1}\bar{1}$) selenium faces.

Using this technique it has been established that all our crystals
grew with their long axes close to a ($\bar{1}\bar{1}\bar{1}$) direction, i.e. the growing
interface lay close to a {$\bar{1}\bar{1}\bar{1}$} plane, with the {111} zinc plane facing the
tip of the crystal, so that the growing face lay close to a {$\bar{1}\bar{1}\bar{1}$} selenium
face. It is interesting to note in passing that similar etching experi-
ments on boules of CdS and CdSe grown by the same vapour phase technique
show a similar effect, i.e. the c-axes of all boules examined lay within
$20^{\circ}$ of the geometric axes of the boules, and the growth interface there-
fore lay within $20^{\circ}$ of a basal plane. This basal plane was found to be
the non-metal ($000\bar{1}$) face in all samples examined.


## 5.4    Electron microscope studies

Polished discs were thinned for transmission studies using the
HPC solution and the "window" technique described by Hirsch et al[8].
After thinning, the specimens were washed first in distilled water, and
then in absolute alcohol. They were then ready for examination in the
JEM 120 electron microscope.


### 5.4.A Zinc Selenide

The dominant defects observed in the zinc selenide samples were

narrow twins extending completely across thin regions of the specimen, see Figure 5.4.1. Although some of these twins exceeded 1 µm in width the majority were slightly narrower than this and were often found close together in small groups which were separated by larger regions of untwinned material. With the wider twins, where the boundaries were well separated, some irregularity was apparent at the edge of the specimen at the intersections with the twin boundaries. This is illustrated in Figure 5.4.2 and is attributed to differential etching of the different crystallographic faces of the twinned material. Electron diffraction patterns from the regions containing the twins showed that twinning occurred on {111} planes in all the samples.

There are two types of twin which can occur on {111} planes in the sphalerite structure, namely the ortho- and the para-twin[12]. The ortho-twin is not associated with any change of polarity along the (111) axis, whereas the para-twin is. The following experiment was performed in order to identify the nature of the twins in zinc selenide. A boule containing large grains was selected, and a slice was cut from it so that its large area surface lay close to a {111} plane on which twinning occurred in the largest grain. Since the cut was made at an angle of a few degrees to the {111} plane, the twin boundaries intersected the cut surface at this low angle. After mechanical and chemical polishing with diamond paste and HPC, the slice was etched in bromine in methanol for about one minute. Subsequent examination in the optical microscope showed that both the twinned and untwinned regions developed etch pits with a three-fold symmetry, and that the twinned material had suffered a 180° rotation about the <111> axis in comparison with the untwinned material. The similar nature of the pits in the twinned and untwinned

material, indicating maintained polarity, and the relative 180° rotation are the characteristics expected of ortho-twins.

Although very few other defects have been observed in the zinc selenide slices, the micrograph in Figure 5.4.3 does illustrate one interesting grain boundary which is worth recording. A knowledge of the orientations of the two grains, at the top and bottom of the micrograph, together with the information that the boundary lies approximately parallel to the [100] direction in the upper grain, suggests that the fault is a tilt boundary with a <100> axis, of the type described by Holt[9]. Such a grain boundary, in contrast with an ortho-twin boundary for example, contains an array of wrong bonds which makes the fault a favourable site for the formation of precipitates. In fact small regions of dark contrast are seen along this boundary, Figure 5.4.4, and are believed to be such precipitates.

The incidence of dislocations in the as-grown crystals of zinc selenide was very low, and apart from the twinning described above very few crystallographic defects were observed. Many of the diffraction patterns however did exhibit extensive streaking as shown in Figure 5. This effect is attributed to thermal diffuse scattering which is observed in many materials with the diamond or zinc blende structure (see for example Honjo et al[10]). The diffuse streaking was most prominent in patterns where the zone axis was close to a <100> direction as in Figure 5.4.5. Unlike streaking associated with stacking faults and planar defects, which is very sensitive to specimen orientation, the streaking associated with thermal diffuse scattering is maintained as the crystal is tilted with respect to the incident beam.

The reason why the thermal diffuse streaking is most prominent in patterns with a <100> zone axis is that the 'zig-zag' chains in

0·2 μM

G 220
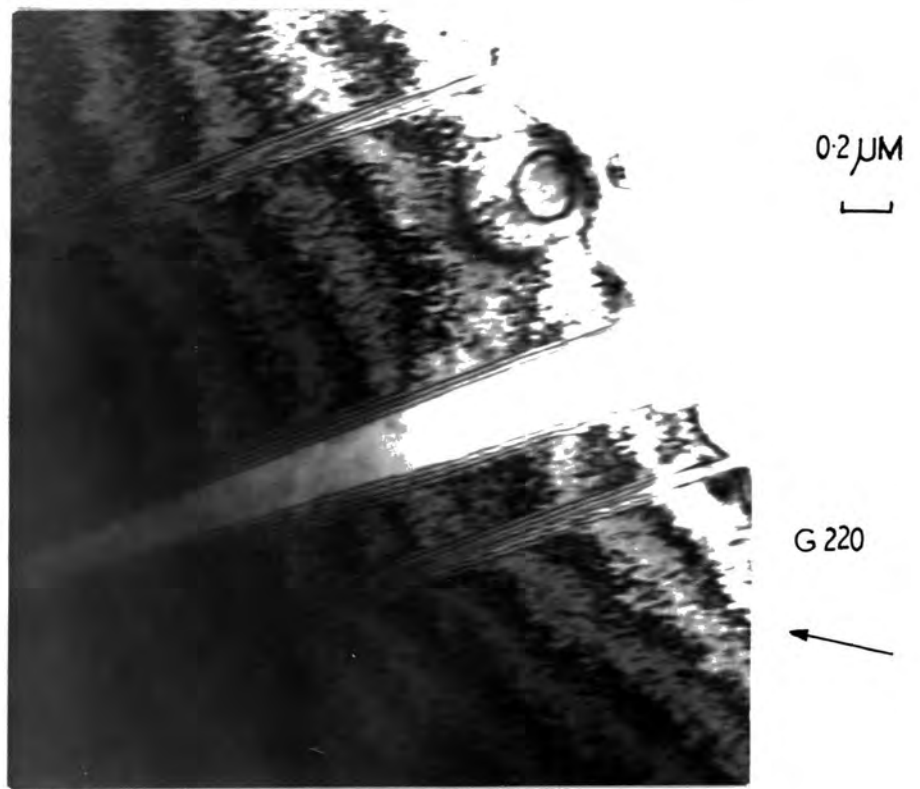
Figure 5.4.1: A group of narrow twins in ZnSe



0·1 μM

G 220

Figure 5.4.2: An irregularity in the specimen edge
near a twin boundary

<110> directions which connect nearest neighbour atoms, and which give rise to 'intensity walls' in reciprocal space perpendicular to their length are perpendicular to the direction of the electron beam in this orientation. In other orientations when the zig-zag chains are not perpendicular to the electron beam, the intensity walls intersect the Ewald sphere at an angle inclined at less than $90°$ to the direction of the electron beam so that the streaking is less pronounced.

### 5.4B Zinc sulpho-selenide

The defect content of this material differed from that of zinc selenide in that, with increasing sulphur content, the degree of stacking disorder increased. In addition many more thin twins were observed which were less wide than those in zinc selenide. A typical region containing such faults is shown in Figure 5.4.6, which once again suggests that the twins occur in groups, while most of the area shown in the micrograph remains of the same crystallographic orientation.

Some examples of the stacking faults which have been observed are shown in Figure 5.4.7. Such faults which frequently occurred in groups, all lie on the same slip plane. This suggests that they owe their origin to slip processes. All the faults investigated were found to be intrinsic, by relating the direction of the diffraction vector operating to the asymmetry of the corresponding dark-field image (see for example Gevers et al.[11]). Although no stacking-fault tetrahedra have been found, a few planar faults which slip from one {111} plane to another have also been observed, see Figure 5.4.8.

The planar faults just described were relatively easy to identify because they were situated between fairly large regions of defect free material. However the crystals of zinc sulpho-selenide
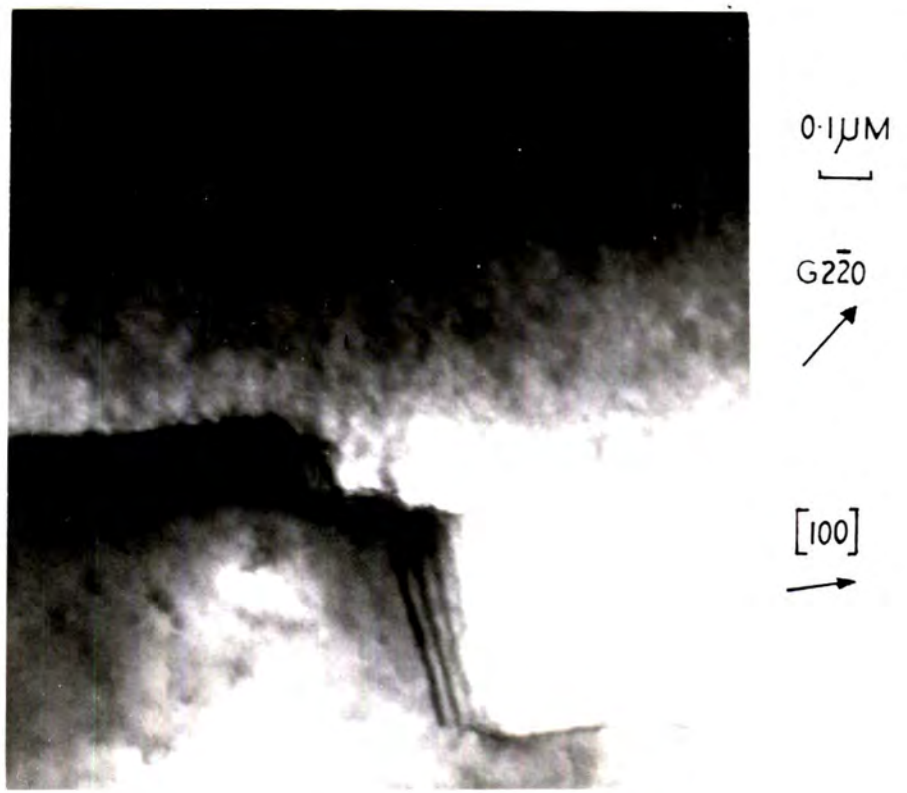
0·1μM

G2̄2̄0

[100]

Figure 5.4.3:  Fringe contrast at a <100> tilt boundary
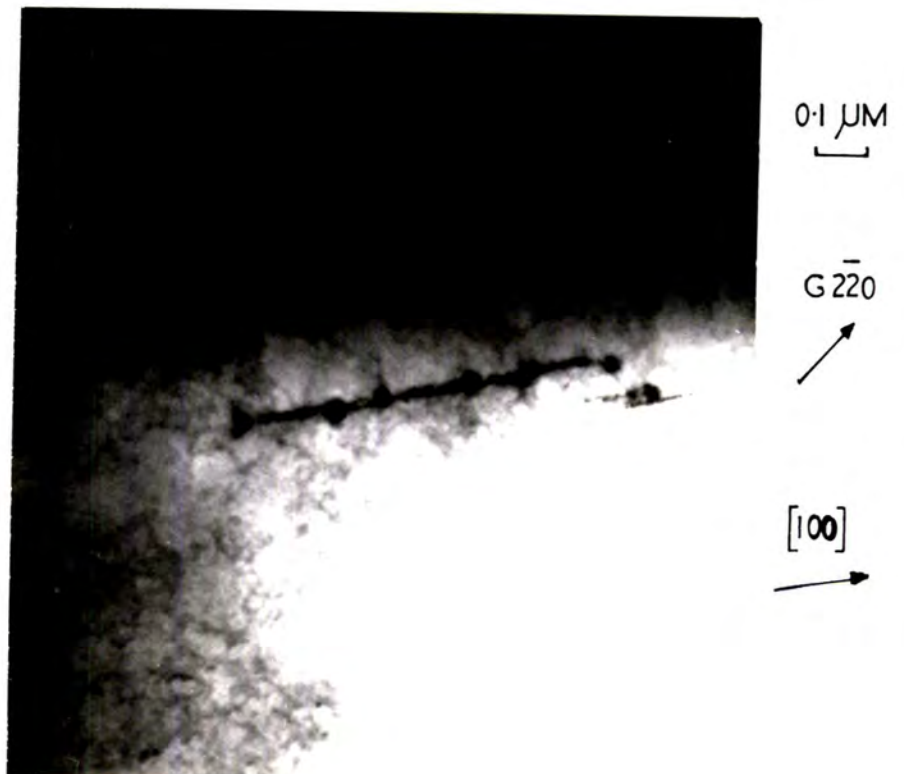


0·1 μM

Ḡ2̄20

[100]

Figure 5.4.4:  Another region of the boundary in
Figure 5.4.3 after tilting through a
few degrees
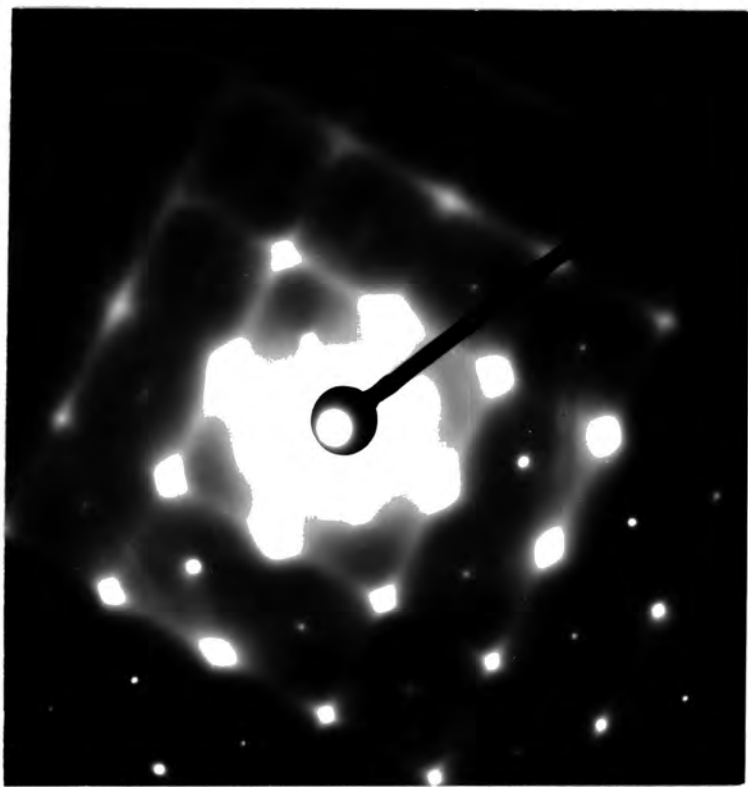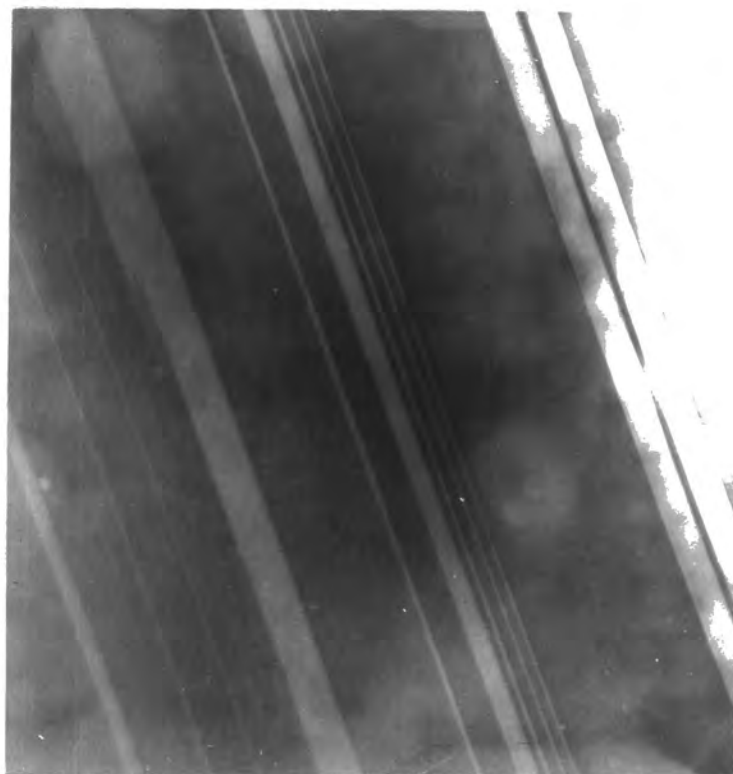
Figure 5.4.5:    Selected area diffraction from a <100>
                 axis of ZnSe using 100 kV electrons

0·1 μM



Figure 5.4.6:    A group of thin twins in ZnSe$_{0.4}$S$_{0.6}$

also contained a few small regions where the concentration of planar faults was very high, as shown in Figure 5.4.9. The selected area diffraction patterns from these regions contained extra spots which could be attributed to twinning on a $\{111\}$ plane. In addition there was a suggestion of diffraction streaks passing through the matrix reflections in a direction perpendicular to the length of the faults. This streaking is probably due to a shape effect associated with the thickness of the overlapping planar defects. The composition of the material within the heavily faulted regions is clearly uncertain, but the degree of stacking disorder suggests that thin lamellae of hexagonal or polytypic material may be present.

The presence of a hexagonal phase in one sample has been firmly established by electron diffraction. In the sample examined, the hexagonal material was in the form of a thin layer in the plane of the foil. The consequent overlapping of the layers of wurtzite and zinc blende gave rise to the moiré fringes shown in Figure 5.4.10. The variation in orientation and spacing of these fringes is attributed to different diffraction conditions and changes in orientation of the phase boundary in different regions of the specimen.

A study of the diffraction pattern showed that the orientational relationship between the cubic and hexagonal phases was such that the (111) cubic plane was parallel to the (10$\bar{1}$0) hexagonal plane, while the $[21\bar{1}]$ cubic direction was parallel to the $[0001]$ direction in the hexagonal material. Thus the fringes belong to a parallel moiré pattern where the fringe spacing, M, is given by

$$M = d_1 d_2 / |d_1 - d_2|$$

where $d_1$ and $d_2$ are the interplanar spacings of the planes in the two
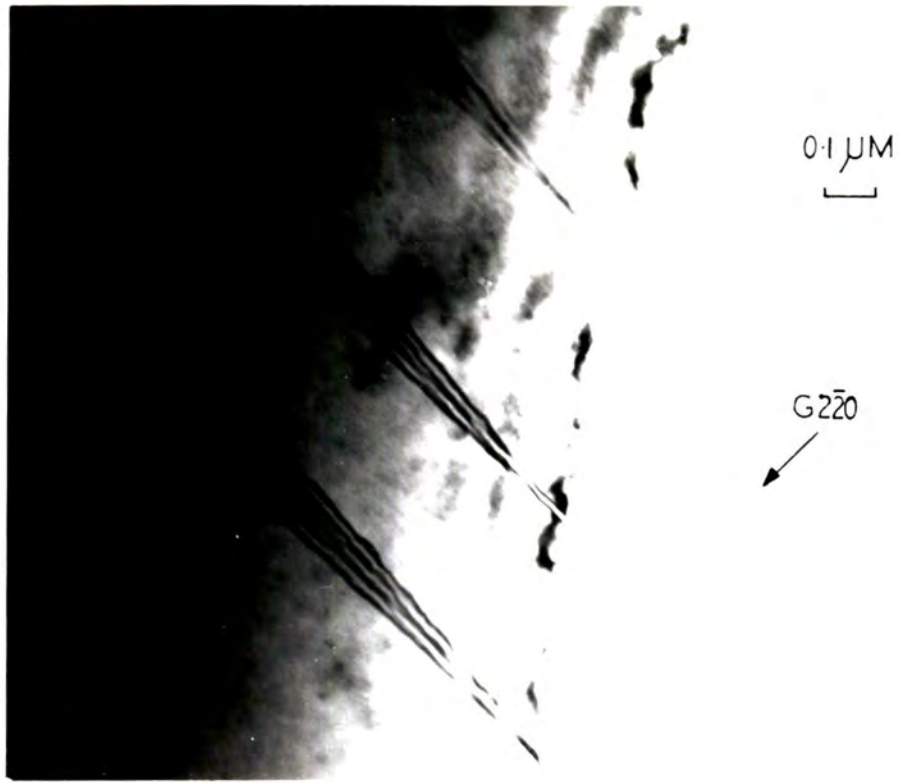
Figure 5.4.7: Long intrinsic stacking faults in $ZnSe_{0.4}S_{0.6}$



Figure 5.4.8: Intrinsic stacking fault in $ZnSe_{0.4}S_{0.6}$ arising from slip on two different {111} planes.

phases which are parallel to one another and responsible for the fringe contrast. To account for the observed value of M of 100 $\overset{o}{A}$, for example at P in Figure 5.4.10, the difference in the values of $d_1$ and $d_2$ must have been of the order of 2%. The magnitude of this difference is consistent with the fact that the separation of the reflections from these planes was not resolved in the diffraction pattern.

To conclude this account of the experimental results on the mixed crystals some measurements of lattice parameters should perhaps be mentioned. The sample containing the small regions of hexagonal phase which led to the production of the moiré fringes was cut from a boule of the nominal composition $ZnSe_{0.4}S_{0.6}$. Nominal in the sense that the boule was grown from a charge of this molar composition. The lattice parameters calculated from the electron diffraction data were as follows; for the cubic phase $a_o = 5.46 \pm 0.11 \overset{o}{A}$ ; for the hexagonal phase $a_o = 3.90 \pm 0.08 \overset{o}{A}$, $c = 6.32 \pm 0.13 \overset{o}{A}$. The values obtained from the ASTM index for ZnSe and ZnS are: for the cubic structure $a_o = 5.667 \overset{o}{A}$ for ZnSe and $a_o = 5.406 \overset{o}{A}$ for ZnS ; for the hexagonal structure $a_o = 3.996 \overset{o}{A}$, $c = 6.530 \overset{o}{A}$ for ZnSe and $a_o = 3.820 \overset{o}{A}$, $c = 6.260 \overset{o}{A}$ for ZnS.

Thus assuming Vegard's law holds for this solid solution, as much work on the photoluminescence and energy band gap of powdered samples suggests, the measurement of lattice parameters indicates that the composition of the cubic phase was approximately $ZnS_{0.79}Se_{0.21}$, while that of the hexagonal was between $ZnS_{0.55}Se_{0.45}$ and $ZnS_{0.78}Se_{0.22}$, depending on whether the values of $a_o$ or c are taken into consideration. The uncertainty in the lattice parameters derived from electron diffraction patterns really permits of a qualitative conclusion only,

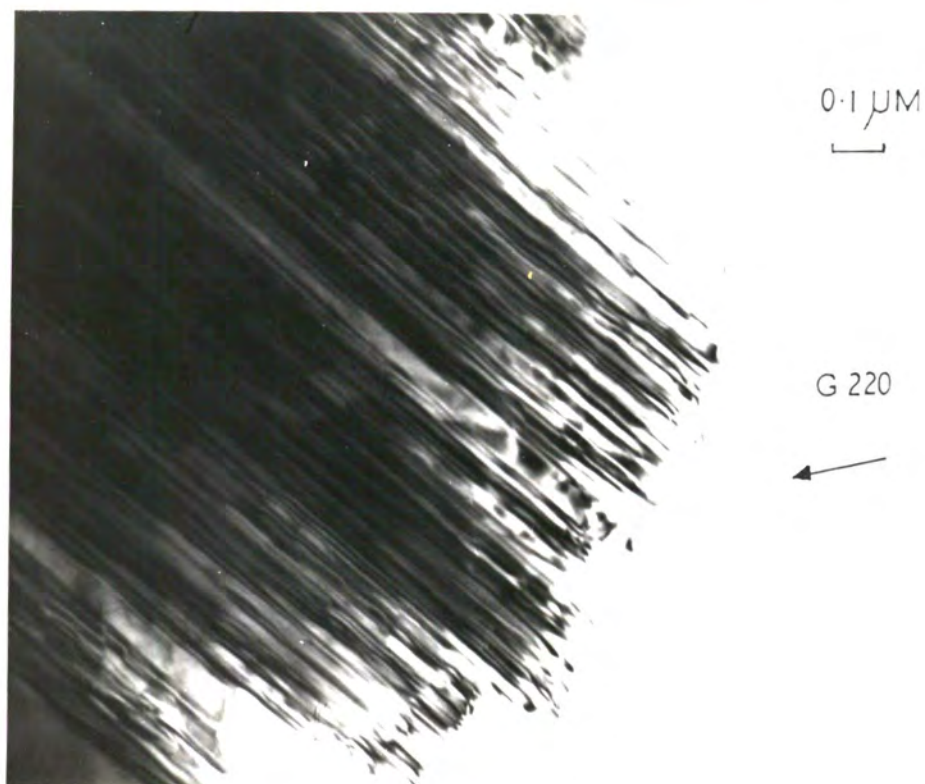0·1 μM

G 220

Figure 5.4.9: A large number of very thin overlapping
planar faults in ZnSe$_{0.4}$S$_{0.6}$



0·1 μM

P

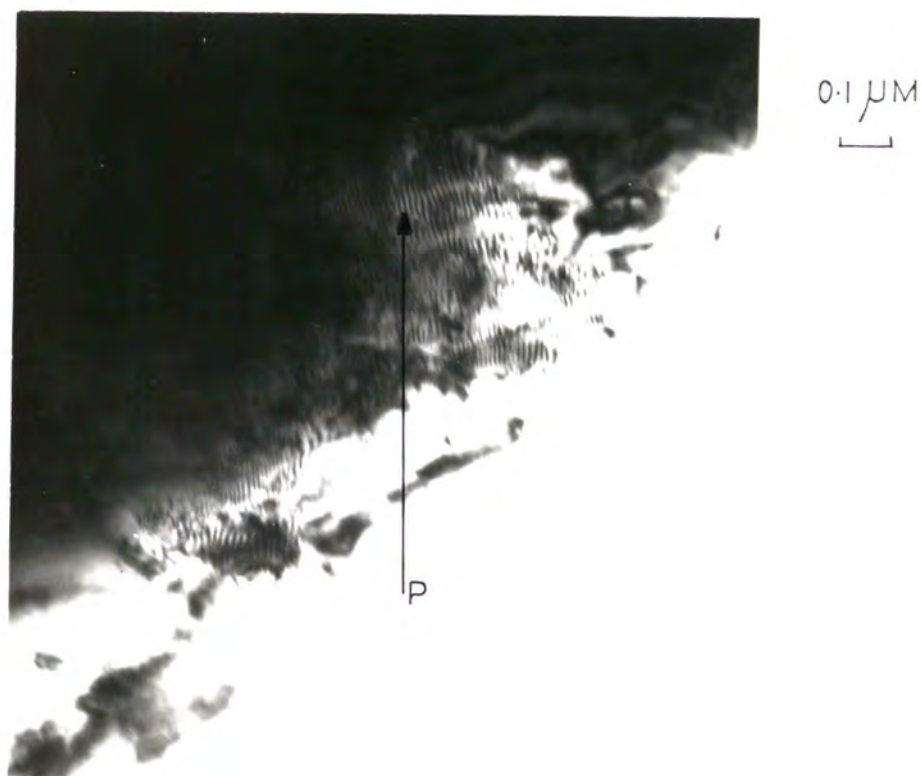Figure 5.4.10: Moiré fringe contrast arising from overlapping
layers of wurtzite and sphalerite planes in
ZnSe$_{0.4}$S$_{0.6}$

namely that this particular boule contained a higher molar proportion of sulphur than selenium and indeed was a solid solution with a composition not too far removed from the nominal composition. This was confirmed later by the X-ray powder photograph technique.

## 5.5    Discussion

The experiments reported here show that the vapour phase technique used to grow homogeneous single crystals of $ZnSe_{1-x}S_x$ is basically successful for values of x up to 0.6 at least. Electron microprobe analysis indicated that the crystals were homogeneous and this and X-ray powder techniques, together with electron diffraction studies, have shown that the crystals produced had compositions close to those of the starting charges, which were simple mixtures of the sulphide and selenide. Examination in transmission in the electron microscope revealed that the zinc selenide samples were of particularly high crystallographic quality with surprisingly few dislocations between grain boundaries. Those defects which were observed were mostly associated with stacking disorder. Thus long, thin twins were common in zinc selenide while zinc sulpho-selenide was considerably more disordered and contained intrinsic stacking faults as well as a higher density of even thinner twins.

In discussing twinning in compounds with the zinc blende structure it is important to realise that there are two possible twin boundaries with a $\{111\}$ composition plane, see Holt[12]. In cubic zinc selenide, for example, the $[111]$ axis is polar and the stacking of zinc and selenium layers in (111) planes can be represented as

$$a \alpha b \beta c \gamma a \alpha b \beta c \gamma a \alpha b \beta c \gamma$$
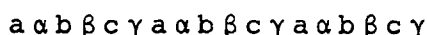
where abc represent zinc layers and $\alpha\beta\gamma$ represent selenium layers.

If the $[1\bar{1}1]$ axis is vertical, the atoms of any layer lie vertically
above the atoms of lower-lying planes designated by the same letter.
α is separated from a by one quarter the distance between two succes-
sive a planes. Similar remarks apply to b and β , and c and γ . The
two possible twins described by Holt[12] are the para- and ortho-twin
which can be represented in the following way:

$$a\,\alpha\,b\,\beta\,c\,\gamma\,a\,\alpha\,b\,b\,\alpha\,a\,\gamma\,c\,\beta\,b\,\alpha\,a \;-\; \text{para-twin} ,$$

$$a\,\alpha\,b\,\beta\,c\,\gamma\,a\,\alpha\,c\,\gamma\,b\,\beta\,a\,\alpha\,c\,\gamma\,b\,\beta \;-\; \text{ortho-twin.}$$

The true mirror image, or para-twin, is characterised by wrong bonds
and the polarity of the $[111]$ axis changes to $[\bar{1}\bar{1}\bar{1}]$ across the twinning
boundary. In contrast the ortho-twin has no wrong bonds and the
polarity does not change. Because of its bonding, the para-twin has
higher energy than the ortho-twin and is therefore less likely to be
observed. Indeed in the etching experiment described in Section 5.4A,
the twins observed in crystals of $ZnSe_xS_{1-x}$ were all of the ortho-type.

The question of the origin of the twins cannot be completely
resolved. The twins must form either during growth or as a result of
post-growth stress. Consider first the possibility that the twins form
during growth. It is believed that the formation of growth twins
depends on a particular characteristic of the growth of our crystals.
For example it is usually found that when crystals of II-VI compounds
are grown by the technique described here, the growth face lies within
$20^{\circ}$ of the $(\bar{1}\bar{1}\bar{1})$ or $(000\bar{1})$ non-metal face. Taken in conjunction with
the findings of Parker[13], who investigated the growth of epitaxial
layers of zinc selenide on gallium arsenide and found that the growth
rate of the $(\bar{1}\bar{1}\bar{1})$ selenium face was two and a half times that of the

(111) zinc face, this suggests that the growth of zinc selenide is strongly polar.
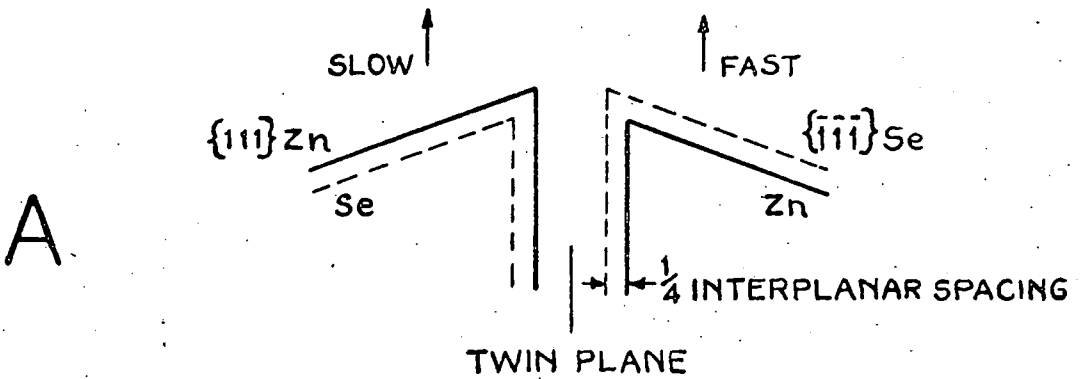
Now when an unseeded ampoule is used, multiple nucleation may well occur. Often one seed grows faster than the others, fills the ampoule and a single crystal results. This is probably what happens with crystals with the wurtzite structure, such as CdS and CdSe, which are relatively easy to grow in single crystal form by the vapour phase technique. However with a cubic material such as zinc selenide, the higher symmetry will promote fast growth in four times as many directions, thus leading to the greater polycrystallinity typical of boules of this material. Now as a grain of zinc selenide grows in a fast $<\bar{1}\bar{1}\bar{1}>$ direction at a small angle to the axis of the ampoule, see Figure 5.5.1, twinning may well occur to preserve the overall axial growth direction. If the twin boundary is of the ortho-type the growth interface will be of opposite polarity on either side of the twinning plane. Since the metal (111) face grows more slowly, this is an inherently unstable situation so that the crystal would rapidly twin back to establish the original fast growing interface. It is suggested that this mechanism may account for some of the long, thin twins observed in zinc selenide and zinc sulpho-selenide. However, it cannot be responsible for the formation of all the twins because some of them are found lying perpendicular to the growth axis. The proposed mechanism is only able to account for twins lying on the three {111} planes which intersect the growth interface.

As to the possibility that the twins are introduced by post-growth stress, it seems unlikely that stress due to the differential contraction of the crystal and its container during cooling will

normally be significant. This is because the coefficients of thermal

expansion of zinc sulphide and selenide are substantially larger than

that of silica glass, as evidenced by the fact that the grown boules

usually become completely free from the walls of the capsule during

the cooling process following the completion of growth. However sticking

sometimes occurs, and then differential contraction leads to stress.

In addition there is some evidence to suggest that the walls of evacuated

silica glass ampoules creep slowly at $1200^{\circ}C$ under external atmospheric

pressure. For example evacuated capsules with cross sections which are

circular initially are sometimes found to have become slightly elliptical

in section following heating at $1200^{\circ}C$ for ten days. The gradual collapse

of the walls of the ampoule could therefore readily introduce stress

into the growing boule. Another source of stress occurs, of course,

during cooling, when a certain amount of differential contraction between

the core and periphery of the boule is unavoidable in the presence of a

radial temperature gradient. These results indicate that the major

defects in zinc selenide are ortho-twins, and that as selenium is

replaced with sulphur, the twins become narrower, and the incidence of

stacking faults increases. It has not been possible to study zinc

sulphide, but the available evidence[14] suggests that the major defects

in that material are stacking faults. It is believed that many of the

stacking faults in zinc sulphide, and of the twins in zinc selenide,

owe their origin to post-growth stress, and that the reason for the

occurrence of different defects in the two materials is to be sought

in the slight difference in the degree of ionicity of the bonding in

the two compounds. Consider, for example, the stacking of double atom

layers along a <111> axis in a cubic crystal. In the notation used

# TWINNING DURING CRYSTAL GROWTH.

## Fig. 5 : 5 : 1

A

SLOW ↑          ↑ FAST

{111}Zn                    {ī̄ī}Se

Se            Zn

$\frac{1}{4}$ INTERPLANAR SPACING

TWIN PLANE

SHOWING HOW A TWIN BOUNDARY PARALLEL TO
THE GROWTH DIRECTION LEADS TO FAST AND
SLOW GROWING FACES.

B

GROWTH ↑ DIRECTION

CAPSULE

PROBABLE GROWTH FACE.

IDEAL GROWTH FACE.

FAST{ī̄ī} PLANE            SLOW {111} PLANE
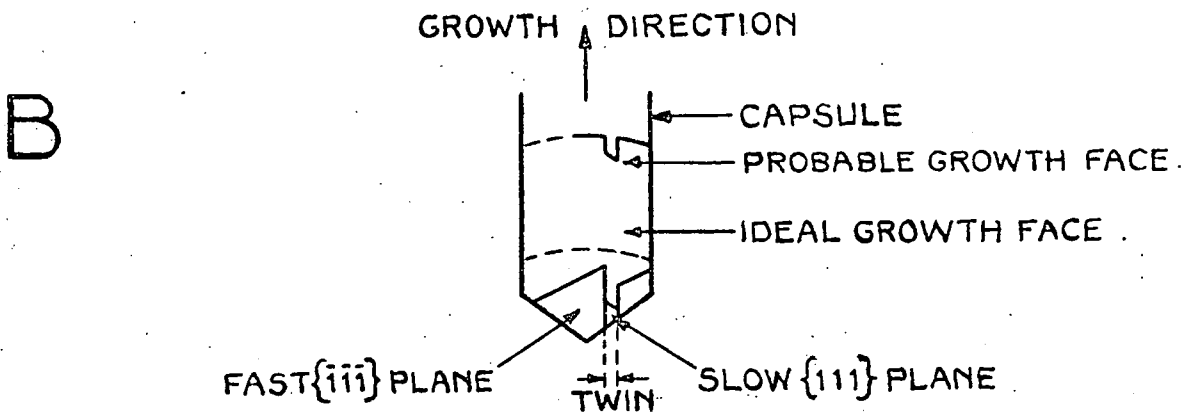
TWIN

ILLUSTRATING THE GROWTH OF AN ORTHO-TWIN.

earlier this can be represented as

$$a \alpha b \beta c \gamma \uparrow a \alpha b \beta c \gamma a \alpha b \beta c \gamma \qquad (i)$$
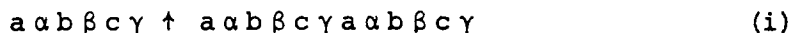
A stress nucleated dislocation will split into two partials separated by an intrinsic stacking fault, and one partial will sweep across a {111} plane in a position such as that marked by the arrow in (i) above. The stacking fault energy in zinc sulphide is very low, or even negative, so that the fault covers the whole plane. Following the passage of the partial the stacking sequence becomes

$$\overset{\text{hexagonal}}{a \alpha b \beta c \gamma b \beta} \uparrow c \gamma a \alpha b \beta c \gamma a \alpha \qquad (ii)$$

This intrinsic stacking fault (ii) can be regarded as containing four double layers of hexagonal material with a stacking sequence $b \beta c \gamma b \beta c \gamma$. This configuration will be particularly stable in zinc sulphide, and in the mixed crystals with high sulphur content, because the higher ionicity of the bonding in zinc sulphide favours the formation of the wurtzite structure. (This of course is the meaning of a negative stacking fault energy). To relieve thermal stress, a large number of partials must pass over {111} slip planes, but this will occur at random and in consequence numerous intrinsic stacking faults will be found.

Now with zinc selenide the bonding is more covalent, which favours the formation of the sphalerite structure. The stacking fault energy associated with a sequence such as (ii) will be higher than in zinc sulphide and sequence (ii) will not be as stable. Thus when further stress is to be relieved it is probable that a partial dislocation will pass over a {111} plane adjacent to an existing intrinsic

fault, for example at the position indicated by the arrow in (ii). This leads to the following stacking sequence

$$a\,\alpha\,b\,\beta\,c\,\gamma\,b\,\beta\,a\,\alpha\,\uparrow\,b\,\beta\,c\,\gamma\,a\,\alpha\,b\,\beta \qquad\qquad (iii)$$
$$\quad\;\; T \qquad\;\; T$$

This arrangement can be regarded equally as an extrinsic stacking fault or as a thin twin, with composition planes indicated by the letters T. If now yet another partial passes over the plane indicated by the arrow in (iii), the twin widens by one double atom layer and the stacking sequence becomes

$$\xleftarrow{\quad\;} H \xrightarrow{\quad} \xleftarrow{\quad} H \xrightarrow{\quad}$$
$$a\,\alpha\,b\,\beta\;\;\uparrow\;c\,\gamma\,b\,\beta\,a\,\alpha\,c\,\dot\gamma\;\;\uparrow\;a\,\alpha\,b\,\beta\,c\,\gamma \qquad (iv)$$
$$\qquad\quad\; T \qquad\qquad T$$

Obviously the repeated passage of partial dislocations over adjacent {111} planes will lead to the widening of the ortho-twin. It is suggested that the reason why the partials continue to traverse planes adjacent to the twin plane is because the bonds in those particular planes, marked by arrows in (iv), will be weaker than the bonds in properly co-ordinated double {111} layers in wholly cubic material. Thus in the stacking sequences (ii) and (iii) the double layers to the left of the arrows (and the double layer to the left of the right-hand arrow in (iv)) are in an immediately hexagonal environment. The covalent nature of zinc selenide ensures that this is a relatively unstable arrangement so that there will be an inherent weakness on the planes marked with arrows. Stress relief will therefore occur preferentially on these planes with the result that the twins widen in preference to the formation of random stacking faults. Energy considerations make this point clearer. The passage of three partials on successive {111} planes leads to configuration (iv) with two 3-layer

hexagonal regions marked H. If three partials had passed on three {111} planes at random, a total of twelve double layers with the hexagonal stacking would have been formed. This is clearly an unfavourable situation in a crystal with a higher degree of covalency in its bonding. The disparity between the energies required to form wider twins or random stacking faults increases with the number of partials required to relieve the stress.

In conclusion therefore it is suggested that the relief of thermal stress in zinc selenide leads to the formation of ortho-twins. Incidentally it is perhaps worth recording that zinc telluride is more covalent than zinc selenide, and crystals of zinc telluride are usually heavily twinned[15]. As the selenium in zinc selenide is replaced by sulphur, the increasing ionicity of the bonds and the corresponding tendency to form the wurtzite structure leads to the formation of random stacking faults. In the mixed material therefore both thinner twins and isolated stacking faults would be expected, particularly if microscopic homogeneity is not strictly maintained.

# CHAPTER 5

## REFERENCES

1. J W Allen, A W Livingstone and K Turvey (1972) Sol. St. Electron 15 1363

2. Y S Park, C R Geesner and B K Shin (1972) Appl. Phys. Lett. 21 567

3. M E Ozsan and J Woods (1975) Sol. St. Electron. 18 519

4. M E Ozsan and J Woods (1974) Appl. Phys. Lett. 25 489

5. M R Lorenz (1967) in Physics and Chemistry of II-VI Compounds, Eds. M Aven and J S Prener (North Holland Amsterdam) p.80

6. N Hemmatt and M Weinstein (1967) Electrochem. Soc. 114 851

7. S Gezci and J Woods (1972) J. Mat. Sci. 603

8. P B Hirsch, A Howie, R B Nicholson, D W Pashley and M J Whelan (1965) Electron Microscopy of Thin Crystals (Butterworths, London) p.31

9. D B Holt (1964) J. Phys. Chem. Sol. 25 1385.

10. G Honjo, S Kodera and N Kitamura (1964) J. Phys. Soc. Japan 19 351

11. R Gevers, A Art and S Amelinckx (1963) Phys. Status Solidi 3 1563

12. D B Holt (1966) J. Mat. Sci. 1 280

13. S G Parker (1971) J. Cryst. Growth 9 177

14. H Blank, P Delavignette and S Amelinckx (1966) Phys. Status Solidi 2 1660

15. M R Lorenz (1967) in Physics and Chemistry of II-VI Compounds, Eds. M Aven and J S Prener (North-Holland Amsterdam) p.103

## CHAPTER 6

## CHEMICAL VAPOUR TRANSPORT AND HIGH TEMPERATURE CRYSTAL GROWTH

6.1    Introduction

In this chapter descriptions are given of two crystal growth techniques used to grow a relatively small number of crystals which could not be produced in the usual vertical system.  The crystals in question were pure ZnS, untwinned ZnSe:Mn, and ZnSe heavily doped with manganese to a concentration of 0.1 - 1%.

Untwinned ZnSe was required for E.S.R. experiments, while very heavily doped material was needed for optical absorption spectroscopy in an attempt to identify the zero phonon line in the manganese absorption spectrum.  Unfortunately the ZnSe obtained from the vertical system was often twinned, which gave rise to extra peaks in the E.S.R. spectrum due to the hexagonal structure associated with the twins.  Hartman[1] reported that hexagonal ZnSe grew in the temperature range $800 - 1050^{\circ}C$, and it was hoped that by preparing crystals at a higher or lower temperature untwinned ZnSe would be produced.  To reduce the temperature an iodine transport system was used, and to increase the temperature a modified Piper-Polich system was employed in a horizontal arrangement.  The furnace was heated by a 'Crucilite' element capable of operating up to $1500^{\circ}C$.  The two techniques were later applied to zinc sulphide and zinc sulpho-selenide. Iodine transport was found to be useful for introducing high levels of manganese (0.3%) into ZnSe.  It had proved impossible to incorporate such high levels of manganese even when several molar percent of manganese was added to the charge.  However, the required concentration was obtained with the iodine transport system quite easily.  This is not surprising because Weidemeier and Sigai[2] used this method to grow crystals of MnSe.

## 6.2    Crystal Growth  by a Modified Piper-Polich Technique

The vertical furnaces available for crystal growth were limited to use below 1200°C in order to obtain a reasonable life from their Kanthal A1 windings.  It was hoped that ZnSe would twin less readily at 1300°C than 1150°C and it was thought that the higher temperature might assist the transport of any manganese added to the ZnSe charge, thus enabling ZnSe:Mn to be produced free of chlorine or iodine.  A horizontal furnace with a 'Crucilite' element, in which CdS had previously been grown by a modified Piper and Polich[3] technique was available.  Initial attempts to grow ZnSe in a sealed and evacuated capsule failed.  A ten millimetre I.D. capsule with walls 2 - 3 mm thick was pulled through a temperature gradient in three days.  In a series of experiments the temperature of the furnace was progressively increased.  No transport occurred until the temperature reached 1300°C, when the tube collapsed and the charge sintered into several dense rounded pieces.  As the temperature was increased further some of the capsules expanded as the pressure inside exceeded one atmosphere.  Sintered pieces of ZnSe with a deep red colour were obtained from those capsules which did not fracture before cooling.  Silica glass devitrifies rapidly above 1200°C and because of this the capsule often shattered during cooling. Oxidation of the crystals was prevented by quenching the capsule when it had cooled to the region of 400 - 600°C.

To promote material transport the open tube arrangement of Figure 6.2.1 was adopted.  Argon was passed slowly along the 15 mm silica tube at a rate somewhat less than 50 ml/sec and allowed to escape into a fume cupboard.  The whole tube containing the capsule was pushed through the temperature gradient at between 1 and 3 cms/day.  The charge sintered to a single piece with a deep green colour while the transported material was light green.

Unfortunately, even at the maximum growth temperature used, $1375^{\circ}C$, the transported material possessed a cellular structure and was not homogeneous. A variety of shapes of capsule and heat sink were tried without success.

Further work was postponed until the need to grow crystals of $ZnSe_xS_{1-x}$ at temperatures greater than $1200^{\circ}C$ provided an incentive. Using the vertical capsule with a reservoir, crystals with a composition from ZnSe to $ZnSe_{.4}S_{.6}$ could be grown, but although pure ZnS was transported the distillate consisted of a mass of dendritic needles. $ZnS_{.75}Se_{.25}$ behaved similarly.

As a result the modified Piper-Polich furnace shown in Figure 6.2.2 was devised. A capsule with a long neck (Figure 6.2.3) was moved through the temperature gradient by a stainless steel pull rod passing through an '0' ring seal. The 'purox' furnace tube could be evacuated with a mercury diffusion pump.

Pressures between 5 torr and 1 atmosphere could be maintained inside the 'purox' tube by leaking argon into the system through one needle valve, and pumping through a second. A flow of between 50 and 100 ml/min was required to keep the pressure stable.

The growth procedure was similar for ZnSe, $ZnSe_xS_{1-x}$ and ZnS. Flow run material was ground to a coarse powder and loaded into a growth tube. Before use each tube was soaked in aqua regia for two hours and then washed in methanol and deionised water. A hook and the constrictions in the nozzle were added after the material had been loaded.

The tube was positioned in the furnace so that the first constriction between the capsule and the nozzle was in the hottest part of the furnace. After the system had been flushed with argon, the furnace was evacuated with the diffusion pump and baked for 24 hours at $800^{\circ}C$.

INITIAL ARRANGEMENT FOR HIGH TEMPERATURE GROWTH

Fig. 6:2:1

A

EXHAUST
TO FUME
CUPBOARD

A

15 mm O.D. SILICA
TUBE

FURNACE

TRAVEL
3 cms / DAY
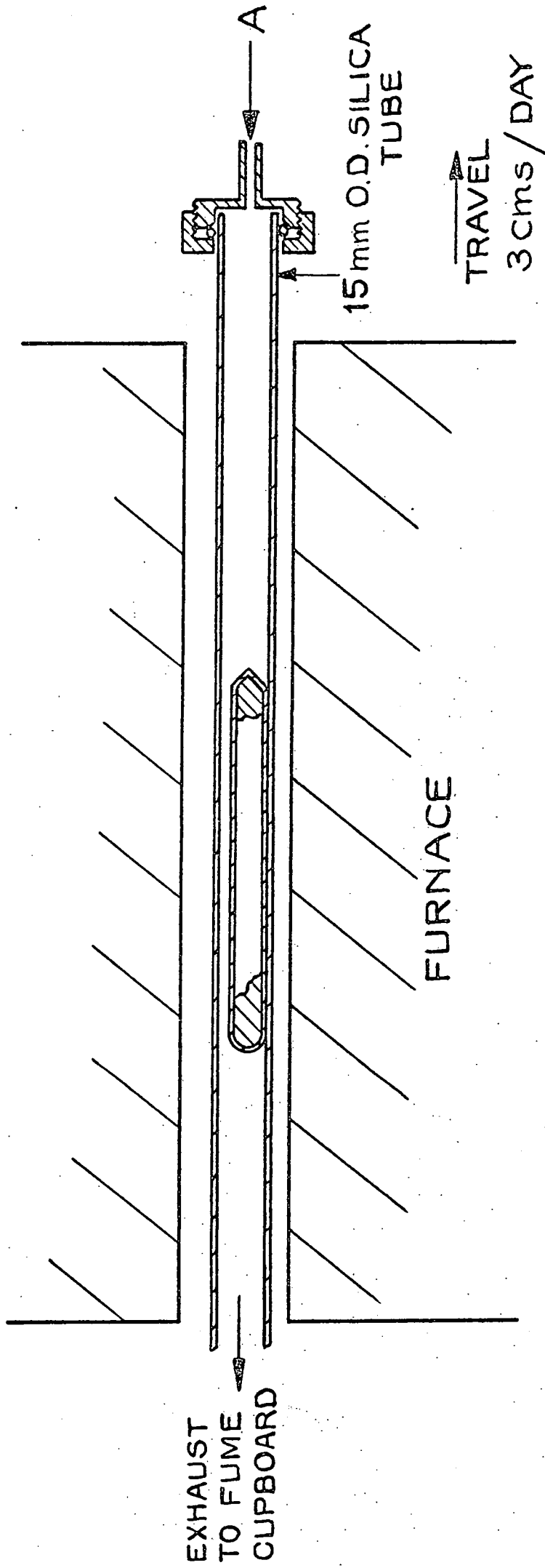
NOT TO SCALE.

Argon, or an argon and hydrogen mixture was then admitted to the system to the required pressure and the furnace temperature was increased to that required for growth. The pulling mechanism was started immediately when the binary compounds ZnSe or ZnS were being grown, but 24 hours under a reverse temperature gradient was allowed to promote the formation of a solid solution before the crystal growth was begun.

Material was transported rapidly towards the growth tip and nucleation occurred at several of the constrictions, thus sealing off the capsule. Using a pull rate of 3 cms per day complete transport of a 10 gm ZnSe charge occurred in 36 hours. Initially argon was used as the atmosphere, but some of the ZnSe crystals grown were red in colour and shattered on cooling. The silica was also stained yellow instead of the usual white. It was suspected that the cause was the diffusion of oxygen through the walls of the furnace tube. When 10% hydrogen was added to the argon the colour of the crystals improved and the cracking stopped. Initial experiments with zinc sulphide and zinc selenide suggested that the most successful temperatures and pressures were $1350 - 1400^{\circ}C$ at 0.25 atmopsheres for ZnS and $1300^{\circ}C$ at 1 atmosphere for ZnSe. A charge of $ZnS_{.5}Se_{.5}$ was transported when treated in the same way as the sulphide.

The apparatus yielded interesting initial results, but it became clear that the system was not particularly reliable, and the stainless steel was probably introducing some contamination. An improved design in which the furnace moved and the furnace tube and capsule were rigidly held is shown in Figure 6.2.4.

## 6.3    Chemical Vapour Transport

The technique of chemical vapour transport (C.V.T) has been exploited for the purification of metals since the 1930's. At that time

MODIFIED PIPER-POLICH FURNACE SYSTEM.

Fig. 6:2:2

PUROX FURNACE TUBE.

FURNACE.

NEEDLE VALVE

VACUUM SYSTEM

T/C

PULL ROD

H₂

ARGON

NEEDLE VALVE
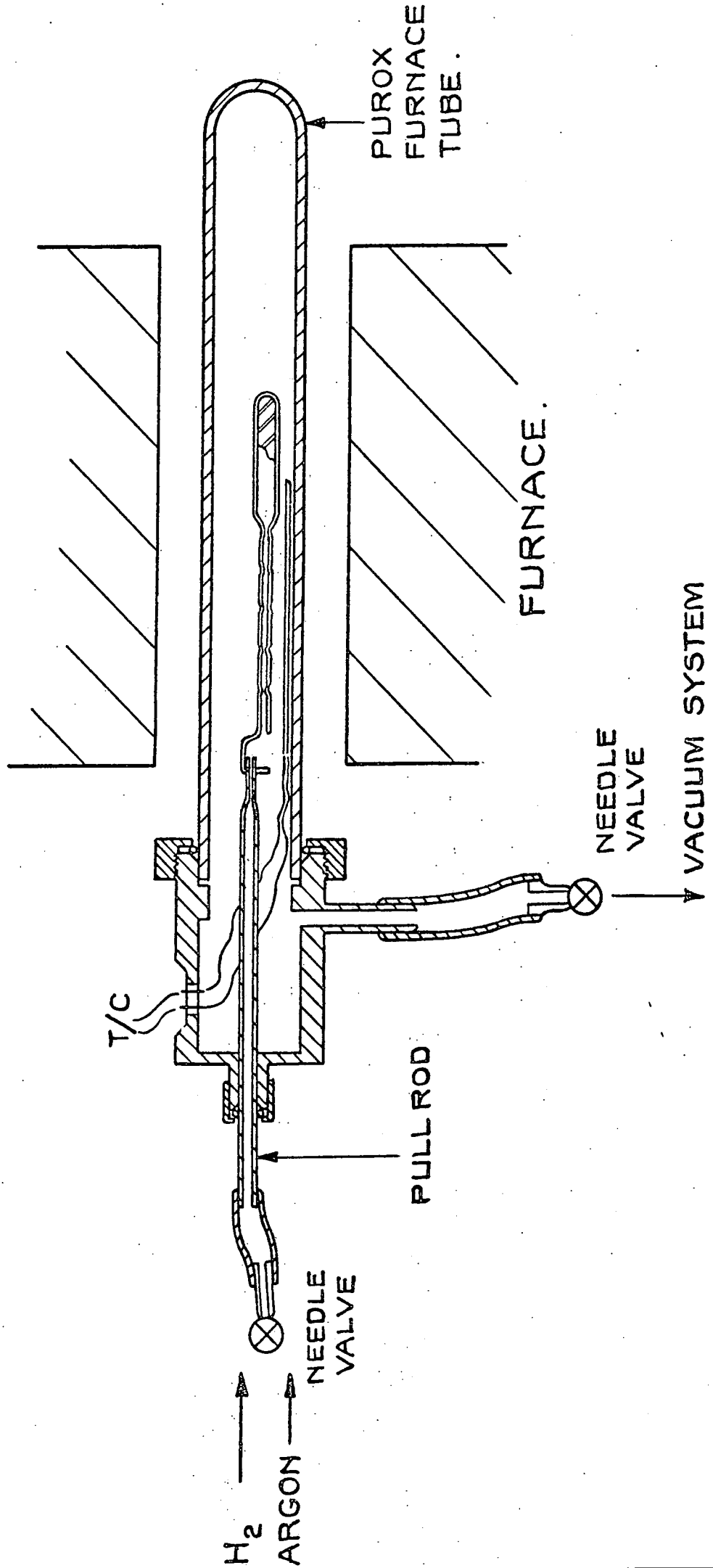
NOT TO SCALE.

it was used for the production of tungsten and zirconium. In the 'Van-Arkle' process,[4] a wire of the material is heated to $\sim 2000°C$ while a zirconium source is maintained at a few hundred degrees centigrade. Zirconium is transported under a pressure of $10^{-2}$ atmospheres by the reaction

$$\text{Zr} \quad + \quad 4\text{I} \quad \underset{\text{HOT}}{\overset{\text{COLD}}{\rightleftharpoons}} \quad \text{Zr I}_4$$
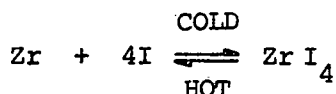
A similar reaction is used in quartz halogen spotlamps to redeposit tungsten which evaporates from the hot filament of the lamp back on the filament.

Nische[5], Shaeffer[6] and Parker[7] have all investigated the transport of II-VI compounds by C.V.T. and they found that iodine at a pressure of 1 atmosphere is most suitable for the purpose.

ZnSe is transported by the reaction

$$2\,\text{ZnSe} \quad + \quad 2\,\text{I}_2 \quad \underset{\text{HOT}}{\overset{\text{COLD}}{\rightleftharpoons}} \quad 2\,\text{ZnI}_2 \quad + \quad \text{Se}_2$$

The reaction occurs at around $800°C$ and a special furnace system was built to obtain the required standard of temperature control, Figure 6.3.1. A double furnace was used with two temperature controllers, one maintaining a backing furnace at $800°C$, while the other allowed a temperature difference of up to $30°C$ to be superimposed using a differential control thermocouple. The two junctions of the differential thermocouple were located at each end of the capsule and hence gave the difference in temperature along it. As may be seen from Figure 6.3.1, the inner furnace had two windings so that the temperature gradient inside the furnace could be reversed without disturbing the capsule. The growth tube employed,

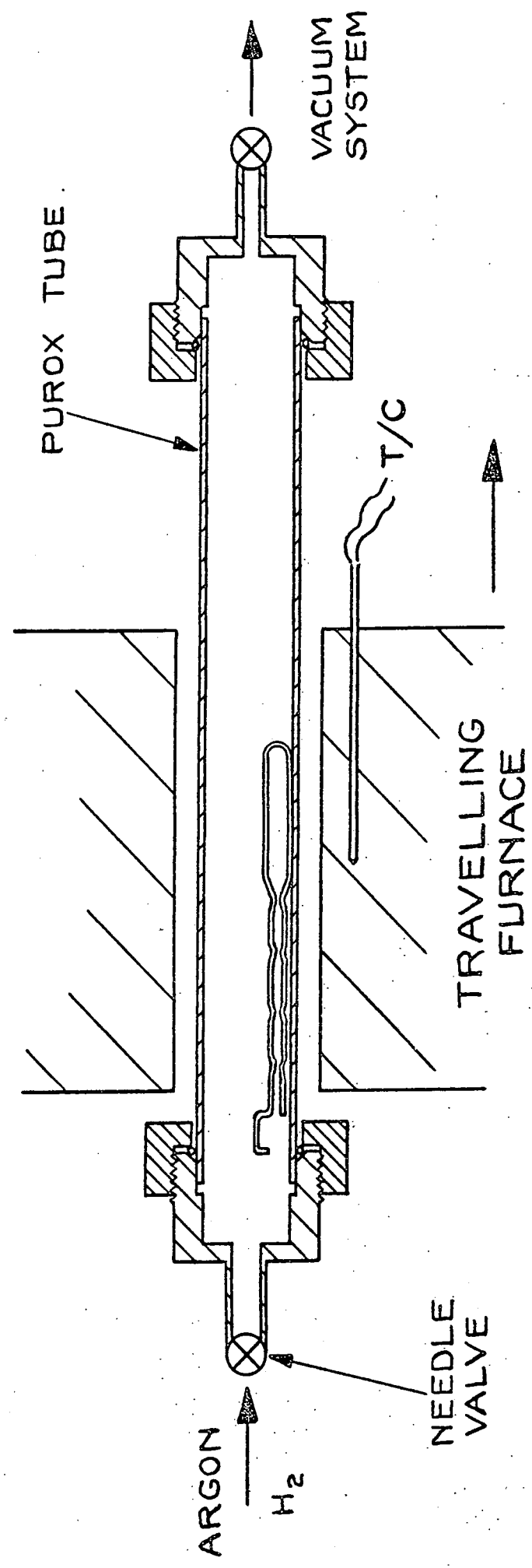GROWTH TUBE FOR MODIFIED PIPER-POLICH TYPE FURNACE.

Fig. 6:2:3

CHARGE

10-I.D.

80

4-I.D.

150
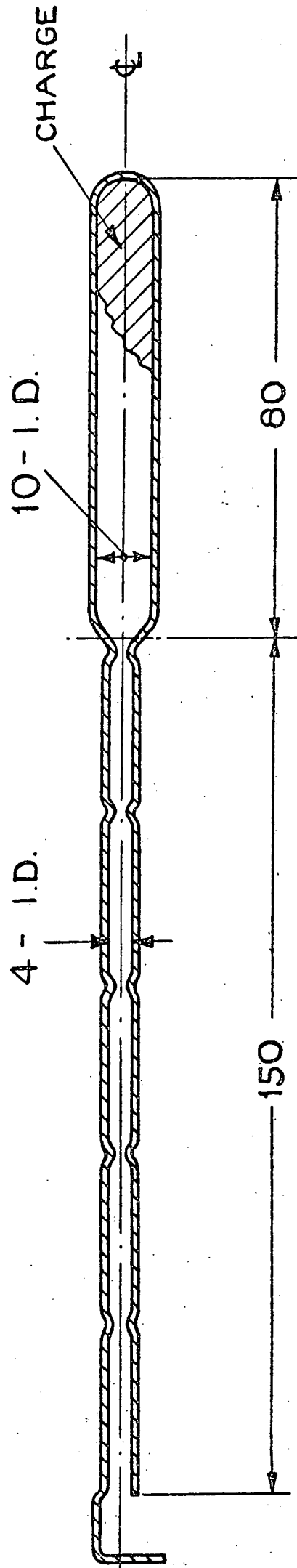
ALL DIMENSIONS IN MILLIMETRES

ACTUAL SIZE.

FINAL HIGH TEMPERATURE GROWTH SYSTEM.

Fig. 6:2:4

NOT TO SCALE.

PUROX TUBE.

VACUUM SYSTEM

T/C

TRAVELLING FURNACE

ARGON

H₂

NEEDLE VALVE

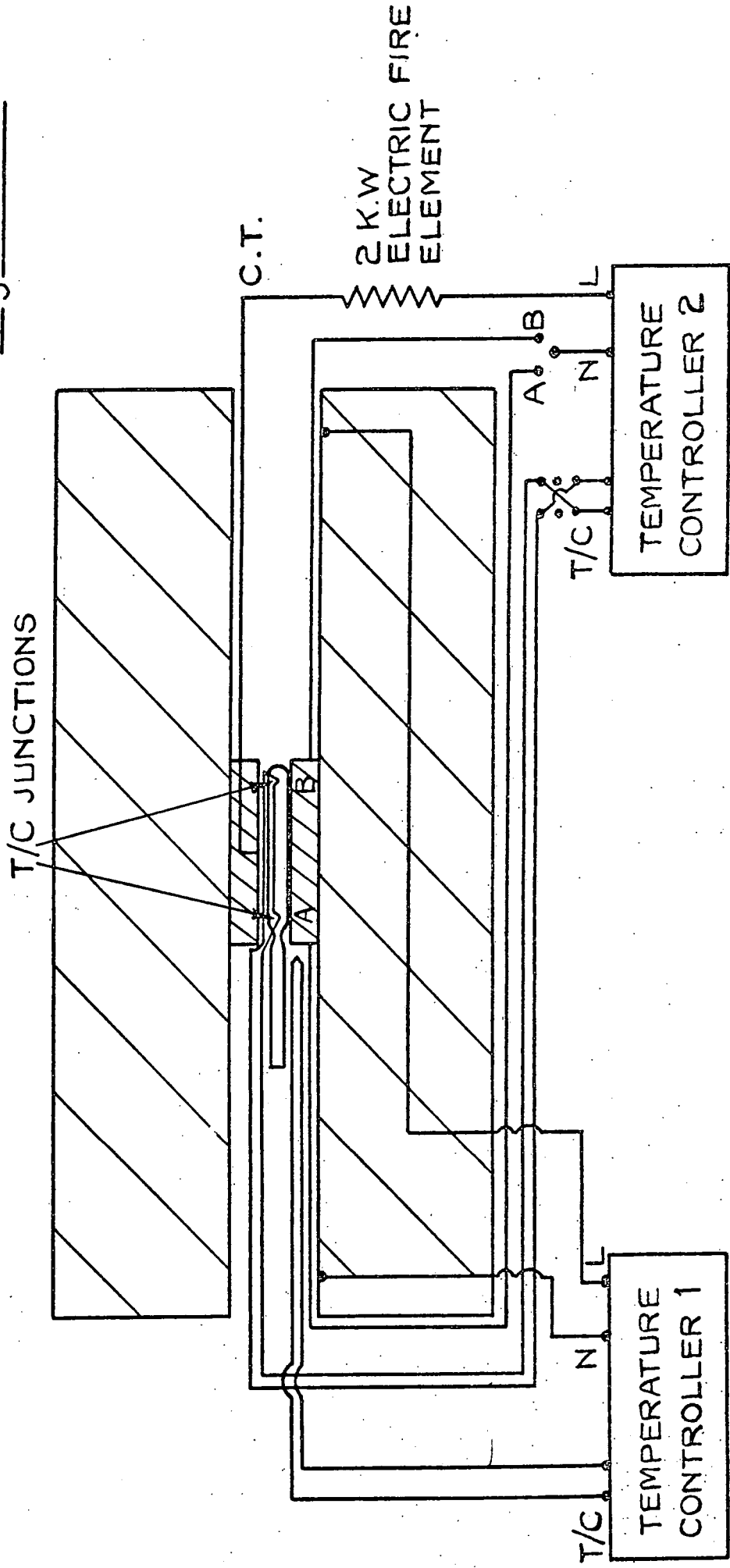(see Figure 6.3.2,)had a quartz heat sink attached to the growth tip to encourage a single crystal to nucleate.

The experimental method was simple, two grams of crushed ZnSe were loaded into a capsule with 4 mg/ml of iodine. The capsule was rapidly flushed with argon and sealed at rotary pump pressure. A solid silica rod was attached as the heat sink and the capsule was ready for use. It was positioned in the furnace as shown in Figure 6.3.3 and the backing furnace was switched on to bring the furnace temperature to $800^{\circ}$C. When this had been reached the inner furnace was switched on. Since section A was connected to the controller which maintained a temperature difference of $30^{\circ}$C between the ends of the capsule, a reverse temperature gradient could be maintained for 24 hours to clean the growth tip. To start the growth the temperature controller was connected to zone B and the thermocouple connections reversed. The temperature difference $\Delta T$ was maintained at $10 - 15^{\circ}$C for ZnSe.

A similar procedure was followed to grow ZnS from ZnS powder, except a temperature difference of $20 - 30^{\circ}$C was employed. Small crystals weighing about ½ gm could be grown in $10 - 14$ days. The capsules were removed from the furnace to check on progress after 7 days. Often very good quality pieces of crystal were produced although their size was small. The material often terminated in prisms or tetrahedra. All the facets examined were of the {111} or {110} type. No twins were observed.

To grow material doped with manganese the elemental dopant was ground up with the charge and the standard procedure was followed. After a few days the furnace was switched off and the capsule removed. None of the charge had been transported but zinc displaced by the manganese was found in the growth tip. The charge thus formed was inserted into a

IODINE TRANSPORT SYSTEM

Fig. 6:3:1.

T/C JUNCTIONS

C.T.

2 K.W ELECTRIC FIRE ELEMENT

TEMPERATURE CONTROLLER 2

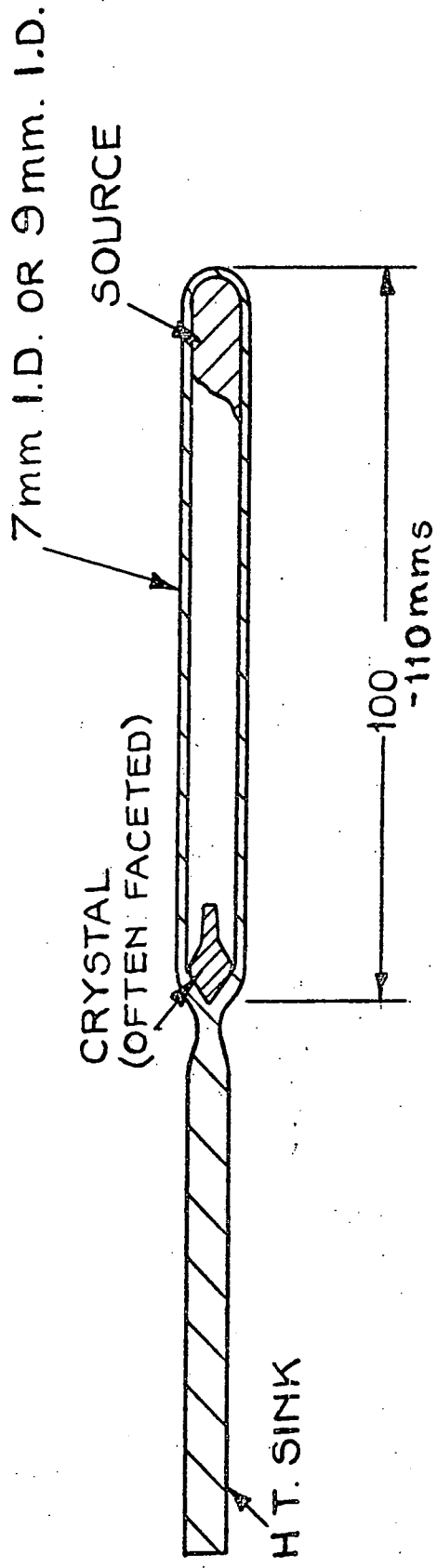TEMPERATURE CONTROLLER 1

T/C = THERMOCOUPLE

C.T. = CENTRE TAP FROM FURNACE WINDING

second capsule, and growth now proceeded in the same way as for undoped ZnSe. There was little change in the growth rate or crystallinity, although manganese doped crystals appeared much darker.

The capsules usually employed in these experiments were 100 mm long and 6 - 7 I.D. When the diameter was increased to 9 or 10 mms the growth became irregular and often dendritic. It was concluded from this that the normal 7 mm I.D. capsule promoted diffusion controlled growth, while in the larger diameter tube convection currents led to instability.

IODINE TRANSPORT CAPSULE.

Fig. 6:3:2

7mm. I.D. OR 9mm. I.D.

SOURCE

CRYSTAL
(OFTEN FACETED)

100
~110mms

H.T. SINK

DETAILS OF FURNACE CONSTRUCTION FOR THE IODINE TRANSPORT SYSTEM.

Fig. 6:3:3

MULLITE TUBE

CENTRE TAP WITH GLASS TUB AS INSULATION

JUNCTION

POWER INPUT TO

JUNCTION

WINDING B

KANTHAL A1 WOUND ON TRANSPARENT SILICA

WINDING A

T/C

F I R E B R I C K

POWER INPUT TO A

THERMOCOUPLE FOR BACKING FURNACE
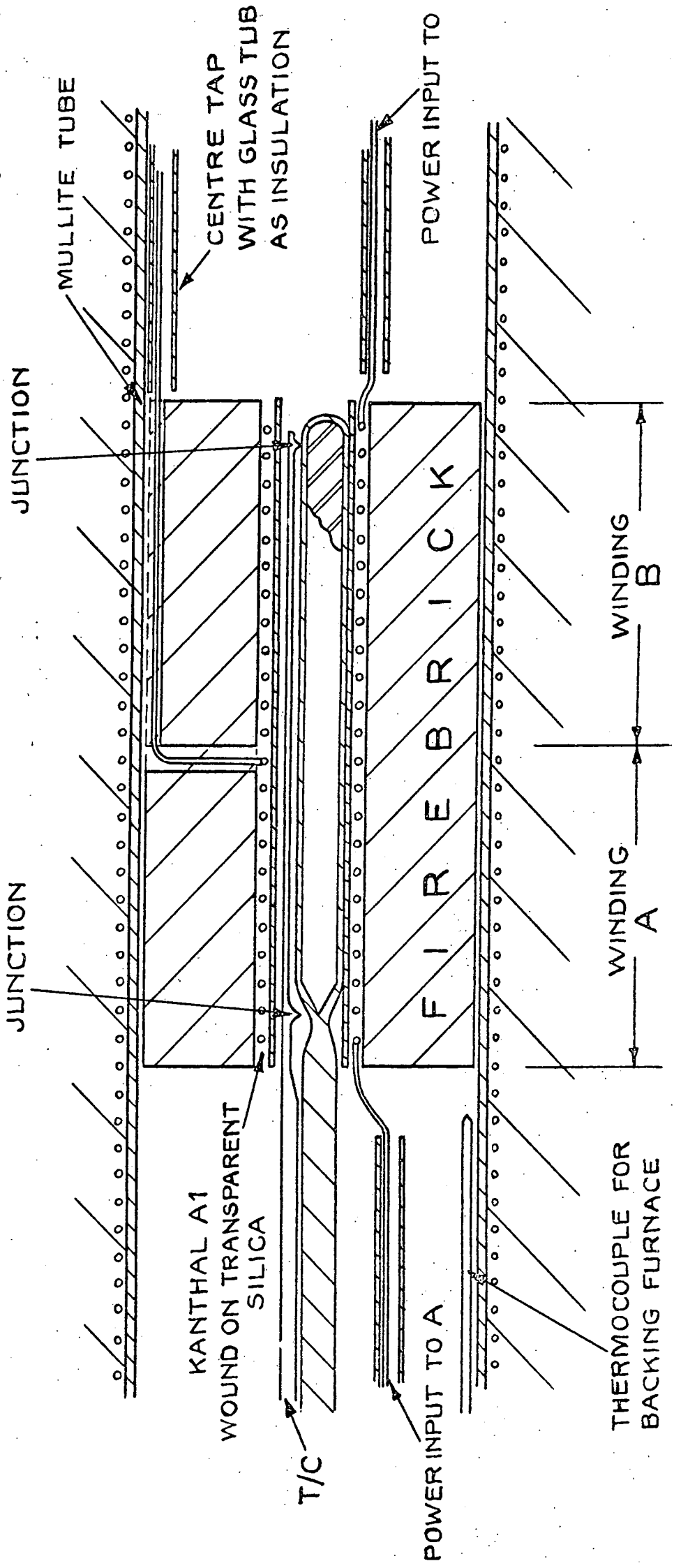
ACTUAL SIZE

# CHAPTER 6

## REFERENCES

1. H Hartmann (1970) Kristall and Technik. 5 4 527-534

2. H Weidemeier and A G Sigai (1969) J. Cryst. Growth 6 67-71

3. W W Piper and J J Polich (1961) J. Appl. Phys. 32 1278

4. J H E Jeffes (1968) J. Cryst. Growth 3,4 13-32

5. R Nische, H V Boelsterli and M Lichtensteiger (1961) J. Phys. and Chem. Sol. 21 199

6. H Shafer (1964) Chemical Transport Reactions Academic Press New York

7. S G Parker (1971) J. Cryst. Growth 9 177-182

## CHAPTER 7

### THE ANOMALOUS PHOTOVOLTAIC EFFECT

7.1    Introduction to the anomalous photovoltaic effect

The anomalous photovoltaic effect in single crystals of zinc sulphide is a well-known but little-understood phenomenon which has been reported by several authors (Ellis et al 195 ,[1] Cheroff and Keller 1958,[2] Merz 1958,[3] Lempicki 1959,[4] Cheroff et al 1959,[5] Brafman et al 1964[6]). Under examination in the polarizing microscope between crossed polarizers, the crystals which show the effect are seen to contain bands of uniform birefringence parallel to the close packed planes. The widths of these bands vary considerably and are of the order of micrometres. The coloured birefringent bands are separated by dark lines (striations) which are accompanied by kinks in the crystal and by surface steps (Daniels 1966[7]). Together with silicon carbide and cadmium iodide, zinc sulphide is a classic example of a material showing polytypism. In their book, Verma and Krishna (1966)[8] listed ten known polytypes of ZnS, and Steinberger and Mardix (1967)[9] have identified more than sixty. It is often supposed that a band of uniform birefringence corresponds to a particular polytype, and that the dark striations are associated with one-dimensional stacking disorder. In any event the anomalous photovoltage only appears when the electrodes are applied along an axis perpendicular to the striations and birefringent bands. The dominant features of the observed photovoltage are (i) that it can exceed 100 V in a crystal a few millimetres long, and (ii) it reverses sign at least once, and sometimes twice, as the wavelength of the exciting radiation is increased from about 3000 to 4000 Å. Merz (1958)[3]

has offered an explanation of the effect which suggests that each structural change in the crystallographic stacking sequence, from dominantly cubic to dominantly hexagonal and vice versa, produces a photovoltage of the order of 0.15 V, and that all those voltages are additive. Neumark (1962)[10], however, has criticized Merz's explanation and proposed that the effect is due to spontaneous polarization of hexagonal zinc sulphide which leads to opposing electric fields in hexagonal and cubic material.

This work is believed to be the first observation of the anomalous photovoltaic effect in zinc selenide, although Hartmann[11] reported polytypes amongst needles of disordered structure in 1970. The crystals which showed an anomalous photovoltaic effect all exhibited numerous birefringent bands and dark striations when examined in the polarizing microscope. These observations demonstrate that the effect in zinc selenide is entirely analogous to that in zinc sulphide and have led the author to propose a rather different qualitative explanation of the phenomenon.


7.2    Crystal Growth

The crystals used were prepared as described in Chapter 2. Hartmann[11] reported his polytypes amongst material prepared by a similar technique. However, he used mixtures of HCl, $H_2$ and $N_2$ as his carrier gases.

The zinc selenide produced was normally used for growing the bulk crystals described in Chapter 3. However, it occasionally contained some well shaped needles and platelets. This work was performed exclusively on needles selected from such material, which were typically

1 cm long and approximately hexagonal in cross section with a width

of one side of the hexagon of about 0.1 mm. In the dark the electric

resistivity of these samples was of the order of $10^{10}$ Ωcm corresponding

to a resistance of $10^{14}$ Ω.

First, the needles were examined under crossed polarizers, in

the polarizing microscope. A typical micrograph is shown in Figure 7.2.1.

The crystals examined had several common features. For example, all

of them were birefringent, exhibiting bands of uniform colour separated

by dark striations, which were perpendicular to the c-axes of the

crystals. This axis lay along the length of a needle. Each needle

was hollow. A hole ran along the axis of each crystal, as the dark

line along the centre of Figure 7.2.1 shows. Figure 7.2.2 is a micro-

graph of a different crystal with an even larger hole along its axis.

The micrographs show that the holes were not perfectly continuous but

appeared to suffer slight lateral displacements at their intersections

with the dark striations. Hollow needle crystals of zinc sulphide have

previously been described by Lendvay and Kovacs (1970)[12]. Figure 7.2.3

shows growth features at the tip of the crystal, and 7.2.4 coloured

birefringent bands.


## 7.3    Experimental Procedures and Results

In initial trials, conducted to select samples suitable for

further investigations, the needles were equipped with silver paste

electrodes at either end of their long dimension and were mounted on

sample holders as shown in Figure 7.3.1. The sample formed a bridge

between two copper contacts stuck to a glass slide. If a bridge

arrangement was not used the crystals were shorted out by the silver

paste which crept by surface tension between the glass and the crystal. Many of the samples were so delicate that they could only be handled with an artist's fine brush.

When the paste was dry the samples were irradiated with focussed light from a 250 Watt, compact source, mercury vapour lamp. For measurements of the open-circuit photovoltage, the sample was connected in series with a backing-off voltage and an EIL 'Vibron' electrometer type 33B. The electrometer, which had an input impedance of $10^{14}$ $\Omega$, was used as a null meter. All the crystals exhibited an open-circuit photovoltage. With many, this was smaller than the band gap of zinc selenide ($E_g \sim 2.7$ eV), but with several the OCV (open-circuit voltage) exceeded 5 V, and with one in particular, it exceeded 100 V. The results which are described below refer specifically to this latter crystal, but it is clear that the photovoltaic properties of all the needles studied were basically similar.

Although it was important to measure the OCV of the samples in order to demonstrate the true anomalous nature of the photoeffect, it was more convenient when studying the spectral response etc., to measure the short-circuit current (SCC). The reason for this was that the high input impedance of the electrometer made the null measurement of the OCV an essentially slow process. During the time required to adjust the backing voltage the zero-drift of the electrometer might have been appreciable so that substantial error would be involved. No such difficulty occurred when the SCC was measured using a Rank DC amplifier type NE 503B.

The SCC increased with increasing temperature, as illustrated by the curve in Figure 7.3.2, and its variation with intensity of

Figure 7.2.1: Micrograph of a crystal exhibiting birefringent
banding and dark striations. Notice the kinking of
the surface and the axial hole. (Magnification x 200)



Figure 7.2.2: Micrograph of a second crystal similar to those shown
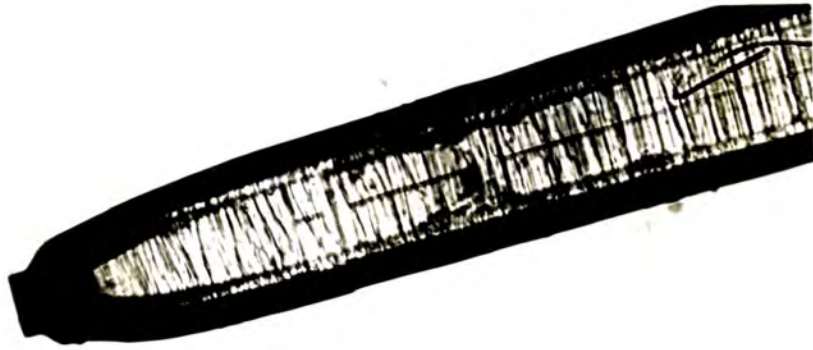in Figure 7.2.1, but with larger axial hole.
(Magnification x 200)

Figure 7.2.3:  Growth features at the tip of a
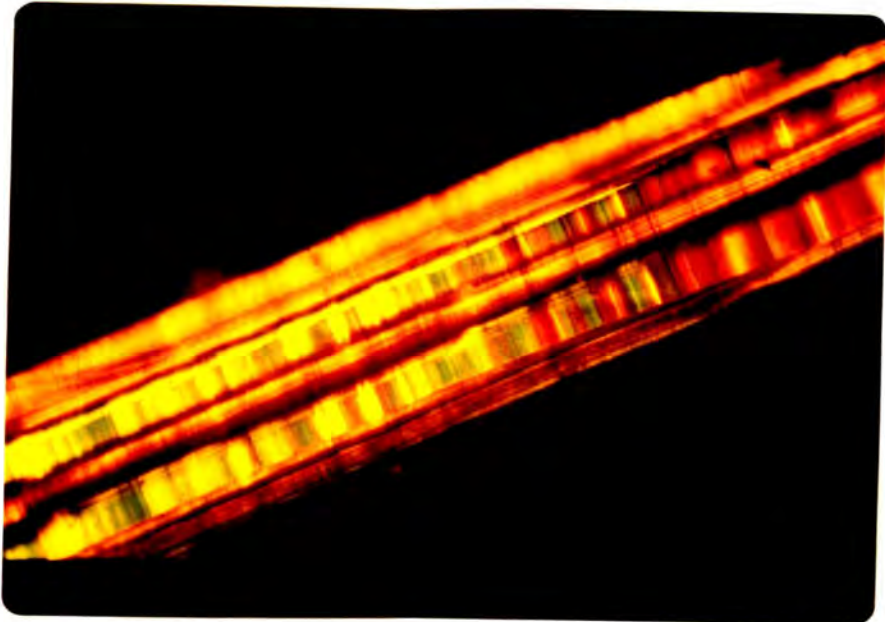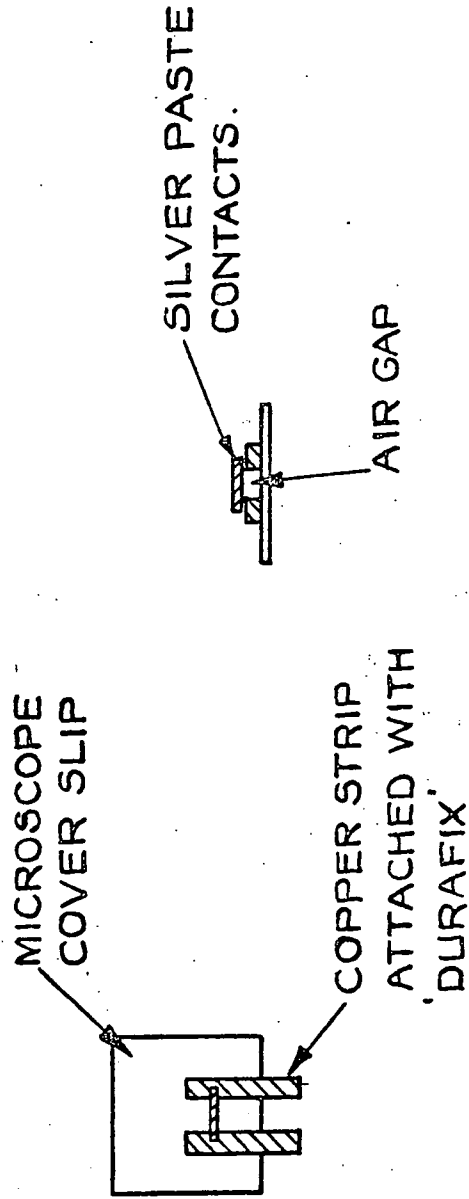needle crystal (Mag x 100)



Figure 7.2.4:  Coloured birefringence bands in ZnSe
needle viewed through crossed
polarisers (Mag x 200)

# METHOD OF MOUNTING SAMPLES TO MEASURE
## ANOMALOUS PHOTOVOLTAIC EFFECT.

Fig. 7 : 3 : 1



MICROSCOPE COVER SLIP

COPPER STRIP ATTACHED WITH 'DURAFIX'

SILVER PASTE CONTACTS.

AIR GAP

illumination was found to be linear over five orders of magnitude when the illumination from the mercury lamp was reduced by interposing neutral density filters.

The spectral distribution of the SCC to unpolarized light is shown in Figure 7.3.3. The measurements were made using light from the exit slit of a Barr and Stroud double monochromator type VL2 with a 250 W tungsten-halogen lamp as source. When the light from the exit slit was polarized with the electric vector parallel or perpendicular to the axis of the needle, the resultant spectral distribution curves were displaced slightly from one another in wavelength, as shown in Figure 7.3.4. The spectral distribution of the SCC was measured in two ways, namely by scanning from long to short wavelengths and vice versa. There was no detectable difference in the resultant curves, which indicates that trapping effects played no significant part in the process.

## 7.4 Discussion

Polytypism and one-dimensional stacking disorder have been studied fairly extensively in zinc sulphide, see for example, Verma and Krishna (1966)[8]. The phenomena occur because of the close similarity between the wurtzite and zinc blende structures and the small difference in energy between the two modifications. Wurtzite is the stable modification of zinc sulphide at temperatures above $1020^{\circ}C$, whereas zinc blende is stable at lower temperatures. However, it is not usual for synthetic crystals of zinc sulphide to be either wholly cubic or wholly hexagonal. Crystals grown at high temperatures ($\sim 1200^{\circ}C$) contain polytypes and stacking faults, and under crossed

ANOMALOUS PHOTOCURRENT PLOTTED AGAINST TEMPERATURE.

Fig. 7:3:2

PHOTOCURRENT ARBITRARY UNITS.

TEMPERATURE °K ⟶
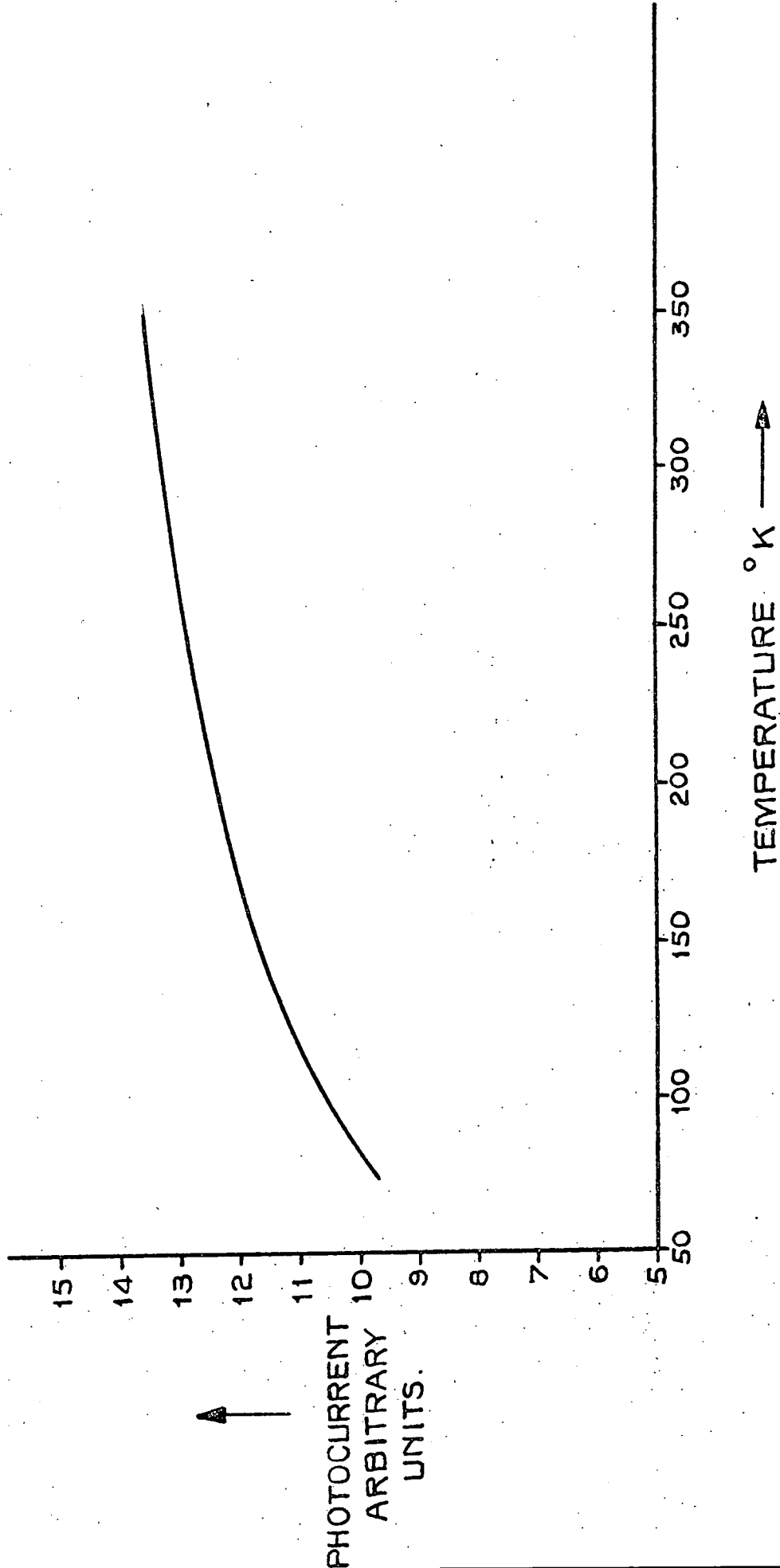
polarizers in the polarizing microscope exhibit birefringent bands and dark striations. Such crystals show the anomalous photovoltaic effect.

Although zinc selenide can also crystallize in hexagonal (wurtzite) and cubic (zinc blende) modifications, the situation appears to be slightly different from that with zinc sulphide. For example, no consensus of opinion in the literature as to the temperature ranges in which the two modifications of zinc selenide would be expected to be stable has been found. The experience of several years of growing crystals of zinc selenide by a flow process as described earlier, by the iodine transport method and in sealed tubes, suggests that the cubic modification is stable at temperatures below $800^{\circ}C$ and above $1000^{\circ}C$. In the intermediate range from 800 to $1000^{\circ}C$, hexagonal crystals can be obtained, particularly if the flow process is employed. It is interesting to note that Fitzgerald et al (1966)[13] grew hexagonal crystals of zinc selenide at $1000^{\circ}C$ using a flow process. Crystals grown by them in the range 900-950$^{\circ}C$ showed mixed cubic-hexagonal structure. Hartmann[11] found similar results.

The crystals used in this investigation were all grown in the temperature range 800-1000$^{\circ}C$, and they all showed coloured birefringent bands and dark striations when examined in the polarizing microscope. Indeed all the needles were hollow, and it is believed that they grew as hexagonal crystals from axial screw dislocations with very large Burgers' vectors. The crystals are hollow because the hole reduces the energy of the dislocation considerably. Periodically occurring slip in basal planes after growth would lead to the formation of polytypes by the mechanism discussed by Daniels (1966)[7]

## SPECTRAL DISTRIBUTION OF S.C.C. USING UNPOLARISED LIGHT.
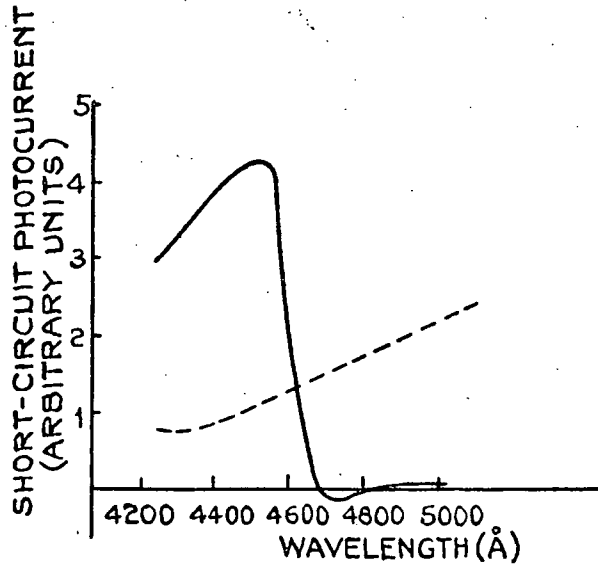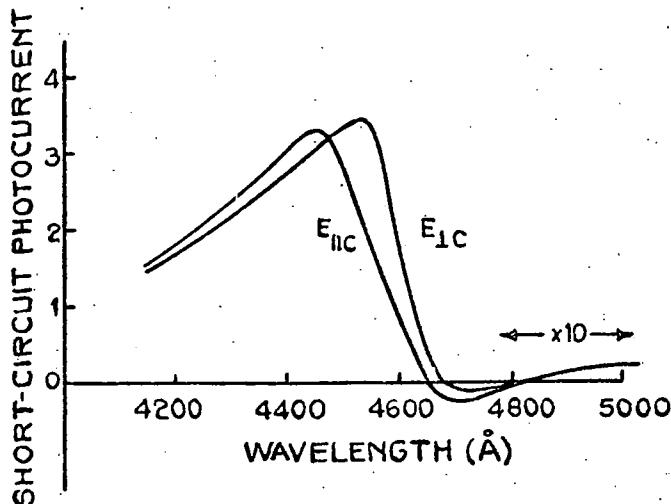
SPECTRAL DISTRIBUTION AT ROOM TEMPERATURE OF THE SHORT-CIRCUIT PHOTOCURRENT WITH UNPOLARIZED LIGHT. THE BROKEN CURVE REPRESENTS THE ENERGY PER UNIT BAND WIDTH OF THE EXCITATION USED.

## SPECTRAL DISTRIBUTION OF S.C.C. USING POLARISED LIGHT.

SPECTRAL DISTRIBUTION OF THE SHORT-CIRCUIT PHOTOCURRENT WITH LIGHT POLARISED PARALLEL $(E_{\parallel c})$ AND PERPENDICULAR $(E_{\perp c})$ TO THE C-AXIS OF THE NEEDLE.

and Mardix and Steinberger (1966)[14]. It is important to note that the polarity of the stacked double layers of zinc and selenium atoms in the basal planes does not change along the length of the crystal. Further, the crystals contained very few (and in most crystals no) extended cubic regions; i.e. with the exception of the dark striations, the crystals exhibited birefringent banding along the whole of their lengths. It is concluded, therefore, that the anomalous photovoltage occurs in a material when the structure changes frequently from one polytype to another without any change of polarity.

Neumark's[10] theory seems to be unsatisfactory because it assumes that the cubic material is nonpolar. Cubic material, however, is polar in the same sense as the hexagonal. It is also difficult with Neumark's theory to understand why the photovoltage changes sign when the wavelength of the incident light is varied. It is believed that the effect can be explained in terms of the heterojunction which occurs at the interface between two polytypes. In the following discussion the crystal is imagined to be composed of alternate segments of crystal with the hexagonal and polytype structure. It seems reasonable to suppose that the hexagonal and cubic modifications represent the two extremes of the possible range of polytypic structures and that the band gaps of the various polytypes are intermediate between those of hexagonal and cubic zinc selenide.

The exact values of the forbidden gaps of cubic and hexagonal zinc selenide reported in the literature vary slightly from one author to another. However, it is certain that the band gap of hexagonal zinc selenide is larger than that of the cubic. For example Segall and Marple (1967)[15] quote $E_g$ = 2.818 eV for cubic ZnSe at 4 K,

whereas Liang and Yoffe (1967)[16] give a value of 2.8697 eV for the hexagonal modification at 15 K. According to Segall and Marple[15] the band gap of the cubic material at room temperature is 2.67 eV. It seems reasonable to assume that the band gap of hexagonal zinc selenide is about 2.73 eV at room temperature.

Consider what happens in one unit of the crystal along the c-axis, where one unit contains two potential barriers which occur when the crystal structure changes from a polytype to hexagonal and back to the polytype. The Fermi level, which lies approximately in the middle of the forbidden gap of all the crystal modifications, must be at the same energy throughout in the dark. Since the work-functions of the polytype and hexagonal modifications are different, band-bending will occur, as illustrated for one junction in Figure 7.4.1, to permit the Fermi level to attain its equilibrium position. To achieve additive photovoltages along the crystal it must be postulated that consecutive barriers contain some degree of asymmetry, as shown for example in Figure 7.4.1b, which illustrates the two barriers of the unit under discussion. In fact it would be rather surprising if no asymmetry were present, as the following argument will demonstrate.

To fix ideas, consider the unit to be made up of a sandwich of hexagonal material between two cubic layers (cubic is simply taken to represent the extreme polytypic variation from the hexagonal structure). In the cubic region on the left-hand side of Figure 7.4.1b the double layers of zinc and selenium are assumed to be stacked in the ABC cubic sequence along the axis of the needle. Suppose that the (111) zinc plane is to the left and the ($\overline{111}$) selenium plane to the right. Then at the junction X, Figure 7.4.1b, a selenium layer in a

mainly cubic environment neighbours a zinc layer in the hexagonal modification. In contrast at the next junction, Y, a selenium layer in a mainly hexagonal environment neighbours a zinc layer in a cubic matrix, i.e. the environments are reversed. It seems reasonable, therefore, to suppose that the potential energy diagrams at the two junctions will differ slightly from one another. In Figure 7.4.1b, the two barriers are drawn with slightly different heights.

To check the validity of the idea an experiment was performed on ZnSe containing no major structural defects. Large-area cubic platelets of ZnSe have been studied fairly extensively in this department (Gezci and Woods)[17]. The only defects observed in these particular crystals have been dislocations and three-dimensional defects which may have been stacking-fault tetrahedra. Twelve such crystals were equipped with silver contacts on the large-area faces, and were then illuminated with the focused light from the mercury lamp. In all the samples a photovoltage of the same sign was generated. This photovoltage was about 20 mV in magnitude, and in all samples the zinc (111) face became negative. This experiment indicates that the work-functions of the (111) and ($\bar{1}\bar{1}\bar{1}$) faces are different and supports the contention that the two junctions in a crystal unit such as discussed above will be asymmetric.

Now assuming that some such potential energy diagram as that in Figure 7.4.1b is correct, the behaviour of the photocurrent can be explained quite simply. First, although the two junctions produce photovoltages in opposition, there is nonetheless a net photo-EMF per pair when the sample is illuminated. This net EMF is small, being of the order of a few millivolts, but there may well be several thousand barriers per centimetre along the c-axis. Indeed Merz was

# ENERGY DIAGRAM OF CUBIC/HEXAGONAL JUNCTION IN Zn Se NEEDLE.

Fig. 7 : 4 : 1



A
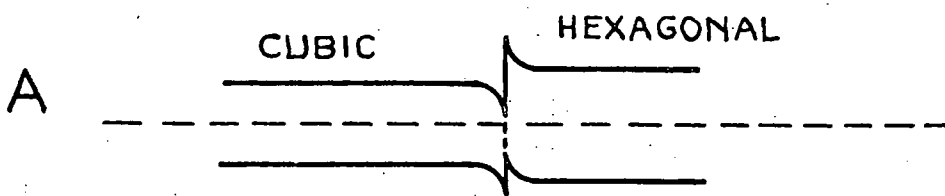
CUBIC    HEXAGONAL

PROPOSED POTENTIAL ENERGY BARRIER AT A
HEXAGONAL/POLYTYPE INTERFACE.



B

X    Y
HEXAGONAL
CUBIC                CUBIC
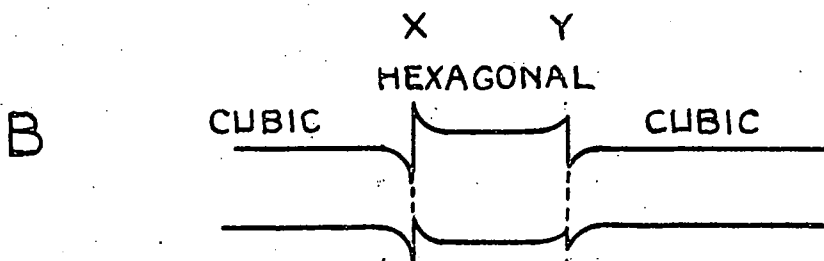
PROPOSED ENERGY DIAGRAM OF TWO ADJACENT
BARRIERS WHERE A REGION OF HEXAGONAL
CRYSTAL IS SANDWICHED BETWEEN THE SAME
POLYTYPE OR CUBIC REGION.

able to count 2000 barriers per cm in his crystals. (There may well, of course, have been more which were not resolved in the polarizing microscope).

Consider next what happens when the wavelength of the exciting light is changed. At long wavelengths, light is absorbed at deep-lying donors in both the cubic and hexagonal regions (ZnSe is a dominantly n-type semi-insulator). The concentrations of electrons excited to the conduction bands of the cubic and hexagonal regions are therefore very similar. However, the electrons in the hexagonal region will see a lower barrier at Y than at X and will therefore flow out of the hexagonal region preferentially to the right. Thus a current will be generated with electrons flowing to the right under short-circuit conditions, and with an open circuit a net voltage will be set up to oppose their flow.

As the wavelength of the excitation is decreased, a situation is reached where free electrons can be excited across the band gap of the cubic material, but the photon energy is still insufficient to generate free electrons and holes in the hexagonal region. Now the major electron concentration is in the cubic regions, with the result that electrons flow more readily over the barrier at Y from right to left, than they do over the barrier at X in the opposite direction. Under open-circuit conditions, this means that the hexagonal region at Y becomes more negative than that at X, and as a result under short-circuit conditions electrons will flow from right to left. In brief, the direction of the short-circuit current is reversed.

As the wavelength of the excitation is reduced still further, electrons can be excited across the band gap of the hexagonal region.

Eventually a large population of electrons would be created in the conduction band of the hexagonal layer with the result that electrons would again flow out of the hexagonal region to the right, thus leading to a further reversal of the short-circuit current. In total therefore, the model can explain two reversals of the sign of the photocurrent as the wavelength is changed.

The model requires that the tail of the fundamental optical absorption region in cubic zinc selenide extends to 4800 $\overset{o}{A}$ at room temperature, where the first reversal of sign occurs as the wavelength is reduced. Experiments in this laboratory by S. Gezci on the optical absorption of cubic crystals have shown that significant absorption is usually observed beginning at 4750 $\overset{o}{A}$ at room temperature. Furthermore, no dichroism would be expected and the threshold for significant absorption in cubic zinc selenide should occur at the same wavelength for light polarized with the electric vector parallel or perpendicular to the needle axis. Thus, if this explanation of the anomalous photovoltaic effect is correct, the first sign reversal of the photocurrent to occur as the wavelength is reduced should be independent of the polarization of the incident light. The curves in Figure 5 show this to be an observed fact.

In the cubic modification of zinc selenide the uppermost valence band has $\Gamma_s$ symmetry and optical transitions to the conduction band are allowed for either state of polarization of the incident light. With hexagonal zinc selenide the uppermost valence band has $\Gamma_9$ symmetry and the next highest $\Gamma_7$ symmetry. Optical transitions from the $\Gamma_9$ band to the conduction band are only allowed for $E_{\perp c}$ (light polarized with the E-vector perpendicular to the c-axis), whereas transitions from

$\Gamma_7$ are allowed for $E_{\parallel c}$ and $E_{\perp c}$. Then if light polarized with $E_{\perp c}$ is used, the threshold for optical absorption will occur at a longer wavelength than it will when light polarized with $E_{\parallel c}$ is used. The curves in Figure 7.1.4 show that the second reversal of the sign of the photocurrent occurs at longer wavelengths with light polarized with $E_{\perp c}$, which is in accord with our interpretation. Unfortunately the wavelengths at which the photocurrent changes sign cannot be used to determine the band gaps of the various polytypic and hexagonal regions because the experimental curves are likely to be superpositions of many individual curves for barriers corresponding to phase changes between particular polytypes.

# CHAPTER 7

## REFERENCES

1. S G Ellis, F Herman, E E Loebener, W J Merx, C W Struck and J G White, (1958) Phys. Rev. 109 1860.

2. G Cheroff and S P Keller (1959) Phys. Rev. 116 1091-3

3. W J Merx (1958) Helv. Phys. Acta 31. 625-635

4. A Lempicki (1959) Phys. Rev. 113 1204-9

5. G Cheroff, R C Erick, and S P Keller (1959) Phys. Rev. 116 1091-3

6. O Brafman, E Alexander, B S Fraental, Z H Kalman and I T Steinberger (1964) J. Appl. Phys. 35 1855-60

7. B K Caniels (1966) Phil. Mag. 14 487-500

8. A R Verma and P Krishna (1966) Polymorphism and Polytypism in Crystals (New York, Wiley)

9. I T Steinberger and S Mardix (1967) Proc. Int. Conf. in II-VI Semiconducting Compounds, Brown University, Rhode Island, U.S.A. Ed. G.D. Thomas (New York W.A. Benjamin) pp.167-78

10. G F Neumark (1962) Phys. Rev. 125 838-45

11. H Hartmann (1970) Kristall and Technik 5 4 527-534

12. E Lendvay and P Kovacs (1970) J. Crystal Growth 7 61-4

13. A G Fitzgerald, M Mannami, E B Pagson and A D Yoffe (1966) Phil. Mag. 14 197-200

14. S Mardix and I T Steinberger (1966) Israel J. Chem. 3 243

15. B Segall and D T F Marple (1967) Physics & Chemistry of II-VI Compounds, ed. M. Aven and J.S. Prener (Amsterdam: North-Holland) p.335

16. W Y Liang and A D Yoffe (1967) Proc. R. Soc. A300 326-36

17. S Gezci and J Woods (1972) J. Mat. Sci. 7 603-8

## CHAPTER 8

## CONCLUSIONS

The main object of the research described in this thesis was to produce boules of zinc selenide with centimetre dimensions for research purposes. Having established a reliable technique for undoped boules the work progressed to doped material, with particular emphasis on the incorporation of manganese. Finally the growth of crystals of the solid solution $ZnSe_xS_{1-x}$ was investigated.

The most satisfactory production technique for ZnSe was found to be the method of Clark and Woods[1] which was originally used for CdS. In brief, this method is a vacuum distillation in a sealed and evacuated capsule. The capsule is connected via a narrow orifice to a reservoir containing either zinc or selenium which is used to control the composition of the vapour in the capsule. Theoretically, in order to obtain the maximum transport rate, the composition of the gas in the capsule should be the stoichiometric ratio of two parts monatomic zinc to one part of diatomic selenium. However, this is not necessarily the best condition for crystal growth. Faktor and Garret[2] suggest that growth off stoichiometry should give more stable growth conditions. A theoretical consideration of the growth system revealed that growth a little off stoichiometry must always occur in the Clark and Woods system. Experimentally it was found that for undoped boules the best growth occurred when the tail temperature was maintained so as to give a pressure of the reservoir element equal to $\frac{1}{3}P_{MIN}$ in the case of selenium or to $\frac{2}{3}P_{MIN}$ in the case of zinc. With a charge temperature of $1165°C$ this meant a reservoir temperature of $560°C$ for zinc or $360°C$ for selenium. The theoretical analysis of the tail reservoir system was of necessity mainly qualitative. However, it has been demonstrated that the use of

the reservoir will correct for a non-stoichiometry in the charge exceeding 1000 p.p.m., and that a much greater quantity of volatile material may be removed if it is released as the system warms up, e.g. zinc released by the reaction between the charge and manganese. Further, it has been shown that the tail reservoir will not hold an exact vapour pressure over the material in the capsule, but one which depends on the physical dimensions of the system, the amount of residual gas present, and the temperature of the reservoir. It was discovered that to account theoretically for the rate of loss of material to the tail tube from the capsule, an inert gas pressure of $\sim 1-5$ torr was required in the capsule. Several different experiments were performed to check if this gas was in fact present. A pressure of residual gas of the right order of magnitude was discovered in capsules which had been in the furnace for a period of 14 days. Mass spectrometer analysis suggested that the gas was at least partly carbon monoxide. In fact, if this gas were not present the rate of loss of material to the tail tube would be sufficient to block it within a few hours. This was con-firmed experimentally by pumping the tail tube of a capsule with a rotary pump while crystal growth proceeded. When this inert gas pressure is taken into consideration, it was found that the maximum deviation of $A_\ell$ (the ratio $P_{Se_2}/P_{Zn}$ at the charge) from the stoichiometric value of 0.5 was $A_\ell = 0.264$ (zinc tail) and $A_\ell = 0.849$ (for a selenium tail). From this it may be calculated that $A_o$, the value at the interface, was between $A_o = 0.194$ (Zn tail) and $A_o = 1.12$ (Se tail). It was calculated that to account for the observed growth rate a value of $\Delta T$ between 8.2 and $19.6^{\circ}C$ was required. The experimentally observed values of $\Delta T$ were less than $20^{\circ}C$. This is a strong indication that the growth was transport limited.

The crystal itself can be grown with a different stoichiometry from the charge and the stoichiometry remains constant throughout the growth

period, in contrast to the stoichiometry of a crystal grown in a simple sealed capsule. A much wider range of dopants may be incorporated before growth is inhibited. In general it was concluded that crystals grown with selenium reservoirs should be of higher purity than those with zinc reservoirs, because the lower vapour pressure in the tail helps impurities to escape from the capsule. Also growth conditions should be more stable because $P_T$ increases faster for a selenium rich atmosphere than for a zinc rich one. These findings were confirmed by experience during the growth of several hundred ZnSe and CdS boules.

The dopants copper, gallium and indium were found to enter the boule easily when added to the charge in the form of the elements. However, it was more effective to add erbium and manganese to the reservoir in the form of the chloride. It is believed that the growth of such materials is assisted by a chlorine transport reaction. This could be of assistance in the incorporation of many dopants which are not easily transported in elemental form. The amount of manganese incorporated into the lattice can be increased by adding ground manganese metal to the charge in addition to using manganese chloride in the tail. This fact provides support for the argument about a chlorine transport mechanism. To obtain really large amounts of manganese in the crystal ($\sim 1\%$) it was necessary to use C.V.T. with iodine at $\sim 800^{\circ}C$. A temperature different of $15^{\circ}C$ was employed between the ends of the capsule and small ($\frac{1}{2}$ gm) crystals were grown in 10 days in a 7 mm I.D. capsule.

Solid solutions of $ZnSe_xS_{1-x}$ were grown in the Clark and Woods[1] system. The charge was a ground mixture of ZnSe and ZnS and the reservoir contained Zn. A satisfactory reservoir temperature was found to give $P_{Zn}$ = (2 Kpa), where $\ell nKpa = X \ell nKp(ZnSe) + (1-X) \ell nKp (ZnS)$. Theoretically it was found that segregation of selenium and sulphur could occur

through a physical separation in the transport system. This would be worst if transport occurred entirely by diffusion. The reservoir system prevents this happening but could allow the loss of more selenium than sulphur to the tail reservoir. Fortunately in practice this was not significant and boules were grown satisfactorily up to a maximum sulphur content of $ZnS_{0.6}Se_{0.4}$. Growth then became unstable with the distillate consisting of an agglomeration of dendritic needles.

The main defects found during an examination in the electron microscope were thin twins in the case of ZnSe, changing progressively to stacking faults as the sulphur content of the boules increased. As might be expected the quantity of defects increased in the solid solutions. It is thought that the defects are mainly the result of post growth stress, although some twinning probably occurs to maintain the fast growth direction in an appropriate orientation at the growth face.

Finally, the anomalous photovoltaic effect has been discovered in ZnSe. The results were found to be entirely analogous to those reported in ZnS. A potential of over 100 volts was obtained from one needle crystal of ZnSe, which exhibited coloured birefringence bands. The short circuit current was plotted for varying wavelengths of sample excitation. The short circuit current was found to change sign twice as the wavelength of the illumination was reduced from 5000 to 4000 Å. Qualitatively this was explained in terms of the asymmetry of heterojunctions along the polar axis of the needle. As the wavelength of the exciting light is decreased, the electron populations in the conduction bands of the cubic and hexagonal regions of the needle crystal are increased first by trapped electrons and then by electrons excited across the band gap. Normally there is a net flow of electrons from the hexagonal to the cubic regions because of the asymmetric junctions. However, when the energy of the wavelength of the

radiation corresponds to the band gap of the cubic material, there is a sudden jump in the electron population of the cubic region. This reverses the electron flow until the energy of the radiation is sufficient to excite electrons across the band gap of the hexagonal material, when the current flow reverts to normal. Because the effective band gap of hexagonal material is slightly different parallel and perpendicular to the c-axis, the short wavelength reversal should occur at slightly different wavelengths for radiation polarised parallel and perpendicular to the c-axis. This was indeed found as predicted by the theory.

# CHAPTER 8

## REFERENCES

1. L Clark and J Woods (1968) J. Cry. Growth 3, 4 127-130

2. M M Faktor and I Garrett (1974) Growth of Crystals from the Vapour, Chapter 4 (Chapman and Hall London)

# APPENDIX 1

## CONVERSION OF ETHER 19/90 TEMPERATURE CONTROLLER TO

## SOLID STATE SWITCHING

A very simple circuit was used to convert the 'Ether Mini 19/90' temperature controller to Triac firing in order to improve reliability. The circuit is illustrated in Figure A1.1.

In principal, the idea is to remove the relay from the controller and use the power to drive an oscillator circuit which fires a triac instead. The '19/90' has a power supply on the bottom circuit board giving +20, 0, and -20 volts, and the relay is operated by a circuit which holds one terminal at +20 volts, while the other is switched between 0 volts (ON) and 20 volts (OFF). The relay was removed and a transistor used to invert the logic. (It conducts when the base is at 0 volts, but not when it is at 20 volts). When the transistor is conducting the 0.47 $\mu$F capacitor charges from the transistor output via a 1.2 K resistor until it exceeds the breakdown voltage (32 volts) of the diac, when it is discharged and the cycle repeated. The voltage at the collector of the transistor drops to 20 volts when the controller goes 'OFF' and the oscillations stop. Because the circuit pulses every $3 \times 10^{-3}$ secs, it is unnecessary to synchronise the pulses with the mains cycles, there is always a pulse to fire the triac soon after the mains has passed through zero. Investigation with a cathode ray oscilloscope showed the pulses applied to the triac gate to be about 4 volts in magnitude and followed by a ringing oscillation at greater than 100 kHz which died in 2 or 3 oscillations. The action of the controller appeared unaffected by this modification, but it should be noted that it is useful only with resistive loads.

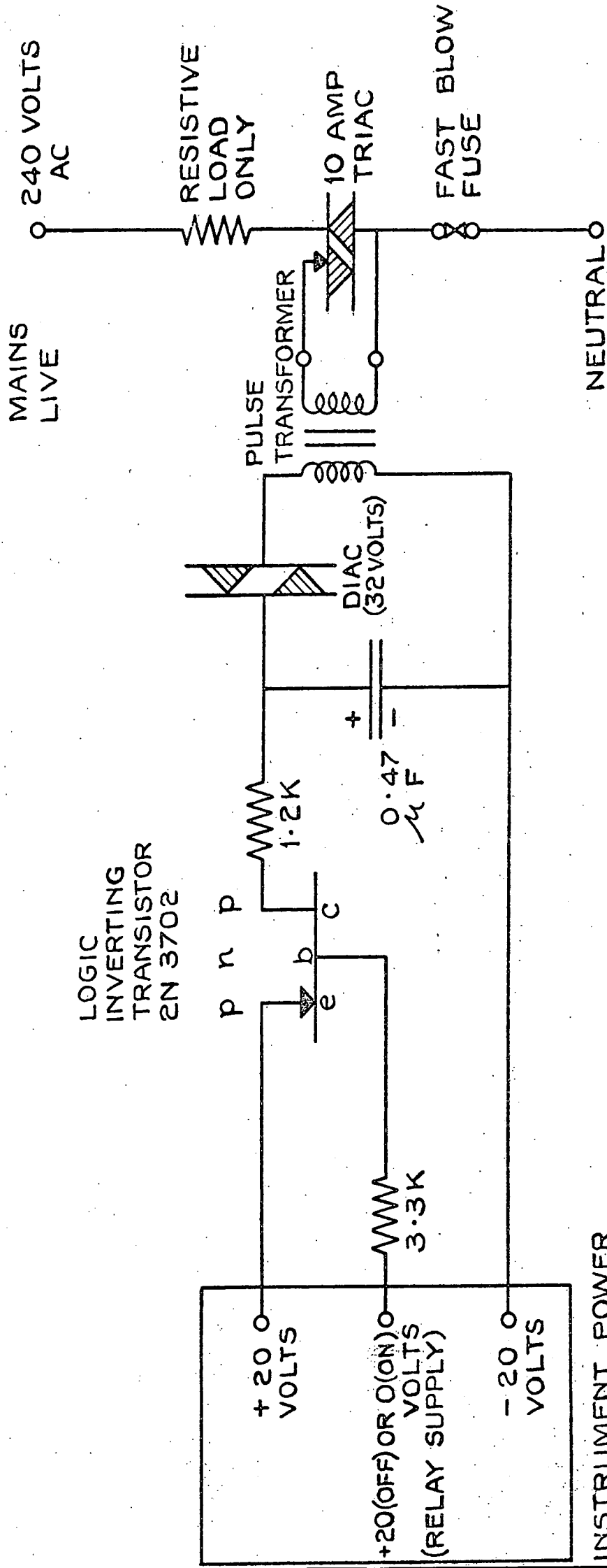# CONVERSION OF ETHER MINI 19/90 TO SOLID STATE SWITCHING.



Fig. A1:1.

## APPENDIX 2

### AN AMPLIFIER TO MEASURE THE SHORT CIRCUIT CURRENT OF A

### PHOTOVOLTAIC CELL

While carrying out a preliminary investigation of the possibility

of depositing epitaxial ZnTe on ZnSe from tin solution the author

became interested in measuring the S.C.C. of the device produced. He

thus became aware of the need for improved instrumentation to measure

the performance of CdS cells produced within the research group. The

amplifier described below was unnecessary for ZnTe films on ZnSe because

only one epitaxial film was produced, but it proved very useful for CdS

cells.

When investigating the performance of experimental photovoltaic

cells it is often necessary to measure the short-circuit current as a

function of the intensity and the wavelength of the illumination. Because

the cell may be constructed from photoconductive materials, the internal

resistance of the cell may alter as these two parameters are varied.

Traditionally, the 'short-circuit' current is determined by measuring

the voltage developed across a small series resistor. To achieve an

accuracy of 1% the voltage measured must be less than 1% of the open

circuit voltage (this may be relaxed to 5% or more if the cell is known

to have a good voltage current characteristic, see Figure A2.1).

In Figure A2.2 a simple circuit is shown which has been used to

measure short-circuit currents accurately. It is based on an integrated

circuit operational amplifier with a FET input, which was selected for

its high input impedance and low input bias current. The gain is $10^5$.

When the test cell is illuminated the short circuit current flows through

the feedback loop of amplifier $A_1$ giving a voltage output equal to the
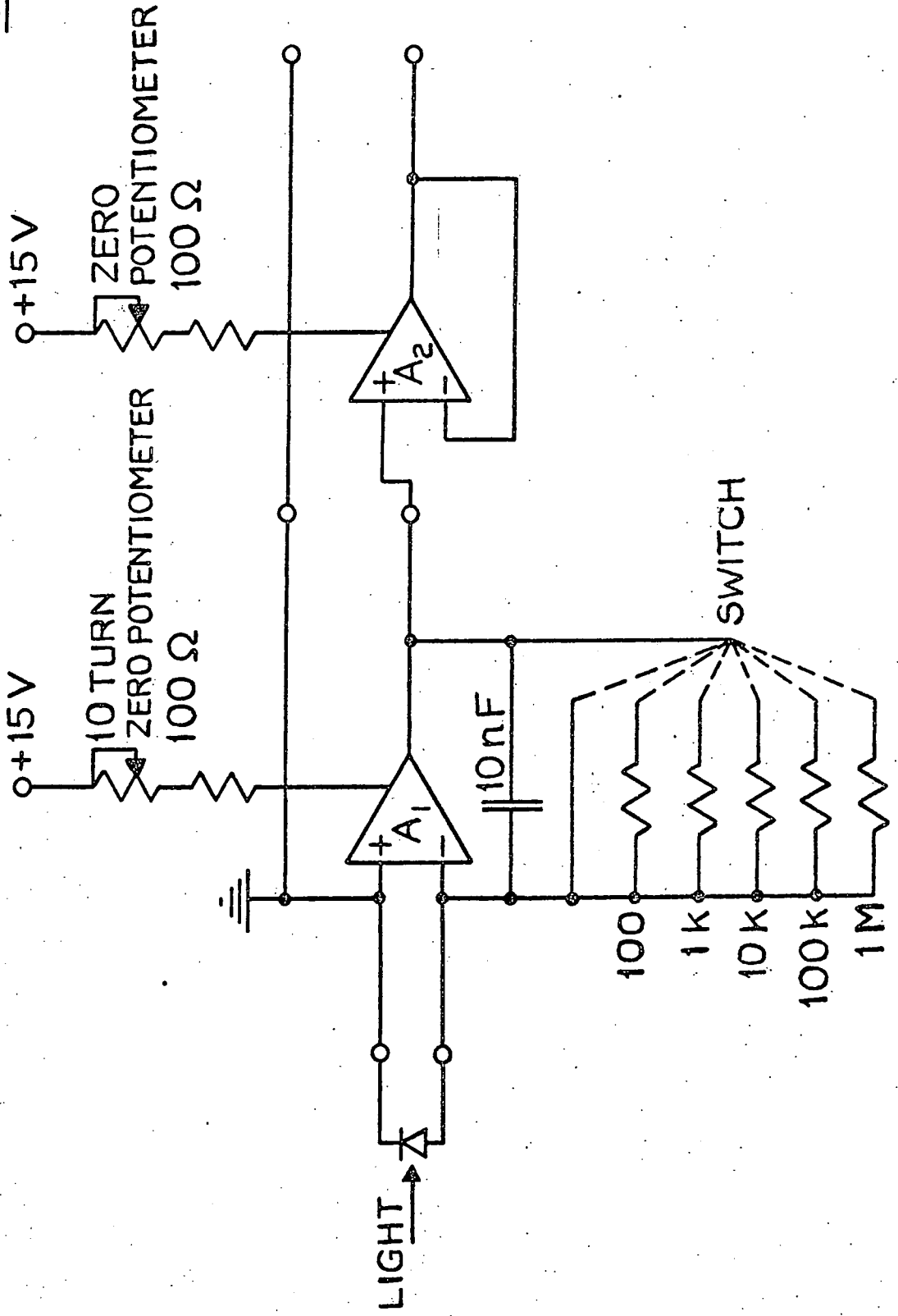
# PHOTOVOLTAIC CELL CHARACTERISTICS.

Fig. A2 : 1
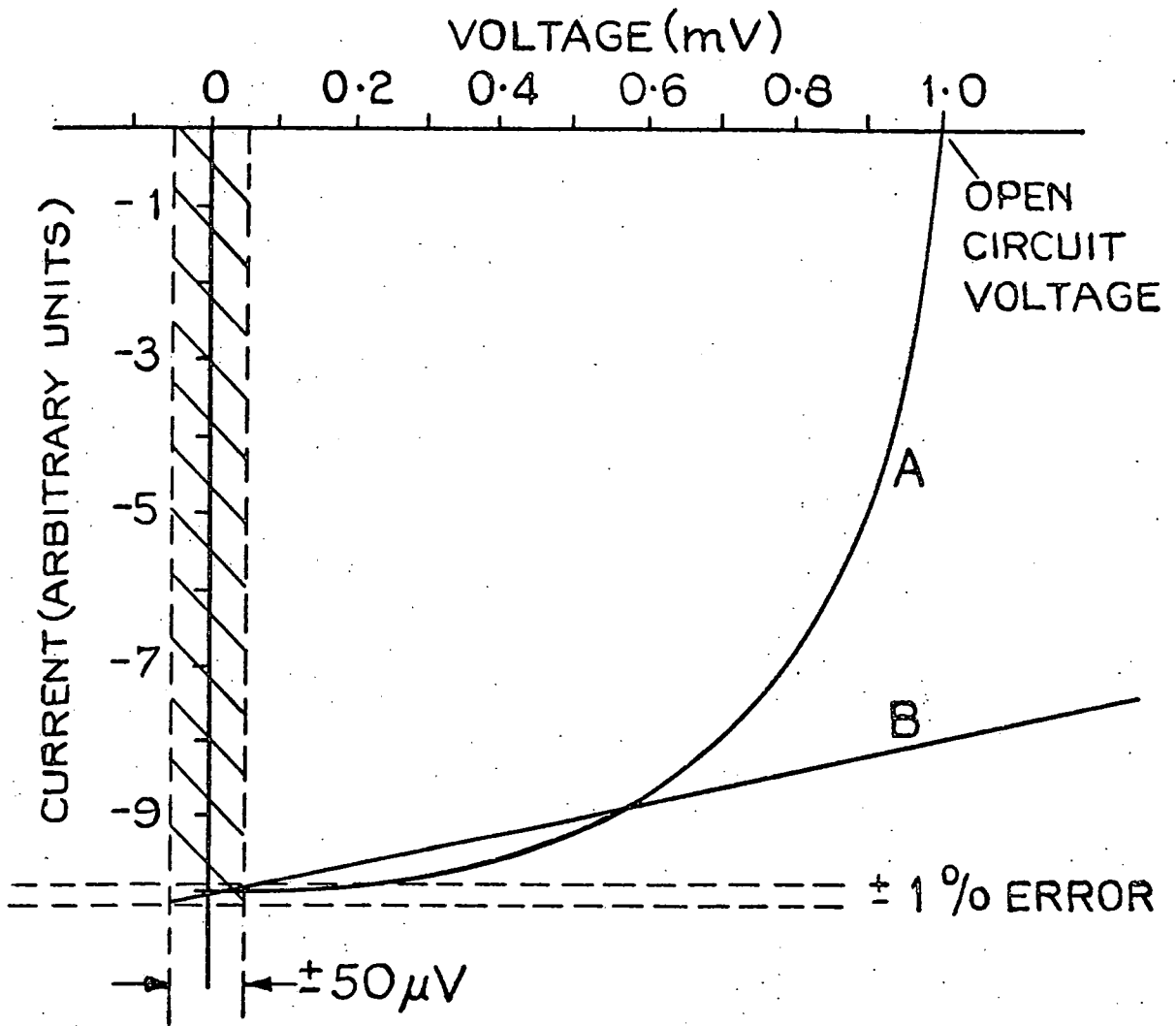
VOLTAGE (mV)



AMPLIFIER KEEPS TEST CELL WITHIN ±50μV SHADED AREA.

A, TYPICAL CELL - GOOD KNEE SHAPED CHARACTERISTIC.

B, WORST CELL - LINEAR CHARACTERISTIC.

CIRCUIT DIAGRAM

Fig. A2:2

LIGHT

+15V
10 TURN
ZERO POTENTIOMETER
100 Ω

+15V
ZERO
POTENTIOMETER
100 Ω

$A_1$

$A_2$

10nF

SWITCH

100
1k
10k
100k
1M

product of the feedback resistance and the short circuit current. The voltage at the virtual earth, and hence at the terminals of the test cell, is $V_{out}/G$ where G is the gain. A feedback resistor is selected by a switch to give an output which does not exceed 100 mV, corresponding to 1 $\mu$V at the terminals of the cell (the capacitor merely prevents oscillations with some values of feedback resistor). For a true measurement of the short-circuit current, the voltage at the input of the cell should be zero. It varies from this because of the 1 $\mu$V mentioned above, and the input drift of the amplifier. The drift was measured as less than 50 $\mu$V h$^{-1}$ by replacing the test cell with a 1 k$\Omega$ resistor and selecting the 100 k$\Omega$ feedback resistor to give a gain of 100. Thus, the performance of the amplifier is limited solely by the input drift. For 1% accuracy the open-circuit voltage of the test cell should be 100 x 50 $\mu$V = 5 mV (or 1 mV for a cell with a normal characteristic, see Figure A2.1).

In our arrangement the output voltage was fed into a buffer amplifier $A_2$ which protected $A_1$ from oscillations which sometimes occurred when it was connected directly to an external circuit. Any instrument with an input impedance greater than 5 k$\Omega$ could then be connected to the amplifier, e.g. a chart recorder or digital voltmeter.

Using the 1 M$\Omega$ feedback resistor, a short-circuit current of 10 nA could be measured in a high impedance sample. A plot of current against wavelength was also made for a silicon cell with an internal resistance of 2 $\Omega$. (Note the 100 mV output limit must be observed).

To achieve similar results with the conventional method, a voltmeter capable of measuring 5 $\mu$V to 1% would be required.
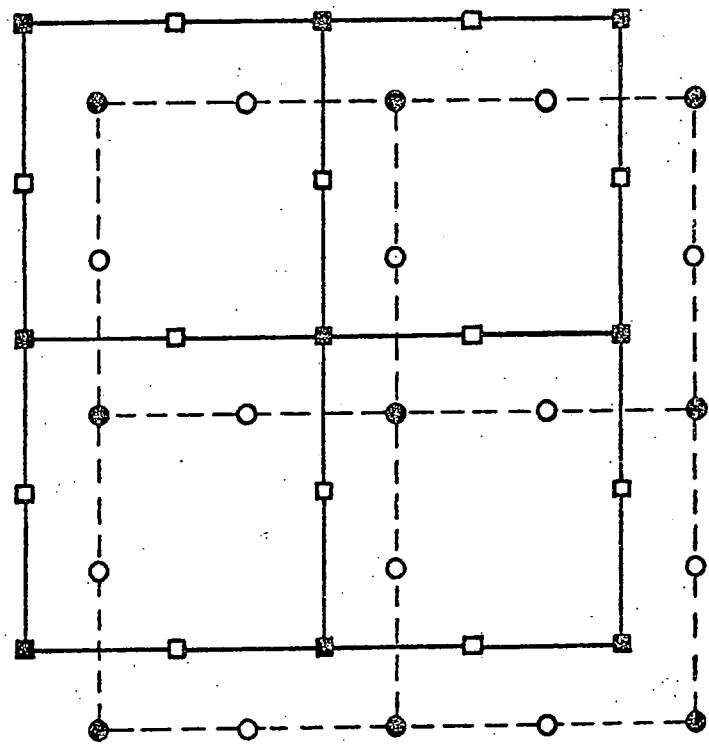
## APPENDIX 3

## POLAR PLANES IN THE ZINC BLENDE STRUCTURE

The etching experiments mentioned in Chapter 5.3 drew attention to another small point. While it is commonly recognised that the {111} plane is polar in the zinc blende structure, it is not often noticed that in fact this is only one of a family of planes that ought to show polar effects. Figures A3.1 and A3.2 show the difference between non-polar faces ( A3.1) and the family of polar planes that intersect the {$\bar{1}$01} plane perpendicularly. A polar plane has metal atoms and non-metal atoms in separate planes at a distance $\frac{1}{4}$d apart (where d is the interplane spacing).

Planes of the type {1, 2n-1, 2n-1} are of the same polarity as the {1,1,1}, as are {4n-3, 1, 1} planes. However, {4n-1, 1, 1} planes are of opposite polarity. n is an integer $\geqslant 1$. Effects may well be noticed when etching planes with small values of n; high index planes are usually made up of steps of lower index planes.

# Fig. A3:1

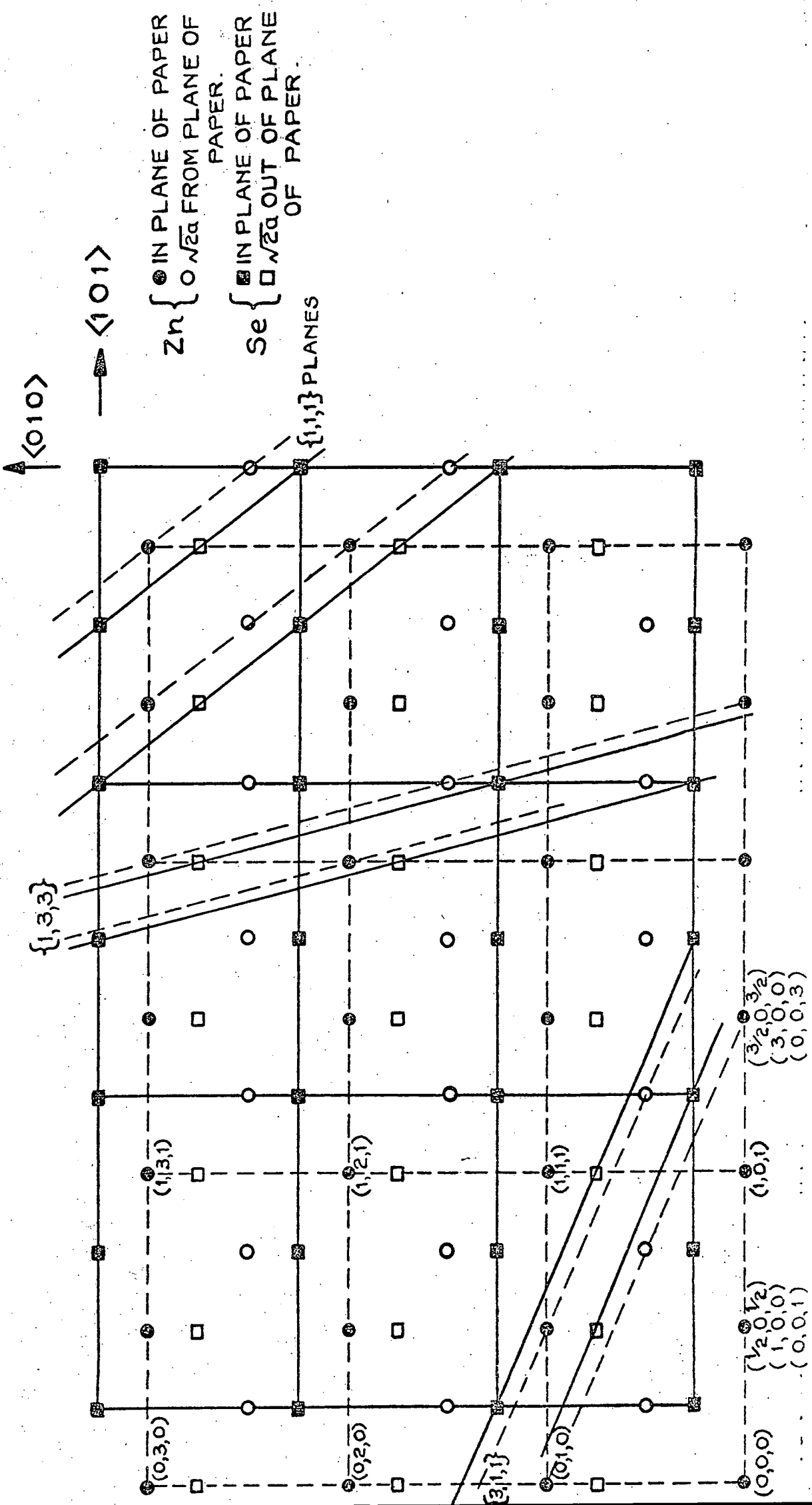## CUBE FACE



A CUBE FACE {100}

$Zn \begin{cases} \bullet & \text{CUBE CORNER} \\ \circ & \text{FACE CENTRE} \end{cases}$

$Se \begin{cases} \blacksquare & \text{CUBE CORNER} \\ \square & \text{FACE CENTRE} \end{cases}$

Fig. A3:2

{$\overline{1}$0 1} FACE

Zn { ● IN PLANE OF PAPER
      ○ √2a FROM PLANE OF PAPER.

Se { ▦ IN PLANE OF PAPER
      □ √2a OUT OF PLANE OF PAPER.

$\langle 010 \rangle$
$\langle 101 \rangle$

{1,1,1} PLANES

{1,3,3}

{3,1,1}

(0,3,0)
(1,3,1)

($\overline{0}$,2,0)
(1,2,1)

(1,1,1)

(0,1,0)
(1,0,1)

(½,0,½)
(3/2,0,3/2)
(1,0,0)
(3,0,0)
(0,0,1)
(0,0,3)

(0,0,0)

### APPENDIX 4

### The Calculation of $A_\ell$ and $A_o$ after a Crystal Growth Run

The value of $\frac{u\ell}{D}$ describes, in physical terms, the balance of diffusion and Stefan flow during the transport of material by sublimation. When the transport equations are applied to the tail part of the crystal growth tube, they may be used to determine $A_\ell$ as shown in Section 4.8. In fact to determine $A_\ell$ after a crystal growth run it is only necessary to know the value of $\exp\left(\frac{u\ell}{D}\right)$ and the ratio $P_{RESERVOIR}/P_{MIN}$. The former can be measured by weighing the amount of material deposited in the tail, the time taken, and the physical dimensions of the capsule, the latter is fixed by the temperatures of the reservoir and charge.

First consider transport from the capsule to the tail tube, let

$$Q = \exp\left(\frac{u\ell}{D}\right) = \frac{3 P_{Zn}(\ell) - 2 P_T}{3 P_{Zn}(0) - 2 P_T} = \frac{3 P_{Se_2}(\ell) - P_T}{3 P_{Se_2}(0) - P_T} \tag{A4.1}$$

Then

$$2 P_T (1 - Q) = 3 (P_{Zn}(\ell) - Q P_{Zn}(0)) \tag{A4.2}$$

and

$$P_T (1 - Q) = 3 (P_{Se_2}(\ell) - Q P_{Se_2}(0)) \tag{A4.3}$$

From A4.2 and A4.3

$$2 (P_{Se_2}(\ell) - Q P_{Se_2}(0)) = P_{Zn}(\ell) - Q P_{Zn}(0) \tag{A4.4}$$

so

$$2 P_{Se_2}(\ell) - P_{Zn}(\ell) = Q( 2 P_{Se_2}(0) - P_{Zn}(0)) \tag{A4.5}$$

At this point it is necessary to separate the two possible cases;

for a tube with zinc in the reservoir, $P_{Se_2}(0) = 0$ and $P_{Zn}(0) = E.P_{MIN}$,

for a tube with selenium in the reservoir $P_{Zn}(0) = 0$ and $P_{Se_2}(0) = F.P_{MIN}$.

Then for a tube with a zinc reservoir A4.4 gives

$$(2 P_{Se_2}(\ell) - P_{Zn}(\ell)) = -Q.E.P_{MIN} \qquad (A4.6)$$

But

$$K_p^3 = \frac{4}{27} . P_{MIN} = P_{Zn}^2(\ell) . P_{Se_2}(\ell), \qquad (A4.7)$$

so

$$(2 P_{Se_2}(\ell) - P_{Zn}(\ell)^3 = -Q^3 . E^3 . \frac{27}{4} . P_{Zn}^2(\ell) . P_{Se}(\ell) \qquad (A4.8)$$

Also,

$$A_\ell = \frac{P_{Zn}(\ell)}{P_{Se_2}(\ell)},$$

so,

$$(2 A_\ell - 1)^3 + \frac{27}{4} Q^3 E^3 A_\ell = 0 \qquad (A4.9)$$

If $E = \frac{2}{3}$ (the usual case of the reservoir set to give the partial pressure of the element at $P_{MIN}$ in the capsule) the equation reduces to

$$(2 A_\ell - 1)^3 + 2 A_\ell Q^3 = 0 \qquad (A4.10)$$

Similarly, for a reservoir containing selenium,

$$(2 A_\ell - 1)^3 - 54 F^3 Q^3 A_\ell = 0 \qquad (A4.11)$$

Usually $F = \frac{1}{3}$, so

$$(2 A_\ell - 1)^3 - 2 A_\ell Q^3 = 0 \qquad (A4.12)$$

It may be seen that only the coefficient of $A_\ell$ varies in equations A4.9 and A4.11, so it is very easy to solve these equations graphically.

Figure A4.1 gives the variation of $A_\ell$ with $\frac{3}{2}$ EQ. (Reducing to Q in the usual case $E = \frac{2}{3}$). Figure A4.2 gives the variation of $A_\ell$ with $3FQ$ (Reducing to Q in the usual case of $F = \frac{1}{3}$).

Returning to A4.10 and A4.12, it is possible to learn a little more about these special cases. $Q = \exp\left(\frac{U\ell}{D}\right)$, and $\frac{U\ell}{D}$ is always negative because of the sign convention used. (Figure 4.1.1). Therefore $0 < Q < 1$. $Q \to 0$ represents very high flow velocities when diffusion may be ignored, and $Q \to 1$ represents very slow flow when Stefan flow may be ignored. In practice this would mean a high inert gas pressure.

$Q = 0$ gives the trivial solution $A_\ell = \frac{1}{2}$ (i.e. perfectly stoichiometric gas over the charge) as would be expected.

$Q = 1$ gives $A_\ell = 0.1588$ for a tube with zinc in the reservoir, and $A_\ell = 1.1623$ for a tube with selenium in the tail.

Equations (A4.11) and (A4.12) are similar to (4.8.17) and (4.8.18), the differences are because it is assumed here that the diffusion coefficients for zinc and selenium are equal, where previously they were assumed to be in the ratio 1:1.5 because of the differing molecular masses.

In Table 4.8.1 the values of $A_\ell$ and $A_o$ are the same whichever value of $P_{MIN}$ was selected (i.e. that due to Aven and Prener or Kirk and Raven) because the value of E was fixed at $\frac{2}{3}$ and that of F at $\frac{1}{3}$ in the calculations. It is believed that the fastest transport occurred under these conditions.

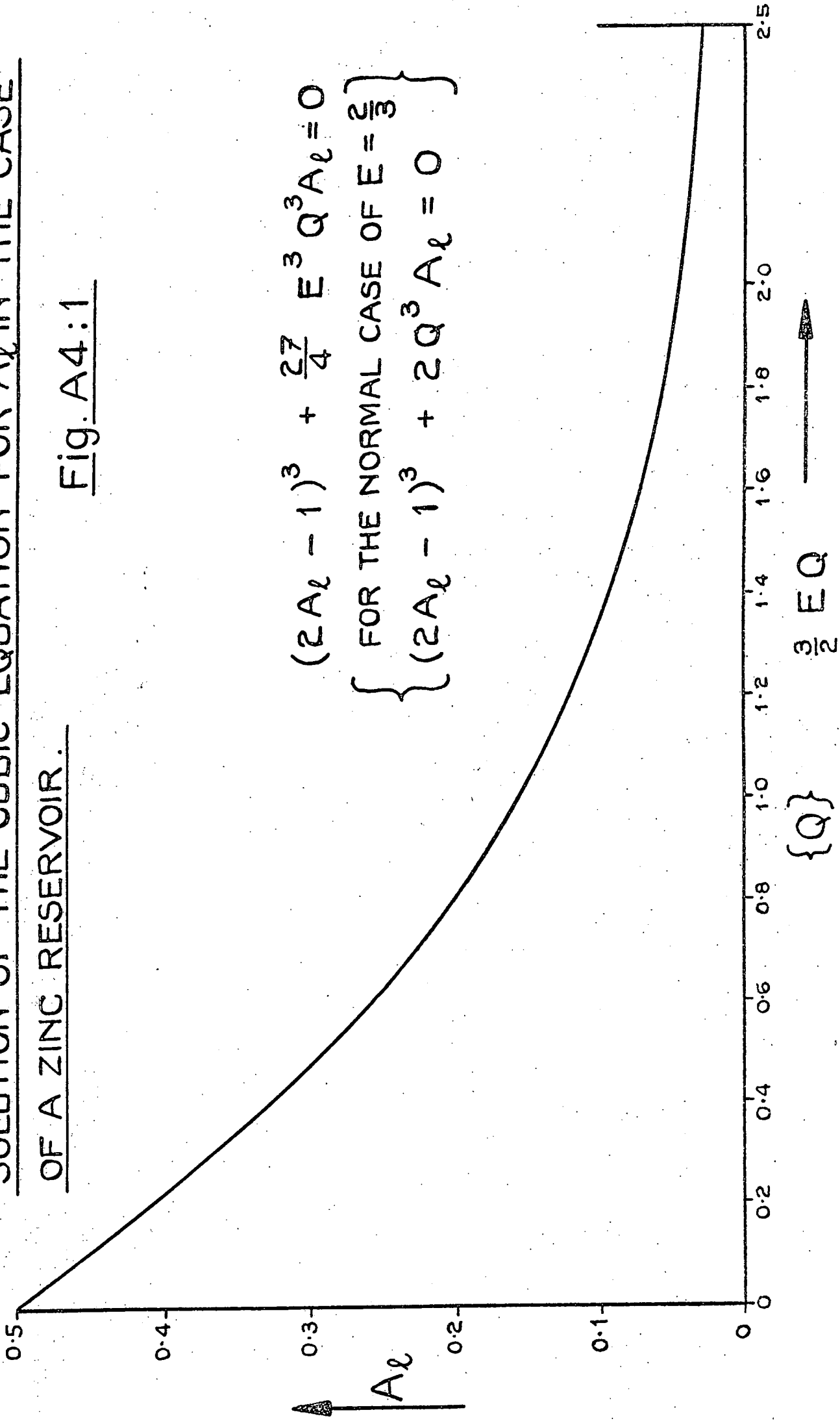To derive $A_o$ from $A_\ell$, the transport equations must be used again, let

$$z = \exp\left(\frac{U\ell}{D}\right) = \frac{3\,P_{Zn}(\ell) - 2\,P_T}{3\,P_{Zn}(0) - 2\,P_T} = \frac{3\,P_{Se_2}(\ell) - P_T}{3\,P_{Se_2}(0) - P_T} \qquad (A4.13)$$

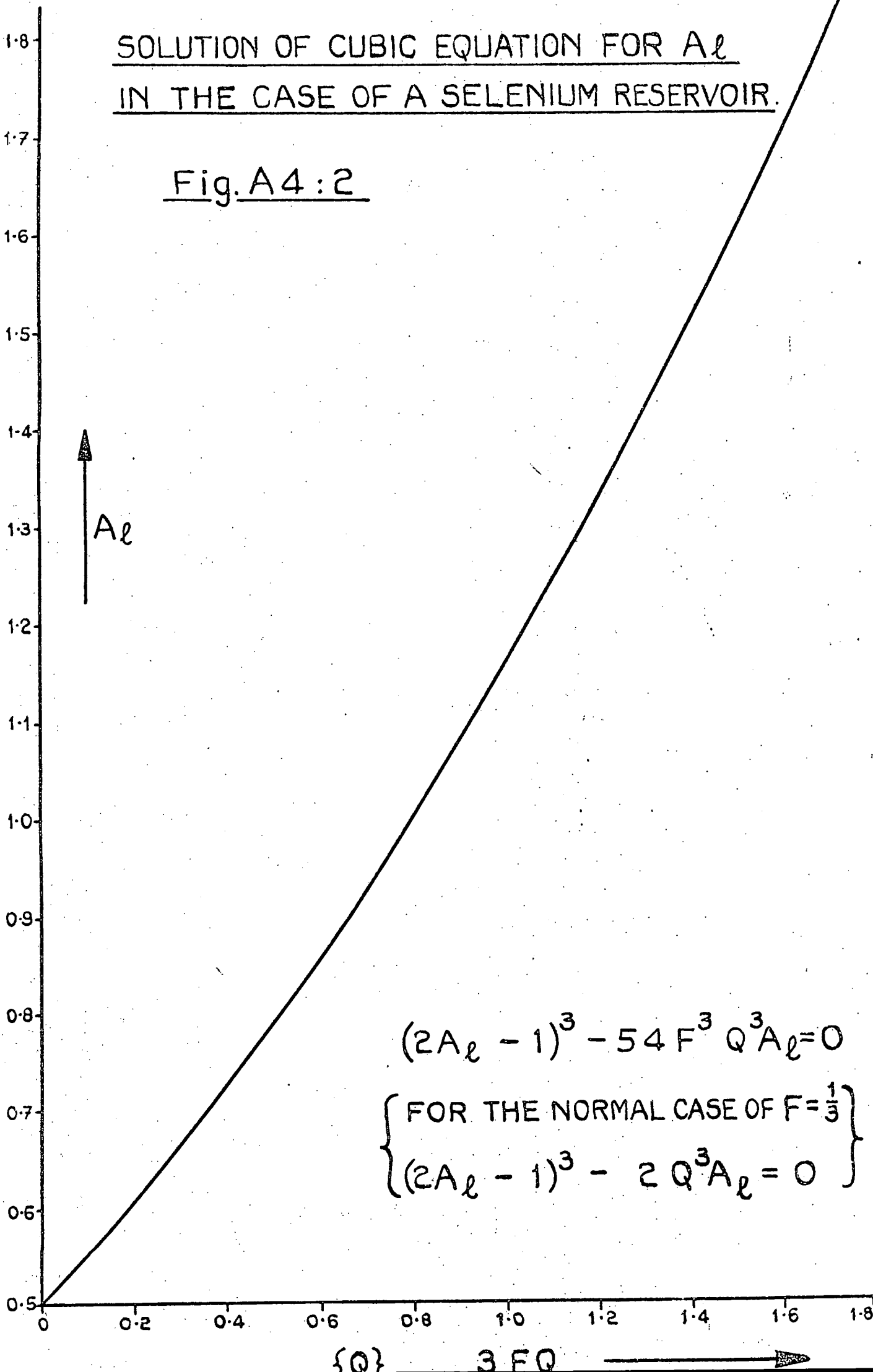From A4.2 and A4.3 it is possible to write;

# SOLUTION OF THE CUBIC EQUATION FOR $A_\ell$ IN THE CASE OF A ZINC RESERVOIR.

## Fig. A4:1



$$(2A_\ell - 1)^3 + \frac{27}{4} E^3 Q^3 A_\ell = 0$$

$$\left\{ \begin{array}{l} \text{FOR THE NORMAL CASE OF } E = \frac{2}{3} \\ (2A_\ell - 1)^3 + 2 Q^3 A_\ell = 0 \end{array} \right\}$$

$\frac{3}{2} E Q$

$\{Q\}$

$A_\ell$

SOLUTION OF CUBIC EQUATION FOR $A\ell$
IN THE CASE OF A SELENIUM RESERVOIR.

Fig. A4:2

$A\ell$

$$(2A_\ell - 1)^3 - 54 F^3 Q^3 A_\ell = 0$$

$$\left\{ \begin{array}{l} \text{FOR THE NORMAL CASE OF } F = \tfrac{1}{3} \\ (2A_\ell - 1)^3 - 2 Q^3 A_\ell = 0 \end{array} \right\}$$

$\{Q\}$    $3 FQ$ ⟶

$$2 P_T (1 - Z) = 3 (P_{Zn}(\ell) - Z P_{Zn}(0)) \tag{A4.14}$$

and

$$P_T (1 - Z) = 3 (P_{Se_2}(\ell) - Z P_{Se_2}(0)) \tag{A4.15}$$

$$= 3 (A_\ell P_{Zn}(\ell) - A_o P_{Zn}(0)) \tag{A4.16}$$

because

$$A = \frac{P_{Se_2}}{P_{Zn}} .$$

Eliminating $P_{Zn}(0)$ from A4.14 and A4.16 yields

$$P_T (1 - Z)(2 A_o - 1) = 3 (P_{Zn}(\ell) A_o - P_{Zn}(\ell) A_\ell) .$$

But from equation A4.1 , for a zinc reservoir $(P_{Se_2}(0) = 0)$ ,

$$P_T = \frac{3 P_{Se_2}(\ell)}{1 - Q} = \frac{3 P_{Zn}(\ell) A_\ell}{1 - Q} \tag{A4.17}$$

and for a selenium reservoir , $(P_{Zn}(0) = 0)$ ,

$$P_T = \frac{3}{2} \cdot \frac{P_{Zn}(\ell)}{1 - Q} \tag{A4.18}$$

So for a tube with zinc in the reservoir

$$A_o = \frac{A_\ell (Z - Q)}{(1 - Q - 2 A_\ell (1 - Z)}$$

and for a tube with selenium in the reservoir ,

$$A_o = \frac{2 A_\ell (1 - Q) + Z - 1}{2 (Z - Q)} .$$